

MICROELECTROPHORETIC STUDIES OF
AQUEOUS SUSPENSION SYSTEMS
OF PHARMACEUTICAL INTEREST

by

John Bratt Kayes

THESIS
615.2 KAY
184913 26 NOV 1975

A dissertation submitted for the
Degree of Doctor of Philosophy
in the
Department of Pharmacy
of the
University of Aston
in Birmingham

May, 1975.

Microelectrophoretic studies of aqueous suspension systems
of pharmaceutical interest

Summary

The relationship between electrophoretic properties and suspension characteristics has been studied. A monodisperse polystyrene latex dispersion was used as a model system, the results found from this have been applied qualitatively, and where possible quantitatively, to suspensions of the drugs Betamethasone, Griseofulvin, Nalidixic Acid and Thiabendazole.

The effect of adding anionic (sodium alkyl sulphates), cationic (alkyltrimethylammonium bromides) and nonionic (polyoxyethylene glycol monoethers of n alkanols) surface active agents, and mixtures of these ionic and nonionic species, on the electrophoretic properties of the above dispersions has been measured, and the results correlated with sedimentation volume studies of the drug suspensions.

Mobility versus pH plots for the drugs showed that the charge on the particle varied with pH, suggesting the advisability of this sort of study before formulation. The nonionic surfactants are adsorbed in a looped monolayer as was shown by a plateau region in the mobility versus pH plot, these nonionic surfactants were effective as steric stabilizers in preventing suspension caking.

With cationic surfactants adsorption is a two stage process characterized by neutralization of negative charge followed by charge reversal. The free energy of adsorption was measured and depended on alkyl chain length, the driving force for adsorption being the hydrophobic effect. Displacement of the reversal of charge concentration by nonionic surfactant depended on its concentration and the type of

cationic surfactant.

Adsorption of anionic surface active agents caused an increase in zeta potential. An estimate of the free energy of adsorption was made from the slope of the zeta potential versus \log_{10} concentration surfactant plot. The zeta potentials found with varying concentration of anionic surfactant were used to calculate the DLVO potential energy plot for the Thiabendazole/sodium dodecyl sulphate system. Added nonionic surface active agents were found to complex with anionics, complexation being dependent on ethylene oxide chain length.

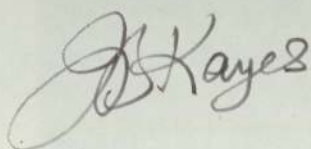
From sedimentation volume studies the existence of coagulated, deflocculated and secondary minimum flocculated systems is discussed and correlated with zeta potential measurements.

The concept of controlled flocculation, or perhaps more correctly controlled coagulation, as a means of preparing a stable pharmaceutical suspension, is supported.

It is concluded that there is need for revision in the terminology describing coarse suspension systems, most suspensions described as flocculated being in fact coagulated.

MEMORANDUM

This dissertation, which is being submitted for the degree of Doctor of Philosophy of the University of Aston in Birmingham, is an account of the work carried out under the supervision of Dr. S. S. Davis in the Department of Pharmacy of the University of Aston in Birmingham from October 1971 to May 1975. Except where acknowledged by reference in the text, the work described herein is claimed to be original and has not been submitted for any other award.

A handwritten signature in cursive script, appearing to read 'J. B. Kayes', is written in dark ink on the page.

J. B. Kayes

May 1975

ACKNOWLEDGEMENTS

I wish to express my appreciation to Dr. S.S. Davis for his interest and advice during the course of this work.

I would also like to thank Professor M.R.W. Brown for making facilities and time available for me, and my colleagues for their support.

Microelectrophoretic studies of aqueous suspension systems
of pharmaceutical interest

Summary

Memorandum

Acknowledgements

Page

Section I.	<u>Introduction</u>	1.
	1.1.	Suspensions	1.
	1.2.	Historical review of the controlled flocculation approach to suspension formulation.	2.
	1.3.	Outline of present work.	11.
Section 2.	<u>Theory</u>	12.
	2.1.	<u>The Electric Double Layer</u>	12.
	2.1.1.	Diffuse double layer, Gouy-Chapman theory for flat surfaces.	13.
	2.1.2.	Double layer around a spherical particle. ...	16.
	2.1.3.	The inner part of the double layer.	17.
	2.1.4.	Discreteness of charge effect.	19.
	2.1.5.	Corrections to the Poisson-Boltzmann equation	20.
	2.1.6.	Interaction of two overlapping diffuse layers	21.
	2.2.	<u>Attraction between particles</u>	23.
	2.2.1.	The de Boer-Hamaker Microscopic Theory of attraction between condensed objects ...	25.
	2.2.2.	The effect of the liquid medium on the attractive forces between particles. ...	26.
	2.2.3.	Electromagnetic retardation	26.
	2.2.4.	The Lifshitz Macroscopic theory of attraction between condensed objects.	27.
	2.3.	<u>The effect of adsorbed layers on the stability of dispersions</u>	30.
	2.3.1.	The effect of the adsorbed layer on the Stern Potential.	31.

Section 2.	<u>Theory, continued</u>	<u>Page</u>
2.3.2.	Steric stabilization	31.
2.3.3.	The van der Waals attraction between colloid particles having adsorbed layers.	36.
2.3.4.	Combined effects of steric stabilization and electrostatic repulsion on the stability of dispersions.	38.
2.4.	<u>Electrophoresis</u>	39.
2.4.1.	Calculation of zeta potentials.	40.
2.4.2.	Permittivity and viscosity	45.
2.4.3.	Non spherical particles.	46.
2.4.4.	Surface charge density from electrophoresis measurements.	46.
2.4.5.	The relation between the Stern potential and surface active agent concentration	48.
2.4.6.	Hydrophobic bonding (the hydrophobic effect).	51.
Section 3.	<u>Experimental</u>	54.
3.1.	<u>Materials</u>	54.
3.1.1.	Surface active agents.	54.
3.1.2.	Polystyrene latex.	55.
3.1.3.	Drugs; Betamethasone, Griseofulvin, Nalidixic Acid and Thiabendazole.	56.
3.2.	<u>Characterisation of Materials</u>	57.
3.2.1.	Surface active agents.	57.
3.2.2.	Polystyrene latex	58.
	(a) Particle size distribution	58.
	(b) Surface groupings.	59.
3.2.3.	Particle size distributions of drugs	61.
3.3.	<u>Apparatus and experimental procedure</u>	63.
3.3.1.	Microelectrophoresis	63.
	(i) Apparatus	63.
	(ii) Experimental procedure.	68.
3.3.2.	Sedimentation volumes.	70.

	<u>Page</u>
Section 4. <u>Microelectrophoresis of polystyrene latex, results and discussion</u>	72.
4.1. <u>Effect of pH on the electrophoretic mobility and zeta potential</u>	72.
4.1.1. Surface and bulk dissociation constants. ...	73.
4.1.2. Calculation of surface charge densities. ...	75.
4.1.3. Calculation of the potential at the surface. ...	76.
4.2. <u>Effect of nonionic surface active agents on the electrophoretic mobility and zeta potential</u>	78.
4.2.1. Effect of concentration	79.
4.2.1.1. Evidence for a closely packed vertically orientated monolayer.	80.
4.2.1.2. Evidence for multilayer formation.	82.
4.2.1.3. Evidence for monolayer formation with attachment by hydrocarbon chain and ethylene oxide groups.	82.
4.2.1.4. Other evidence for the adsorption of non-ionic surfactants on charged particles. ...	83.
4.2.1.5. Conclusions concerning the form of the adsorbed layer in this work.	84.
4.2.2. Effect of number of ethylene oxide units ...	85.
4.2.3. Effect of altering the length of the alkyl chain ...	88.
4.3. <u>Effect of cationic surface active agents on the electrophoretic mobility and zeta potential</u>	88.
4.3.1. General characteristics of the zeta potential- \log_{10} concentration plots.	89.
4.3.2. Conversion of mobility to zeta potential. ...	92.
4.3.3. Calculations from zeta potential- \log_{10} concentration CxTAB plots.	92.
4.4. <u>Effect of mixtures of cationic and nonionic surface active agents on the electrophoretic mobility and zeta potential</u>	94.
4.4.1. General characteristics of the zeta potential- \log_{10} concentration CxTAB plots.	95.
4.4.2. Calculations from zeta potential- \log_{10} concentration surfactant plots.	97.

	<u>Page</u>
Section 4. <u>Microelectrophoresis of polystyrene latex, results and discussion, continued.</u>	
4.4.2.1. Effect of concentration of nonionic surfactant on the reversal of charge concentration.	97.
4.4.2.2. Effect of ethylene oxide chain length on the reversal of charge concentration.	98.
4.5. <u>Effect of anionic surface active agents on the electrophoretic mobility and zeta potential.</u>	99.
4.5.1. General characteristics of the zeta potential- \log_{10} concentration plots.	99.
4.5.2. Calculations from zeta potential- \log_{10} concentration sodium alkyl sulphate curves.	100.
4.6. <u>Effect of mixtures of anionic and nonionic surface active agents on the electrophoretic mobility and zeta potential.</u>	102.
4.6.1. General characteristics of the zeta-potential - \log_{10} concentration sodium alkyl sulphate plots.	102.
4.6.2. Effect of anionic surface active agent type, and nonionic surface active agent ethylene oxide chain length, on the zeta potential- \log_{10} concentration plots.	106.
Section 5. <u>Microelectrophoretic studies on Griseofulvin, Betamethasone, Nalidixic Acid and Thiabendazole suspensions, results and discussion.</u>	109.
5.1. <u>Effect of pH on the electrophoretic mobility and zeta potential.</u>	109.
5.1.1. Conversion of mobility to zeta potential. ...	110.
5.1.2. Mobility/zeta potential-pH plots.	111.
5.2. <u>Effect of nonionic surface active agents on the mobility and zeta potential.</u>	114.
5.3. <u>Effect of dodecyl trimethyl ammonium bromide on the electrophoretic mobility and zeta potential.</u>	115.
5.3.1. General characteristics of the zeta potential \log_{10} concentration C_{12} TAB plots.	116.
5.3.2. Calculation of free energies of adsorption from zeta potential- \log_{10} concentration C_{12} TAB plots.	118.
5.4. <u>Effect of mixtures of cationic and nonionic surface active agents on the electrophoretic mobility and zeta potential.</u>	118.

Section 5.	<u>Microelectrophoretic studies on Griseofulvin, Betamethasone, Nalidixic Acid and Thiabendazole suspensions, results and discussion, continued.</u>	
5.4.1.	General characteristics of the zeta potential- \log_{10} concentration C_{12}^{TAB} with C_{16}^{Ey} plots.	118.
5.5.	<u>Effect of sodium dodecyl sulphate on the electrophoretic mobility and zeta potential.</u>	119.
5.5.1.	General characteristics of the zeta potential- \log_{10} concentration SDS plots. ...	120.
5.5.2.	Calculation of free energies of adsorption from zeta potential- \log_{10} concentration SDS plots.	121.
5.6.	<u>Effect of mixtures of sodium dodecyl sulphate and nonionic surface active agents on the electrophoretic mobility and zeta potential.</u>	121.
5.6.1.	General characteristics of the zeta potential- \log_{10} concentration SDS with C_{16}^{Ey} plots. ...	122.
5.6.2.	Effect of sodium dodecyl sulphate with non-ionic surface active agents of varying ethylene oxide chain length.	123.
Section 6.	<u>Relationship between zeta potential, sedimentation volume and redispersibility of Betamethasone, Griseofulvin, Nalidixic Acid and Thiabendazole suspensions.</u>	124.
6.1.	<u>General considerations.</u>	124.
6.1.1.	Sedimentation volume.	124.
6.1.2.	Redispersibility.	125.
6.1.3.	Zeta potential, sedimentation volume and suspension stability.	125.
6.2.	<u>Characteristics of the zeta potential/sedimentation volume versus concentration of surface active agent plots, and calculation, in selected cases, of the total potential energy of interaction between particles.</u>	128.
6.2.1.	Drug particle, nonionic surfactant systems ...	128.
6.2.2.	Drug particle, cationic surfactant systems ...	129.
6.2.3.	Drug particle, cationic/nonionic surfactant systems.	130.
6.2.4.	Drug particle, anionic surfactant systems. ...	131.
6.2.5.	Drug particle, anionic/nonionic surfactant systems	132.

	<u>Page</u>
Section 7. <u>General discussion and conclusions.</u>	134.

References

Appendix I	Tables 3 and 4 of reference 99.
Appendix II	Tables I, III to V, VII to XIX, XXI to XXXIV, XXXVI, XXXVIII and XXXIX.

SECTION I.

INTRODUCTION

1.1. Suspensions

A pharmaceutical suspension is a coarse dispersion in which insoluble particles are dispersed in a liquid medium, usually aqueous. The discussion here is limited to this form.

The particles have diameters for the most part greater than $1\mu\text{m}$ although some may be as small as $0.1\mu\text{m}$ or less, it is in this factor of size that pharmaceutical suspensions differ from colloidal dispersions. The accepted definition of a colloidal particle indicates that one or more of the components has at least one dimension within the range of about 1nm to $1\mu\text{m}$. There is however no sharp distinction between colloidal and non colloidal systems particularly at the upper size range and suspensions show most of the properties of colloidal systems. However the relatively large particles of a suspension are liable to sedimentation due to gravitational forces.

An aqueous suspension is a useful formulation system for administering an insoluble or poorly soluble drug. The large surface area of dispersed drug ensures a high availability for dissolution and hence absorption; the dissolution of all drug particles commences immediately on dilution in gastro-intestinal fluids. Suspensions contribute further to pharmacy and medicine, by supplying insoluble and often distasteful substances in a form which is pleasant to the taste, of particular importance for administration of drugs to young children; by providing a suitable form for the application of dermatological materials to the skin and sometimes to the mucous membranes; for parenteral administration of insoluble drugs; and for application to the eyes. Suspensions are used similarly in veterinary practice where, for example, a number of anthelmintics are presented in this form. In the veterinary field the

product is often supplied as a dispersible powder; this product has to be of such a character that when stirred with water a suspension results which is sufficiently stable to permit withdrawal of numerous doses with, for practical purposes, equal drug content. In such cases, when settlement takes place when a bulk mix is left, it is essential that stirring should readily reconstitute a uniform suspension. Suspensions thus constitute an important dosage form both in human and veterinary medicine. A closely allied field is that of pest control; pesticides are frequently presented as suspensions for use as fungicides, insecticides, acaricides and herbicides, such are usually intended to be applied as sprays with water as a diluent.

Further important uses of suspensions are seen in the paint and printing industries.

A pharmaceutically acceptable suspension possesses certain desirable qualities among which are the following(1): the suspended material should not settle too rapidly; the particles which do settle to the bottom of the container must not form a hard mass but should be readily dispersed into a uniform mixture when the container is shaken; and the suspension must not be too viscous to pour freely from the orifice of the bottle or to flow through a syringe needle. For pharmaceutical purposes physical stability of suspensions may be defined as the condition in which the particles do not aggregate and in which they remain uniformly distributed throughout the dispersion. Since this ideal situation is seldom realized it is appropriate to add that if the particles do settle they should be easily resuspended by a moderate amount of agitation.

1.2. Historical review of the controlled flocculation approach to suspension formulation

A theory which describes quantitatively some aspects of the stability of a lyophobic colloidal system is that put forward by Derjaguin and

Landau (2) and independently by Verwey and Overbeek (3). The basic premise of their theory, the so-called DLVO theory, was that the potential energy of interaction between a pair of particles could be considered to consist of two components:- (a) that arising from the overlap of the electrical double layers and leading to repulsion V_R (a measure of the magnitude of V_R can be made from the potential at the plane of shear around the particle, the so-called zeta potential (ζ)); (b) that arising from electromagnetic effects and leading to van der Waals attraction, V_A .

These were considered to be additive so that the total potential energy of interaction, V , could be written as

$$V = V_R + V_A \quad 1.1$$

The general features of the curve of potential energy of interaction against the distance of separation between particle surfaces, H_0 , are given in Fig. I.

At small distances of separation, the combination of strong short range repulsive forces and van der Waals attraction leads to a deep minimum termed the primary minimum, P , of magnitude V_p . The position of the primary minimum determines the distance of closest approach. At high surface potentials and low ionic strengths and at intermediate distances the electrical repulsion term is the dominant one and hence a maximum occurs in the potential energy curve; this is normally termed the primary maximum with a magnitude V_m . At larger distances, the energy of electrical repulsion falls off more rapidly with increasing distance of separation than the van der Waals attraction and a second minimum appears in the curve of depth V_{SM} ; this is termed the secondary minimum.

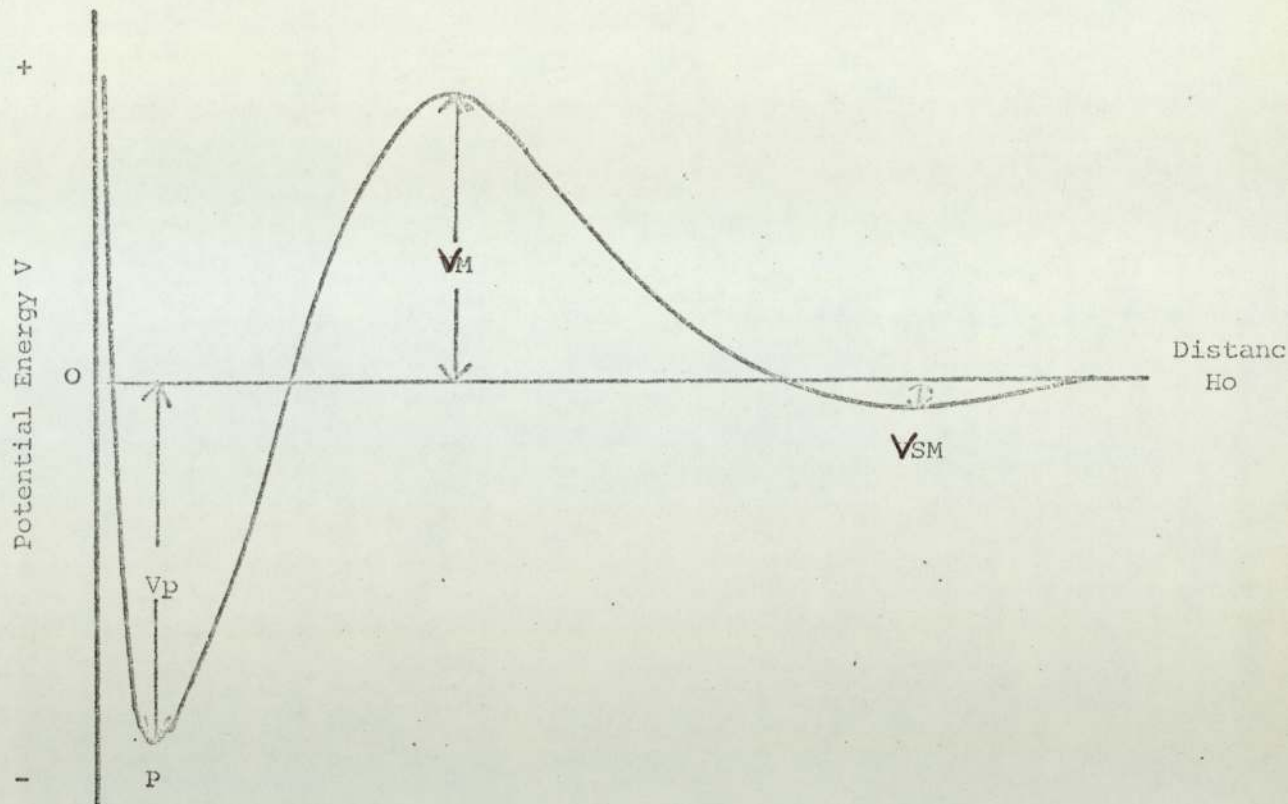


Fig I Potential energy curve ($V = V_R + V_A$) against distance between particles

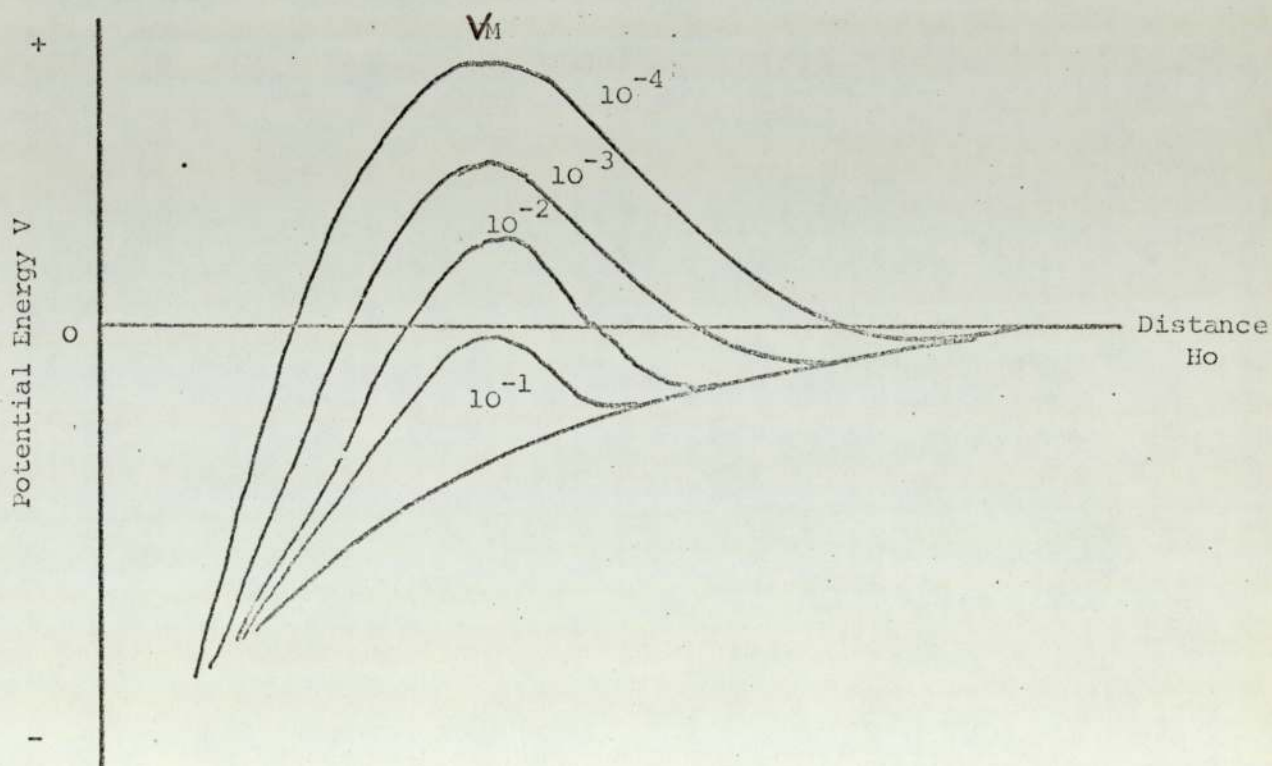


Fig II Effect of electrolyte concentration, mol dm^{-3} , (e.g. Sodium Chloride) on Potential Energy of Interaction at constant surface potential (concentrations illustrative only)

The kinetic energy barrier to particle association in the primary minimum is represented by $V_M + V_{SM}$ and the energy barrier to redispersion from a primary minimum is represented by $V_p + V_M$. The effect of added electrolyte on the potential energy of interaction is shown in Fig. II. At low ionic strength when the surface potential is high (as illustrated with $10^{-4}M$ electrolyte), repulsion dominates and the secondary minimum V_{SM} will not be deep enough to overcome the kinetic energy of the particles. Further addition of electrolyte effectively reduces the repulsive force and hence lowers the height of V_M and also deepens V_{SM} (this could also be described as moving the position of the secondary minimum closer to the particle surface) thus increasing the tendency of the particles to associate in the secondary minimum. Lowering of V_M to a critical value, as with the $10^{-1}M$, and probably $10^{-2}M$, curves, will lead to association in the primary minimum as the particles will possess sufficient kinetic energy to overcome the repulsive barrier and attraction will predominate.

The terms coagulation and flocculation tend to be used indiscriminately in the literature and no attempt has been made to correct terms used in the following review, however here, and in the report of the writer's experimental work, particle association in the primary minimum will be termed COAGULATION, association in the secondary minimum FLOCCULATION (4). The latter term is also used to describe polymer bridging between particles and cross linking of particles produced by metal-ion interactions with polyelectrolytes; thus flocculation describes particle association in which the average distance between the particles is considerably greater than the order of atomic dimensions and hence the aggregate formed in this way has an open structure. On the other hand coagulation leads to the formation of a compact aggregate structure in which the average distance of separation between the particles

can be of the order of atomic dimensions.

It has been known for many years that substances such as nonionic surfactants may, if adsorbed at the particle surface, stabilize a dispersion in the absence of a significant zeta potential. When such an adsorbed layer is present the approach of the particle surfaces and their aggregation in the primary minimum is hindered by the presence of the adsorbed layers. It is clear that an additional term has to be included in the potential energy of interaction for what is called, somewhat loosely, STERIC STABILIZATION V_s .

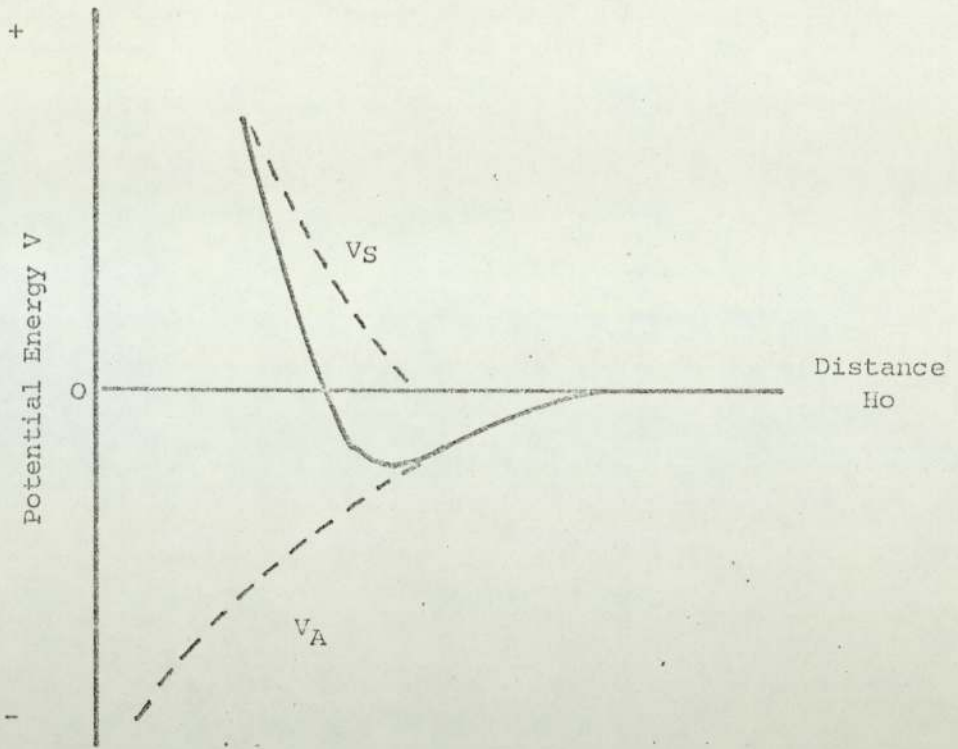
$$\text{Thus } V = V_R + V_A + V_s \quad 1.2$$

It was pointed out by Koelmans & Overbeek (5) that if the potential energy diagram is considered, the particles cannot approach closer than a distance of twice the thickness of the adsorbed layer, and hence passage into the primary minimum is inhibited.

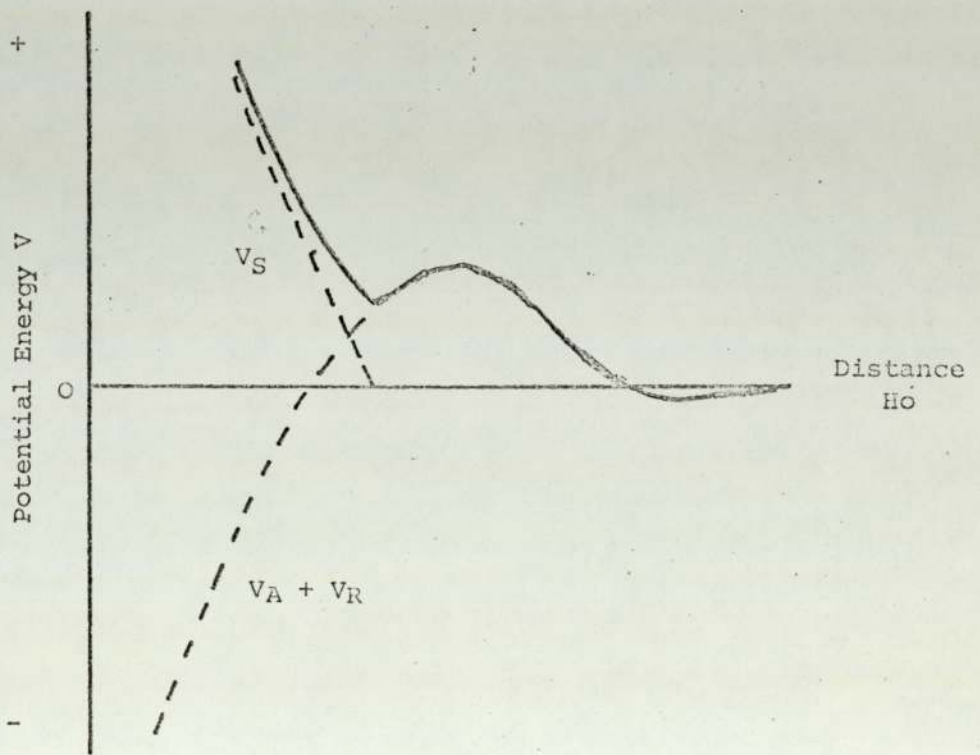
The effect of V_s is shown in Fig. III for the situations which occur in the presence and absence of an electrostatic barrier.

A pharmaceutical suspension which would be thought of as a stable dispersion if considered in terms of the DLVO theory will be deflocculated but will sediment due to the size of the particles. When sedimentation is complete the particles form a close packed arrangement with the small particles filling the voids between the larger ones. Those particles lowermost in the sediment are gradually pressed together by the weight of the ones above, the energy barrier is thus overcome allowing the particles to pass into close contact with each other, coagulation followed by 'caking' (the formation of a compact mass at the bottom of the container) then occurs and re-dispersion of particles is not easily achieved, dispersion forces greater than agitation usually being required.

Physical bonding, leading to cake formation, may be brought about by crystal formation which depends upon the degree of solubility of the



(a) No electrostatic repulsion
 $V = V_A + V_S$



(b) Electrostatic repulsion present
 $V = V_A + V_R + V_S$

Fig III Influence of Steric Stabilization V_S on the potential energy versus distance between particles curve.

dispersed material in the vehicle (6). At the points of contact between microcrystals, a thin layer of supersaturated solution exists. The smaller crystals slowly dissolve and cause the larger crystals to grow. This phenomenon known as Ostwald ripening (7), leads to coarsening of the sediment and in some instances according to Kolthoff and Noponen (8) may also result in caking. Further, chemical bonding due to hydration effects may cause the porous particles to cement together into a hard crystalline mass (9).

Coagulation in the primary minimum, resulting from a reduction in the zeta potential to a point where attractive forces predominate, produces coarse compact masses with a curdled appearance which are not easily dispersed (10). The aggregates are dense and non-porous and form a caked sediment (11). On the other hand particles flocculated in the secondary minimum, V_{SM} , form a loosely bonded structure which settles rapidly, caking does not normally occur, and the particles are easily resuspended. However with particles stabilized by nonionic polymers and flocculated in the secondary minimum, it is possible, particularly with irregularly shaped and polydispersed particles, for coagulation to occur by a "tunnel effect". Due to incomplete coverage of a particle by the polymer, when approached by another particle as they rotate, coagulation can occur through the "tunnel" (12). Further, with such systems, Everett et al (13) have indicated that attractive forces may be of sufficient strength to bring about desorption of the nonionic stabilizer, thus causing coagulation.

Although completely flocculated particles are easily redispersed such suspensions are not wholly satisfactory, sedimentation of flocs is rapid - consequently dose measurement will be difficult - they are unsightly and the volume of flocs produced may be greater than that of the original suspension volume.

It is usual therefore in pharmaceutical suspension formulation to induce "controlled flocculation" - the aim here being to produce assemblages of particles where the average distance between the particles is relatively small, but the particles are prevented (either by electrostatic repulsive forces or by other means) from approaching so close that primary minimum coagulation occurs - such assemblages will be easily redispersible and less bulky and unsightly than a secondary minimum flocculated system.

The principle of "controlled flocculation" was first described by Haines & Martin in a series of papers (6), (14), (15) on studies of sulphamerazine and bismuth subnitrate dispersions; they suggested that suspension 'flocculation' could be controlled by modifying the charge surrounding the particles by the addition of electrolyte. For example the addition of aluminium chloride to 2% sulphamerazine suspensions containing dioctyl sodium sulphosuccinate effectively lowered the zeta potential (estimated from microelectrophoretic mobilities) and produced a pharmaceutically stable suspension characterised by a high sedimentation volume (the ratio of the final volume of sediment to the original volume before settling). They thus showed a correlation between apparent zeta potential, sedimentation volume, caking and "flocculation".

Wilson and Ecanow (16) and subsequently Ecanow et al (17) questioned the work of Haines and Martin for several reasons: (a) they doubted whether this procedure could be applied to macroscopic particles, they thought that, although van der Waals forces exist at the surface of all solid particles, they would be effective in bonding only when the solid was in an extremely fine state of subdivision ($< ca. 2\mu m$) and that therefore flocculation in the secondary minimum with coarse suspension particles could not occur. However, the existence of secondary minimum

flocculation with large particles has been shown with $10\mu\text{m}$ polystyrene latex particles (18), $3\mu\text{m}$ paraffin wax particles (19) and $2-35\mu\text{m}$ globules (20) and it is accepted that it is likely to occur, at low electrolyte concentration, with particles $\text{ca.} > 1\mu\text{m}$. Wiese and Healy (21) state "there is much evidence that such coagulation (secondary minimum flocculation) does occur in systems for which the interaction energy curves show large energy barriers and deep secondary minima. Undoubtedly it can also occur in systems for which the secondary minima are still deep but the energy barriers are smaller". The presence of effective van der Waals forces between macroscopic bodies has been proved beyond doubt by, for example, the work of Tabor and Winterton (22), (23), (24) who measured the force of attraction between molecularly smooth sheets of muscovite mica. The presence of an aqueous medium between the particles does, however, reduce the van der Waals attraction as is discussed in Section 2.2.2; (b) they doubted the usefulness of measurement of zeta potential as a means of assessing the "flocculation", deflocculation state of a suspension as, since "flocculation" was reported to have occurred spontaneously, the true zeta potential could not have been measured; and (c) the effect of the electrolyte on the surfactant was not taken into account. During a subsequent investigation they observed the formation of a precipitate when dioctyl sodium sulphosuccinate at concentrations used by Haines and Martin was mixed with aluminium chloride. "Flocculation" was interpreted as being due to a chemical reaction between the surfactant and the electrolyte instead of a reduction of the zeta potential.

Mathews & Rhodes (25) in studies of coagulation and flocculation with aluminium chloride of suspensions of griseofulvin and polystyrene latex, prepared with sodium dodecyl sulphate, which is precipitated by aluminium chloride, and sodium dioxyethylated dodecyl sulphate which

apparently is not precipitated by aluminium chloride, showed that both flocculation, probably involving chemical bridging, and coagulation resulting from zeta potential reduction, can be used to prevent caking.

The same workers (26) demonstrated that in suspensions of griseofulvin with a mean particle size in the range 3-4 μ m "flocculation" was essentially similar in character to that in lyophobic colloids, and that such "flocculation" was accompanied by changes in the zeta potential of the particles. They also showed that comparisons may be made between coagulation in model disperse systems (a polystyrene latex) and in heterogenous drug suspensions. They strongly support the concept of "controlled flocculation" in the formulation of pharmaceutical suspensions.

Jones, Mathews & Rhodes (27) carried out a similar study on the physical stability of sulphaguanidine suspensions, varying electrolytes, surface active agents and the vehicle, they further support the concept of "controlled flocculation" in suspensions of this drug. Mathews & Rhodes (28) extended the above work including griseofulvin, fine and coarse particle, sulphamerazine and hydrocortisone as drugs for suspension, ammonium and sodium dioxyethylated dodecyl sulphates as surface active agents, and aluminium, calcium, and sodium chlorides as electrolytes. They interpreted the aggregation mechanism using the DLVO theory to predict energy of interaction curves and suggested that coagulation occurs at the primary minimum but that the depth of V_p is restricted due to steric stabilization by the surface active film, so that particle dispersion occurs on agitation. They made quantitative estimations using the DLVO expression modified to include the steric energy term V_s , which they obtained from calculations of chain length and data taken from the work of Ottewill and Walker (29); V_R was obtained from zeta potential measurements and V_A calculated using accepted values of the Hamaker constant.

Their work is further supported by that of Short & Rhodes (30) who

carried out stability studies on suspensions of hydrocortisone and norgestrol and Bondi et al (31) who measured the degree of 'flocculation' of sulphamerazine suspensions as represented by relative sedimentation volumes as a function of both surfactant and electrolyte concentration. Their results emphasise the importance of knowing the location as well as the concentration of the surfactant and are consistent with the DLVO theory. The concept of "controlled flocculation" is therefore firmly established as a means of producing an acceptable pharmaceutical suspension. However the term "controlled flocculation" is perhaps a misnomer, as it covers:-

(a) secondary minimum flocculation - particularly where V_M is reduced by addition of an electrolyte thus deepening V_{SM} - this is controlled flocculation;

(b) flocculation produced by bridging, either by polymers or by metal ion - polyelectrolyte, ~~this~~ could also be called controlled flocculation; and

(c) primary minimum coagulation caused by addition of electrolyte or other charged species, the depth of the primary minimum being restricted by the steric effect of an added surface active agent or polymer - more correctly termed controlled coagulation.

The term "controlled flocculation" could with advantage be replaced by another such as "controlled aggregation".

Other workers who have used the techniques of microelectrophoresis to measure zeta potentials and assess pharmaceutical suspension stability include Stanko & Dekay (32) who examined sulphamerazine suspensions with methylcelluloses and alginates; Nash and Haeger (33) who studied silica dispersions with electrolytes and surface active agents; James and Goddard (34), (35) barium sulphate preparations, used as x-ray opaque media, in the presence of hydrophilic colloidal material; Uno and Tanaka

(36) who, in studying chloramphenicol suspensions, measured the adhesion of suspension particles on the wall surface of the container; Green and Hern (37) who examined the effect of washing with water on the physico-chemical properties of aluminium hydroxide gel; and Nakamura et al who have studied the effect of addition of ionic surfactants on the flocculation-deflocculation behaviour of sulphathiazole, α alumina and graphite suspensions (38).

1.3. Outline of present work

The importance of the use of surface active agents and more particularly the measurement of particle charge, in terms of the apparent zeta potential in pharmaceutical suspension formulation has thus been well established.

The effect that various surface active agents have on the zeta potential of particles in a suspension system is therefore of importance and worthy of investigation; Mathews and Rhodes (26) having demonstrated that comparisons may be made between coagulation in a model disperse system and in heterogenous drug suspensions, it was decided to choose a monodisperse polystyrene latex, the surface properties of which can be well characterized, as a model system. The effect various surface active agents, alone and as mixtures of ionic and nonionic, have on the electrophoretic mobility - and hence the zeta potential - of the latices, has been measured. An attempt has also been made to apply the results found with the model system by carrying out similar measurements with real drug suspension systems.

Any investigation into 'zeta potentials' and the effect of surface active materials as "steric stabilizers" requires a knowledge of:

- (a) Double layer phenomena and electrokinetics, and
 - (b) The effect of adsorbed layers on the stability of dispersions,
- these are discussed in the next section.

SECTION 2.

THEORY

2.1. The Electric Double Layer

Most solids, when in contact with an aqueous medium, acquire a surface electric charge. Possible charging mechanisms include:

(a) Ionization, controlled by the ionization of surface ionogenic groups, for example acidic groups at the surface of polystyrene latices, and is pH dependent. A particle may thus be positively charged at low pH and carry a negative charge at high pH; the pH at which electrophoretic mobility, and hence apparent zeta potential is zero is termed the iso-electric point. The iso-electric point may be more generally defined as the negative logarithm, to the base 10, of the concentration of potential determining ions when the zeta potential becomes equal to zero.

(b) Ion adsorption. A net surface charge can be acquired by the unequal adsorption of oppositely charged ions, which may be of positive or negative charge. Haydon (39) points out that the negative zeta potentials cannot in general be due to hydroxyl ion adsorption because the negative potentials occur principally because the cations are unable to approach the interface as closely as the anions i.e. it is not usually necessary to assume any adsorptive forces between the anion and the surface in order to explain qualitatively the negative zeta potentials. This situation is a general one and holds in various degrees for a number of simple 1:1 and 2:1 inorganic salts. In fact wherever there exists an appreciable area of solution/solid interface it is liable to acquire an apparent negative charge by this mechanism. The influence of hydrogen ions on the zeta potential of these surfaces can be explained qualitatively by an ion exchange mechanism controlled by the size of the hydrated ions.

(c) Ion dissolution, controlled by the difference between the thermodynamic potential between the solid and the solution, e.g. silver iodide.

This surface charge influences the distribution of nearby ions in the aqueous medium. Ions of opposite charge (counter ions) are attracted to the surface and ions of like charge (co-ions) are repelled away from the surface. This effect, together with the mixing tendency of thermal motion, leads to the formation of an electric double layer made up of the charged surface and a neutralising excess of counter ions over co-ions distributed in a diffuse manner in the aqueous medium.

The electric double layer can be regarded as consisting of two regions: an inner region which may include adsorbed ions, and a diffuse region in which ions are distributed according to the influence of electrical forces and random thermal motion as indicated above.

2.1.1. Diffuse double layer, Gouy-Chapman theory for flat surfaces

A theory of the diffuse double layer for infinite plane surfaces was developed independently by Gouy (40) and Chapman (41).

The charge on the solid is treated as a surface charge smeared out uniformly over the surface. The space charge in the solution is considered to be built up by unequal distribution of point-like ions. The solvent is treated as a continuous medium influencing the double layer only through its dielectric constant. It is assumed that the work required to bring an ion from the bulk of the solution to a point near the surface, is entirely due to the electrical potential differences between the initial and final positions. The ions in the solution are assumed to obey a Boltzmann distribution expressing that at places of positive potential the negative ions are concentrated and the positive ones are repelled, whereas for places of negative potential the reverse is the case.

$$n_i = n_0 \exp (-Z_i e \psi / kT)$$

2.1

where n_i is the concentration of ions of kind i at a point x where the

potential is ψ ; n_0 is the concentration in the bulk of the solution; z_i is the valency (sign of the charge included); e is the electronic charge; k the Boltzmann's constant; T the absolute temperature. The space charge density ρ (the net charge per unit volume at a point) is given by the algebraic sum of the ionic charges

$$\rho = \sum Z_i e n_i \quad 2.2$$

The relationship between the electrical potential and the space charge density ρ is given by the Poisson equation which, for variations in the x direction only, takes the form

$$\frac{d^2\psi}{dx^2} = -\frac{\rho}{\epsilon} \quad 2.3$$

where ϵ the dielectric constant of the solution is assumed not to vary with distance from the surface. Therefore combining equations 2.1, 2.2 and 2.3 we obtain the Poisson-Boltzmann equation

$$\frac{d^2\psi}{dx^2} = -\frac{1}{\epsilon} \sum Z_i e n_0 \exp(-Z_i e \psi/kT) \quad 2.4$$

A first integration of (2.4) can be made after multiplying both sides of the equation by $2 d\psi/dx$ to give

$$\left(\frac{d\psi}{dx}\right)^2 = \frac{2kT}{\epsilon} \sum n_0 (\exp(-Z_i e \psi/kT) - 1) \quad 2.5$$

where the condition that for $x \rightarrow \infty \psi \rightarrow 0$ and $\frac{d\psi}{dx} \rightarrow 0$ has been used.

If the case of a solution of a single symmetrical electrolyte, of valency z , is considered, then equation 2.5 can be considerably simplified, thus:

$$\begin{aligned} \frac{d\psi}{dx} &= -\sqrt{\frac{2nkT}{\epsilon}} (\exp(Ze\psi/2kT) - \exp(-Ze\psi/2kT)) \\ \text{or } \frac{d\psi}{dx} &= -\sqrt{\frac{8nkT}{\epsilon}} \sinh \frac{Ze\psi}{2kT} \end{aligned} \quad 2.6$$

From this equation a relation between the surface charge density, σ , and the surface potential, ψ_0 , can be established. The condition of electroneutrality of the total double layer requires that the surface

charge is oppositely equal to the total space charge in the solution

$$\sigma = - \int_0^{\infty} \rho \, dx \quad 2.7$$

using Poisson's equation, equation 2.7 can be integrated to give:

$$\sigma = + \int_0^{\infty} \epsilon \frac{d^2\psi}{dx^2} \, dx = - \epsilon \frac{d\psi}{dx} \quad (x = 0) \quad 2.8$$

inserting the value of $\frac{d\psi}{dx}$ from 2.6

$$\sigma = \sqrt{8nkT\epsilon} \sinh \frac{Ze\psi_0}{2kT} \quad 2.9$$

A second integration of equation 2.6 with the condition $\psi = \psi_0$ for $x=0$ gives

$$\kappa x = \ln \frac{(\exp(Ze\psi/2kT) + 1)(\exp(Ze\psi_0/2kT) - 1)}{(\exp(Ze\psi/2kT) - 1)(\exp(Ze\psi_0/2kT) + 1)} \quad 2.10$$

where κ is identical to the reciprocal length parameter of Debye-Hückel theory; i.e. for a symmetrical electrolyte

$$\kappa = \left(\frac{2 Z^2 e^2 n}{\epsilon kT} \right)^{1/2} \quad 2.11$$

At low potentials, if $Ze\psi_0/2kT \ll 1$, equations 2.9 and 2.10 can be simplified as under these conditions it is permissible to expand the exponential terms and neglect all but the first and second order terms in the resulting series. Equation 2.9 then becomes

$$\sigma = \sqrt{8nkT\epsilon} \frac{Ze\psi_0}{2kT} = \epsilon \sqrt{\frac{2nZ^2e^2}{\epsilon kT}} \psi_0 = \epsilon \kappa \psi_0 \quad 2.12$$

In this case charge and potential are proportional to each other and the double layer behaves as a flat condenser with a distance $1/\kappa$ between the plates.

Equation 2.10 reduces to

$$\kappa x = \ln \psi_0/\psi \quad \text{or} \quad \psi = \psi_0 \exp^{-\kappa x} \quad 2.13$$

showing that at low potentials the potential decreases exponentially over a distance of the order of magnitude $1/\kappa$. It is customary to refer

to $1/\kappa$ as the 'thickness' of the diffuse double layer. Close to the charged surface where the potential is relatively high, i.e. the approximation cannot be made, the potential is predicted by 2.10 to decrease at a greater than exponential rate. κ the reciprocal length parameter is dependent on concentration, c , of added electrolyte, through n , the number of ions, or

$$\kappa \propto \sqrt{n} \quad \propto \sqrt{c}$$

hence $1/\kappa$, "the double layer thickness", $\propto 1/\sqrt{c}$, increasing the concentration of added electrolyte means therefore that $1/\kappa$ "the double layer thickness" is reduced i.e. the double layer is being 'compressed'.

2.1.2. The double layer around a spherical particle (39)

The electrical potential ψ and the space charge density ρ in the solution surrounding a sphere are related by a form of the Poisson equation:

$$\frac{d^2\psi}{dx^2} = \frac{1}{r^2} \frac{d}{dr} \left(r^2 \frac{d\psi}{dx} \right) = - \frac{\rho}{\epsilon} \quad 2.14$$

where r is the distance from the centre of the particle and ϵ the dielectric constant of the surrounding solution; equation 2.5 then becomes

$$\frac{1}{r^2} \frac{d}{dr} \left(r^2 \frac{d\psi}{dr} \right) = - \frac{1}{\epsilon} \sum Z_i e n_0 \exp(-Ze\psi/kT) \quad 2.15$$

This equation cannot be integrated analytically without approximations. For values of ψ_0 sufficiently small for the first two terms only of the expanded exponential to be considered an expression for a sphere of radius, a , is obtained:

$$\psi(r) = \psi(a) \frac{a}{r} \exp \kappa(a - r) \quad 2.16$$

analogous to 2.13 and the surface charge density of the sphere can be shown to be

$$\sigma = - \frac{\epsilon}{a} \psi(a) (1 + \kappa a) \quad 2.17$$

analogous to 2.12.

For higher potentials it is necessary to solve equation 2.15 numerically and a most comprehensive set of results has been obtained by Loeb et al (42) who gave results for uni-univalent electrolytes for surface potentials of 25-400 mV and $Ka = 1$ to 20. The data are readily transformed to those for symmetrical electrolytes. Data for unsymmetrical electrolytes are also given. Their results are valuable in the field of electrophoresis for obtaining zeta potential values from electrophoretic mobility measurements.

2.1.3. The inner part of the Double Layer

The Gouy-Chapman theory assumes that the ions behave as point charges in the electrolyte medium. The theory of Stern (43) extends this double layer theory by the introduction of two modifications. One of these, concerned with ion size, is essentially a correction and takes into account the fact that ions of finite size cannot approach more closely to the surface than a distance equal to their effective radius (the ion may or may not be hydrated). But the other is a new concept which recognises that at short distances from the surface there may exist a specific 'chemical' interaction between the ions and the surface i.e. the ions may become specifically adsorbed. The definition of specific adsorption is usually given as the adsorption which occurs when the electrostatic potential is zero (39). The energies involved are thus best regarded as chemical by nature. It is usually considered that the chemical interaction energy of adsorption of a specifically adsorbed ion is sufficient to cause it to lose part of its water of hydration.

Stern proposed a model in which the double layer is divided into two parts separated by a plane (the Stern plane) located at about an effective ion radius from the surface. The centres of any specifically adsorbed ions are located in the Stern layer, i.e. between the surface

and the Stern plane. Ions with centres beyond the Stern plane form the diffuse part of the double layer for which the Gouy-Chapman treatment with ψ_0 replaced by ψ_δ (the potential at the Stern plane) is considered to be applicable. The potential changes from ψ_0 at the particle surface to ψ_δ (the Stern potential) in the Stern layer and decays from ψ_δ to zero in the diffuse double layer.

Stern assumed that a Langmuir type adsorption isotherm could be used to describe the equilibrium between ions adsorbed in the Stern layer and those in the diffuse part of the double layer. The adsorption energy of ions of kind i , is considered to be composed of two parts, a purely electrical term ($-z_i e \psi_\delta$) and a chemical potential (ϕ_i) independent of the electrical circumstances.

The surface charge density σ_1 of the Stern layer is given by

$$\sigma_1 = \frac{N_1 z_+ e}{1 + \frac{N}{n_+ M} \exp + \left(\frac{z_+ e \psi_\delta + \phi_+}{kT} \right)} - \frac{N_1 z_- e}{1 + \frac{N}{n_- M} \exp - \left(\frac{z_- e \psi_\delta - \phi_-}{kT} \right)} \quad 2.18$$

where N_1 is the available number of adsorption sites per cm^2 . N is Avogadro's number, and M the molecular weight of the solvent. In practice usually only one of the terms in equation 2.18 needs to be considered because either the positive or the negative ions are completely expelled from the molecular condenser. The equation then becomes:-

$$\sigma_1 = \frac{N_1 z_i e}{1 + \frac{N}{n_i M} \exp \left(\frac{z_i e \psi_\delta + \phi}{kT} \right)} \quad 2.19$$

Treating the Stern layer as a molecular condenser of thickness δ and with a dielectric constant ϵ'

$$\sigma_0 = \frac{\epsilon'}{\delta} (\psi_0 - \psi_\delta) \quad 2.20$$

where σ_0 is the charge density at the particle surface. For overall electrical neutrality throughout the whole of the double layer

$$\sigma_0 + \sigma_1 + \sigma_2 = 0 \quad 2.21$$

where σ_2 is the surface charge density of the diffuse part of the double layer and is given by equation 2.9 with the sign reversed and with ψ_0 replaced by ψ_δ .

Substituting from equations 2.20, 2.19 and 2.9 into 2.21 gives a complete expression for the Stern model of the double layer

$$\frac{\epsilon'}{\delta} (\psi_0 - \psi_\delta) + \frac{N_1 z_i e}{1 + \frac{N}{n_1 M}} \exp\left(\frac{Ze\psi_\delta + \phi}{kT}\right) - (8nkT\epsilon)^{1/2} \sinh\left(\frac{Ze\psi_\delta}{2kT}\right) = 0 \quad 2.22$$

This expression contains a number of unknown quantities; information about these can be derived from other sources and will be discussed elsewhere. The use of the Stern model as a basis for the interpretation of adsorption of surface active agents is developed in Section 2.4.5.

Grahame (44) proposed modifications to the Stern treatment by taking into account that in the Stern layer there may be these two types of ion, one of which is specifically adsorbed, whereas the other, which may be hydrated, is localised only by the electrostatic force at its distance of closest approach to the surface. In Grahame's model the specifically adsorbed ion is assumed to lose some of its water of hydration and to be closer to the surface than the other ion. The concept of a single layer of ions with their centres all in one plane, must then be replaced by a model which consists of two parallel planes at different potentials, one associated with each type of ion. These two layers are usually called INNER and OUTER Helmholtz Layers.

2.1.4. Discreteness of charge effect

Both the Gouy-Chapman and the Stern treatments of the double layer assume a uniformly charged surface. The surface charge, however, is not smeared out but is located at discrete sites on the surface. The adsorbed ion does not experience the potential which would have characterized its adsorption site before the ion was adsorbed. The space

around the adsorption site must be cleared of all charge before the ion is placed on it and so the potential at the centre of this 'hole' is smaller, in absolute value, than the average potential before adsorption occurs. The effect, first introduced by Esin & Markov, has been discussed by Haydon (39). Grahame (see (39)) claimed that the energy required to rearrange the existing ions to make room for the incoming ion is negligible and so the important problem was the calculation of the potential in the hole.

The incorporation of the discreteness of charge effect into the Stern adsorption isotherm has been accomplished by Levine et al (45) who show that it is able to explain a number of previously puzzling features of colloid behaviour.

Equation 2.19 then becomes

$$\sigma_1 = \frac{N_1 z_i e}{1 + \frac{N}{n_i M}} \exp \left(\frac{z_i e (\psi_\delta + \phi_\beta) + \phi}{kT} \right) \quad 2.23$$

where ϕ_β is the potential correction for the discreteness of charge effect. The main consequence of including this term is that the theory now predicts that, under suitable conditions, ψ_δ goes through a maximum as ψ_0 is increased. The discreteness of charge effect explains, therefore, the experimental observations that zeta potentials for sols such as silver iodide go through a maximum as the surface potential is increased. Wiese et al (46) have recently invoked the theory to explain similar effects for the adsorption of 2:2 and 3:3 electrolytes on silica.

2.1.5. The corrections to the Poisson Boltzmann Equation

The assumption has been made that the potential in the diffuse part of the double layer can be reasonably well represented by the solution of the Poisson Boltzmann equation as suggested by Gouy and Chapman. Haydon (39), in a review, has shown that this is generally

true for at least 1:1 electrolytes at concentrations below 10^{-2} mol dm⁻³. For higher concentrations and valencies certain corrections become significant but in these regions the more sophisticated treatments become very complicated. The work of Levine and Bell (47) indicates that one must take all of the relevant corrections into account simultaneously (volume of ions, variation in dielectric constant, ion self atmosphere effects and electrostriction) since they tend, to a considerable extent to balance one another out. Their calculations show that the effect of taking the corrections into account is not likely to be significant for electrolyte concentrations of 10^{-1} mol dm⁻³ or less. At higher concentrations the Debye-Hückel reciprocal length is less than 1nm (in aqueous solution at 25°C) and it is arguable whether such double layers can be considered diffuse.

Detailed discussions of the effects of the corrections are contained in the reviews by Hayden (39) and by Macdonald and Barlow (48). From these works it seems reasonable to assume that in almost all of the situations of interest to colloid scientists the simple Gouy-Chapman theory is adequate to describe the potential in the region outside the Outer-Helmholtz plane for 1:1 electrolytes (47) (44). For higher valency types the corrections are so large and so uncertain that it is doubtful whether any useful purpose is served by using the present theory (49).

2.1.6. The interaction of two overlapping diffuse layers

Consider two flat surfaces each of identical surface potential ψ_0 and at a distance H_0 apart. Assume that the double layers are diffuse and that the potentials can be added (principle of linear superposition). The potential at the mid plane (d) between the two surfaces is ψ_d .

Langmuir (50) was able to show that the pressure P acting between

the two surfaces as they approach one another is

$$P = 2nkT (\cosh u - 1) \quad 2.24$$

where $u = ze\psi_d/kT$ and n the number of ions per unit volume. $\cosh u$ is always ≥ 1 so that the pressure is always repulsive.

The potential mid-way between the plates as expressed by u is related to the plate distance $H_0 = 2d$, by the expression

$$\frac{KH_0}{2} = \int_u^z \frac{dy}{\sqrt{2 \cosh y - 2 \cosh u}} \quad 2.25$$

where $Y = \frac{Ze\psi}{kT}$; $Z = \frac{Ze\psi_0}{kT}$; $u = \frac{Ze\psi d}{kT}$

To convert pressure into repulsive energy, V_R , use is made of the expression

$$\begin{aligned} V_R &= - \int P dH_0 \\ &= - \int 2nkT (\cosh u - 1) dH_0 \end{aligned} \quad 2.26$$

there is no analytical method for complete solution of these integral equations but numerical solutions have been given by Verwey & Overbeek

(3). A simple approximation for the condition of weak interaction can be made, with the restrictions $KH_0 > 2$, i.e. the surfaces cannot be closer together than $2/K$ and $u < 1$.

Then $u = 8 \gamma \exp - \frac{KH_0}{2} \quad 2.27$

where $\gamma = \frac{\exp (Ze\psi_0/2kT) - 1}{\exp (Ze\psi_0/2kT) + 1} \quad 2.28$

combining equations 2.24 and 2.28, for unit area of each surface,

$$P = 64nkT\gamma^2 \exp^{-KH_0} \quad 2.29$$

hence

$$\begin{aligned} V_R &= \int_{\infty}^{\frac{H_0}{2}} 64nkT\gamma^2 \exp^{-KH_0} dH \\ &= \frac{64nkT\gamma^2 \exp^{-KH_0}}{K} \end{aligned} \quad 2.30$$

The repulsive energy is therefore, through γ , a function of the surface potential Ψ_0 . A measure of this can be obtained from the potential at the Stern layer Ψ_δ , for which the zeta potential is usually a valid approximation, see for example Watillon and Joseph-Petit (51). In the case of interaction between spherical particles, for high potentials and short distances the situation is complex, requiring numerical integration of the Poisson-Boltzmann equation, see for example Loeb et al (42).

For small potentials a number of useful approximations exist:

- (a) Spheres of same radius (a) and same potential Ψ_0

$$\text{for } \kappa a > 10 \quad V_R = \frac{\epsilon \alpha \psi_0^2}{2} \ln (1 + \exp^{-\kappa H_0}) \quad 2.31$$

holds for ψ_0 ca \leq 50 mV

- (b) Spheres of radii a_1 and a_2 , potentials Ψ_{01} and Ψ_{02}

for $\kappa a > 10$

$$V_R = \frac{\sum a_1 a_2}{4(a_1 + a_2)} \left(\psi_{10}^2 + \psi_{20}^2 \right) \left[\frac{2\psi_{10} \psi_{20}}{\psi_{10} + \psi_{20}} \ln \frac{1 + \exp^{-\kappa H_0}}{1 - \exp^{-\kappa H_0}} + \ln (1 - \exp^{-2\kappa H_0}) \right] \quad 2.32$$

see Hogg et al (52)

- (c) Spheres radii a_1 and a_2 and potential Ψ_0

$$V_R = \frac{\epsilon a_1 a_2 \psi_0^2}{(a_1 + a_2)} \ln (1 + \exp^{-\kappa H_0}) \quad 2.33$$

Any of these situations is possible with suspensions of pharmaceutical particles.

A number of other approximations can be made and these have been summarised by Honig & Mul (53)

2.2 Attraction between particles

The concept of interaction between molecules was introduced by van der Waals in 1893 see, for example Glasstone (54). It was clear, from experimental work at that time, that the ideal gas laws did not account

for the behaviour of real gases, except at very low pressures. van der Waals suggested that intermolecular interactions were in part responsible for the observed deviations from ideality.

Three types of such intermolecular attraction are recognised:-

(a) Two molecules with permanent dipoles mutually orientate one another in such a way that, on average, attraction results, first postulated by Keesom (55). For two molecules with dipole moments μ_1 and μ_2

$$V_K = - \frac{2\mu_1^2 \mu_2^2}{3kT r^6} \quad 2.34$$

where r is the distance of separation.

(b) Dipolar molecules induce dipoles in other molecules so that attraction results, Debye (56)

$$V_D = - \frac{\alpha_1 \mu_2^2 + \alpha_2 \mu_1^2}{r^6} \quad 2.35$$

where α_1 & α_2 are the polarisabilities of molecules 1 & 2.

(c) Attractive forces are also operative between non-polar molecules, as is evident from the liquefaction of hydrogen, helium etc. These universal attractive forces (known as dispersion forces) were first explained by London (57) and are due to the polarisation of one molecule by fluctuations in the charge distribution in a second molecule. The energy of attraction, for hydrogen like atoms, from the London theory is given by:-

$$V_L = - 3/4 \frac{h \nu_0 \alpha^2}{r^6} \quad 2.36$$

where ν_0 is the characteristic oscillatory frequency of an electron and h is Planck's constant.

London pointed out that, for dilute gases, the molecular dispersion force is additive. It is thus to be expected that an attraction can occur between condensed bodies containing many atoms, provided that some additivity is retained in dense media. Kallman and Wilstatter (58) have

suggested that such an attraction could lead to long range attraction and hence play a part in the coagulation of colloids. This, and the phenomena of adhesion and adsorption suggest that an attraction between condensed objects does exist.

2.2.1. The de Boer-Hamaker Microscopic Theory of attraction between condensed objects

Following on the idea of attractive forces between condensed objects, it was further suggested by Kallman and Willstatter that the attractive forces could be quantified by integrating the van der Waal's attraction between their constituent atoms or molecules. Although the attractive energy between two molecules is very short range, varying inversely with the sixth power of the intermolecular distance, it was shown by de Boer (59) and Hamaker (60) that the total interaction energy, between two flat surfaces of infinite thickness, V_A , was given by

$$V_A = - \frac{\pi^2 q^2 3/4 h \nu \alpha^2}{12 \pi H_0^2} = \frac{-A}{12 \pi H_0^2} \quad 2.37$$

where A is the HAMAKER Constant, with the value shown, and q the number of atoms per unit volume. The force of attraction, F_A , per unit area is given by

$$F_A = - \frac{A}{6 \pi H_0^3} \quad 2.38$$

Hamaker further derived the attractive interaction between two spheres, radius a_1 and a_2 :

$$V_A = - \frac{A}{12} \left[\frac{y}{x^2 + xy + x} + \frac{y}{x^2 + xy + x + y} + 2 \ln \frac{x^2 + xy + x}{x^2 + xy + x + y} \right] \quad 2.39$$

where $x = \frac{H_0}{2a_1}$ and $y = \frac{a_2}{a_1}$

if $x \ll 1$, i.e. the case where $H_0 < 2a_1$, then,

$$V_A = \frac{-A a_1 a_2}{6 H_0 (a_1 + a_2)} \quad 2.40$$

For two spheres of the same radius, a , an analogous approximation is:

$$V_A = \frac{-Aa}{12H_0} \quad 2.41$$

this expression is valid for large particles, i.e. including those of pharmaceutical interest.

2.2.2. The effect of the liquid medium on the attractive forces between particles

The above expressions were obtained for interactions in a vacuum; for two particles in a liquid medium interaction will only take place if the medium has material properties which are different to those of the particles. Hamaker suggested that the interaction can be deduced from the in vacuo Hamaker constants for the particles and the medium, the effective constant being:

$$A_H = A_1 + A_2 - 2A_{12} \quad 2.42$$

and for similar materials assuming a geometric mean relationship:

$$A_{12} = (A_{11} A_{22})^{1/2} \quad 2.43$$

and

$$A_H = (A_{11}^{1/2} - A_{22}^{1/2})^2 \quad 2.44$$

where A_{11} and A_{22} are the constants calculated on the basis of interactions between pairs of atoms of those materials.

The various methods of calculating Hamaker constants have been reviewed by Gregory (61) and selected values are given by Visser (62).

2.2.3. Electromagnetic retardation

The expression for attraction energy, equation 2.41,

$$V_A = \frac{-Aa}{12H_0}$$

is not valid when the London forces operate over distances comparable with, or larger than, $0.1\lambda_0$ where λ_0 is the wavelength of intrinsic oscillations of the atoms. This is due to the "retardation effect" which is caused by the finite time necessary for electromagnetic waves to

travel from one atom to the other atom in which it is inducing a dipole. Under these conditions, the force of attraction is given by

$$F_A = \frac{B}{H_0^4}$$

where B is the retarded Hamaker constant; its relation to A is given by $B = 1.24 \times 10^{-2} A \lambda_0$. Hence under retarded conditions the force of attraction between two plates is inversely proportional to the fourth power of the separation distance, compared with the third power in the non-retarded region (63).

Schenkel and Kitchener (18) have analysed the retardation effect and have derived empirical equations which enable attractive energies to be calculated allowing for this effect. These may be applied to coarse suspensions. The equation for the fully retarded situation is

$$V_A = \frac{-2.45 A a \lambda_0}{120 \pi H_0^2} \quad 2.45$$

where A is the Hamaker constant describing the attraction between two similar particles in a given medium. This equation is used for particle separations greater than 15nm.

2.2.4. The Lifschitz Macroscopic Theory of attraction between condensed objects

The macroscopic approach of Lifschitz (64) treats the interacting phases as being continuous and the interaction as occurring through a continuous medium. For small distances of separation between the surfaces of flat plates, $H_0 \leq \lambda_0 / 2\pi$, the force of non retarded attraction is given by

$$F_A = \frac{\bar{h}\omega}{16\pi^3 H_0^3} \quad 2.46$$

In this equation, if the plates are of material 1 interacting in a vacuum then

$$\bar{\omega} = \int_0^\infty \left(\frac{\epsilon_1 - 1}{\epsilon_1 + 1} \right)^2 d\epsilon \quad 2.47$$

and for plates of material 1 and 3 interacting in a medium 2

$$\bar{w} = \int_0^{\infty} \left(\frac{\epsilon_1 - \epsilon_2}{\epsilon_1 + \epsilon_2} \right) \left(\frac{\epsilon_3 - \epsilon_2}{\epsilon_3 + \epsilon_2} \right) d\epsilon \quad 2.48$$

These expressions contain the permittivity, ϵ , as a function of the frequency of the field. The calculation of an interaction constant, therefore, requires considerably more data than those needed to calculate a Hamaker constant. Recently the work of Ninham and Parsegian et al (65), (66) has shown that the use of the London- de Boer-Hamaker theory is restricted by a number of assumptions:-

- (1) of pairwise additivity of individual interatomic interactions in condensed media;
- (2) the approximation that the contributions centred around a single dominant frequency of the electromagnetic spectrum are the only important ones; and
- (3) that the insertion of material between the plates, such as a liquid, can be dealt with by the insertion of an arbitrary dielectric constant at a single frequency.

They conclude (67) that:-

- (1) because of the highly polar nature of liquid water much of the van der Waals force in this medium comes from polarization at infra-red and microwave frequencies rather than the ultra-violet;
- (2) it is incorrect to think of the van der Waals force between liquid layers as being the sum of individual interactions between unit segments of the constituent materials.
- (3) by virtue of the low frequency contribution, the van der Waals force also contains a temperature dependent component.
- (4) dielectric data are often well enough known through the range of frequencies to draw these conclusions and to make quantitative numerical estimates with little ambiguity.

Ninham and Parsegian (68) argue that forces which arise from electromagnetic fluctuations should be called by the general name of "van der Waals interactions". In addition, they suggest that the temperature independent part should be called a 'dispersion force' and the remainder or temperature-dependent part a 'molecular force'. Thus, for example, there is a large long-range van der Waals contribution from the molecular interactions of the permanent dipoles in liquid water. This occurs essentially at zero frequencies and increases almost linearly with temperature.

From Lifshitz theory the potential energy of interaction between two semi-infinite plates of material 1 separated by a medium 2 is given by:

$$V_A = - \frac{A_L}{12 \pi H_0^2} \quad 2.49$$

which can be compared with equation 2.37. Here A_L , which is also a function of the distance of surface separation H_0 , and temperature T , is obtained from:

$$A_L = 1.5 kT \sum_{n=0}^{\infty} I' (\epsilon_n H_0) \quad 2.50$$

where I is a function of permittivity and distance. The prime on the summation sign indicates that the $n = 0$ term must be multiplied by $\frac{1}{2}$. Langbein (69), (70) has derived expressions for use with spheres.

The correctness of the new approach can be gauged by its prediction of a value of an effective Hamaker constant, A_L , for the n decane triple film, of $5.5-6.1 \times 10^{-21}$ J when experiment suggests a value of 5.6×10^{-21} J, whereas pairwise summation of the London dispersion forces predicts a value of A_H of 0.9×10^{-21} J (71).

The idea that the attractive and repulsive interactions are completely separable in colloid systems must be applied with caution. Because the

nature of the dispersion medium profoundly affects the van der Waals attraction - Ninham and Parsegian (67) have shown that the presence of water profoundly reduces the attraction and indicate the difficulty in accurately allowing for its presence - any changes in the intervening liquid, designed to alter the repulsive component, may also influence the attraction. The effect may be small for some electrostatic systems but may be quite large for some sterically stabilized dispersions.

2.3. The effect of adsorbed layers on the stability of dispersions

The adsorbed layer can effect stability in three main ways:

(a) by increasing or decreasing the charge on the particles, thus affecting V_R .

(b) by sterically hindering the approach of the particles, giving V_S .

(c) by altering the value of the Hamaker constant, thus affecting V_A .

2.3.1. The effect of the adsorbed layer on the Stern potential Ψ_δ

Adsorption of ionic surface active compounds, such as sodium dodecyl sulphate or dodecyl trimethyl ammonium bromide, onto particles in an aqueous dispersion, can significantly alter the Stern potential Ψ_δ . Such adsorption is likely to occur when there are more adsorption sites on the particle surface than the number of potential determining groups originally present, as was found by, for example, Ottewill et al (see 39) with silver iodide. Large areas for adsorption of surface active agents by hydrophobic bonding are available with the materials now studied, as is shown in Section 3 on the characterisation of polystyrene latex.

It is possible with surface active counter ions for reversal of charge to take place within the Stern layer i.e. for Ψ_0 and Ψ_δ to have opposite signs; with the polystyrene latex, used in the work, which carries a negative charge due to ionization of $-COOH$ groups, an adsorbed

layer of dodecyl trimethyl ammonium bromide effectively reverses the charge. On the other hand adsorption of a surface active co-ion, for example sodium dodecyl sulphate on polystyrene latex, has the effect of increasing Ψ_0 .

2.3.2. Steric Stabilization

The term steric stabilization was probably first used by Heller and Pugh (72) to denote the fact that uncharged particles can be prevented from coagulating by the adsorption of nonionic polymer molecules. The classical description 'protective' action is also employed (73).

Knowledge of the forces which can lead to short range repulsion is uncertain, however, Barclay and Ottewill (74) have shown that steric stabilization forces are of shorter range than electrostatic and van der Waals forces and that the force increases very rapidly with decrease of distance; this latter fact is supported by the work of Krieger (75) and the theoretical approach of Bagchi (76).

In writing the total energy of interaction as

$$V = V_R + V_A + V_S \quad 2.51$$

where all steric and solvation terms are put together in the term V_S , the position for the origin of the energy terms on the distance axis is not always clear. For example, in the case of V_R and V_A either both interactions can be assumed to emanate from the particle surface or the origin of the van der Waals interaction can be taken as the surface and the origin of the electrical interaction as the Stern layer. Once the particle has an adsorbed layer, however, this can also affect the position of the Stern layer and the thickness of the adsorbed layer may well have to be taken into account in calculating the van der Waals interactions, see for example the work of Vincent et al (77) and the discussion of this problem later on in this thesis; interpenetration

of the adsorbed layers may also occur.

The stability of lyophobic aqueous dispersions to coagulation by electrolytes has been shown to be enhanced by the use of nonionic surface active agents (78), (79) and macromolecules (80). Mathews and Rhodes (26) found the same effect with pharmaceutical suspensions.

Since uncharged colloidal particles coated by nonionic surface active agents or polymers exhibit stability there must exist a repulsive potential barrier between two such particles. This barrier counterbalances the van der Waals attraction between the core particles.

Repulsion is characterised by the change in the Gibbs ~~free~~^{free} energy, ΔG_s , of the particles on close approach. The second law of thermodynamics implies that a positive value of ΔG_s is necessary for stability and Napper (81) has pointed out that since ΔG_s can be written as

$$\Delta G_s = \Delta H_s - T\Delta S_s \quad 2.52$$

three ways of obtaining a positive value for ΔG_s can occur:-

(a) if ΔH_s and ΔS_s are both negative but $T\Delta S_s > \Delta H_s$, then ΔG_s will be positive. The effect of the entropy change opposes flocculation and outweighs the enthalpy term, hence it was suggested that this should be called entropic stabilization. Since $-T\Delta S$ usually decreases in magnitude with decreasing temperature, on reduction of the temperature to the θ temperature the enthalpy and entropy would become equal and flocculation would occur. Thus entropically stabilized dispersions are characterized by a flocculation process which would occur on cooling.

(b) if both ΔH_s and ΔS_s are positive and $\Delta H_s > T\Delta S_s$ then a positive value for ΔG_s results, or enthalpy aids stabilization and entropy aids flocculation. This has been termed enthalpic stabilization. On heating $T\Delta S_s$ should normally increase more rapidly than ΔH_s and hence flocculation should occur.

(c) both the enthalpy and entropy changes oppose flocculation if ΔH_s

is positive and ΔS_s is negative. Dispersions stabilized by this combined enthalpic-entropic mechanism cannot in principle be flocculated at any accessible temperature.

The above classification implies that the generic term steric stabilization encompasses entropic, enthalpic and combined enthalpic-entropic stabilization. It appears that enthalpic effects are probably more important in the stabilization of aqueous dispersions and entropic contributions more important in the stabilization of non aqueous systems.

The classical thermodynamic approach outlined above is independent of any molecular models that might be advanced to describe how ΔG_s arises. It therefore provides little information on how ΔG_s is generated nor does it permit theoretical estimation of its magnitude.

There have been a number of attempts to calculate by statistical thermodynamics the actual magnitude of ΔG_s . This is of course a model dependent procedure. The usual model examined consists of polymer chains irreversibly attached to the particles. The chains project into, and are dissolved by, the dispersion medium (which may also be termed the solvent).

Mackor (82) was the first to attempt to calculate the repulsive potential energy in steric stabilization. He argued that the close approach of two colloidal particles resulted in a decrease in the volume accessible to the stabilizing moieties and thus to a decrease in the configurational entropy, ΔS_{conf} , of the stabilizing chains. The magnitude of ΔG_s was calculated solely in terms of this loss in configurational entropy. Clayfield and Lumb (83) using essentially this approach, performed elaborate calculations for stabilizing polymer chains to find ΔS_{conf} and hence ΔG_s .

It is clear that calculations of this type ignore the presence of any molecules of the solvent that are associated with the chains. The macromolecules alone are assumed to contribute to ΔS_{conf} . This approach

implies that a stable dispersion once formed, cannot be flocculated merely by changing the solvency of the dispersion medium. However Napper et al (see 83) have produced compelling experimental evidence to show that the solvency of the dispersion medium critically determines the stability of sterically stabilized dispersions. The same workers have put forward thermodynamic arguments which imply that those dispersions that flocculate on heating (e.g. many aqueous latices) are enthalpically stabilized, not entropically stabilized. Mackors approach ignores all enthalpy changes.

The critical nature of the solvent properties of the dispersion medium in steric stabilization was first realised by Fischer (84). According to Fischer's theory, if the dissolved polymer sheaths surrounding two sterically stabilized particles were to interpenetrate, the chemical potential of the solvent in the interaction zone would decrease. A gradient in chemical potential would thus be established between the solvent molecules in the interaction zone and those in the external dispersion medium. As a result solvent external to the interaction zone would diffuse into the zone and so force the stabilizing moieties, and the particles, apart. This corresponds to the generation of an excess osmotic pressure. Fischer related the repulsive potential energy to the second virial coefficient(B) of the polymer in free solution using the Flory-Huggins theory (85)

$$\Delta G_S \approx 2BRT \langle C_g \rangle (\Delta V) \quad 2.53$$

where $\langle C_g \rangle$ is the mean segment concentration and (ΔV) is the overlap volume.

According to equation 2.53, a repulsive potential is generated in a dispersion medium of good solvency for the polymer chains because B is positive. In contrast, in a bad solvent, B is negative and the particles are sensitised to flocculation. An interesting case is that

of a theta (Θ) solvent in which the polymer chains can interpenetrate one another without prejudice because B and therefore ΔG_s is zero.

Ottewill and Walker (78) have shown how to express Fischer's formula in terms of ^{an}enthalpy ^{term}, X , which characterized the interaction of the stabilizing group with the solvent, and an entropy of mixing term, Ψ , for the stabilizing layers. They determined the thickness of the adsorbed layer of dodecylhexaoxyethylene glycol monoether on polystyrene latex particles and found it to be ca. 5 nm, just greater than the length of the extended molecule, they estimated that the concentration of water in the adsorbed layer was 0.74 g cm^{-3} indicating the importance of solvation. They then showed theoretically that the free energy of interaction ΔG_s arising from nonionic interactions for two spheres of radius, a , depended on the thickness of the adsorbed layer, d , the distance H_0 between the basic particle surfaces and the thermodynamic terms, X and Ψ .

The expression obtained was

$$\Delta G_s = V_s = \frac{4kT\pi C^2}{3\bar{V}_1 \rho_2^2} (\psi - \chi) \left(d - \frac{H_0}{2}\right)^2 \left(3a + 2d + \frac{H_0}{2}\right) \quad 2.54$$

where \bar{V}_1 is the molecular volume of the solvent molecules and ρ_2 the density of the adsorbed film. Several important criticisms of Fischer's theory may be raised: first, the use of a mean segment concentration is obviously an approximation because the segment density is a function of the distance from the particle surface; second, Fischer's theory by concentrating on interpenetration tends to ignore the compression of the polymer chains that must occur when the minimum distance between the particle surfaces is less than the contour length of the polymer chains. The theory also disregards all virial coefficients higher than the second. However despite these quantitative shortcomings, Fischer's

theory predicts all the qualitative features of flocculation that have been observed by Napper et al (see 83).

The assumption that a mean segment density may be used in calculating the repulsion is undoubtedly an approximation. It corresponds to approximating the segment density by a step function. The density distribution function relevant to a polymer chain attached to an impenetrable interface is in fact required. Fischer's work has now been extended by papers which examine the latter point, by Hesselink, following Clayfield & Lumb, Meier and Hesselink, Vrij and Overbeek (86). Napper & Evans (83) have compared the qualitative predictions of the various theories of steric stabilization with the results of experiments. They have shown that, with the exception of Fischer's solvency theory, all of the theories advanced to date are at odds with results of experiments.

The same workers (87) have developed a theory of steric stabilization that is essentially an extension of Fischer's solvency theory. It treats both interpenetrations and compression using a lattice approach. This permits the introduction of segment density distribution functions. The theory, although with limitations, is in good qualitative agreement with the results of experiment. Bagchi (76) has similarly approached the problem theoretically from a consideration of interpenetrations (which he terms mixing) and compression (which he terms denting) and obtained agreement for this theory with the experimental observations of Napper.

2.3.3. The van der Waals attraction between colloid particles having adsorbed layers

The effect of solvation sheaths, and of adsorbed layers of varying Hamaker constant, on the van der Waals attraction between spherical colloid particles has been considered by Vold (88) and re-evaluated by

Vincent et al (77).

Vold showed that solvation sheaths always lead to a decrease in attraction, but that the effect is only appreciable in the case of very small particles < 50nm, or thick sheaths > 2nm. She also concluded that in the case of adsorbed layers, the attraction was further decreased if the Hamaker constant of the adsorbed layer was not the same as, but slightly different from, that of the medium. Vincent et al have queried Vold's final conclusion concerning the actual sequence of the Hamaker constants necessary to produce this further decrease in attraction. They presented a formal analysis of the conditions necessary to produce maximum effects, determined the conditions under which the presence of adsorbed layers leads to a net increase in attraction, and considered, in greater detail than Vold had done, the case of double sheaths - the latter are relevant in the case of adsorbed surface active agents. They showed that certain values of the Hamaker constant can in fact lead to a reduction in the attraction (over and above that of the simple increase increase in core spacing effect) which is no longer trivial.

Ottewill and Walker (79) used a number of models when considering the stability of polystyrene latices with an adsorbed layer of n dodecyl hexaoxyethylene glycol monoether. The basic expression, derived by Vold, they used for calculating the van der Waal's potential energy of attraction was

$$V_A = -\frac{1}{12} \left\{ (A_M^{\frac{1}{2}} - A_S^{\frac{1}{2}})^2 H_S + (A_S^{\frac{1}{2}} - A_P^{\frac{1}{2}})^2 H_P + 2(A_M^{\frac{1}{2}} - A_S^{\frac{1}{2}})(A_S^{\frac{1}{2}} - A_P^{\frac{1}{2}}) H_{PS} \right\} \quad 2.55$$

where A is the Hamaker constant of the medium, adsorbed layer and the particle as designated by the subscripts, M, S, and P respectively. The function H is given by,

$$H(x,y) = \frac{y}{x^2 + xy + x} + \frac{y}{x^2 + xy + x + y} + 2 \ln \left[\frac{x^2 + xy + x}{x^2 + xy + x + y} \right] \quad 2.56$$

for the interaction between two spheres of unequal radii. In Hamaker's original work x is the distance of surface separation/radius of particle 1 and y is the radius of particle 2/radius of particle 1. Thus if Δ is taken as the distance between the surfaces of the adsorbed layers on the particle the values of H_S , H_{PS} and H_P have x and y values as follows:

$$H_S: \quad x = \frac{\Delta}{2(a+\delta)}, \quad y = 1,$$

$$H_{PS}: \quad x = \frac{\Delta+\delta}{2a}, \quad y = \frac{a+\delta}{a}$$

$$H_P: \quad x = \frac{\Delta+2\delta}{2a}, \quad y = 1.$$

In the limit, as $x \rightarrow 0$, eqn (256) approximates to,

$$H(x,y)_{x \rightarrow 0} = \frac{y}{x(1+y)} \quad 2.57$$

a is the particle radius and δ the thickness of the adsorbed layer, this approach is further discussed and used in calculating V_A in Section 6.

2.3.4. Combined effects of steric stabilization and electrostatic repulsion on the stability of dispersions

In an extension of their work on steric stabilization Napper and Netschey (89) studied the combined effects of steric stabilization and electrostatic repulsion; once the electrical double layer had been compressed, the particle remained sterically stabilized and the flocculation concentrations obtained were those of the sterically stabilized dispersions.

However, in the case of weakly anchored stabilizing molecules, flocculation occurred in the presence of hydrolysed cations owing to the displacement of the stabilizer by the hydrolysed species. This was in agreement with the work of Mathai and Ottewill (90) who came to

similar conclusions after studying the flocculation by hydrolysed cations of silver iodide sols stabilized by nonionic surface active agents.

The importance of a combination of electrostatic factors and steric stabilisation on the stability of pharmaceutical suspensions was investigated by Mathews and Rhodes (20) using, as surface active agents, salts of dioxyethylated dodecyl sulphate in conjunction with particles of sulphamerazine, hydrocortisone and griseofulvin. Their results were interpreted, including the effect of particle size, using equation 2.54 to calculate the energy of interaction due to steric effects; qualitatively, the experimental results were found to be in agreement with those expected theoretically.

2.4. Electrophoresis

Electrophoresis, the movement of a charged surface plus attached material relative to a stationary liquid by an applied electric field, is one of four related electrokinetic phenomena arising from the relative tangential motion between charged phases. The others that can be distinguished are:

- (a) electro-osmosis - the movement of liquid relative to a stationary charged surface by an applied electric field;
- (b) streaming potential - the electric field which is generated when liquid is made to flow along a stationary charged surface; and
- (c) sedimentation potential - the electric field produced when charged particles move relative to stationary liquid.

The electric potential yielded by any of the electrokinetic phenomena is referred to as the electrokinetic or zeta (ζ) potential, which is defined as the potential at the surface or plane of shear, between the phases in relative motion. The exact location of the shear plane (which, in reality is a region of rapidly changing viscosity) is an unknown feature of the electric double layer. In addition to ions in the Stern layer, a

certain amount of solvent will probably be bound to the charged surface and form a part of the electrokinetic unit. It is, therefore, reasonable to suppose that the shear plane is located no more than a small distance further out from the surface than the Stern plane and that the zeta potential is, in general, marginally smaller in magnitude than ψ_δ . In calculations involving double layer theory it is usual to assume identity of ψ_δ and ζ , and the bulk of experimental evidence suggests that errors introduced through this assumption are generally small especially at lyophobic surfaces. Any differences between ψ_δ and ζ will be most pronounced at high potentials and at high electrolyte concentration (91).

Electrokinetic theory involves both the theory of the double layer and that of liquid flow. For curved surfaces the shape of the double layer can be described in terms of the dimensionless quantity Ka , which is the ratio of the radius of curvature, a , of the particle, to double layer thickness, $1/K$. When Ka is small a charged particle may be treated as a point charge, when Ka is large the double layer is effectively flat and may be treated as such.

2.4.1. Calculation of zeta potentials

The calculation of zeta potentials from electrophoretic mobility measurements - the electrophoretic mobility, U , of a particle is its velocity over unit distance under the influence of an applied unit potential - requires a theoretical relation between the two quantities. One of the most commonly used relations of this kind is the equation derived by Helmholtz (92) and improved by Smoluchowski (93):

$$u = \frac{\epsilon \zeta}{\eta} \quad 2.58$$

where ϵ and η are the dielectric constant and viscosity respectively of the solution surrounding the particle and these are assumed to take bulk solution values. The particle is assumed to be non-conducting and the surrounding liquid is assumed to have an electric conductance equal to that

in the bulk phase. In addition, the distribution of the ionic double layer is assumed to be not affected by the applied field. Under these conditions equation 2.58 is valid for $Ka > 300$. It follows from this expression that the electrophoretic mobility of a non-conducting particle for which Ka is large at all points on the surface should be independent of its size provided that the zeta potential is constant. Hückel (94) equated the electrical force on the particle (assuming it to be small enough to be treated as a point charge) with the frictional resistance of the medium:

$$u = \frac{e\zeta}{1.5 \eta} \quad 2.59$$

and for values of $Ka < 1$ the Hückel equation may be used.

Equations 2.58 & 2.59 differ only by a numerical coefficient. Henry (95) resolved this apparent contradiction, he pointed out that the difficulty was associated with the assumption that the applied potential was undisturbed by the migrating particle. This assumption is only correct when the conductance of the particle is the same as that of the medium, and when the particle is so small that no appreciable distortion of the external field occurs in the region of the double layer. Smoluchowski had assumed that, in the entire double layer, the direction of the d.c. field is parallel to the particle surface; Hückel's treatment contains the assumption that, everywhere in the double layer, lines of force run straight from anode to cathode. When the electric field is applied it exerts a force on the ions in the mobile part of the double layer, this force is transferred to the solvent. The resulting flow of solvent molecules causes a hydrodynamic force on the particles in the opposite direction to that in which it is moving; this effect is called electrophoretic retardation. Hückel's treatment results in a higher value of the electrophoretic retardation force than does Smoluchowski's. Application of the electric field also causes the colloidal

particle to move away from the centre of its ion atmosphere and a finite time (the relaxation time) is required for the original symmetry to be restored by diffusion and conduction. In electrophoretic motion the centre of the atmosphere does not coincide with the centre of the particle, the consequence is an additional retarding electrical force on the particle, the relaxation effect.

Henry derived a general electrophoretic equation for conducting and non conducting spheres which takes into account the effect of retardation and is of the form:

$$u = \frac{\zeta \epsilon}{1.5 \eta} [1 + \lambda F(\kappa a)] \quad 2.60$$

where $F(\kappa a)$ varies between zero for small values of κa and 1.0 for large, and

$$\lambda = \frac{k_0 - k_1}{2k_0 + k_1}$$

where k_0 is the specific conductance of the bulk electrolyte solution and k_1 is the specific conductance of the particles. For small κa the effect of particle conductance is negligible. For large κa the Henry equation predicts that λ should approach -1 and the electrophoretic mobility $\rightarrow 0$ as particle conductance increases; however in most practical cases, 'conducting' particles are rapidly polarised by the applied electric field and behave as non-conductors.

For non conducting particles ($\lambda = \frac{1}{2}$) the Henry equation can be written in the form

$$u = \frac{\epsilon \zeta}{1.5 \eta} \zeta f(\kappa a) \quad 2.61$$

In the limiting case $\kappa a \rightarrow \infty$ (i.e. when the double layer is very thin compared with the radius), $f(\kappa a) = 3/2$ and Henry's equation is reduced to the Helmholtz-Smoluchowski equation. When $\kappa a \rightarrow 0$, $f(\kappa a) = 1$ and the Hückel equation is obtained.

The simplifications upon which the Henry equation is based are:-

- (1) The Debye-Hückel approximation is made

(2) The applied field and the field of the double layer are simply superimposed. Mutual distortion of these fields could affect electrophoretic mobility in two ways (a) through abnormal conductance (Surface conductance) in the vicinity of the charged surface, and (b) through loss of double layer symmetry (Relaxation effect).

(3) ϵ and η are assumed to be constant throughout the mobile part of the double layer.

The distribution of ions in the diffuse part of the double layer gives rise to an electrical conductance in this region which is in excess of that in the bulk electrolyte medium. Surface conductance will affect the distribution of electric field near to the surface of a charged particle and so influence its electrokinetic behaviour. Surface conductance can be neglected when Ka is small, but when Ka is not small, calculated zeta potentials may be significantly low on account of surface conductance.

Overbeek (96) and Booth (97) derived equations for spherical particles which allow for retardation, relaxation and surface conductance in the mobile part of the double layer, and which express electrophoretic mobility as a power series in $\epsilon\zeta/kT$. A major mathematical problem was caused by the fact that, for spherical particles, the Poisson-Boltzmann equation has no known tractable solution and these equations were only solved for a restricted number of terms and quantitative validity could only be claimed for $\epsilon\zeta/kT < 1$.

The treatments of Overbeek and Booth have now been superseded by that of Wiersema et al (98), who using the complete Poisson-Boltzmann equation, have obtained numerical solutions of the problem using a computer. The main assumptions upon which this treatment is based are:

(1) The particle is a rigid, non conducting sphere with its charge uniformly distributed over the surface.

- (2) The electrophoretic behaviour of the particle is not influenced by other particles in the dispersion.
- (3) Dielectric constant and viscosity are constant throughout the mobile part of the double layer.
- (4) Only one type each of positive and negative ions are present in the double layer.
- (5) The electrical double layer is described by the Gouy-Chapman theory.
- (6) Brownian motion of the particle is neglected.

The results of Wiersema et al were presented in the form of tables of a dimensionless quantity, E, defined as

$$E = \frac{6\pi\eta eU}{\epsilon kT} \quad (\text{unrationalized}) \quad 2.62$$

The function E was computed for several combinations of the parameters Z_+ , Z_- , Ka , y_0 , m_+ and m_- . The quantity y_0 is given by

$$y_0 = \frac{\epsilon \zeta}{kT} \quad 2.63$$

The parameters m_+ and m_- are given by:

$$m_{\pm} = \frac{N\epsilon kT}{6\pi\eta} \frac{Z_{\pm}}{\lambda_{\pm}^0} \quad (\text{unrationalized}) \quad 2.64$$

where N is the Avogadro number and λ_{\pm}^0 the limiting equivalent conductance of the small ions. Most of the computations were carried out for univalent electrolytes and for $m_+ = m_- = 0.184$ i.e. $\lambda_{\pm}^0 = 70 \Omega^{-1} \text{cm}^2 \text{equiv}^{-1}$ in aqueous solution at 25°C. The maximum value of y_0 computed was 6 which corresponded to $\zeta = 154.1 \text{mV}$ at 25°C. The dependence of E on $m_+ + m_-$ was investigated by a few special computations and for univalent electrolytes only. Other types of electrolyte were also considered although those were limited to rather low values of y_0 .

Ottewill and Shaw (99) have tabulated some of the results of Wiersema et al in a more readily usable form. Mobilities are presented as a function of zeta potential and Ka . For the present work, mobilities were converted to zeta potentials with the aid of these tables. With studies involving characterisation of the latex and the effects of non-

ionic surface active agents on mobility and zeta potential Table 4 of the above reference was used (see appendix I), for mixed surfactant systems Table 3 (see section 4.3.2).

However, with the drug systems discussed in section 5, it was decided for the reasons indicated there, and in section 2.4.3, to use the Smoluchowski equation, 2.58, for those mobility zeta potential conversions.

2.4.2. Permittivity and viscosity

All the treatments mentioned above have assumed that the viscosity, η , and permittivity (dielectric constant) ϵ , are constants. Further difficulty in the calculation and interpretation of zeta potentials will arise if the electric field strength, $d\psi/dx$, close to the shear plane is high enough to significantly decrease ϵ and/or increase η by dipole orientation; both effects reduce the mobility for a given zeta potential. Lyklema and Overbeek (90) have examined this problem and concluded that the effect of $d\psi/dx$ on ϵ is insignificant, but that its effect on η may be significant, especially at high potential and high electrolyte concentration. The variation of η with field strength is given by:

$$\eta = \eta_0 \left[1 + f_0 \left(\frac{d\psi}{dx} \right)^2 \right] \quad 2.65$$

where η_0 is the viscosity in zero field strength. A significant (and positive) viscoelectric effect would result in the effective location of the shear plane moving farther away from the particle surface with increasing ζ and/or increasing K , in other words, the physical meaning of the term 'zeta potential' would vary. Unfortunately, the value of the viscoelastic constant f_0 in aqueous solution is not known with any certainty. Lyklema and Overbeek used $f_0 = 10^{-11} \text{ cm}^2 \text{ v}^{-2}$ but it now appears that this may be very much over estimated (100), (101). Hunter (102) has concluded that the variations of ϵ & η with field strength are

of similar significance and their combined effect is probably small in most cases.

2.4.3. Non spherical particles

The particles of drugs studied in this work are not, for the most part, spheres although they may approximate sphericity. Obviously any other particle shape makes the calculation of the electrophoretic retardation and of the relaxation effect more complicated. In addition, the electrophoretic velocity of a non spherical particle depends, generally speaking, on the orientation of the particle with respect to the direction of the external field and the theory for these particles is incomplete. However, when the particle is insulating, and the thickness l/k of the double layer is small compared with the radius of curvature of any point of the particle surface, Smoluchowski's equation is valid irrespective of the form of the particle (103). Overbeek (104) has also shown that for any particle shape, the relaxation effect can be neglected when the double layer is thin compared to any radius of curvature. Hence in this limiting case, which is applicable to the drug systems used, Smoluchowski's equation can be applied to all particle shapes, and the electrophoretic mobility does not depend on the orientation of the particle.

2.4.4. Surface charge density from electrophoresis measurements

As mentioned in section 2.1.2, the full Poisson-Boltzmann equation for a spherical particle has been solved by Loeb, Overbeek and Wiersema (42). With electrophoretic measurements, the surface charge density calculated from the zeta potential is the charge density at the surface of shear. For convenience, this charge density is often identified with the charge density in the diffuse double layer i.e. σ_2 .

Surface charge density can be interpolated from the tables of Loeb et al. which for 1:1 electrolyte at 25°C is given by (unrationa^slized)

$$\sigma_2 = 1.7603 \times 10^4 (C)^{\frac{1}{2}} \text{ I e.s.u. cm}^{-2} \quad 2.66$$

where values of I as a function of q_0 and y_0 (equation 2.63) are given

$$q_0 = Kr$$

and

$$y_0 = \frac{e}{kT}$$

where r is the distance of the surface of shear from the centre of the sphere and c is the concentration of electrolyte in equivalents per dm^3 .

Some of the values are given below.

$I(q_0, y_0)$ as a function of q_0 and y_0 for 1:1 electrolytes

$q_0 \backslash y_0$	10	20	∞
1	1.1403	1.0912	1.0422
2	2.5361	2.4430	2.3504
3	4.5146	4.3861	4.2586
4	7.5614	7.4068	7.2537
5	12.443	12.271	12.100

The values of $I(q_0, y_0)$ in the last column, i.e. $q_0 \rightarrow \infty$, are calculated from the Gouy-Chapman-Stern diffuse layer theory,

$$\sigma_2 = \left(\frac{2n_0 \epsilon kT}{\pi} \right)^{\frac{1}{2}} \sinh \frac{Ze\zeta}{2kT} \quad (\text{unrationalized})$$

2.67

with $I = 2 \sinh \frac{y_0}{2}$. From the table it will be seen that for $Kr \geq 20$, the surface charge density at the surface of shear of a spherical particle can be calculated with reasonable accuracy by equation 2.67.

Particles used in the present electrophoretic work have $Ka \geq 38$ where a is the radius of the particle. Hence it is justifiable to use equation 2.67, which, in its rationalized form is

$$\sigma_2 = (8n_0 \epsilon kT)^{\frac{1}{2}} \sinh \frac{Ze\zeta}{2kT} \quad 2.68$$

for an aqueous medium at 25°C and a 1:1 electrolyte this expression reduces to

$$\sigma_2 = 3.7 \times 10^{-5} \sqrt{c} \sinh 37.9 \zeta$$

where c is expressed in mol m^{-3} and ζ in volts.

2.4.5. The relation between Stern Potential and surface active agent concentration

Ottewill et al (105) have developed a relationship between the Stern potential and surface active agent concentration valid for small spherical particles when $Ka < 1$. Chen (106) has extended this relationship for surface active ions with a charge opposite to that on the particle when $Ka \geq 20$. The surface charge density of a particle in the absence of surface active agent is given by

$$\sigma_1 = \sigma_1^0 + \sigma_2^0 \quad 2.69$$

where σ_1^0 and σ_2^0 are the charge densities in the Stern plane (potential ψ_δ^0) and in the diffuse double layer respectively. When surface active ions are added to the system, these will adsorb in the Stern plane by ion exchange with the inorganic ions in this plane or by direct transfer from the diffuse double layer. The Stern potential will be altered to a value ψ_δ and the charge densities in the Stern and diffuse double layers to σ_1 and σ_2 respectively. Assuming that the surface charge density σ_0 is not affected by adsorption of surface active ions, then

$$\sigma_0 = \sigma_1 + \sigma_2 \quad 2.70$$

From equations (2.69) and (2.70) it follows that

$$\sigma_1 - \sigma_1^0 = \sigma_2^0 - \sigma_2 = \Delta \sigma_2 = \sigma_c \quad 2.71$$

since $\sigma_1 > \sigma_1^0$ due to the adsorption where σ_c is the increase in charge density in the Stern plane. The Stern equation (107) can be written as

$$\sigma_c = \frac{N_1 Z_i e}{1 + \frac{\exp\left(-\frac{\Delta \bar{G}}{kT}\right)}{x_c}} \quad 2.72$$

where N_1 is the number of adsorption sites per m^2 and x_c is the mole fraction of the surface active agent and $\Delta \bar{G}$ is the electrochemical free

energy of adsorption. It has been assumed in the derivation of this equation that there is no lateral interaction between the adsorbing surface active ions.

When the concentration of the surface active agent is low then

$$x_c = \frac{c}{55.6 \times 10^3} \quad 2.73$$

where c is the concentration of the surface active ion mol m^{-3} .

Combination of equations 2.72 and 2.73 putting

$$k_2 = \frac{\exp - \frac{\bar{\Delta G}}{kT}}{55.6 \times 10^3} \quad 2.73a$$

yields

$$\sigma_c = \frac{zeN_1 k_2 c}{1+k_2 c} = \frac{k_1 c}{1+k_2 c} = \Delta \sigma_2 \quad 2.74$$

where $k_1 = zeN_1 k_2$

It is seen that equation 2.74 is the Langmuir (108) adsorption equation and the Stern equation is essentially the Langmuir adsorption equation modified for ionic adsorption on solid in aqueous solution (107). As discussed in section 2.4.4 the charge density in the diffuse double layer for particles with $ka \geq 20$ can be calculated using equation 2.68, whence

$$\sigma_2^0 = (8 \eta_0 \epsilon kT)^{\frac{1}{2}} \sinh \frac{ze\psi_\delta^0}{2kT} \quad 2.75$$

and
$$\sigma_2 = (8 \eta_0 \epsilon kT)^{\frac{1}{2}} \sinh \frac{ze\psi_\delta}{2kT} \quad 2.76$$

Therefore
$$\sigma_c = (8 \eta_0 \epsilon kT)^{\frac{1}{2}} \left[\sinh \frac{ze\psi_\delta^0}{2kT} - \sinh \frac{ze\psi_\delta}{2kT} \right] \quad 2.77$$

Since σ_c can increase continuously, conditions may arise such that the particle charge may reverse sign so that ψ_δ^0 and ψ_δ have different signs.

When this occurs

$$\sigma_c = \sigma_2^0 + \sigma_2 \quad 2.78$$

generally

$$\sigma_c = (8 \eta_0 \epsilon kT)^{\frac{1}{2}} \left[\sinh \frac{ze\Psi_0^0}{2kT} + \sinh \frac{ze\Psi_\delta}{2kT} \right] \quad 2.79$$

Equation (2.74) can be rearranged to yield

$$\frac{1}{c} = k_2 \left[\frac{zeN_1}{\Delta \sigma_c^2} - 1 \right] \quad 2.80$$

Combination of equations 2.79 and 2.80 gives

$$\frac{1}{c} = k_2 \left[\frac{ze N_1}{(8 \eta_0 \epsilon kT)^{\frac{1}{2}} \left[\sinh \frac{ze\Psi_0^0}{2kT} + \sinh \frac{ze\Psi_\delta}{2kT} \right]} - 1 \right] \quad 2.81$$

which expresses the general relationship between the Stern potential and surface active agent concentration. From equations 2.74 and 2.77

$$(8 \eta_0 \epsilon kT)^{\frac{1}{2}} \left[\sinh \frac{ze\Psi_0^0}{2kT} - \sinh \frac{ze\Psi_\delta}{2kT} \right] = \frac{k_1 c}{1+k_2 c} \quad 2.82$$

The slope of $\Psi_\delta - \log_{10} c$ can be obtained by differentiation of equation 2.82 to give

$$\frac{ze}{2kT} (8 \eta_0 \epsilon kT)^{\frac{1}{2}} \cosh \frac{ze\Psi_\delta}{2kT} \frac{d\Psi_\delta}{d \ln c} = \frac{-k_1 c}{(1+k_2 c)^2} \quad 2.83$$

It can be shown from equation 2.74 that

$$\frac{1}{(1+k_2 c)} = - \left[\frac{\Delta \sigma_c^2}{zeN_1} - 1 \right] \quad 2.84$$

Combination of equations 2.74, 2.77, 2.83 and 2.84 yields

$$\frac{d\Psi_\delta}{d \log_{10} c} = \frac{4.606kT}{ze} \left(\frac{\sinh \frac{ze\Psi_0^0}{2kT} - \sinh \frac{ze\Psi_\delta}{2kT}}{\cosh \frac{ze\Psi_\delta}{2kT}} \right) \left[\frac{(8\eta_0 \epsilon kT)^{\frac{1}{2}} (\sinh \frac{ze\Psi_0^0}{2kT} - \sinh \frac{ze\Psi_\delta}{2kT})}{zeN_1} - 1 \right] \quad 2.85$$

when $\Psi_\delta = 0$ equation 2.85 becomes

$$\frac{d\Psi_\delta}{d \log_{10} c} [\Psi_\delta = 0] = \frac{4.606kT}{ze} \left(\sinh \frac{ze\Psi_0^0}{2kT} \right) \left[\frac{(8 \eta_0 \epsilon kT)^{\frac{1}{2}} \sinh \frac{ze\Psi_0^0}{2kT}}{zeN_1} - 1 \right] \quad 2.86$$

It can be seen from equation 2.86 that the slope of the $\Psi_\delta - \log_{10} c$ plot at $\Psi_\delta = 0$ is independent of k_2 but is dependent on N_1 , Ψ_0^0 and z . Since the latter two quantities are usually known, the slope of the curve can

be used to calculate N_1 . So far it has been assumed that k_2 will remain constant over the whole curve. However, this will only be true whilst $\Delta \bar{G}$ remains constant, and since

$$\Delta \bar{G} = \Delta \phi + ze\psi_\delta \quad 2.87$$

where $\Delta \phi$ is the specific chemical free energy of adsorption, this will hold under the condition that $ze\psi_\delta$ is small compared with $\Delta \phi$.

2.4.6. Hydrophobic bonding - the hydrophobic effect

Hydrophobic substances may be defined as those that are readily soluble in many non polar solvents but are only sparingly soluble in water (109). Surface active agents are substances which have both hydrophobic (a hydrocarbon chain) and hydrophilic regions in their molecular structure. From a thermodynamic point of view the outstanding feature of the process of dissolving a surface active agent in water is the large negative entropy change which is intimately related to the structuring of water around the hydrocarbon portion of the surface active agent. To counteract this unfavourable entropy change the hydrocarbon groups tend to withdraw from the aqueous phase, this may occur by the surface active agent molecule orientating itself at an interface with the hydrocarbon chain away from the aqueous phase. At a certain concentration, however, (the critical micelle concentration) the hydrocarbon chains cluster together forming the interior of micelles. This tendency was termed "hydrophobic bonding" by Kauzmann (110).

The position had, in fact, been stated most succinctly by Hartley at an earlier date (111), he said "The antipathy of the paraffin chain for water is, however, frequently misunderstood. There is no question of actual repulsion between individual water molecules and paraffin chains, nor is there any very strong attraction of paraffin chains for one another. There is however, a very strong attraction of water molecules for one another in comparison with which the paraffin-paraffin

or paraffin water attractions are very slight".

The term 'hydrophobic bonding' can therefore be criticized in that there is no bonding between the hydrophobic groups (there will however be van der Waals type attractive forces), and the phenomenon is better described as the 'hydrophobic effect'.

As the hydrophobic effect is due to the entropy changes associated with the structuring of water molecules around the hydrocarbon chain of the surface active agent molecule, it follows, that as the length of the hydrocarbon chain increases there will be a greater entropy increase when the hydrocarbon chain leaves the aqueous phase, i.e. the longer the hydrocarbon chain the more energetically favourable it is for such a molecule to be adsorbed at an interface.

There will be a similar entropy increase when a hydrocarbon chain is specifically adsorbed at a solid hydrophobic surface, as occurs for example, 'between' the acidic groups of a polystyrene latex particle and this will contribute to the free energy of adsorption. Ottewill and Watanabe (112) have shown, with silver iodide, positively charged, that with anionic surface active agents at zero zeta potential, there is sufficient space for all the chains to lie flat on the surface.

However once the adsorbed ions reach a certain critical concentration at the solid liquid interface, they begin to associate into two dimensional patches of ions at the surface in much the same way as they associate into three dimensional aggregates to form micelles in bulk solution. The forces responsible for this association will again be entropic (113). Although the concentration at which clusters form is below bulk solution critical micelle concentration Furstenau^e has shown that the concentration of adsorbed ions within the Stern layer approximates the cmc. There are therefore a number of factors which contribute to the free energy of adsorption of hydrocarbon chains at a

hydrophobic surface.

SECTION 3.

EXPERIMENTAL

3.1. Materials

The distilled water used for all solutions and dispersions was obtained from a Fison's Fi-stream all glass still. General chemicals used were of A.R. quality.

3.1.1. Surface Active Agents

(a) Nonionic surface active agents

The nonionic surface active agents were polyoxyethylene glycol ethers of n alkanols, used as commercially supplied; purification was not attempted as they would be used in this state in pharmaceutical practice. Impurities present are polymers with varying numbers of ethylene oxide groups, n alkanols and ethylene oxide (114).

(i) Polyoxyethylene n dodecanol.

$C_{12}H_{25}(CH_2CH_2O)_n OH$, the average number of n is 23,

$C_{12}E_{23}$. Mol. Wt. 1198.

B.D.H. Chemicals Ltd. "BRIJ 35"

(ii) Polyoxyethylene n hexadecanols.

$C_{16}H_{33}(CH_2CH_2O)_n OH$, n taken as 10, $C_{16}E_{10}$;

18, $C_{16}E_{18}$; 30, $C_{16}E_{30}$; 45, $C_{16}E_{45}$; 60, $C_{16}E_{60}$.

Mol. Wts. 682, 1034, 1562, 2222, 2882 respectively.

Glovers (Chemicals) Ltd. Texofors A10, A18, A30,

A45 and A60

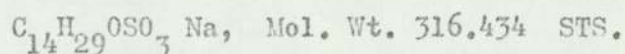
and Cetomacrogol 1000 B.P., $C_{16}E_{23}$.

Mol. Wt. 1254.

Macarthys

(b) Anionic surface active agents

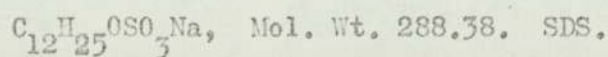
(i) Sodium tetradecyl sulphate



Prepared in the laboratory at the University of Aston

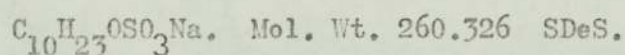
by G. Mukhayer.

(ii) Sodium dodecyl sulphate



B.D.H. Chemicals Ltd "Specially pure"

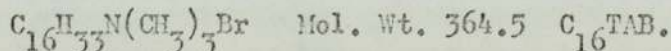
(iii) Sodium decyl sulphate



Eastman Organic Chemicals

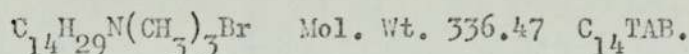
(c) Cationic surface active agents

(i) Hexadecyltrimethylammonium bromide

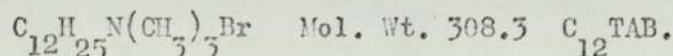


B.D.H. Chemicals Ltd.

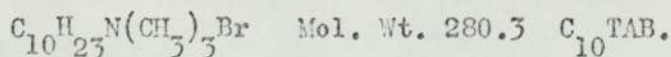
(ii) Tetradecyltrimethylammonium bromide



(iii) Dodecyltrimethylammonium bromide



(iv) Decyltrimethylammonium bromide



The last three surfactants were prepared in the laboratory at the University of Aston by D. Guveli.

The above compounds were used without further purification.

3.1.2. Polystyrene latex

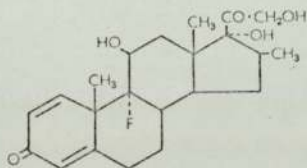
The sample used was prepared, at the University of Bristol, by an aqueous phase initiation suspension polymerisation process (115).

The styrene, redistilled at 5-10mm Nitrogen, was 0.871 molar (calculated on total volume). Initiator potassium persulphate $K_2S_2O_8$ A.R. recrystallized from room temperature solution, 3.4×10^{-4} mol dm^{-3} ; sodium chloride A.R. 11.54×10^{-3} mol dm^{-3} ; both calculated on the volume of the aqueous phase. The polymerisation was carried out in a 1 litre round bottomed flask in a thermostat bath at $70^\circ C$, stirrer speed 350 r.p.m., reaction time 24hours, initial pH 6.5, final 3.0. The latex was extensively dialysed against distilled water with numerous changes of dialysate.

3.1.3. Drugs

(i) Betamethasone B.P.

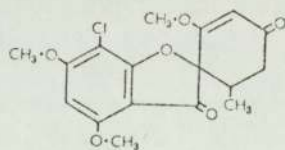
9 α -fluoro-11 β ,17 α ,21-trihydroxy-16 β -methylpregna-1,4-diene-3,20-dione,



Gift from Glaxo Laboratories Ltd.

(ii) Griseofulvin B.P.

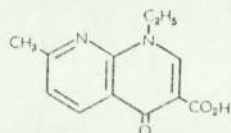
(+)-7-chloro-4,6-dimethoxycoumaran-3-one-2-spiro-1'-(2'-methoxy-6'-methylcyclohex-2'-en-4'-one)



Gift from Glaxo Laboratories Ltd.

(iii) Nalidixic Acid B.P.C.

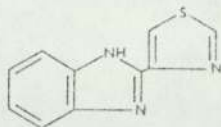
Nalidixic Acid is 1-ethyl-7-methyl-4-oxo-1,8-naphthyridine-3-carboxylic acid



Gift from Winthrop Laboratories

(iv) Thiabendazole B.P.C.

Thiabendazole is 2-(4-thiazolyl)benzimidazole.



Gift from Merck Sharpe and Dohme Ltd.

3.2. Characterisation of materials

3.2.1. Surface active agents

The surface active agents were characterised by measurement of critical micelle concentrations, cmc. For the nonionics the method used was that of dye solubilization using Orange OT (116). The cmc's of the ionic surfactants were found by measuring the conductance of solutions of varying concentration by means of a Wayne Kerr Auto-balance Universal Bridge B642.

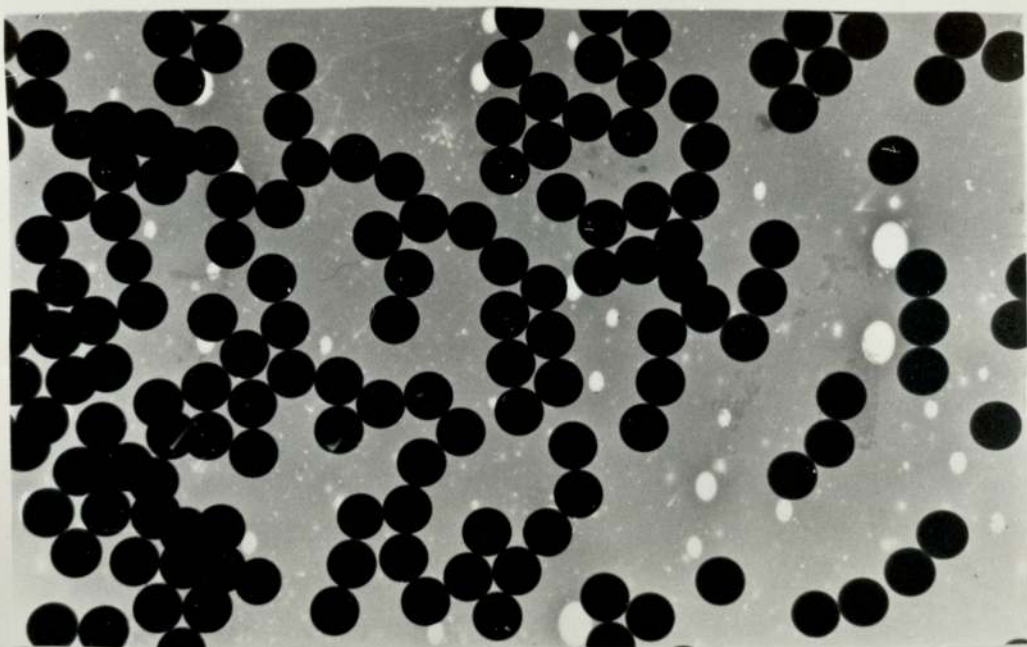
Results are given below together with selected literature values.

Cmc, in water, of surface active agents at 25°C.			
Surface active agent	cmc mol dm ⁻³	Literature value mol dm ⁻³	Reference
C ₁₆ E ₁₀	1.8x10 ⁻⁴	6.0x10 ⁻⁵	} (118)
C ₁₆ E ₁₈	1.55x10 ⁻⁴	3.85x10 ⁻⁵	
C ₁₆ E ₂₃	6x10 ⁻⁵	5.0x10 ⁻⁵	(119)
C ₁₆ E ₃₀	4x10 ⁻⁵	2.20x10 ⁻⁵	(118)
C ₁₆ E ₄₅	1.2x10 ⁻⁵	1.75x10 ⁻⁵	(118)
C ₁₆ E ₆₀	1x10 ⁻⁵	1.15x10 ⁻⁵	(119)
C ₁₂ E ₂₃	1.45x10 ⁻⁴	1.0x10 ⁻⁴	(117)
SDeS	3.25x10 ⁻²	3.26-3.35x10 ⁻²	} (117)
SDS	7.86x10 ⁻³	8.06-8.4x10 ⁻³	
STS	2.06x10 ⁻³	2.05x10 ⁻³	
C ₁₀ TAB	6.06x10 ⁻²	6.5-6.8x10 ⁻²	
C ₁₂ TAB	1.60x10 ⁻²	1.40-1.64x10 ⁻²	} (117)
C ₁₄ TAB	3.58x10 ⁻³	3.51-3.6x10 ⁻³	
C ₁₆ TAB	8.66x10 ⁻⁴	8.0-9.8x10 ⁻⁴	

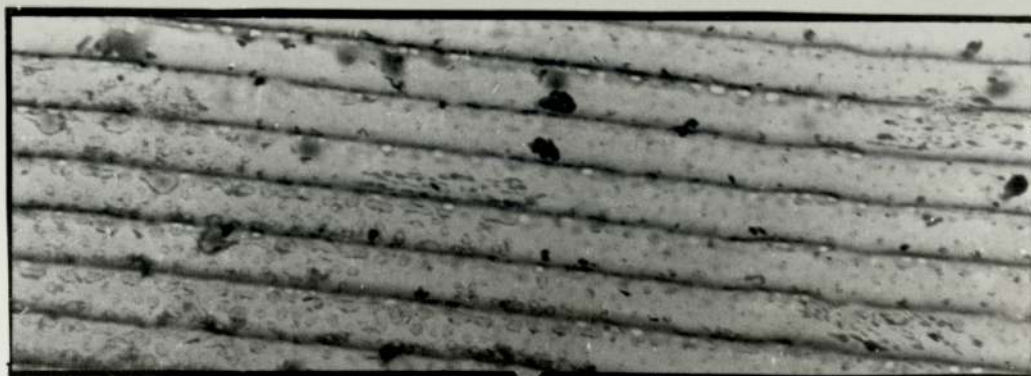
3.2.2. Polystyrene latex characterisation

(a) Particle size distribution

A particle size distribution of the latex dispersion was obtained using a Hitachi HS.7. Electron Microscope, at the University of Bristol. Photographs of particles were taken and analysed using a Zeiss Particle Size Analyser. Computer print out, Fig. IV, histogram, Fig. V, and specimen photograph on the following plate show that the dispersion is monodisperse containing spherical particles with a number average diameter



Polystyrene Latex



Diffraction grating

1 division = 1 μm

SOE NO 2 .N= 895

LOWER BOUND 0.519

UPPER BOUND 0.923

LOWER QUARTILE 0.749

MEDIAN 0.767

UPPER QUARTILE 0.767

MEAN +.76079132

VARIATION +.02204248

SKFW -2.8207961

KURTOSIS +53.003927

SIZE IN MICRONS	FREQUENCY	PERCENT
0.528	1	0.11
0.546	0	0.00
0.565	0	0.00
0.583	0	0.00
0.602	0	0.00
0.620	0	0.00
0.633	0	0.00
0.657	1	0.11
0.675	0	0.00
0.693	2	0.22
0.712	7	0.78
0.730	52	5.81
0.749	245	27.37
0.767	506	56.54
0.785	76	8.49
0.804	4	0.45
0.822	0	0.00
0.841	0	0.00
0.859	0	0.00
0.877	0	0.00
0.896	0	0.00
0.914	1	0.11

END OF DATA

ENTER NEXT PROGRAM

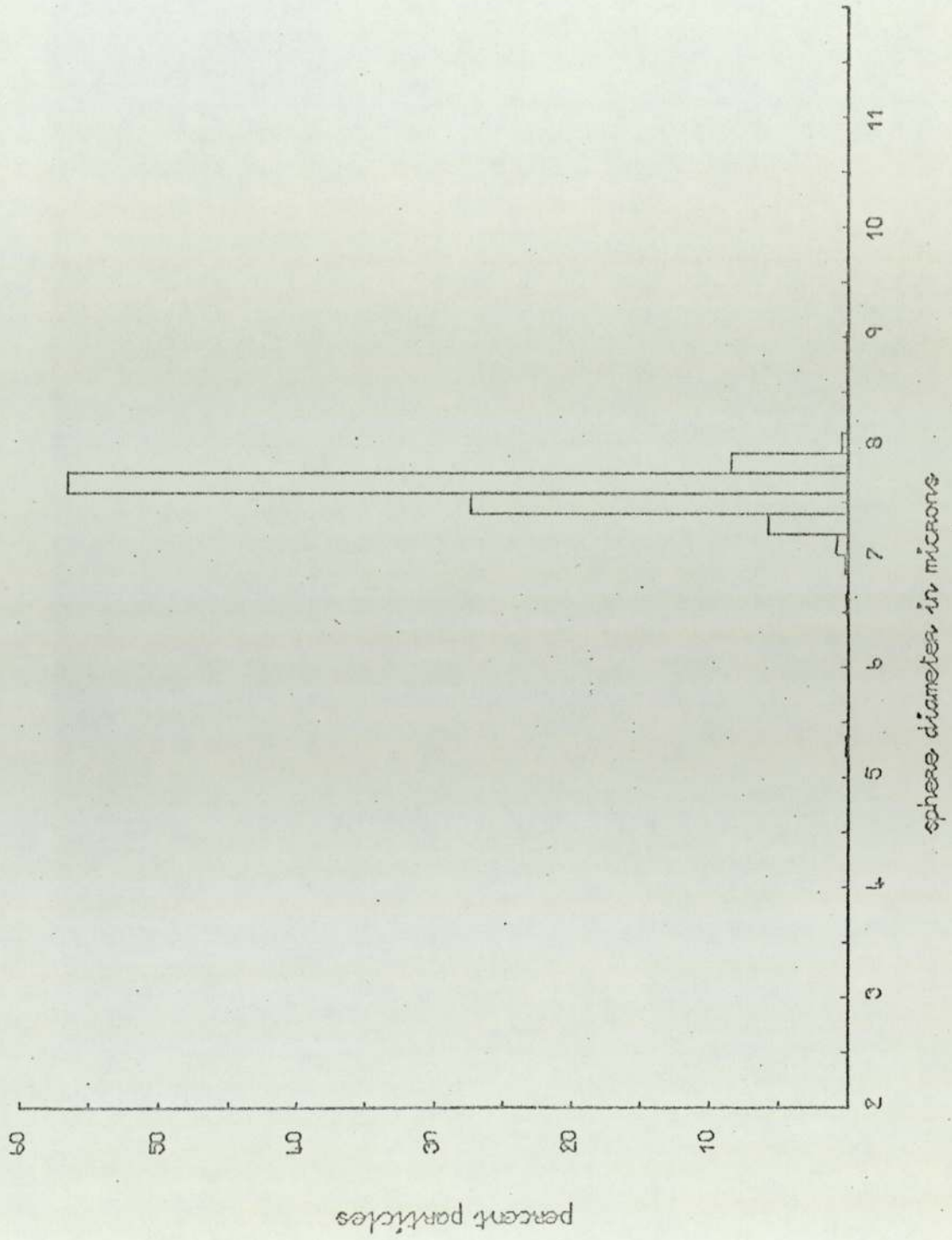


Fig v particle size distribution for sol no. 2

particle size of $0.761\mu\text{m}$ with a variation of $\pm 0.022\mu\text{m}$, the modal diameter is $0.767\mu\text{m}$.

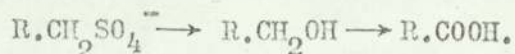
(b) Characterisation of surface groupings

Ottewill and Shaw (120) have shown that polystyrene particles are negatively charged.

Polystyrene produced by suspension polymerisation using hydrogen peroxide as initiator gives a latex with carboxyl groups as the only ionizing groups. The mechanism of formation of the carboxyl groups is not known with certainty. One possible route is that combination of an hydroxyl radical with monomer leads to the formation of an alcohol which is then converted to an acid in the oxidising atmosphere of the polymerisation. An alternative is that in the presence of oxygen a peroxide is formed with styrene which subsequently decomposes to yield an alcohol and hence a carboxyl under oxidising conditions (121).

The use of persulphate as an initiator, as in the method of preparation used here, can produce a latex with two types of acidic groupings. One is a much stronger acid than the other and suggests the formation of a sulphate grouping in addition to a carboxyl (121).

Goodwin et al (115) have shown that the sulphate groupings formed on the latex particle surface are a consequence of the interaction between monomer molecules in the aqueous phase and sulphate free-radicals. Hydroxyl groups are formed due to hydrolysis of sulphate groupings; in addition hydroxyl groups may be formed from the reaction of monomer molecules with hydroxyl radicals formed by the reaction of persulphate with water. Due to the oxidising conditions that exist during the polymerisation, surface hydroxyl groups can also be oxidised to carboxyl groups. The sequence of reactions would seem to be:-



It is possible to decide the type(s) of ionizing end group(s) present by conductometric titration (122) of the latex dispersion with carbonate free sodium hydroxide solution. 5ml. of the dispersion was taken and titrated with $10^{-2} \text{ mol dm}^{-3}$ NaOH, added from an Agla syringe, under nitrogen. The specific conductivity of the dispersion being observed by means of a Wayne-Kerr conductivity bridge, the type and number of acidic groupings can be found from the plot obtained. Results for the latex dispersion are given in Fig. VI., these indicate that the only ionizing groups present are $-\text{COOH}$, this is confirmed in Section 4.1. by electrophoretic measurements.

Results

5ml. of latex dispersion (0.275g) required 0.07ml of $10^{-2} \text{ mol dm}^{-3}$ NaOH

$$\begin{aligned} \text{Equivalents of NaOH} &= \frac{7 \times 10^{-2}}{100 \times 1000} = 7 \times 10^{-7} \text{ per } 0.275\text{g} \\ &= 2.545 \times 10^{-6} \text{ g}^{-1}. \end{aligned}$$

Therefore the number of $-\text{COOH}$ groups per g. is

$$\begin{aligned} 2.545 \times 10^{-6} \times 6.023 \times 10^{23} \\ = 1.533 \times 10^{18} \text{ g}^{-1}. \end{aligned} \quad (\text{a})$$

The mean number average diameter is $0.76 \mu\text{m}$

$$= 7.6 \times 10^{-7} \text{ m}$$

Therefore area per particle, $\Pi d^2 = 1.815 \times 10^{-12} \text{ m}^2$

The volume of a single particle is $\Pi d^3/6$ and the mass is $\Pi d^3 \rho/6$ per particle, where ρ the density of the polystyrene latex is $1.055 \times 10^3 \text{ kgm}^{-3}$

$$\begin{aligned} \text{Therefore area per g} &= \frac{6\rho/d}{7.6 \times 10^{-7}} = \frac{6 \times 1.055 \times 10^6 \text{ m}^2 \text{ g}^{-1}}{7.6 \times 10^{-7}} \\ &= 8.328 \text{ m}^2 \text{ g}^{-1} \end{aligned} \quad (\text{b})$$

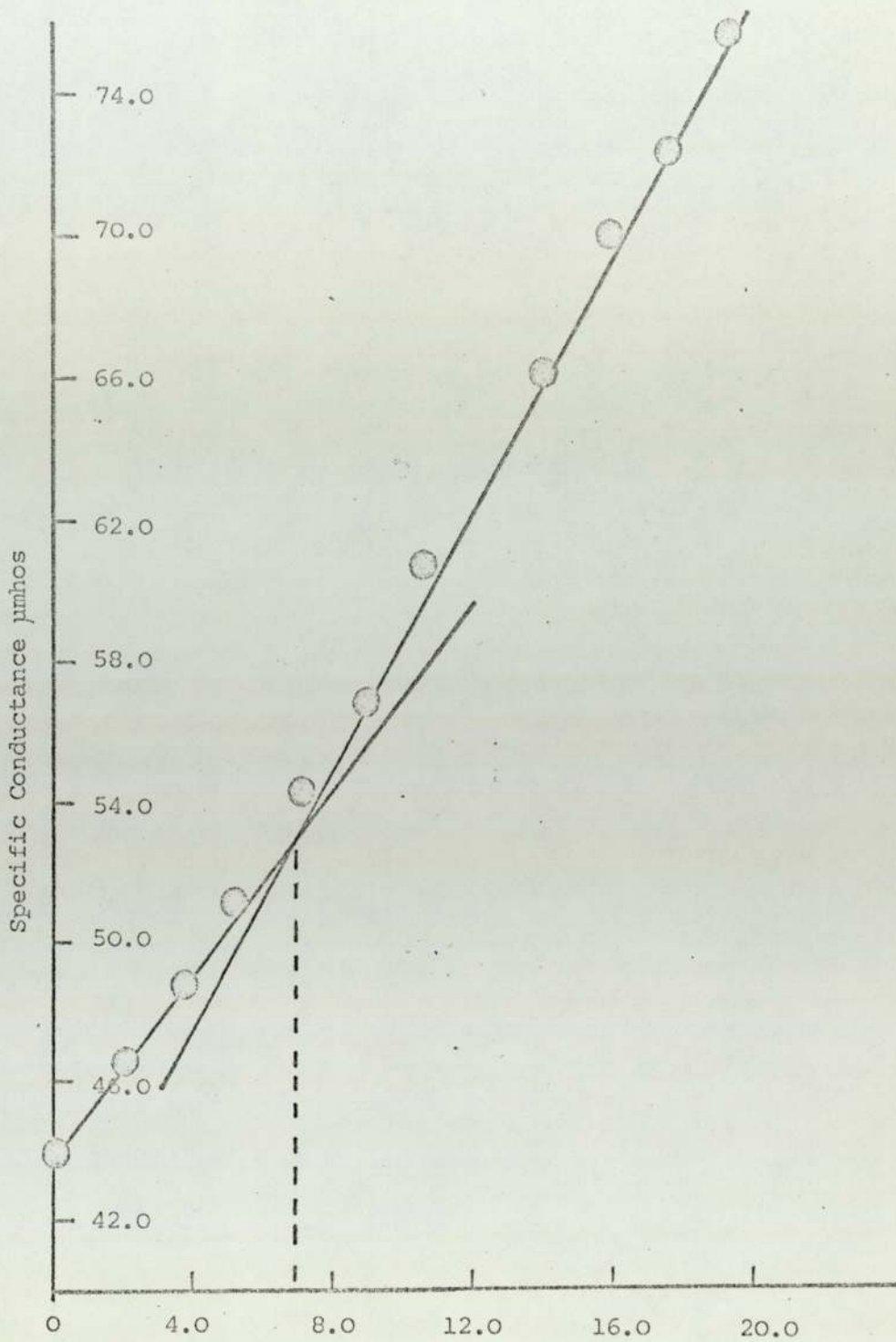
The number of charge groups per unit area is a/b

$$= 1.84 \times 10^{17} \text{ groups m}^{-2}$$

Area per charge group is $5.44 \times 10^{-18} \text{ m}^2$ or 5.44 nm^2

When the group is ionised there is one e of charge for that area i.e.

$$1.60 \times 10^{-19} \text{ C.}$$



10^{-2} mol dm^{-3} Sodium Hydroxide ml. $\times 10^{-2}$

Fig VI Polystyrene Latex characterisation by conductometric titration, estimation of -COOH groups.

3.2.3. Characterisation of drugs

All drugs were used as supplied by the manufacturers.

Particle size distribution

(i) Betamethasone and Griseofulvin

Particle size distributions of Betamethasone and Griseofulvin were obtained using a Joyce Loebel disc centrifuge; a diagram of this instrument is shown in Fig. VII. (123). This uses a two layer centrifugal sedimentation technique, the supernatant liquid is removed after fixed times of rotation and its concentration determined colorimetrically, the fall in optical density being equated with the oversize particles which have passed the sampling distance. Photomicrographs of these two drugs are shown on a following plate. Results, as cumulative percentage undersize frequency curves, are shown in Fig. VIII for Betamethasone and Fig. IX for Griseofulvin.

For Betamethasone:

Median diameter $1.6\mu\text{m}$

Modal diameter $1.5\mu\text{m}$

and

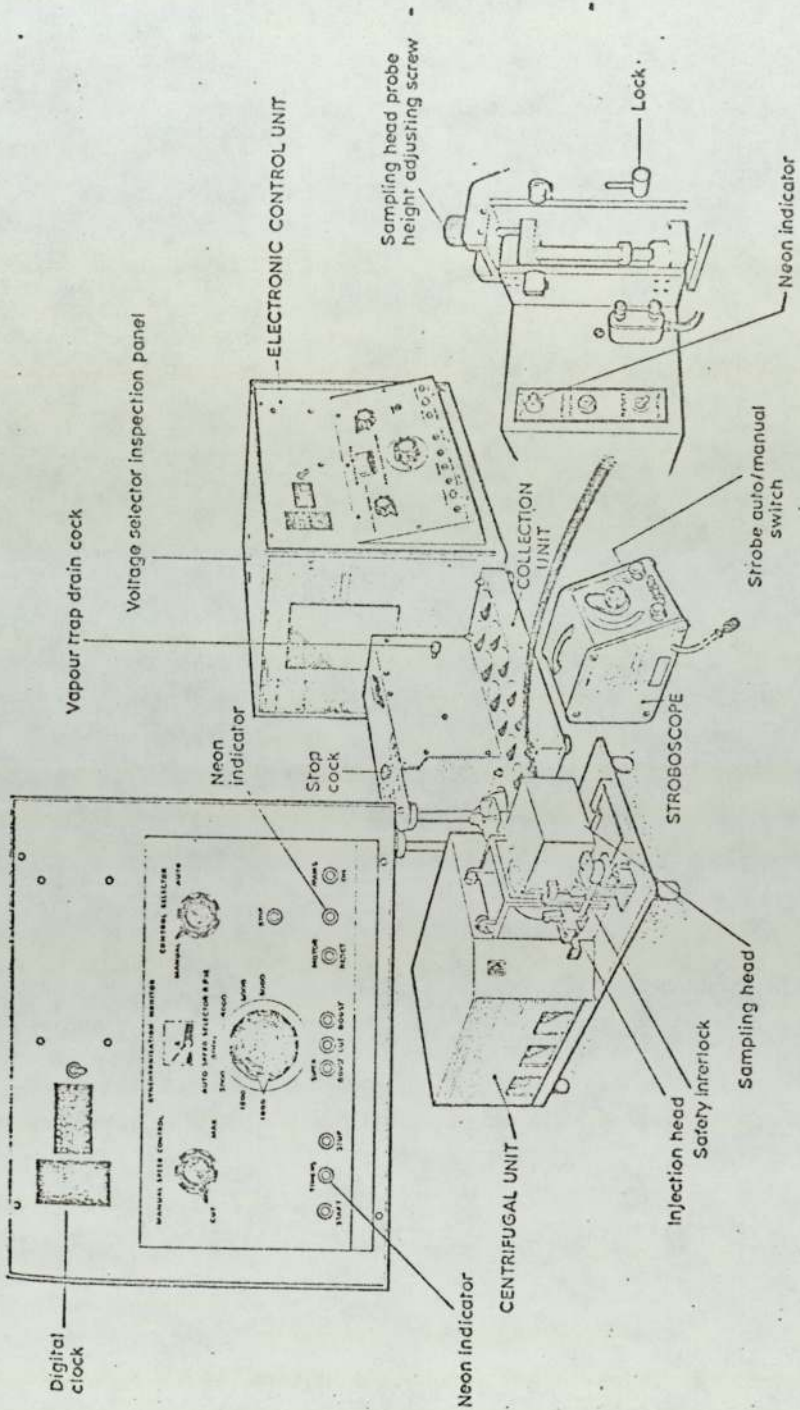
Griseofulvin

Median diameter $1.9\mu\text{m}$

Modal diameter $2.0\mu\text{m}$

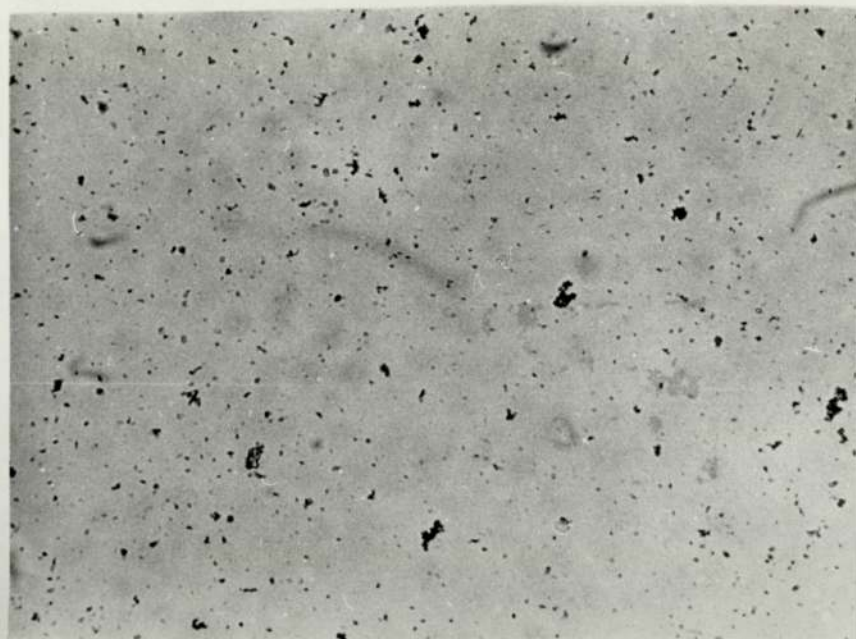
(ii) Nalidixic Acid

As the photomicrograph for this drug shows, a number of the particles are large, some with one measurement $> 100\mu\text{m}$, ^{and} sizing by a sedimentation technique is therefore difficult. It was therefore decided to measure the surface area of the powder. An air permeability method, which measures the flow of air through a packed powder bed of known porosity and from this obtains the surface area of the powder, was chosen. As well as giving surface area a mean particle diameter



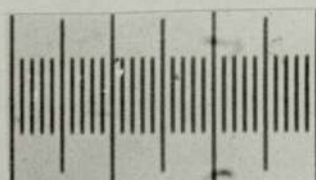
DISC CENTRIFUGE CONTROL POSITIONS

Fig. VII The Joyce Loebel disc centrifuge.



BETAMETHASONE

Scale
1 division
= 10 μm



GRISEOFULVIN

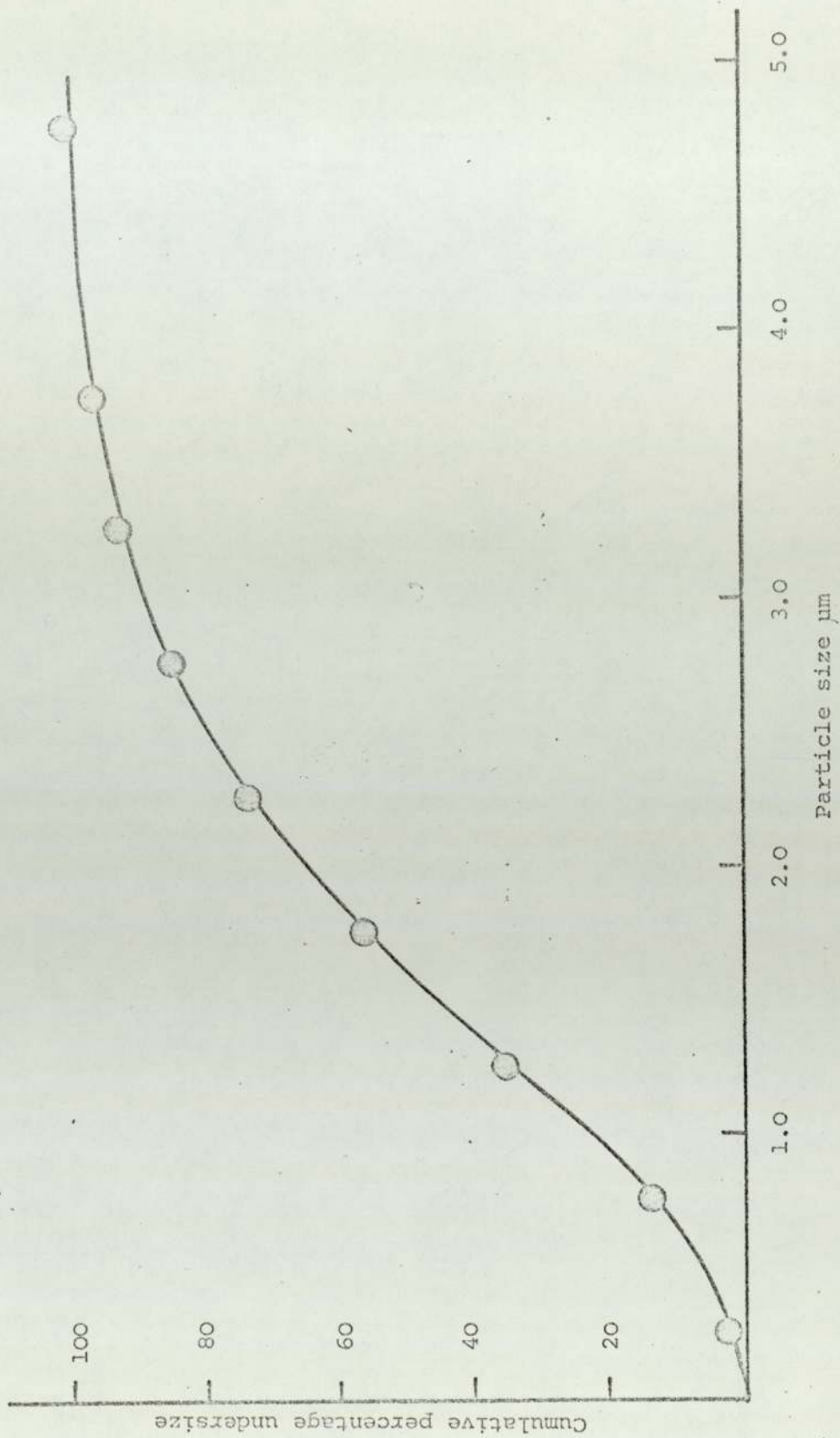


Fig VIII Particle size distribution Betamethasone

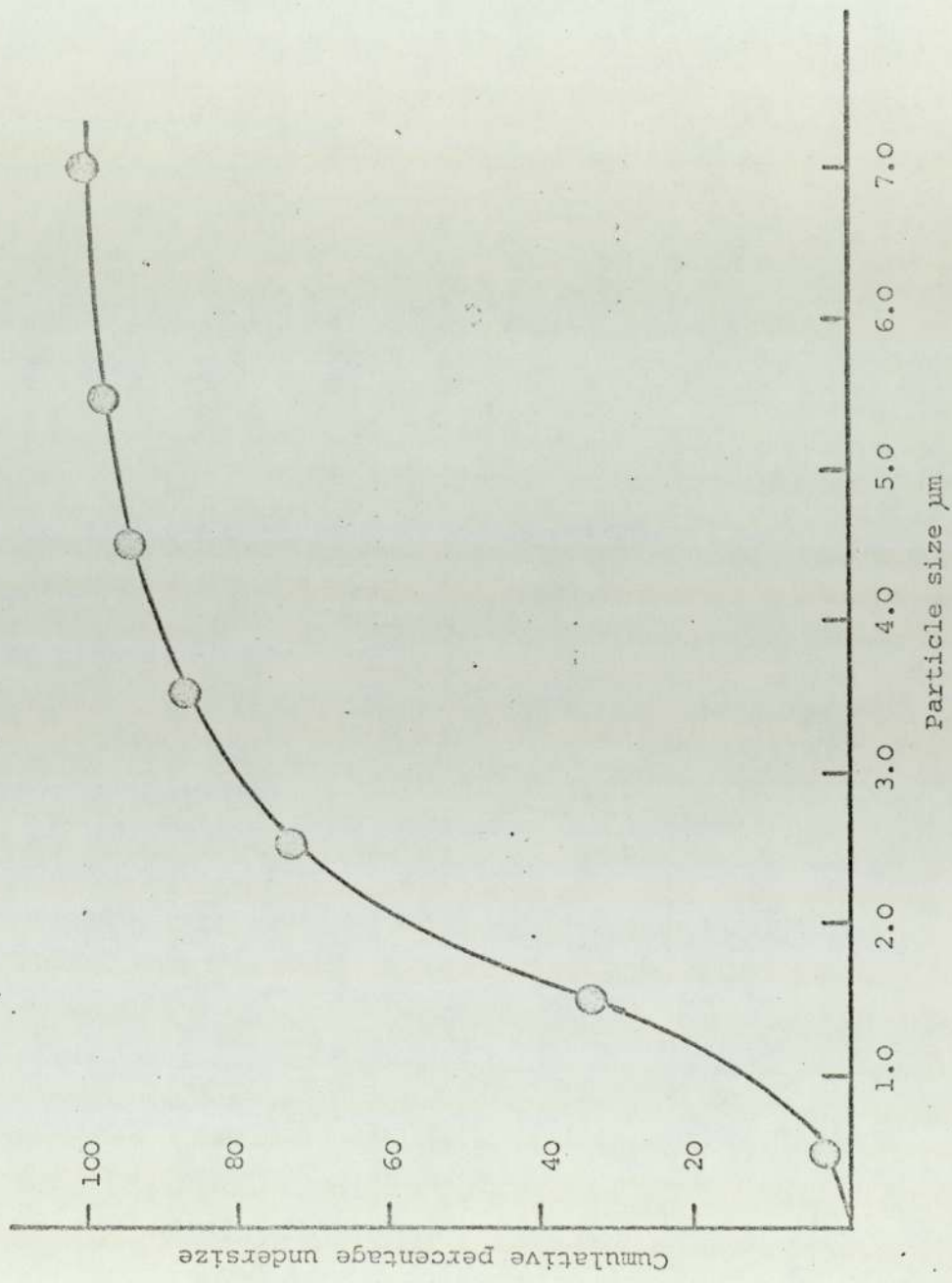


Fig IX Particle size distribution Criseofulvin

can also be obtained.

The particles are coarse and therefore the Fisher sub sieve sizer, a commercial instrument based on the Gooden and Smith modification of the Lea and Nurse apparatus is suitable (124). This instrument embodies a self calculating chart which enables the surface weight mean diameter, d , in μm to be read off directly. d is given by:

$$d = \frac{60,000}{14} \sqrt{\left[\frac{\eta c F \rho L^2 M^2}{[VD-M]^3 [P-F]} \right]}$$

where c = flowmeter conductance in ml/sec per unit pressure (g force/cm²)

F = pressure difference across flowmeter resistance (g force/cm²)

M = mass of sample in grams

D = density of sample in gm/cm³

V = apparent volume of compacted sample in ml.

P = overall pressure head in g force/cm²

L = bed thickness in cm

η & ρ are the viscosity and density of air respectively.

By using a sample weight equal in grams to the true density of the powder and selecting and fixing some of the variables, d is indicated by the value of F only, measured by the height of a column of liquid in a tube. The surface area can be obtained from the mean diameter, d , using:

$$\text{Area} = \frac{6D}{d} \text{ cm}^2 \text{ g}^{-1}$$

where D is the density of the sample.

The density of Nalidixic acid as obtained using a density bottle and water containing nonionic surfactant as a dispersant was found to be 1.4 gm/cm³.

The mean particle diameter measured at a porosity of 0.5 and 0.45 is 36.5 μm . The surface area per gram is therefore $2.30 \times 10^3 \text{ cm}^2 \text{ g}^{-1}$ or $2.30 \times 10^{-1} \text{ m}^2 \text{ g}^{-1}$.

(iii) Thiabendazole

The particle size analysis of Thiabendazole was carried out by Andreasen pipette (125). In this method, the concentration changes occurring within a suspension, settling under gravity, are studied by removing samples of the suspension by means of a pipette. The concentration of solid in the samples is determined by a suitable analytical technique, the largest size present in each sample being calculated from Stoke's equation, due allowance being made for the fall in height of the suspension after each sample is withdrawn.

A photomicrograph of this drug is shown on a following plate. Results as a cumulative percentage undersize frequency curve, are shown in Fig. X.

Median diameter $12\mu\text{m}$

Modal diameter $11\mu\text{m}$

The particle size analyses of Betamethasone, Griseofulvin and Thiabendazole were carried out by R. Buxton at the University of Technology, Loughborough.

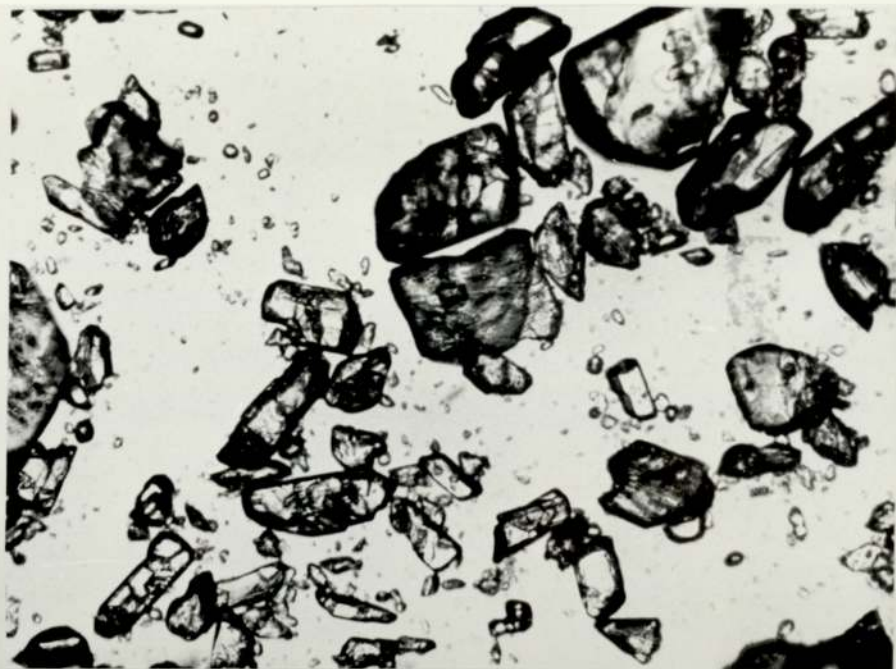
3.3. Apparatus and experimental procedure

3.3.1. Microelectrophoresis

(i) Apparatus

The equipment used for electrophoretic measurements was the Rank Particle Microelectrophoresis Apparatus Mark II (Rank Bros., Bottisham, Cambridge) as illustrated on the following plate.

The basic part of the instrument is the electrophoresis cell which may be thin walled and cylindrical or rectangular in cross section. The cell has an electrode at either end. Movement of the particle, under the influence of an applied potential, is viewed either by use of ultramicroscope illumination with the cylindrical cell, which is used

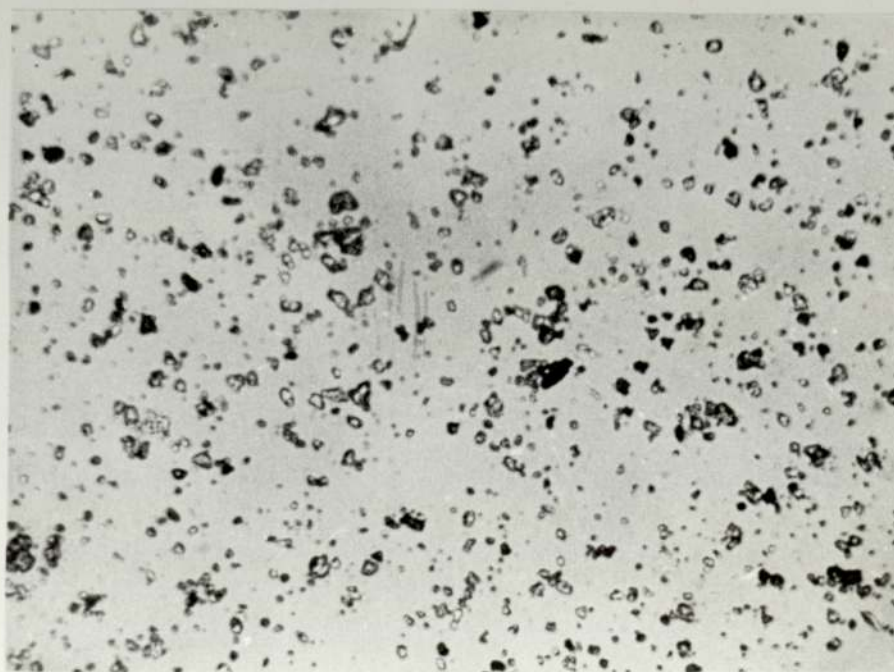
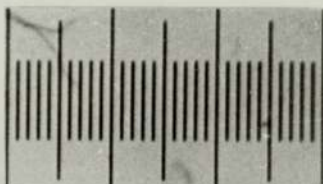


NALIDIXIC ACID

Scale

1 division

= 10 μm



THIABENDAZOLE

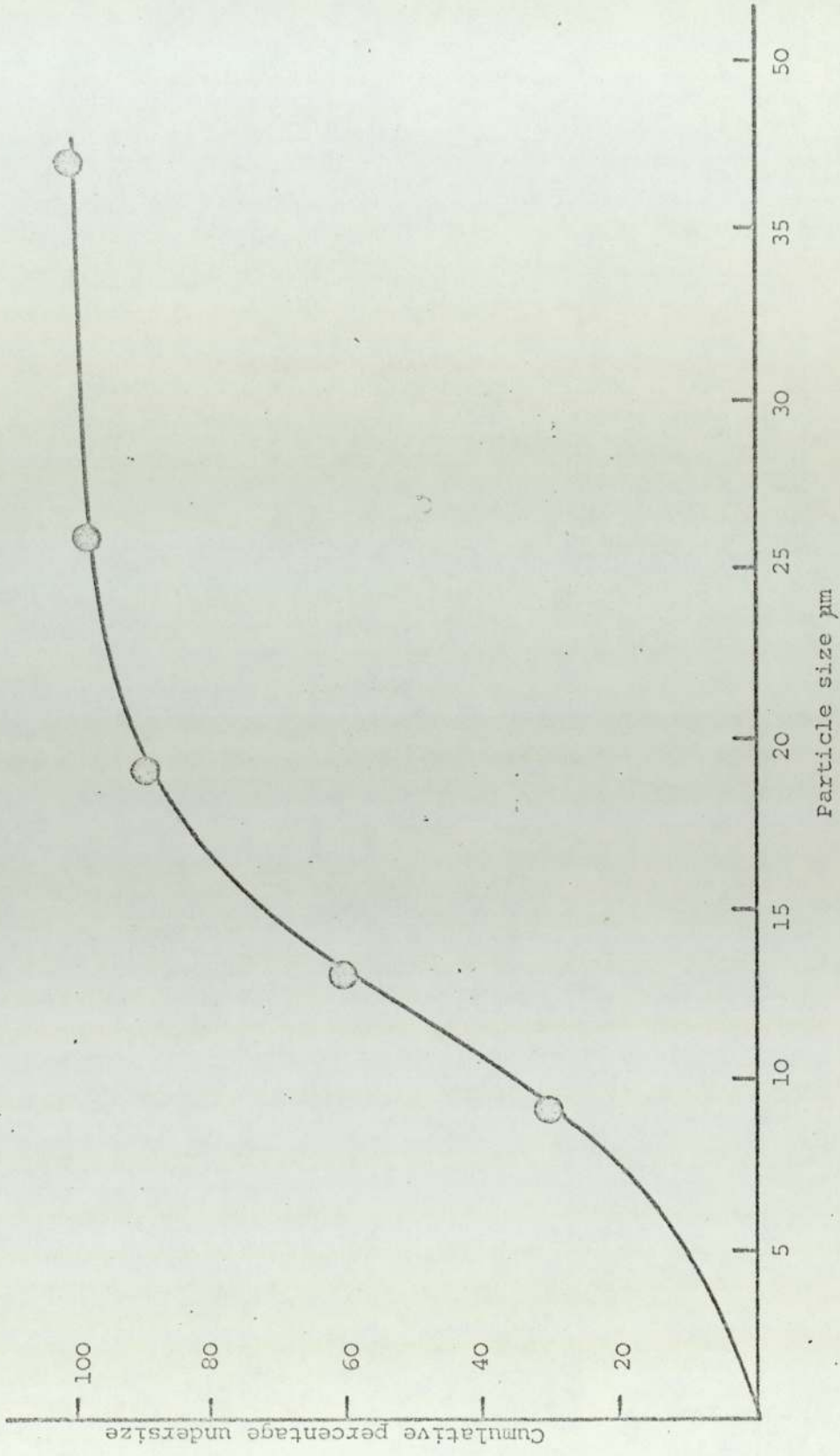
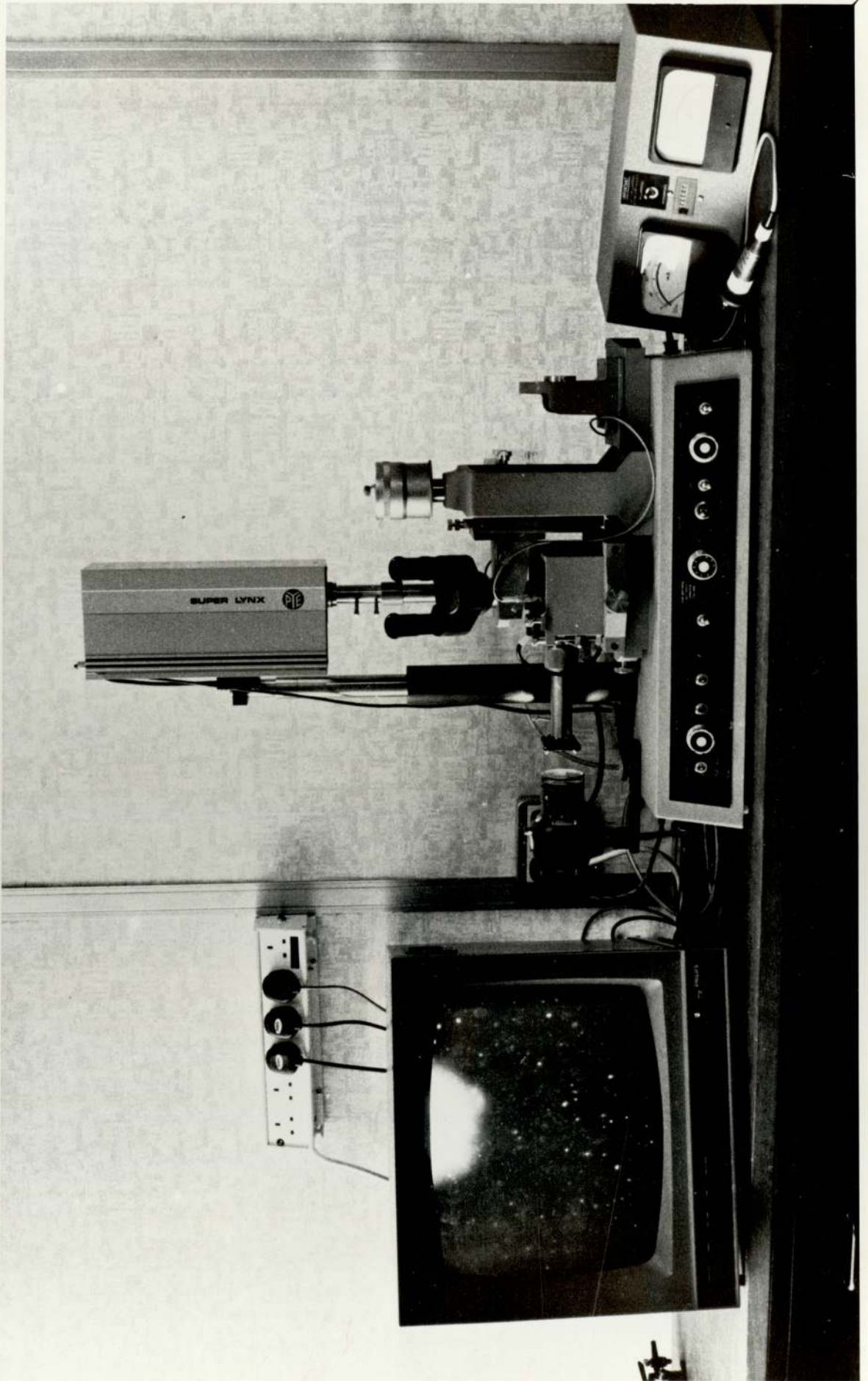


Fig X Particle size distribution Thiabendazole



for small particles, or by direct microscopic observation with the rectangular cell, which is used for large particles which sediment under the influence of gravity.

Each cell is immersed in a water thermostat bath. Illumination is by means of a quartz iodine 100 watt lamp controlled by a rheostat switch. The applied potential, also controlled by a rheostat switch, is recorded on a Voltmeter. The microscope eyepiece contains a graticule enabling the velocity of the particle to be measured by means of an electrical timer calibrated to 0.02 seconds. The instrument was modified by the addition of a Pye Super Lynx LDM 0001 Television Camera mounted on the viewing head so that the same image could be seen by the camera as through the microscope eyepiece. The camera extension tube contains a graticule and this, and the image, are projected onto the screen of a Philips television monitor.

For accurate temperature control of the water baths a Churchill pump and thermostat was used to circulate water at a temperature of $25^{\circ}\text{C} \pm 0.5^{\circ}\text{C}$. The eyepiece and camera graticules were calibrated with the microscope objectives in water and/or air as required, with a stage micrometer, also in water and/or air, for the normal eyepiece each square in the graticule was found to be $70\mu\text{m}$ and with the camera $60\mu\text{m}$, for the cylindrical cell and double these sizes for the flat cell.

(a) Electrodes

Platinum black electrodes were used as these are adequate for most salt concentrations commonly in use (126). At high concentrations of electrolyte "gassing" at the electrodes occurs at high applied potentials and this produces a "back e.m.f." or "polarization". The back e.m.f. however seldom rises to more than one volt in the time of a measurement and even if the applied potential is of the order of 10Vcm^{-1} , this will give an error of only 1% (127).

At high electrolyte concentration and high field strengths Joule heating in the dispersion is a limiting factor and, for example, in a thin walled cell serious difficulties arise at field strengths of 10Vcm^{-1} in concentrations of $2 \times 10^{-1} \text{mol dm}^{-3}$ and above of typical electrolytes. Since the heat produced is given by E^2K (E = field strength and K = specific conductivity of the electrolyte) difficulties due to Joule heating at high electrolyte concentration can be reduced by reducing the field strength (127). The majority of observations made in this work were of dispersions in solutions of $10^{-2} \text{mol dm}^{-3}$ electrolyte or less and difficulties due to heating were noticed on few occasions only.

In order to calculate electrophoretic mobilities it is necessary to determine the interelectrode distance for both the cylindrical and flat cells. This was obtained by measuring, by means of a Wayne-Kerr Conductivity Bridge, the conductance of standard solutions of potassium chloride for which the specific conductivity K has been well documented. The distance between the electrodes l is given by

$$K = \frac{l}{AR}$$

where A is the area of cross section of the cell and R the resistance of the liquid in the cell is given by l/λ , where λ is the measured specific conductance. K is the known specific conductance of the solution of potassium chloride used. The cross sectional areas of the cells can be obtained by microscopic observation of the cell dimensions, measured by means of the adjusting micrometers on the instrument.

By these means the inter-electrode distance of the flat cell was found to be 6.25cm and that of a typical cylindrical cell 7.06cm.

(b) Stationary levels

The walls of the electrophoresis cell will in general be charged in the presence of solvent - usually negative in water - and this will lead to a streaming of the oppositely charged solvent near the walls towards the appropriate electrode. This electroosmotic streaming velocity would be uniform across the cell were it not for the reverse flow at hydrostatic equilibrium (since the cell is closed) which itself obeys Poiseuille's law. The combination of these opposed flows results in a parabolic distribution of liquid speeds with depth, where the solvent itself is only stationary at well defined levels in the cell. Clearly the observed velocity of a particle is only equal to its own electrophoretic velocity when measured at these "stationary levels".

(i) Cylindrical cells (126)

The electro-osmotic effect by itself gives rise to a velocity $V_{E.0}$ across the cross-section of the cell towards the electrode of the same polarity as the charge on the cell wall. The reverse flow is according to Poiseuille's law, so that

$$V_L = V_{E.0} - c(a^2 - r^2)$$

where V_L is the liquid velocity at a distance r from the centre of the tube of radius a , and c is a constant. For zero overall liquid transport

$$\int_0^a V_L (2\pi r) dr = 0$$

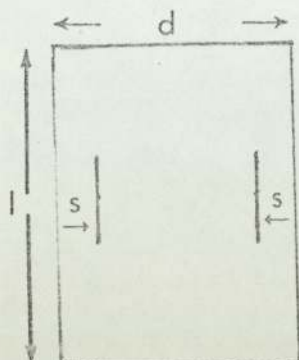
The solution of these expressions gives $c = 2V_{E.0}/a^2$ so that

$$V_L = V_{E.0} \left(\frac{2r^2}{a^2} - 1 \right)$$

The stationary level, i.e. the position where $V_L = 0$, is therefore located at $r = 0.707a$ or 0.146 of the internal diameter from the cell wall.

(ii) Flat cells

Calculation of the stationary levels for electrophoresis cells with an observation channel of rectangular cross section is more complex.



Komagata (128) has shown that the position of the stationary layers, s , is given by

$$\frac{s}{d} = 0.500 - \left[0.0833 + \frac{32}{\pi^5} \frac{d}{l} \right]^{\frac{1}{2}}$$

The stationary layer position is seen to depend on the ratio l/d .

For the flat cell used $d = 0.8\text{mm}$ and $l = 10.5\text{mm}$ and $s = 0.158\text{mm}$. The correctness of the calculated stationary levels of the cylindrical cell was checked using Human red blood cells, which have a mobility of $-1.31 \pm 0.03 \times 10^{-8} \text{ m}^2 \text{ s}^{-1} \text{ V}^{-1}$ in $6.67 \times 10^{-2} \text{ mol dm}^{-3}$ phosphate buffer at pH 7.4 and 25°C (129). For the flat cell, polystyrene latex the mobility of which had been found in the cylindrical cell, was used.

(c) Optical correction for cylindrical cells (127)

A cylindrical cell potentially introduces the complication of observation through curved glass. It is assumed that the cell and its containing tank are water filled, the normal situation for observation. The refractive index of the water is then written n_w and of the glass n_g . When the microscope is focussed on a point at right angles to the major axis of the capillary it is likely that, when viewing the stationary layer, this will be "off centre" i.e. the internal diameter is equal to da less a very small correction which at maximum is $\frac{2t^2}{da}$ where t is given by

$$t = g \left[1 - \frac{n_w}{n_g} \right]$$

where g is the thickness of the glass wall. Since g is itself related

to the apparent thickness of the wall, g_a , by

$$g = g_a \frac{n_g}{n_w}$$

it follows that an alternative form for t is

$$t = g_a \left[\frac{\frac{n_g}{n_w} - 1}{\frac{n_g}{n_w}} \right]$$

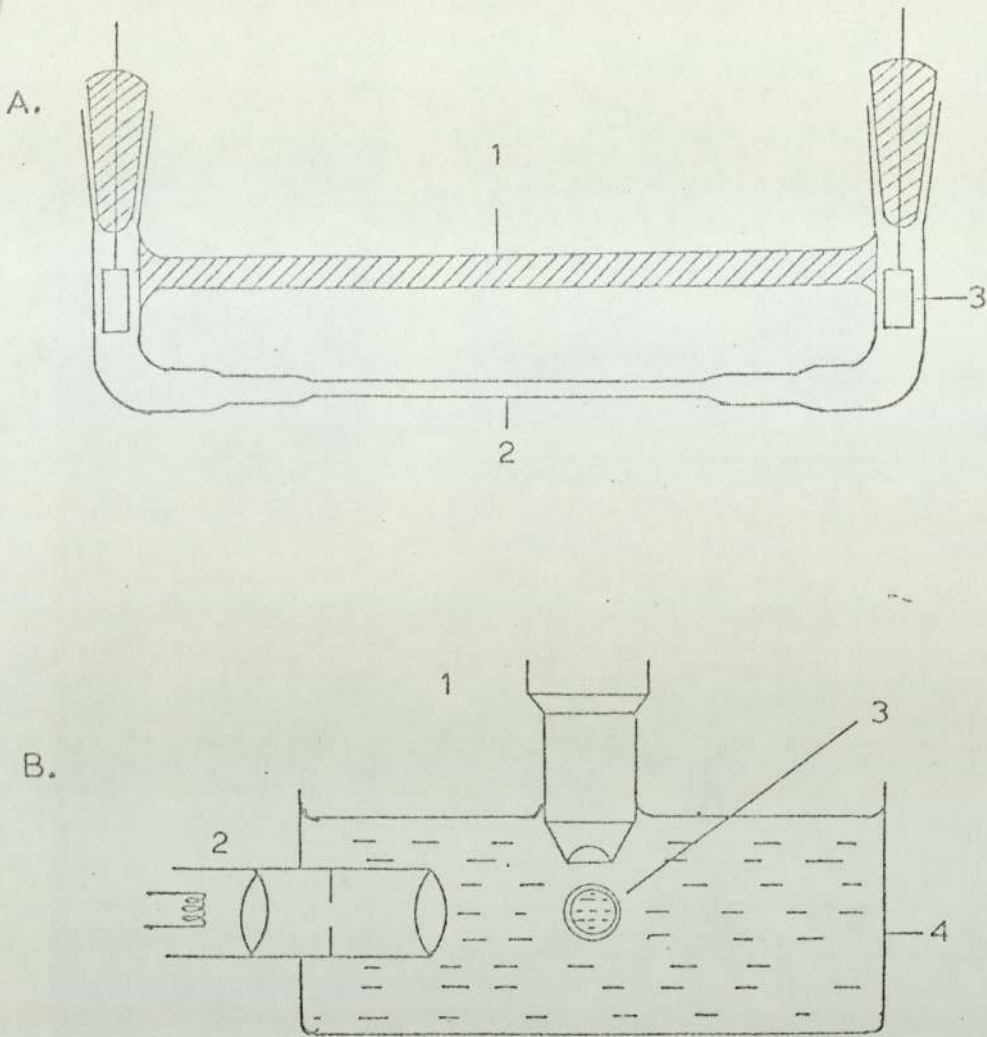
Substitution in these expressions ($n_g = 1.47$ for pyrex glass) shows that even if g_a were as great as $100\mu\text{m}$ the correction would be utterly negligible, the thickness of the cell wall of the cylindrical cell is ca. $65\mu\text{m}$ so that using thin wall cells the optical correction can be ignored. No optical correction is necessary to the position of stationary levels in flat cells.

(ii) Experimental procedure

(a) Cylindrical cell

The thin walled cell, constructed of Pyrex glass, is of the van Gils type (130) and is illustrated in Fig. XI. together with a diagram of the viewing arrangement.

The lamp, focussing lens and slit were adjusted so that the light emerging from the illuminating objective was a well defined beam coming to a focus within the cell, as narrow a slit width as possible being used to give better illumination of the stationary layer. The top surface of the capillary was then illuminated and the microscope focussed onto this, the relevant micrometer reading was noted; this procedure was repeated with the inside of the glass wall, the difference between the two micrometer readings giving the thickness of the cell wall. In use, the microscope was, for convenience, focussed onto the outside wall of the capillary and then the micrometer "racked in" the thickness of the cell wall and the stationary layer; it was then focussed onto the stationary plane and the light beam was adjusted to



A. Electrophoretic Cell

1. Strengthening Rod.
2. Observation Tube
3. Platinum Electrode.

B. Viewing Arrangement

1. Microscope Objective.
2. Light Source.
3. Cross-section of Electrophoresis Cell.
4. Thermostated Bath.

Fig XI A Schematic Diagram for the Electrophoretic Cell and Viewing Arrangement (After Shaw) (126)

illuminate this plane.

The cell was cleaned, before assembly, with chromic acid and well rinsed with distilled water; when assembled it was kept full of distilled water.

All solutions were made in 10^{-3} mol dm^{-3} NaCl to give a solution of suitable conductance and to keep the ionic strength, as far as possible, constant.

A portion of test dispersion, concentration of particles ca. 10^8 ml^{-1} , was taken and its pH measured by means of a Pye Unicam model 290 pH meter, adjustment of pH being made, if required by the addition of NaOH or HCl. The dispersion was then transferred to the microelectrophoresis cell and velocity measurements made. The cell was well washed with distilled water between samples and care was taken to completely fill the tube excluding air bubbles. Particle velocities were determined by timing individual particles over a fixed distance on the eyepiece scale, only light spots in sharp focus being timed. The current was adjusted to give a transit time of 5 to 10 seconds over the measured distance, where possible, as timings of this magnitude are optimum with respect to Brownian motion error and operator timing error. Particles were timed in alternate directions, by use of the reversing switch, so that the effect of drift, (due to leakage, electrode polarization etc.) can be largely eliminated. The velocity was calculated from an average of about 20 timings. Individual observations conform to Gauss' law of errors, hence the necessity to make a number of observations. With electrophoretically homogenous dispersions, careful experimentation will generally lead to single velocity determinations (corrected for any persistent drift) with an average deviation of ca 5 to 7 per cent from the mean. The probable error for an electrophoretic mobility calculated from the mean of 20 velocity determinations

will (at best) be about 2% (126).

(b) Flat cell

The flat cell is constructed of silica. The point of view is midway between the top and bottom of the cell. The focussing onto the outside of the cell wall, and the measurement of the thickness of the cell wall, were carried out as for the cylindrical cell. Viewing is by direct observation with the microscope the stationary plane being illuminated via a low power dark ground condenser. The microscope was focussed onto the stationary layer as described previously. The microscope objective is air mounted outside the thermostat bath, because of this only a low power objective could be used.

Measurements were made with dispersions as described for the cylindrical cell.

(c) Calculation of electrophoretic mobilities

A computer programme was used to calculate electrophoretic mobilities from the timings made. The computer is a Digico Micro 16 digital computer using 'Mathchat' language. A copy of the programme print out and a specimen sheet of calculations are shown in Figs. XII and XIII respectively. Standard deviations were normally of the order of 2-3%, except for low charge particles $< 10\text{mV}$, where deviations of ca. 10% were sometimes found; such errors are normally of only small magnitude when considering the calculated values of mobility and zeta potential.

3.3.2. Sedimentation volumes

2% w/v of the drugs Betamethasone, Griseofulvin, Nalidixic Acid and Thiabendazole were made into suspensions with the requisite vehicle, all of which contained $10^{-3} \text{ mol dm}^{-3}$ NaCl. Suspensions were made in 50ml. stoppered measuring cylinders.

```

5T , "HOW MANY SETS OF READINGS ARE THERE " : A N
10FOR I=1,1,N:DO 30/234
25GO 240
30S SUM=0:S TOT=0
40T !!, "TYPE IN TWENTY READINGS", !!
50FOR J=1,1,20:DO 60
55GO 65
60A REDC(J):S SUM=SUM+REDC(J):T !
65S AV=SUM/20:T !, "THE AVERAGE READING IS " , 20.06, AV
80FOR J=1,1,20:DO 90
85GO 100
90S TOT=TOT+(REDC(J)-AV)**2
100S VAR=TOT/19:T !!, "VARIANCE IS " , 20.06, VAR
110S SDEV=RSQ(VAR):T !!, "STANDARD DEVIATION IS " , 20.06, SDEV
140T !!, "TYPE VALUE 120/140/ETC. " : A GV
150T !!, "TYPE VOLTAGE " : A VOL
160T !!, "TYPE DISTANCE " : A DIS
165T !!, "TYPE VALUE OF Y " : A X(I)
170S A=GV/AV:S B=VOL/DIS:S U(I)=A/B:T !,
200S PAV=(SDEV/AV)*100
210T !!, "STANDARD DEVIATION IS " , 20.06, PAV, " % OF THE MEAN"
220S PU=U(I)*SDEV/AV:T !!, 20.06, PAV, " % OF U IS " , PU
230S YMS(I)=U(I)-PU:S YPS(I)=U(I)+PU
232T !!, 20.06, " X=", X(I), " Y=", U(I), " Y-S=", YMS(I)
234T 20.06, " Y+S=", YPS(I)
240T !!!!!, " Y Y Y-S"
245T , " Y+S", !!
250FOR I=1,1,N:DO 260
255QUIT
260T !, 20.06, " ", X(I), " ", U(I), " ", YMS(I), " ", YPS(I)

```

Figure XII

TYPE IN TWENTY READINGS

:4.66,
:4.74,
:4.96,
:4.66,
:4.82,
:4.74,
:4.58,
:4.68,
:4.7,
:4.9,
:4.68,
:4.82,
:5.04,
:4.82,
:4.66,
:5.08,
:4.88,
:4.52,
:4.66,
:4.68,

THE AVERAGE READING IS 4.784000

VARIANCE IS 0.024825

STANDARD DEVIATION IS 0.157560

TYPE VALUE 120/140/ETC. :140,

TYPE VOLTAGE :60,

TYPE DISTANCE :6.25,

TYPE VALUE OF X :0.00001,

STANDARD DEVIATION IS 3.293485 % OF THE MEAN

3.293485 % OF U IS 0.100397

X= 0.000010 Y= 3.048355 Y-S= 2.947958 Y+S= 3.148752

Figure XIII

Dispersion of the drugs, all of which are hydrophobic to some extent, was achieved by triturating with the vehicle in a mortar and pestle; when surfactant solutions formed the vehicle, these were introduced as concentrated solutions in order to aid dispersion, and afterwards diluted. The suspension was transferred to a measuring cylinder, the pH measured and adjusted as necessary, and then made up to volume.

The suspension was then shaken in a constant temperature water bath at $25^{\circ} \pm 0.5^{\circ}\text{C}$ for 24 hours, to allow for complete adsorption, Elworthy and Guthrie(119) having shown that sixteen hours was necessary for equilibrium adsorption of C_{16}E_y nonionic surfactants on Griseofulvin. The suspension was then stored in an incubator for three days at $25^{\circ} \pm 0.5^{\circ}\text{C}$ for sedimentation to occur, Mathews and Rhodes (26) have shown that this length of time is required for completion of sedimentation in such suspension systems. Sedimentation volumes were then immediately measured, suspension characteristics noted and the solid redispersed as indicated in Section 6. The pH of the suspension was then checked and electrophoretic mobilities measured in the usual way.

SECTION 4.

MICROELECTROPHORESIS OF POLYSTYRENE LATEX,

RESULTS AND DISCUSSION

4.1. Effect of pH on the electrophoretic mobility and zeta potential.

Using the procedure detailed in Section 3 examination was made of the variation of mobility, and hence of zeta potential, of the polystyrene latex dispersion in 10^{-3} mol dm $^{-3}$ sodium chloride solution, as a function of pH at 25°C. Adjustment of pH was made by addition of hydrochloric acid or sodium hydroxide solution. Results are given in Table I and Fig. XIV. The plot in Fig. XIV. shows an increase in mobility (the particle is negatively charged) over the pH range 2 to 5 which is consistent with the ionization of carboxyl groups (120) (121). Above pH 5 the mobility is constant indicating complete ionization of the carboxyl groups. After pH 9 the mobility rises again from 5.8×10^{-8} m 2 s $^{-1}$ V $^{-1}$ to 6.25×10^{-8} m 2 s $^{-1}$ V $^{-1}$ at pH 11, the above references indicate that this is atypical. Goodwin et al (115) have shown that primary alcohol groups and/or hydroxyl groups may be present as the result of acid hydrolysis of sulphate, but the primary alcohol groupings are unlikely to ionise until a much higher pH is reached; the mobility increase could be due therefore to a surface excess of hydroxyl ions as the concentrations of this species increases with pH.

The mobility could be assumed to be constant, however, between pH 6 and 9 provided that the ionic strength was kept constant, and subsequent measurements were carried out between these pH limits and where possible at ca pH 7.0. The sharp fall off in mobility as pH is decreased below 5 is indicative of the presence of -COOH groups only, as Ottewill and Shaw (120) found that the mobility tailed off much more slowly if sulphate groups (from the persulphate used in the polymerisation process) were also present. These results confirm those found

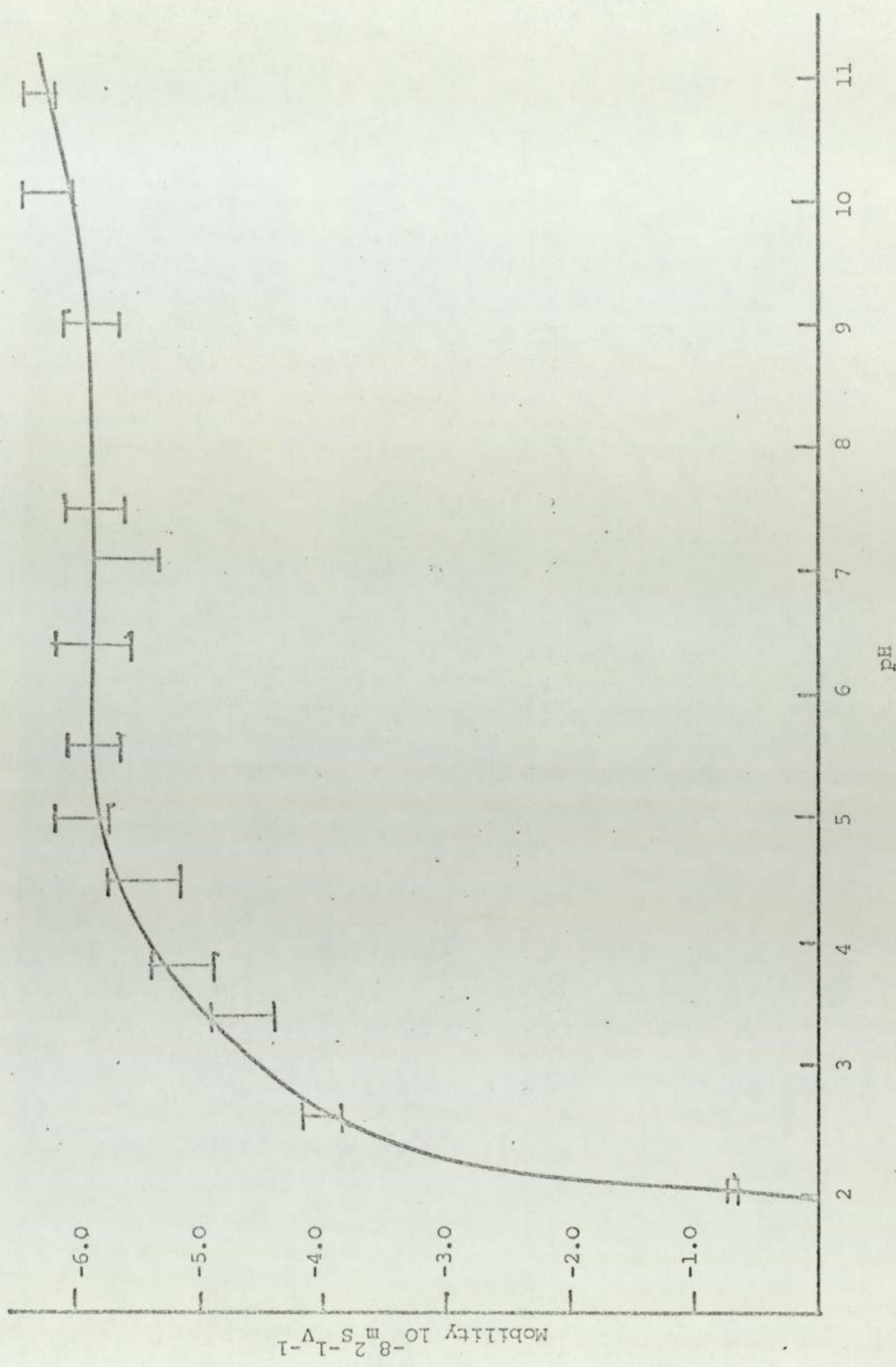


Fig XIV Mobility versus pH for polystyrene latex in $10^{-3} \text{ mol dm}^{-3} \text{ NaCl}$ at 25°C

from conductometric titration that the only ionizing groups present on the latex are carboxyl groups.

4.1.1. Surface and bulk dissociation constants

The problem of determining pK values from electrophoresis data and possibly using them to identify surface groupings has been examined by Ottewill & Shaw (120).

At the shear plane an acid surface dissociation constant can be defined (neglecting activity coefficients) by

$$K_s = \frac{[H_s^+][A_s^-]}{[HA_s]} \quad 4.1.$$

The hydrogen ion concentration at the shear plane $[H_s^+]$ can be related to the bulk hydrogen ion concentration $[H_b^+]$ by the Boltzmann distribution

$$[H_s^+] = [H_b^+] \exp(-e\zeta/kT). \quad 4.2.$$

Combination of 4.1 and 4.2 gives

$$pK_s = pH_b - \log_{10} \frac{[A_s^-]}{[HA_s]} + \frac{e\zeta}{2.303kT} \quad 4.3.$$

Considering only monovalent charged groups, the charge density σ at the shear plane is given by:

$$\sigma = n_{As^-} e$$

where n_{As^-} is the number of ionized groups per unit area contributing to the electrokinetic charge.

If σ_0 is the surface charge density under conditions of complete ionization

$$\frac{[A_s^-]}{[HA_s]} = \frac{\sigma}{\sigma_0 - \sigma} \quad 4.4.$$

At low potentials σ and ζ are proportional, therefore,

$$\frac{[A_s^-]}{[HA_s]} = \frac{\zeta}{\zeta_0 - \zeta} \quad 4.5.$$

where ζ_0 is the limiting zeta potential corresponding to complete ionization.

$$\text{At the bulk pH where } \zeta = \frac{1}{2} \zeta_0, \log_{10} \frac{[A_s^-]}{[HA_s]} = 0,$$

$$\text{therefore } pK_s = pH_b \left(\zeta = \frac{1}{2} \zeta_0 \right) + \frac{e \zeta}{2.303kT} \quad 4.6.$$

This expression will only be valid at low potentials since proportionality between σ and ζ , and constant location of the shear plane have been assumed.

The bulk dissociation constant, K_b , is given (neglecting activity coefficients) by

$$pK_b = pH_b - \log_{10} \frac{[A_b^-]}{[HA_b]} \quad 4.7.$$

$$\text{Assuming that } \log_{10} \frac{[A_b^-]}{[HA_b]} = 0 \text{ at } \zeta = \frac{1}{2} \zeta_0,$$

combination of 4.6. & 4.7. gives

$$pK_s = pK_b + \frac{e \zeta}{2.303kT} \quad 4.8.$$

$$\text{and } pK_b = pH_b \left(\zeta = \frac{1}{2} \zeta_0 \right). \quad 4.9.$$

The mobility of the latex when ionization of the carboxyl groups is complete is $5.8 \times 10^{-8} \text{ m}^2 \text{ s}^{-1} \text{ V}^{-1}$; interpolation of this value in table 4 of Ottewill and Shaw (99) (Appendix 1) gives a value of ζ_0 of 103mV, and the mobility value for a ζ of 51.5mV is 3.55 this corresponds to a pH value and from 4.9. a pK_b of 2.75; this value agrees reasonably well with that of ca 3.0 normally found for carboxyl groups.

Inserting the relevant values into equation 4.8. gives a pK_s value of 3.62, which seems to be in agreement with that found by Ottewill & Shaw (120), at that zeta potential, for carboxylated polystyrene latex dispersions. They found, by extrapolation, a pK_s of 4.64, $\zeta = 0$, which agrees well with the calculated value of 4.31 for phenylacetic acid which

can be looked upon as the 'parent' of the polystyrene carboxylic acid group.

Owing to the neglect of activity coefficients, the assumption that $\log_{10} \frac{A_b}{HA_b} = 0$ at $\zeta = \frac{1}{2}\zeta_0$ is probably not valid except perhaps

at low zeta potential, pK values obtained from electrokinetic experiments cannot, therefore, be related accurately to pK values obtained by titration especially at high potentials.

4.1.2. Calculation of surface charge densities.

1. Surface charge density at the surface

The steady state mobility above ca. pH5 indicates that ionization of the carboxyl groups is, as far as can be detected by electrophoresis, complete. The surface charge density at the surface can be estimated on the basis of one electronic charge, e, per carboxyl group. From conductometric titration data it was found that the number of charged groups ($n_{\text{COO}'}$) per unit area was $1.84 \times 10^{17} \text{ m}^{-2}$ (area per group 5.44 nm^2).

The surface charge density at the surface σ_0 is thus given by:

$$\begin{aligned} \sigma_0 &= (n_{\text{COO}'})e \\ &= 2.94 \times 10^{-2} \text{ Cm}^{-2} \end{aligned}$$

2. Surface charge density at the surface of shear

As shown in Section 2.4.4, equation 2.68, the charge density at the surface of shear can be calculated from:

$$\begin{aligned} \sigma &= \left(8 n_0 \epsilon kT \right)^{1/2} \sinh \frac{ze\zeta}{2kT} \\ &= \left(8 N_A c \epsilon kT \right)^{1/2} \sinh \frac{ze\zeta}{2kT} \end{aligned}$$

where N_A is the Avogadro number, c the concentration in mol m^{-3} and ϵ the permittivity (8.85×10^{-12} times the value for the dielectric constant).

For $10^{-5} \text{ mol dm}^{-3}$ (1 mol m^{-5}) sodium chloride at 25°C , $Z = 1$,

$$\epsilon = 78.3 \times 8.85 \times 10^{-12} \text{ and } \zeta = 103 \times 10^{-3} \text{ V:}$$

$$\sigma = 1.34 \times 10^{-2} \text{ C m}^{-2}$$

The electrokinetic surface charge density is lower than the surface charge density at the surface because counter ion association takes place at the carboxyl groups.

The number of carboxyl groups ionized at any particular pH can be found by use of the dissociation exponent pK_s :



where HA represents the unionized carboxyl group and α the fraction ionized.

The dissociation constant

$$K_s = \frac{[H^+][A^-]}{[HA]} = [H^+] \frac{\alpha}{1-\alpha}$$

taking logarithms:

$$-\log K_s = -\log [H^+] - \log \frac{\alpha}{1-\alpha}$$

or
$$pK_s = pH - \log_{10} \frac{\alpha}{1-\alpha} \qquad \qquad \qquad 4.10.$$

at $\alpha = 0.5$, $pK_s = pH$, pK_s as found previously is 3.62. Hence 50% ionization of carboxyl groups has occurred at pH 3.62.

Equation 4.10 can be used to calculate the degree of ionization for a particular pH, the actual number of carboxyl groups ionized will be $1.84 \times 10^{-17} \alpha \text{ m}^{-2}$. A plot of n_{COO^-} versus pH is shown in Fig. XV and the results in table II. The plot shows a rapid fall off to zero of ionized groups between pH 5 and 2 again consistent with the presence of carboxyl groups.

4.1.3. Calculation of the potential at the surface, Ψ_0

For a diffuse double layer equation 2.12, section 2.1.1., gives the surface charge density at the surface σ_0 as

$$\sigma = \left(8 n_0 \epsilon kT \right)^{1/2} \sinh \frac{ze\Psi_0}{2kT}$$

$$= \left(8 N_A c \epsilon kT \right)^{1/2} \sinh \frac{ze\Psi_0}{2kT} \qquad \qquad \qquad 2.12.$$

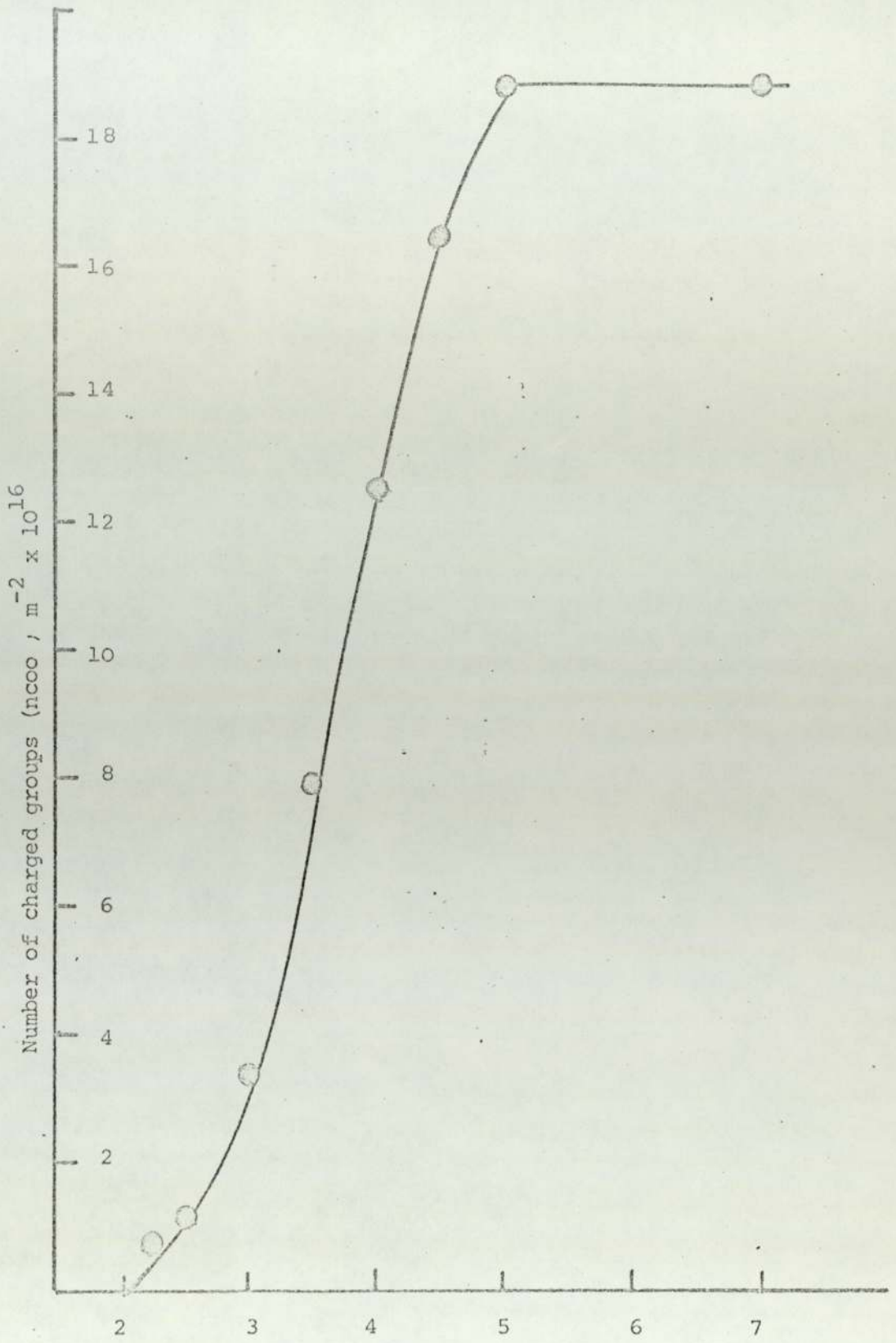


Fig xv Polystyrene latex, variation in number of ionized carboxyl groups with pH.

TABLE II

Polystyrene latex in 10^{-3} mol dm^{-3} Na Cl. Variation of surface ionized carboxyl groups, surface charge density σ_0 (α) and surface potential ψ_0 , with pH. .

pH	Mobility $10^{-8} \frac{\text{cm}^2}{\text{V} \cdot \text{s}}$	Zeta Potential mV	Fraction of carboxyl groups ionized α	$n \text{ } \text{COO}^-$ $\times 10^{17}$	σ_0 $\times 10^{-2} \text{ C}$	ψ_0 mV	ζ/ψ_0
7.0	-5.8	-103	1	1.84	2.94	-142	0.725
5.0	-5.8	-103	1	1.84	2.94	-142	0.725
4.5	-5.5	-93	0.88	1.62	2.59	-136	0.684
4.0	-5.25	-86	0.68	1.25	2.00	-123	0.700
3.5	-4.75	-74	0.43	0.79	1.26	-100	0.74
3.0	-4.1	-61	0.18	0.33	0.53	-59	1.03
2.5	-2.9	-41	0.06	0.11	0.18	-24	1.7
2.25	-2.0	-28	0.037	0.07	0.11	-15	1.86
2.0	0	0	$\rightarrow 0$	$\rightarrow 0$	$\rightarrow 0$	$\rightarrow 0$	$\rightarrow \infty$

At complete ionization $\sigma_0 = 2.94 \times 10^{-2} \text{ C m}^{-2}$, using the condition where we have $10^{-3} \text{ mol dm}^{-3}$ sodium chloride at 25°C .

$$\begin{aligned}\sigma_0 &= 2.94 \times 10^{-2} \text{ C m}^{-2} \\ &= 3.70 \times 10^{-3} \sinh 19.45 \Psi_0\end{aligned}$$

From which

$$\Psi_0 = 0.142\text{V} = 142\text{mV}$$

The surface is negatively charged, hence this is a negative value. The potential therefore drops from -142mV to -103mV , the latter being the zeta potential at the point where ionization is complete.

For each fraction α of the carboxyl groups ionized, there will be a partial dissociation surface charge density σ_α , where

$$\sigma_\alpha = \alpha \sigma_0$$

For each value of α reported in table II a value of σ_α was calculated. From these values using equation 2.12, with σ_α replacing σ_0 , the corresponding surface potential Ψ_0 was found, the ratio of each Ψ_0 to its corresponding zeta potential, i.e. $\frac{\zeta}{\Psi_0}$ was then calculated, results are shown in table II.

Davies and Rideal (131) found that for several experimental systems, the ratio $\frac{\zeta}{\Psi_0}$ was constant of value ca 0.5 provided that the ionic strength or surface charge density were not lowered, when the value $\rightarrow 1$.

The values of the ratio above pH 3.5 found here are constant, but of the order of 0.7, a constant value would be expected if the assumption is made that there is no specific interaction within the Stern plane. The difference in magnitude of the ratios found here from those reported by Davies and Rideal may be due to the method used in calculating the zeta potentials. If the Smoluchowski equation (no account being taken of Ka effects) is used here values of zeta potentials giving ratios $\rightarrow 0.5$ are obtained.

Deviations from the constant ratio which occur at low pH values are due to the lowering of surface charge density and are as reported by Davies and Rideal. The ratio values > 1 may well be due to the choice of pK_s value of 3.62 used in calculating σ_a , the chosen value relating to $\frac{1}{2}\zeta_0 = -51.5\text{mV}$. Ottewill and Shaw (120), plotting pK_s versus $\frac{1}{2}\zeta_0$ for various carboxylated polystyrene latices, obtained an extrapolated pK_s value at zero zeta potential of 4.64. Estimating from their results a pK_s of 4.5 at $\frac{1}{2}\zeta_0 = -14\text{mV}$ to calculate $\frac{\zeta}{\Psi_0}$ at pH 2.25 gives a value of the ratio of ca 1.3 which, within the limits of error involved, would seem a more realistic figure than that of 1.86 reported in table II. It may well be necessary at the lower pH values to choose a pK_s value, for calculation of α , corresponding to the $\frac{1}{2}\zeta_0$ for that pH.

4.2. Effect of nonionic surface active agents on the electrophoretic mobility and zeta potential.

The effect that adsorption of nonionic surface active agents of the polyoxyethylene mono alkyl ether class, $C_x E_y$, can be expected to have on the electrophoretic mobility and zeta potential depends on their affect on the structure of the double layer at the charged solid/liquid interface. The situation may be represented pictorially as in Fig. XVI (132).

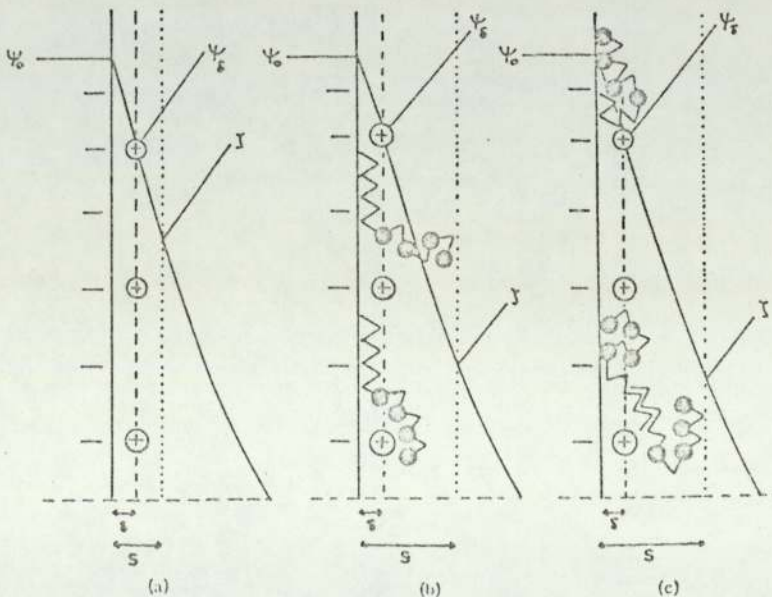


Fig. XVI Schematic representation of the situation at a charged solid/liquid interface in the presence and absence of nonionic surfactants.

Here two possible modes of adsorption at low surface coverages are considered. In Figure XVI(b) adsorption has occurred via the hydrocarbon chain leaving the ethylene oxide chain in the solution. In Figure (c) adsorption has occurred mainly via the ethylene oxide chain, but in addition there is also attachment by the alkyl chain; with both models if the energy of adsorption of the nonionic surfactant is greater than that of the cations in the Stern layer, some of the cations will be displaced, causing a change of the Stern potential. In both cases the adsorbed molecules project some way beyond the original plane of shear, and apart from changes in the zeta potential occasioned by changes in the Stern potential there will also be a change as a result of the mechanical displacement of the plane of shear into the solution.

4.2.1. Effect of concentration.

The nonionics used were $C_{16}E_{10}$, $C_{16}E_{18}$, $C_{16}E_{30}$, $C_{16}E_{45}$ and $C_{16}E_{60}$. Results are given in Fig. XVII & Tables III&IV. Measurements were carried out at ca. pH 7.0 at 25°C in 10^{-5} mol dm⁻³ sodium chloride. All curves show the same effect with increasing concentration of nonionic surfactant, i.e. a decrease in mobility of the polystyrene particles to a value at ca. 10^{-6} mol dm⁻³ which then remains steady until ca. 10^{-5} mol dm⁻³, when, particularly as the number of ethylene oxide unit increases, a fall off in mobility occurs as the concentration is increased to 10^{-2} mol dm⁻³.

The indication is therefore, that, with all these nonionic surfactants, adsorption onto the latex particle takes place until a limiting state is reached, presumably when some form of monolayer is present, and then no further adsorption occurs. In all cases the mobility shows no alteration in the region of the critical micelle concentration.

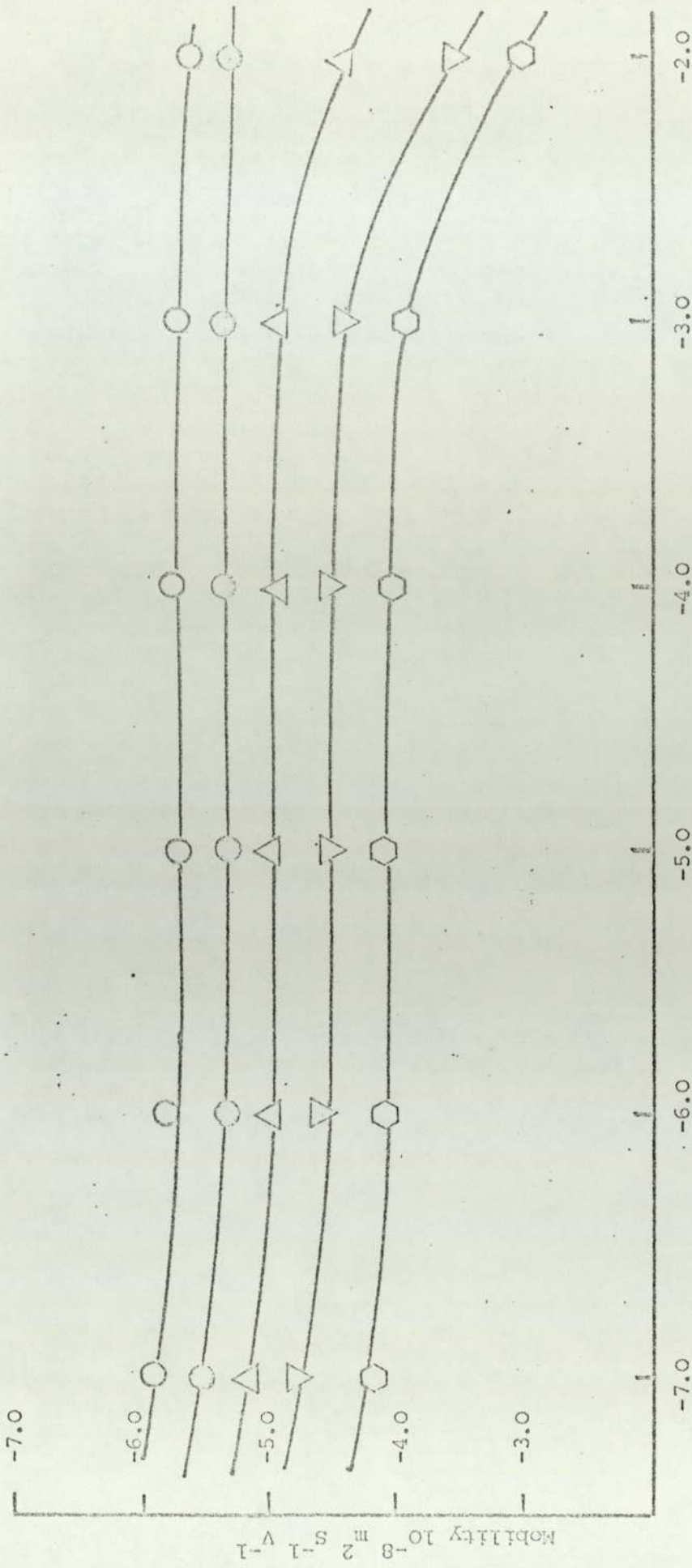


Fig XVII Mobility versus concentration non ionic surfactant
 $\text{C}_{16}\text{E}_{10}$ ○ ; $\text{C}_{16}\text{E}_{18}$ ○ ; $\text{C}_{16}\text{E}_{30}$ △ ; $\text{C}_{16}\text{E}_{45}$ △ ; $\text{C}_{16}\text{E}_{60}$ ○.

Ottewill (133) has reviewed the adsorption of certain nonionic surfactants of this type onto a negatively charged surface. He considered that at low surface coverage, adsorption at the particle surface could occur via the hydrocarbon chain leaving the ethylene oxide chain in solution, or by adsorption mainly via the ethylene oxide chain, but in addition by the alkyl chain, i.e. as illustrated in the previous subsection. This would account for the gradual decrease in mobility until the plateau region is reached.

At higher coverage it is possible that the adsorbed molecules exist either:

- (i) as a closely packed vertically oriented monolayer, or,
- (ii) as a multilayer, or,
- (iii) as a monolayer, with molecules looped around the particle attached by both the hydrocarbon chain and the ethylene oxide groups.

4.2.1.1. Evidence for a closely packed vertically oriented monolayer.

Mathai and Ottewill (134) made electrokinetic measurements, using microelectrophoresis, on silver iodide particles in the presence of a series of homogenous polyoxyethylene monoalkyl ethers, C_8^E6 , C_{10}^E6 , C_{12}^E6 , C_{16}^E6 and C_{16}^E9 . At low concentrations of nonionic surfactant the mobility decreased very slowly with increase in concentration. However, just before the cmc a sharp change of gradient occurred. Comparison of these results with adsorption isotherms for certain of the nonionics used showed that the adsorption behaviour was reflected in the form of the electrokinetic curves; in both cases the shape of the curve commenced to change just below the cmc, the mobility starting to decrease sharply at almost the same concentration of nonionic surfactant as that at which the number of molecules adsorbed per unit area commenced to rise.

They interpreted the results to mean that in the region of low surface coverage the nonionic molecules are lying in a looped or extended

form on the particle surface and only a small decrease in mobility occurs. Since the nonionic surface active agent does not itself contribute any free charges to the electrical double layer, the decrease must occur because of a shift of the plane of shear or of the zero point of charge. Both in fact probably contribute to the decrease in electrokinetic potential and are accompanied by some displacement of ions from the neighbourhood of the surface. In the region of the cmc more extensive adsorption takes place to form surface aggregates and a considerable shift of the plane of shear occurs - this suggests that the molecules are vertically orientated. Above the cmc the increase in amount adsorbed is very small and hence only small changes of mobility were observed - suggesting that multilayer formation has not occurred.

Mathai and Ottewill also found that the mobility against concentration nonionic surfactant plots were very similar for both negatively charged and positively charged silver iodide sols, suggesting that the adsorption of the nonionic material was not very sensitive to the nature of the charge on the solid surface.

Ottewill and Walker (29), in studies of the adsorption of $C_{12}E_6$ on polystyrene latex, concluded, that from the adsorption curves obtained, adsorption of a vertically orientated monolayer of $C_{12}E_6$ molecules was completed on the latex particle surface at about the cmc of the surface active agent. The area per molecule obtained at saturation was in reasonable agreement with this concept. The thickness of the adsorbed layer on the latex surface as obtained by sedimentation studies appeared to confirm that the molecules were vertically orientated. They also suggested that there was a probable change from horizontally adsorbed molecules to vertical orientation in the region of the cmc. These workers also found that the layer was heavily hydrated, probably owing to hydrogen bonding between the ether oxygens of the ethylene oxide

units and the water molecules.

4.2.1.2. Evidence for multilayer formation

The simplest form of multilayer would be a bimolecular leaflet formation, although aggregation may occur on the surface to give less regular structures. It is however probably unlikely that such a bimolecular layer would form on polystyrene latex (135).

Evidence for the formation of multilayers does, however, exist. Watanabe et al (136) measured the differential capacity of the mercury/sodium sulphate solution interface at various concentrations of nonionics of the polyoxyethylene type; their results showed that a transition from monolayer to multilayer adsorption appeared to occur in the region of the cmc, they also concluded that there was some attachment to the surface by means of the ethylene oxide chains.

Daluja and Srivastava (137) examined the effect of polyoxyethylene monoalkyl phenyl ethers on the mobilities of As_2S_3 and Sb_2S_3 sols. Whilst their results were similar to those found by Mathai and Ottewill (134), they attributed the fall off in mobility that occurred with increasing concentration to the adsorption of micelles. However no values were given to show that the mobility fall occurred at the cmc of the nonionic material.

4.2.1.3. Evidence for monolayer formation with attachment by hydrocarbon chain and ethylene oxide groups.

Elworthy and Guthrie (119) carried out an investigation of the adsorption of nonionic surface active agents at the Griseofulvin solution interface, using $C_{16}E_{10}$, $C_{16}E_{23}$, $C_{16}E_{45}$, $C_{16}E_{60}$, (the commercially available forms) $C_{16}E_7$ and $C_{16}E_9$. Isotherms for this $C_{16}E_x$ series were of the Langmuirian type over the concentration range studied, the region of maximum adsorption occurring in most cases at or close to the cmc.

Experiments with polyethylene glycol 400 indicated that the ethylene oxide groups had a tendency to adsorb at the Griseofulvin surface and the area per molecule at monolayer coverage indicated that the glycol is likely to be adsorbed flat on the surface. When the surface active agent corresponding to the polyethylene glycol 400 i.e. $C_{16}E_9$ or $C_{16}E_{10}$, was used the area per molecule decreased by factors of 4 to 5. This indicated that the hydrocarbon chain is adsorbed at the surface, if it were not, the area per molecule would not change significantly. Increasing the ethylene oxide chain length of the surface active agent had the effect of decreasing the maximum amount adsorbed and increasing the area per molecule. They thought that the hydrocarbon chain was adsorbed onto the surface and that the polyoxyethylene chain bent towards it and was also attached to it. Comparison of the values for the areas per molecule at the Griseofulvin interface with those for the closest packing at the air water interface showed that the former were greater, thus indicating that the ethylene oxide chain was contributing more to the area per molecule at the solution solid interface than at the air water interface, and also that the surfactant containing the shortest polyoxyethylene chain was most closely packed, which is in accordance with the work of Corkill et al (138), (139).

4.2.1.4. Other evidence for the adsorption of nonionic surfactants on charged particles.

Glazman (140) working with nonionic polyethers adsorbed onto negatively charged particles, found that the zeta potential was reduced with increasing concentration of nonionic material. A similar result was obtained by Elworthy and Florence (141) with emulsion systems. On the other hand Glazman and Kabysh (142) found that adsorption of polyethers on positively charged silver iodide sols resulted in charge reversal; whilst ether oxygens in the ethylene oxide adducts may form

oxonium ions (143) it is unlikely that positively charged chains could accomplish the sign change.

4.2.1.5. Conclusions concerning the form of the adsorbed layer in this work.

The surface of Griseofulvin - the microelectrophoretic properties of which have been examined and are reported in Section 5 -is predominately hydrophobic. Indications are that its behaviour is similar to that of polystyrene latex.

The polystyrene latex has one carboxylic acid group, area 0.205nm^2 , per 5.44nm^2 of surface area, and although there is the possibility of primary alcohol and or hydroxyl groups being present, this large area is predominately hydrophobic in character. Adsorption of the alkyl chains will occur on this hydrophobic surface by the hydrophobic effect. The ether oxygens of the ethylene oxide units may also associate with polar groupings by hydrogen bonding and this will occur if primary alcohol and or hydroxyl groups are present. Hydrogen bonding may also occur between the ether oxygens and the solvation sheath surrounding the ionized carboxylic acid groups. It appears likely therefore that, as indicated by the concentration against mobility plots, adsorption of these nonionics occurs both by means of the alkyl chain and the ethylene oxide units. The molecules will thus loop themselves around the particle with the ethylene oxide chains at the extreme edge of the adsorbed layer, thus shielding the alkyl chains against further adsorption. Monolayer adsorption would thus appear to be favoured and this would account for the plateau region on the curves even above the cmc.

The fall off in mobility which occurs at high concentration, well above the cmc, is most probably due to the viscosity increase of the bulk solution and its effect on mobility. For example the viscosity

of solutions of $C_{16}E_{60}$ at $25^{\circ}C$ are as follows:

$$10^{-3} \text{ mol dm}^3, 0.9612 \text{ cp} \quad (152)$$

$$10^{-2} \text{ mol dm}^3, 1.3940 \text{ cp}$$

the increase in viscosity with concentration would change the steady state mobility of $4.1 \times 10^{-8} \text{ m}^2 \text{ s}^{-1} \text{ V}^{-1}$ to a calculated value of $2.83 \times 10^{-8} \text{ m}^2 \text{ s}^{-1} \text{ V}^{-1}$ compared with the value of $3.0 \times 10^{-8} \text{ m}^2 \text{ s}^{-1} \text{ V}^{-1}$ found at 10^{-2} mol dm^3 . Similarly for solutions of $C_{16}E_{30}$:

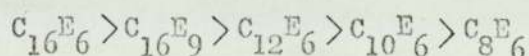
$$10^{-3} \text{ mol dm}^3, 0.9172 \text{ cp.}$$

$$10^{-2} \text{ mol dm}^3, 1.0423 \text{ cp.}$$

changing the steady state mobility of $5.0 \times 10^{-8} \text{ m}^2 \text{ s}^{-1} \text{ V}^{-1}$ to a calculated value of $4.4 \times 10^{-8} \text{ m}^2 \text{ s}^{-1} \text{ V}^{-1}$, experimental $4.5 \times 10^{-8} \text{ m}^2 \text{ s}^{-1} \text{ V}^{-1}$. There is good agreement with the calculated and experimental results in both cases which supports the above explanation.

4.2.2. Effect of number of ethylene oxide units.

Ottewill (132) considered that, for alkyl polyoxyethylene compounds having a straight alkyl chain and polyoxyethylene chains containing 3 or 9 ethylene oxide units, for constant alkyl chain length, increasing the length of the ethylene oxide chain decreased the extent of adsorption at a constant molar concentration. Mathai and Ottewill (134) found that, at equimolar concentrations below the cmc, electrophoretic results suggested that the order of adsorption for polyoxyethylene alkanols was

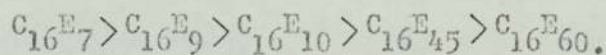


Elworthy and Florence (144) in considering the effect of polyoxyethylene chain length on the stabilization of oil-in-water emulsions by nonionic surface active agents, found that increasing the number of ethylene oxide units increased stability at a given surface active agent concentration. The electrophoretic mobility, u , however decreased

as the ethylene oxide chain length increased, for example from ca. 4 units with 6 ethylene oxide units to ca. 1 unit with 24. Obviously the electrical contribution to stability decreased as the series was ascended and steric stabilizing factors became important.

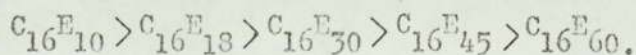
Daluja and Srivastava (137) who studied the effects of a nonionic surfactant series on As_2S_5 and Sb_2S_5 sols, concluded, that the degree of increase in mobility was directly proportional to the decrease in chain length of the ethylene oxide chains for the same hydrocarbon moiety.

Elworthy and Guthrie (119) found that increasing the number of units in the ethylene oxide chain had the effect of decreasing the maximum amount adsorbed and decreased the area per molecule. For the polyoxyethylene mono hexadecyl ethers used.



The suggestion made in the present work is that, with the compounds used a looped monolayer is formed at the polystyrene latex surface. Presumably the effect of the size of the nonionic molecule will be to displace the plane of shear further out from the particle surface. The greater the number of ethylene oxide units the greater will be this displacement and the lower will be the mobility.

Figure XVII shows that the mobility falls as ethylene oxide chain length increases



A plot of mobility versus ethylene oxide chain length - Fig. XVIII is linear showing that the decrease in mobility is proportional to the increase in ethylene oxide chain length as found by Daluja and Srivastava.

A prediction of the decrease in mobility with increase in ethylene chain length can be made by use of equation 2.10 in the form

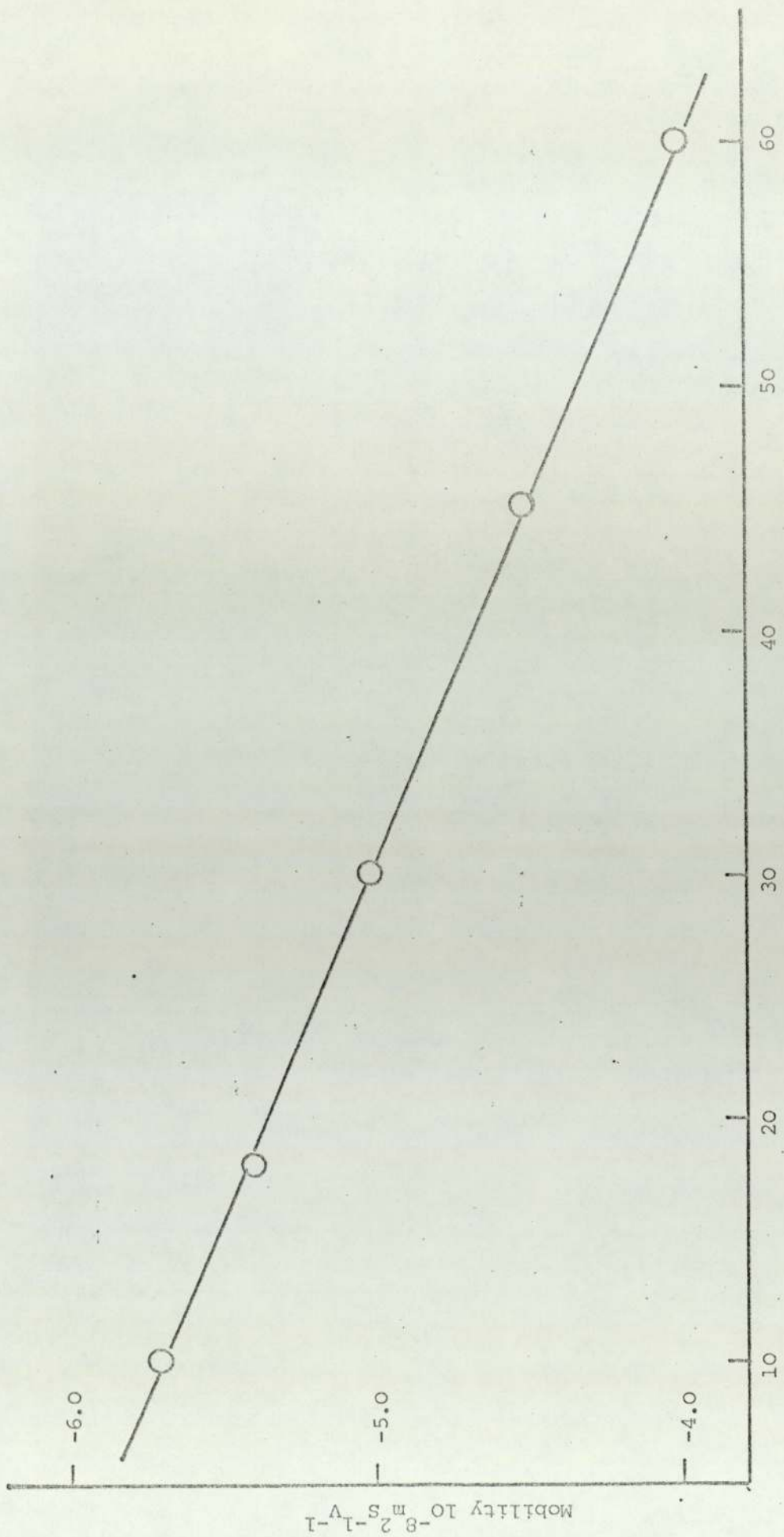


Fig XVIII
Number of ethylene oxide units
in series of C₁₆E_Y

$$\kappa x = \ln \left[\frac{(\exp^{Ze\zeta}/2kT + 1)}{(\exp^{Ze\zeta}/2kT - 1)} \frac{(\exp^{Ze\psi_0}/2kT - 1)}{(\exp^{Ze\psi_0}/2kT + 1)} \right]$$

where x the 'distance' of the plane of shear (ζ replacing ψ) from the particle surface can be estimated (the assumption is made that there is no change of ion adsorption within the Stern plane).

Staudinger and other workers (153) have indicated that the configuration of ethylene oxide groups in the ethylene oxide chain is most probably a zigzag arrangement below 9 ethylene oxide units and a meander configuration above this number. An average value obtained by these workers for the 'length' of an ethylene oxide unit in a meander chain was 0.2nm, whereas the zigzag - which is the fully extended condition - gave a length of 0.35nm.

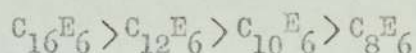
The 'length' occupied by a number of such units can be calculated, added to the value of x found and the zeta potential for a particular number of ethylene oxide units predicted. For example, with $C_{16}E_{30}$ the value of u is $5.0 \times 10^{-8} \text{ m}^2 \text{ s}^{-1} \text{ V}^{-1}$, this corresponds to a zeta potential of 78mV. Calculation of x from the above equation gives a value of 3.18nm. The effective 'length' (meander configuration) of 30 extra ethylene oxide units is 6nm giving for $C_{16}E_{60}$ a total x of 9.18nm, the experimental value of zeta potential of 59mV for this compound gives a calculated x of 5.29nm. These values confirm the suggestion that the arrangement of nonionic surfactant around the particle is a looped monolayer.

The paraffin chain groups of the surfactant molecule are also in zigzag configuration, the distance between alternate $-\text{CH}_2-$ groups of the chain being 0.25nm (153). The extended length of $C_{16}E_{30}$ (meander configuration) is therefore ca. 8nm and $C_{16}E_{60}$ ca. 14nm. These values inserted into the above equation give zeta potentials of 41.5mV and 22mV respectively, the corresponding experimental values being 78mV

and 59mV. These calculations supply further evidence in favour of the looped monolayer configuration.

4.2.3. Effect of altering the length of the alkyl chain.

In his review (133) Ottewill considered that, for alkyl polyoxyethylene compounds having a straight alkyl chain and ethylene oxide chains containing 3 or 9 units, for constant ethylene oxide chain length increasing the alkyl chain length increased the extent of adsorption at a constant molar concentration. This would be expected from a consideration of Traube's rule and free energies of adsorption. Thus Mathai and Ottewill (134) found the order of adsorption



In this work a comparison of the effect of two nonionic surfactants $C_{12}E_{23}$ and $C_{16}E_{23}$ is made. Their concentration mobility plots, Fig. XIX are virtually identical, suggesting that, under the conditions used, the difference in adsorption energies of the alkyl chains is masked by the ethylene oxide chains the latter being the main cause of shear plane displacement, hence as the latter are of equal number with the two compounds the mobilities are virtually the same.

4.3. Effect of cationic surface active agents on the electrophoretic mobility and zeta potential.

The adsorption of cationic surface active agents at the polystyrene solid - liquid interface is a two stage process (145) (146). Firstly, the polar head groups are specifically bound to the surface of the solid - the $-COO^-$ groups of the polystyrene latex which interact with the cationic head group of the surface active agent. Secondly the alkyl chains adsorb onto hydrophobic sites on the latex so that the ions are adsorbed in reverse orientation. This two stage adsorption is characterised electrophoretically by the gradual neutralization of the negative

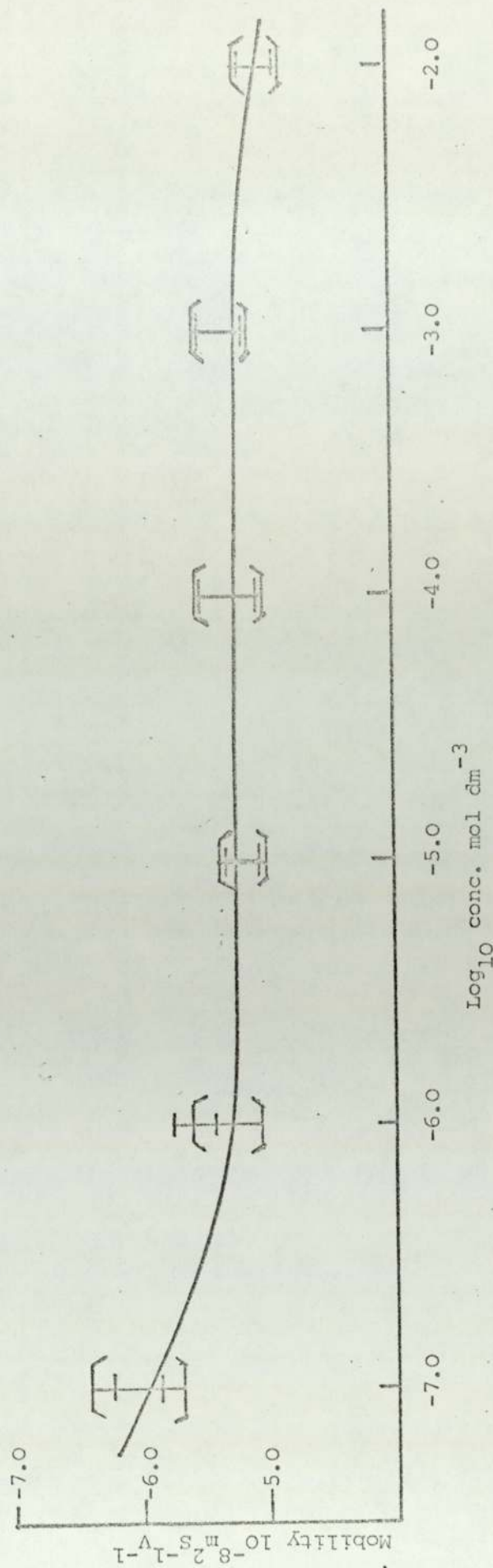


Fig XIX Mobility versus concentration nonionic surfactant $\text{C}_{12} \text{E}_{23} \text{I}$; $\text{C}_{16} \text{E}_{23} \text{T}$.

charge of the latex with increasing concentration until the electrophoretic mobility is zero, followed by reversal of charge which gradually increases with concentration as reverse orientation adsorption occurs. The adsorption of surface active cations can thus be used to determine the number of carboxyl groups on the surface, the adsorption constant and the free energy of adsorption.

4.3.1. General characteristics of the zeta potential- \log_{10} concentration plots.

The cationic surface active agents used were alkyl trimethyl ammonium bromides, CxTAB, with C_{10} , C_{12} , C_{14} and C_{16} alkyl chains. Results are shown in Figure XX and Tables Va and Vb. The curves have an extended S shape as has been predicted and reported previously by Ottewill et al (105) (147).

Generally, and as is shown by for example C_{10} TAB over the concentration range 10^{-6} mol dm $^{-3}$ to 10^{-5} mol dm $^{-3}$, there is a small initial decrease of negative zeta potential with increasing concentration of CxTAB. This is in keeping with the suggestion (106) that adsorption in this concentration region occurs primarily by ion exchange between the CxTA $^{+}$ ions and the inorganic cations, e.g. Na $^{+}$, already present in the Stern layer of the latex particles. Some adsorption of CxTA ions by direct transfer from the solution to the Stern layer probably accounts for the small decrease in potential. Since the particle will only be sparsely covered at this concentration the most probable orientation of the surface active ion on the particle surface is a flat lying orientation, this would allow maximum interaction between the alkyl chain of CxTA $^{+}$ and the particle surface through the hydrophobic effect.

After this initial slow decrease in the negative zeta potential, with increasing concentration, all plots are characterized by a rapid decrease in negative potential until it becomes zero; with further increase

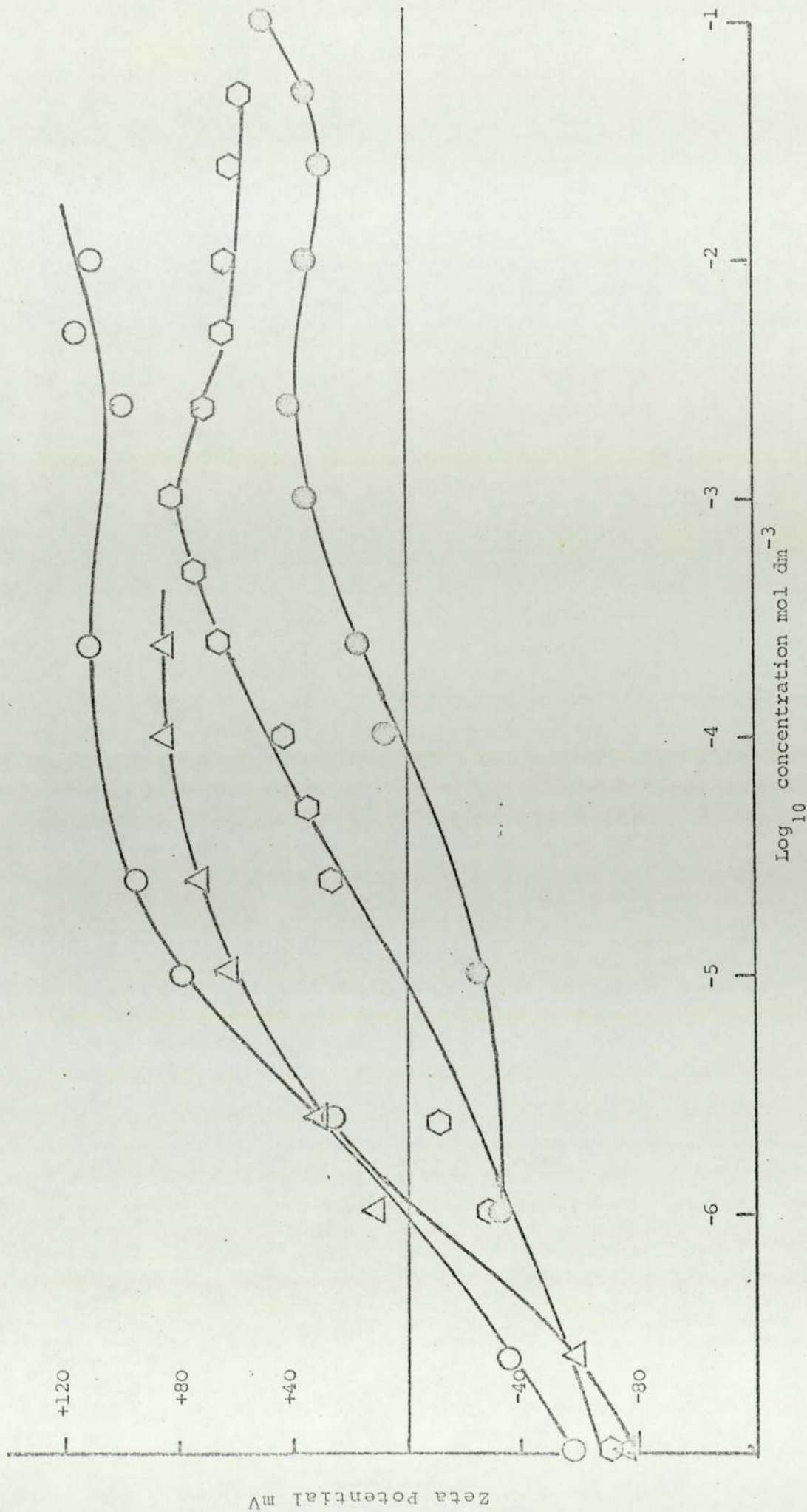


Figure XX Zeta potential - concentration C_{10}^{TAB} C_{12}^{TAB} C_{14}^{TAB} C_{16}^{TAB} .

in concentration a reversal of sign of zeta potential occurs, followed by an increase of positive potential.

Connor and Ottewill (146) have shown that the adsorption process, over the part of the curve where $\zeta \rightarrow 0$, involves ionic interaction between the cationic head group and the negatively charged carboxyl groups on the surface of the particle. Infra red studies (145) indicated that the association is a purely electrostatic one and that formation of a chemical bond does not occur.

These workers have shown, for these cationic surface active agents, that Traube's rule is obeyed, i.e. that the free energy of adsorption increases linearly with increase of $-\text{CH}_2-$ groups (calculation of the relevant free energies of adsorption are made in the next sub-section). This adherence to Traube's rule suggests that, in the region under discussion, the alkyl chains are lying flat on the surface in hydrophobic association with the surface, as mentioned above.

The positive zeta potential increases linearly with concentration until a maximum value is reached, and then stays virtually constant with further concentration increases. The only way that this potential change can occur is for the CxTA^+ ions to be adsorbed in reverse orientation with their head groups towards the solution phase. Saturation adsorption should then be indicated by the zeta potential staying constant as concentration increases. However, Chen has shown (106), that the zeta potential appears to stay constant over a short concentration range even though adsorption studies show that adsorption of CxTA^+ ions continues to increase substantially, i.e. that the maximum zeta potential expected is not actually reached. The explanation for this could be two-fold, firstly, as CxTA^+ ions are being adsorbed, there could be an equivalent adsorption of Br^- ions behind the shear plane thus accounting for the apparent invariance of zeta potential. This might be expected as,

initially when surface active agent is absent, counter ions e.g. Na^+ are specifically adsorbed in the Stern layer of the negatively charged particles. In the concentration range where the particles are positively charged the adsorption of anion occurs. Secondly ionic strength effects at the higher concentrations may also contribute to the value of zeta potential being lower than expected. Furthermore, with increasing adsorption of CxTA^+ and Br^- ions, the displacement of the shear plane away from the particle surface would also cause the zeta potential to decrease. These effects would also account for the fall off in mobility which occurs, with increasing concentration, after the 'flat' ^{portion} ~~position~~ of the curve.

Since, over the positive zeta potential range, the number of CxTA^+ ions adsorbed exceeds the surface charges, electrostatic contribution to the free energy of adsorption is unfavourable to adsorption. Clearly the main driving force for adsorption comes from the hydrophobic effect.

As concentration increases the adsorbed CxTA^+ ions tend to stand up on the particle surface so that at saturation adsorption the indication is (146) that a high proportion of them are vertically oriented, those ions interacting with negatively charged carboxyl groups having their head groups towards the surface and those on hydrophobic sites having their head group towards the solution phase.

One of the zeta potential- \log_{10} concentration plots shows an increase in zeta potential at high concentrations i.e. C_{10}TAB at 10^{-2} mol dm^{-3} , this result is difficult to explain. It seems possible that further adsorption of CxTA^+ ions could occur, by the hydrophobic effect, onto those ions associated with the carboxyl groups of the particle - as the concentration is above the critical micelle concentration some multi-charged species is conceivable - this would increase the number of charged groups, increasing the zeta potential, but would also displace the shear plane leading to a lowering of potential. However, adsorption measure-

ments (106) show no adsorption taking place over this concentration range. It therefore seems more likely that the effect is due to difficulties e.g. heating effects, encountered with the microelectrophoresis technique at high ionic strengths.

4.3.2. Conversion of mobility to zeta potential.

Zeta potentials were obtained from the observed mobilities by interpolation from table 3 of the work of Ottewill and Shaw (99) (see appendix 1), who presented the computation results of Wiersema in the form of mobility as a function of zeta potential and K_a . The limiting equivalent conductance of all ions was taken to be $70 \Omega^{-1} \text{ cm}^2 \text{ equiv}^{-1}$. The differences caused by the limiting equivalent conductance of the other ions present e.g. C_{10}TA^+ $24.08 \Omega^{-1} \text{ cm}^2 \text{ equiv}^{-1}$; Na^+ , $50.15 \Omega^{-1} \text{ cm}^2 \text{ equiv}^{-1}$; Cl^- $76.35 \Omega^{-1} \text{ cm}^2 \text{ equiv}^{-1}$; Br^- , $78.17 \Omega^{-1} \text{ cm}^2 \text{ equiv}^{-1}$ was assumed to have negligible effect as has been shown, for example by Chen (106).

Since all measurements were made in $10^{-5} \text{ mol dm}^{-3}$ sodium chloride which, with the latex being used, gives a value of K_a of 38, the effect of additives below this concentration were presumed to be negligible, hence values of mobility and zeta potential were calculated for $K_a = 38$. When the concentration of additive was above $10^{-5} \text{ mol dm}^{-3}$ the higher value was used to calculate K_a and the corresponding mobilities and zeta potentials.

Values relating K_a , mobility and zeta potential for the various concentrations used are given in Fig. XXI.

4.3.3. Calculations from zeta potential- \log_{10} concentration CxTAB curves.

As discussed under Section 2.4.5. the slope of the curve of the Stern potential against \log_{10} concentration of CxTAB, equation 2.8.6, can be used to calculate the number of sites N_1 available per m^2 when the initial Stern potential is known. For the present work, the Stern

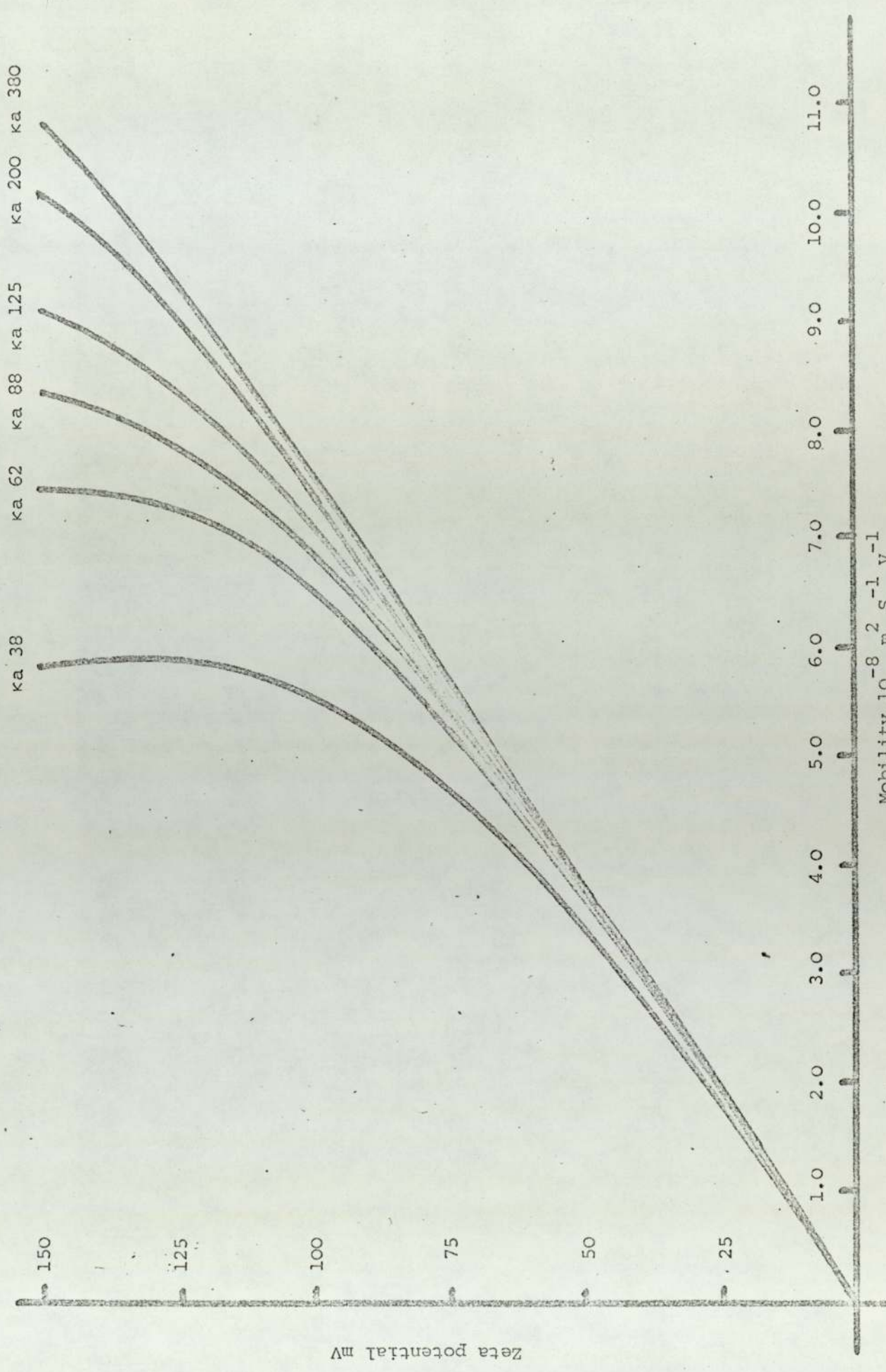


Fig XXI Theoretical values of mobility as a function of zeta potential and Ka for a positively or negatively charged sphere in the presence of a 1:1 electrolyte with $m^* = 0.184$ at 25°C .

potential is replaced by the zeta potential and equation 2.86 becomes

$$\left(\frac{d\zeta}{d \log_{10} C} \right)_{\zeta=0} = \frac{4.606kT}{Ze} \frac{\sinh Ze \zeta_0}{2kT} \left[\frac{(8n_0\epsilon kT)^{\frac{1}{2}} \frac{\sinh Ze \zeta_0}{2kT} - 1}{Z N_1 e} \right]$$

In addition the adsorption constant k_2 can be calculated from equation

$$2.81. \quad 1/C = k_2 \left[\frac{Ze N_1}{(8n_0\epsilon kT)^{\frac{1}{2}} \left[\sinh \frac{Ze \zeta_0}{2kT} \pm \sinh \frac{Ze \zeta}{2kT} \right] - 1} \right]$$

and the chemical free energy of adsorption ΔG from equation 2.73a.

$$k_2 = \frac{\exp \frac{-\Delta G}{kT}}{55.6 \times 10^3}$$

Results are shown in Table VI. As indicated in sub-section 4.3.1.

the zeta potential- \log_{10} concentration plots are linear over the range

$-\zeta \rightarrow 0 \leftarrow \zeta$ The theory outlined in Section 2.4.5. predicts that all

curves should have the same slope in the region of zero zeta potential

provided N_1 , the number of adsorption sites remains constant. There is

however an increase in slope as alkyl chain length increases this must

be due to increased adsorption over and above that necessary to interact

with the carboxylic acid groupings on the latex and results from an

increase in adsorption energy as the alkyl chain length increases.

The concentration required to reverse the charge decreases with

increasing chain length. Fig. XXII shows a plot of the number of carbon

atoms in the chain against the reversal of charge concentration (RCC),

there is a linear relationship for chain lengths C_{10} , C_{12} and C_{14} but for

C_{16} the RCC is much less influenced by increasing chain length.

The number of adsorption sites, N_1 , appears to be only approximately

constant the best agreement being for the C_{14} and C_{16} chains. N_1 can be

taken as the number of carboxyl groupings per m^2 , the values reported

here are at the best an order of magnitude lower than the value of

$1.84 \times 10^{17} m^{-2}$ found by conductometric titration, this may be due to

incomplete ionisation of the carboxylic acid or the adsorption of

inorganic counter ions e.g. Na^+ within the Stern layer.

TABLE VI

Free energies of adsorption Cationic surface active agents

Compound	$(d\zeta/d \log_{10} C)_{\zeta = 0}^{\text{mV}}$	$C_{\zeta = 0} \text{ mol dm}^{-3}$	$C \text{ mol m}^{-3}$ ($\zeta = +35 \text{ mV}$)	$N_1 \text{ m}^{-2}$	$K_2 \text{ m}^3 \text{ mol}^{-1}$	$-\Delta G \text{ kJ mol}^{-1}$
C ₁₀ TAB	33	9.5×10^{-2}	1	2.41×10^{16}	6.10	31.56
C ₁₂ TAB	36	10^{-2}	8×10^{-2}	7.78×10^{15}	79.11	37.91
C ₁₄ TAB	62	10^{-3}	3.5×10^{-3}	2.33×10^{15}	3.24×10^3	47.11
C ₁₆ TAB	75	10^{-3}	3.0×10^{-3}	2.27×10^{15}	5.75×10^3	48.53

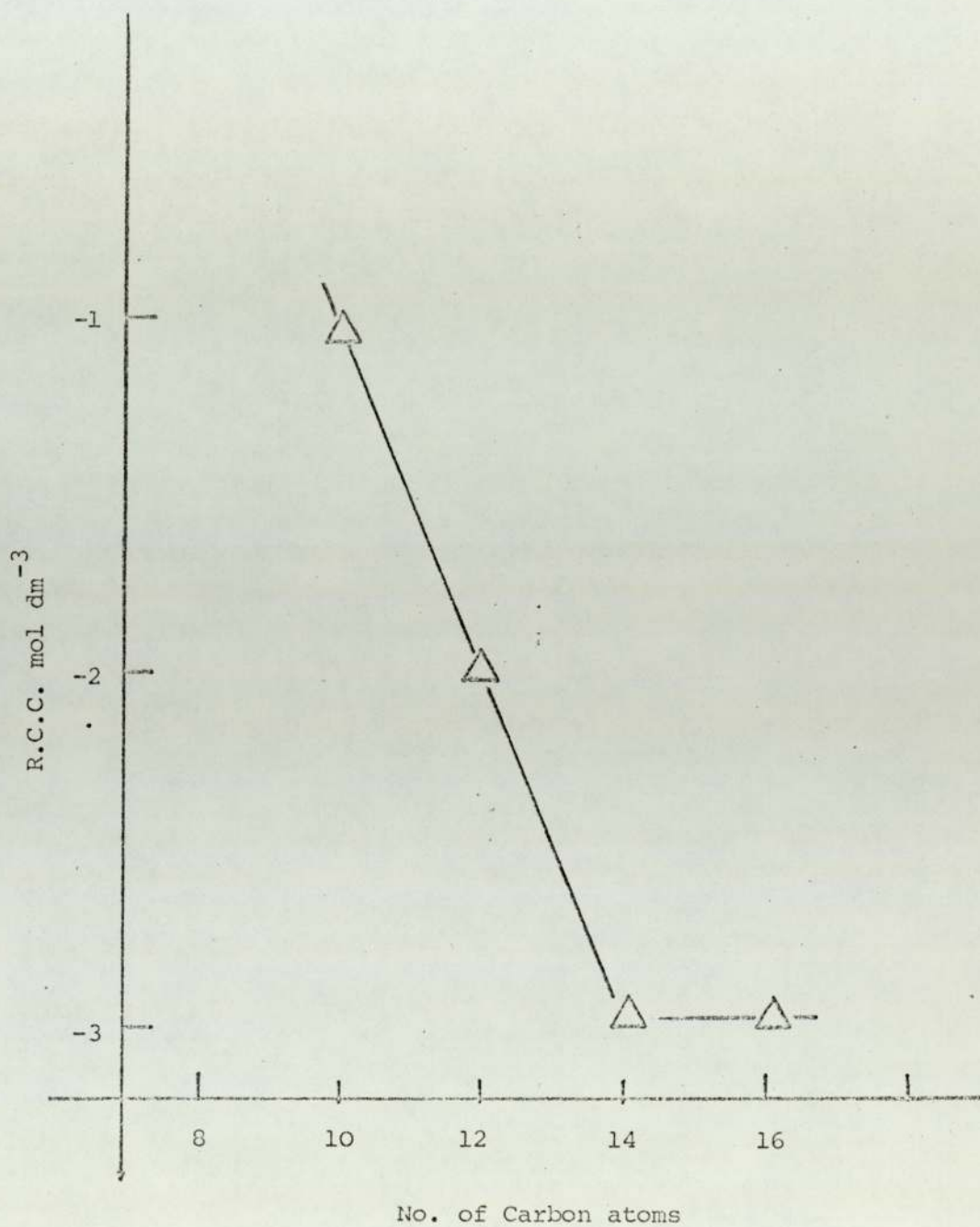


Fig. XXII Effect of hydrocarbon chain length of C_xTAB on reversal of charge concentration (RCC)

In calculating k_2 the adsorption constant from equation 2.81 an additional value of the zeta potential is required. A value, +35mV, the same for each alkyl chain length, was chosen which was on the linear portion of the zeta potential versus \log_{10} concentration plots.

The change in chemical free energy of adsorption with change in chain length is shown in Fig. XXIII. The increment in $\Delta\bar{G}$ per CH_2 group is virtually constant up to C_{16} but above this chain length the $\Delta\bar{G}$ increment per CH_2 decreases. The increment in $\Delta\bar{G}$ per CH_2 group over the linear part of the plot is 3.9kJ mol^{-1} . The reason for the decrease in $\Delta\bar{G}$ above C_{14} is thought to be due to the partial dimerization of the longer chains in dilute solutions below the cmc (145). The results reported here for $\Delta\bar{G}$ agree with those reported by Connor (145).

4.4. Effect of mixtures of cationic and nonionic surface active agents on the electrophoretic mobility and zeta potential.

The effect of adding nonionic surface active agents, C_{16}E_y , to the cationic surface active agents used in Section 4.3. was examined; constant concentrations of the nonionic were used and the concentration of cationic varied as previously. The order of mixing of surface active agent with the latex did not seem to affect the adsorption pattern, i.e. latex + cationic then nonionic added, gave the same results as latex + nonionic and then cationic surfactant added.

The mixtures used were C_{10}TAB with $\text{C}_{16}\text{E}_{30}$ and $\text{C}_{16}\text{E}_{60}$; C_{12}TAB with $\text{C}_{16}\text{E}_{10}$, $\text{C}_{16}\text{E}_{30}$ and $\text{C}_{16}\text{E}_{60}$; C_{14}TAB , C_{16}TAB both with $\text{C}_{16}\text{E}_{30}$ and $\text{C}_{16}\text{E}_{60}$. In addition, in order to obtain the comparative effect of ethylene oxide chain length, studies were made of C_{12}TAB with $\text{C}_{16}\text{E}_{10}$, $\text{C}_{16}\text{E}_{18}$, $\text{C}_{16}\text{E}_{30}$, $\text{C}_{16}\text{E}_{45}$ and $\text{C}_{16}\text{E}_{60}$.

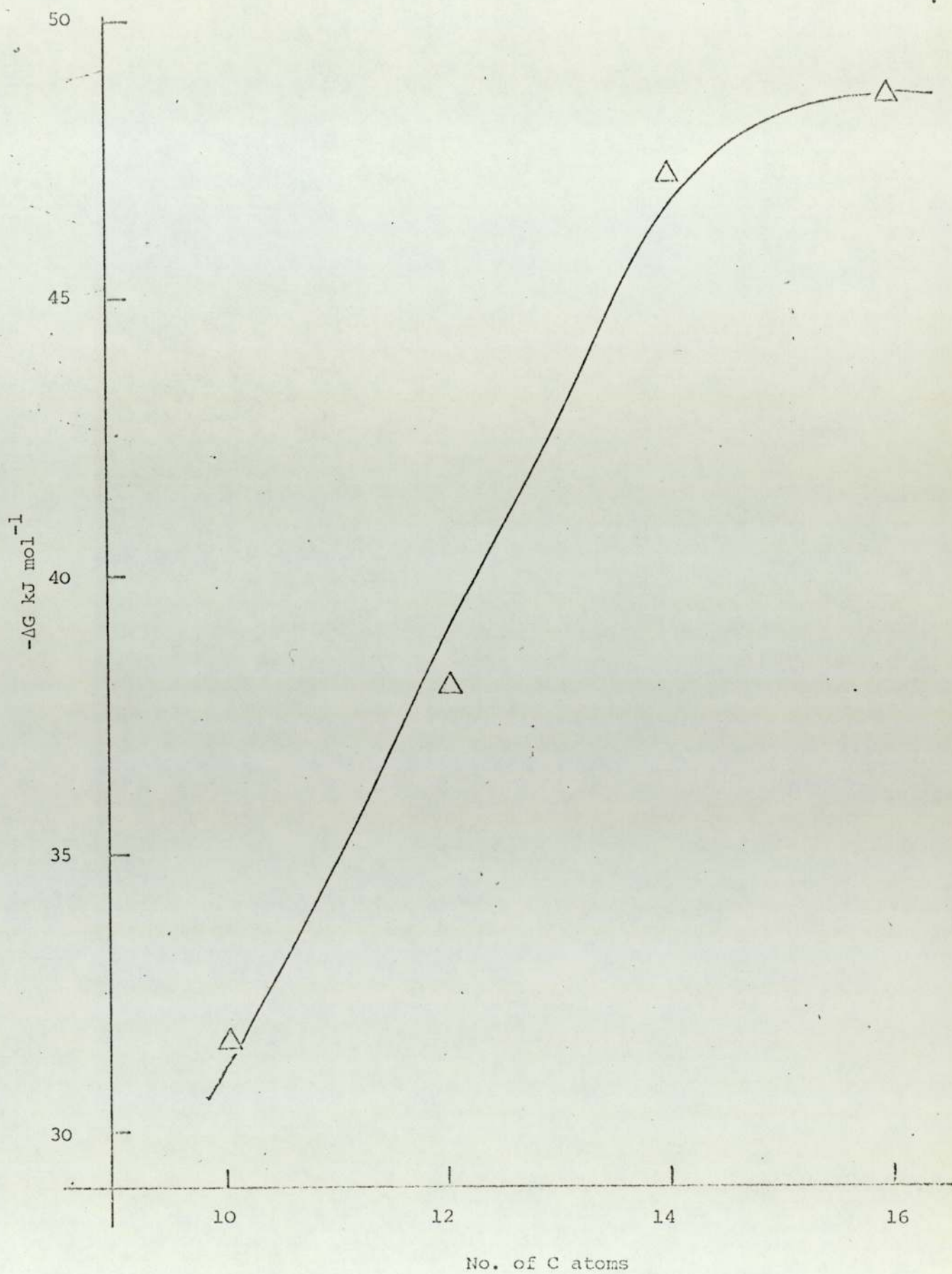


Fig. XXIII Effect of chain length on free energies of adsorption - alkyl trimethyl ammonium bromides.

4.4.1. General characteristics of the zeta potential- \log_{10} concentration CxTAB plots.

Results are shown in Figures XXIV to XXXII inclusive and Tables VII to XVI inclusive, they all follow a pattern which can be studied by examination of the results for C_{12}^{TAB} and C_{16}^E shown in Fig. XXVII and Tables X and XI.

In the presence of the nonionic surface active agent the zeta potential- \log_{10} concentration plot is displaced to the right so that the reversal of charge concentration (RCC) of C_{12}^{TAB} is higher than in the absence of the nonionic surfactant, for example, with 10^{-2} mol dm⁻³ C_{16}^E the RCC is displaced from 10^{-5} mol dm⁻³ to 7×10^{-4} mol dm⁻³. This suggests that both species are adsorbed onto the latex particle and that the nonionic species is hindering the cationic adsorption which brings about charge reversal.

The effect of the adsorption of the nonionic surfactant will be to "push out" the shear plane and hence reduce the zeta potential; it will not neutralize the charge on the particle. The only way that the non-ionic surfactant could reduce the zeta potential towards zero would be by multilayer adsorption and, as has been shown in Section 4.2, that does not occur with the nonionic systems under examination. This lowering of the zeta potential due to the presence of the nonionic surfactant is seen over the major portion of all plots.

As the concentration of cationic material increases so it must displace the nonionic and eventually charge reversal occurs. If it is assumed that the nonionic is more strongly adsorbed than the cationic - the alkyl chain length of the nonionic is C_{16} , a greater free energy of adsorption by the hydrophobic effect would therefore be expected than say from the alkyl chain of C_{12}^{TAB} - whilst the cationic only associates with the ionized carboxylic acid groups, then after

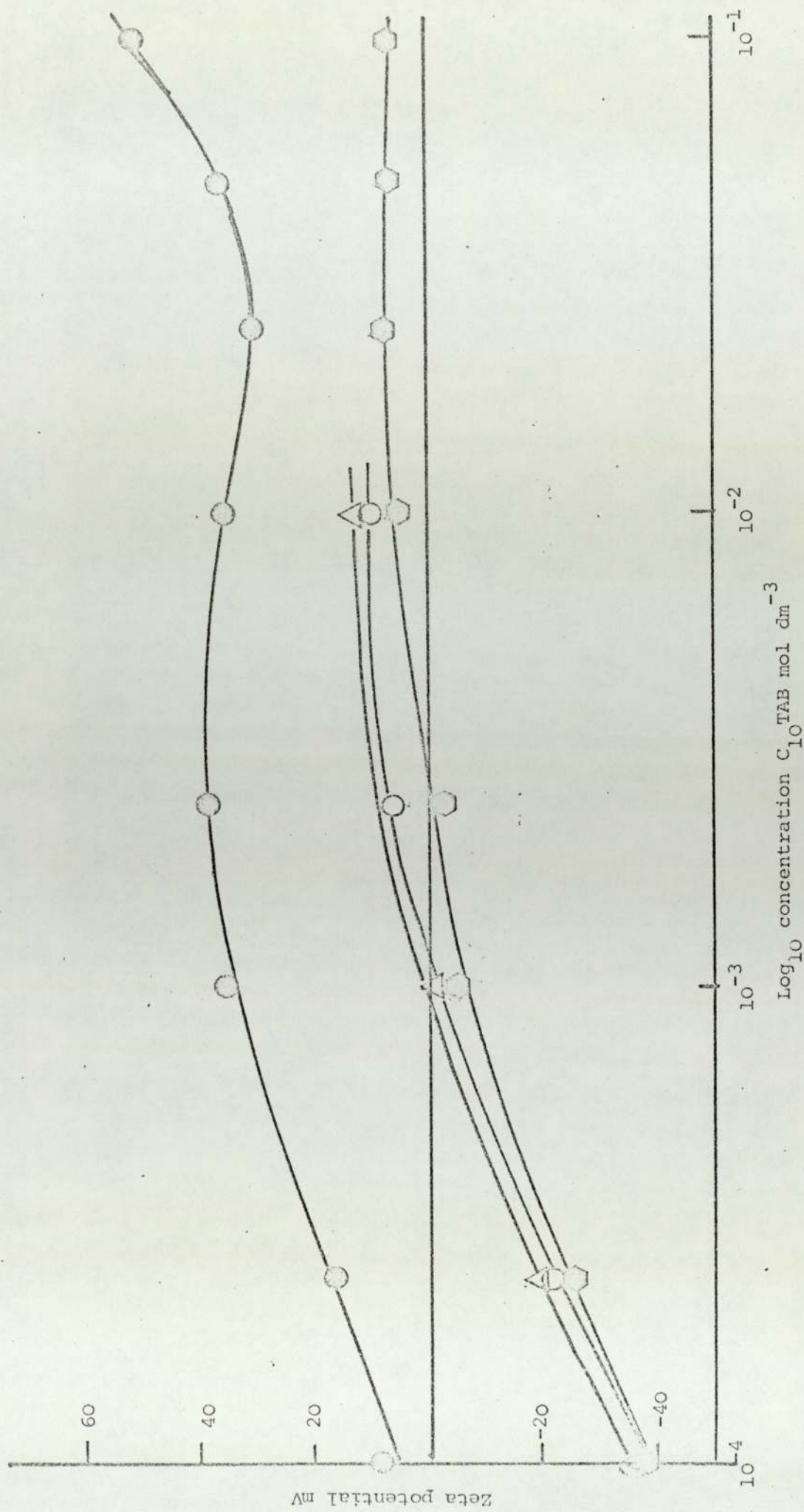


Figure XXIV Zeta potential - concentration C_{10} TAB mol dm^{-3} ; with C_{16} E₃₀, 10^{-2} mol dm⁻³; 10^{-3} mol dm⁻³; 10^{-4} mol dm⁻³; 10^{-1} mol dm⁻³.

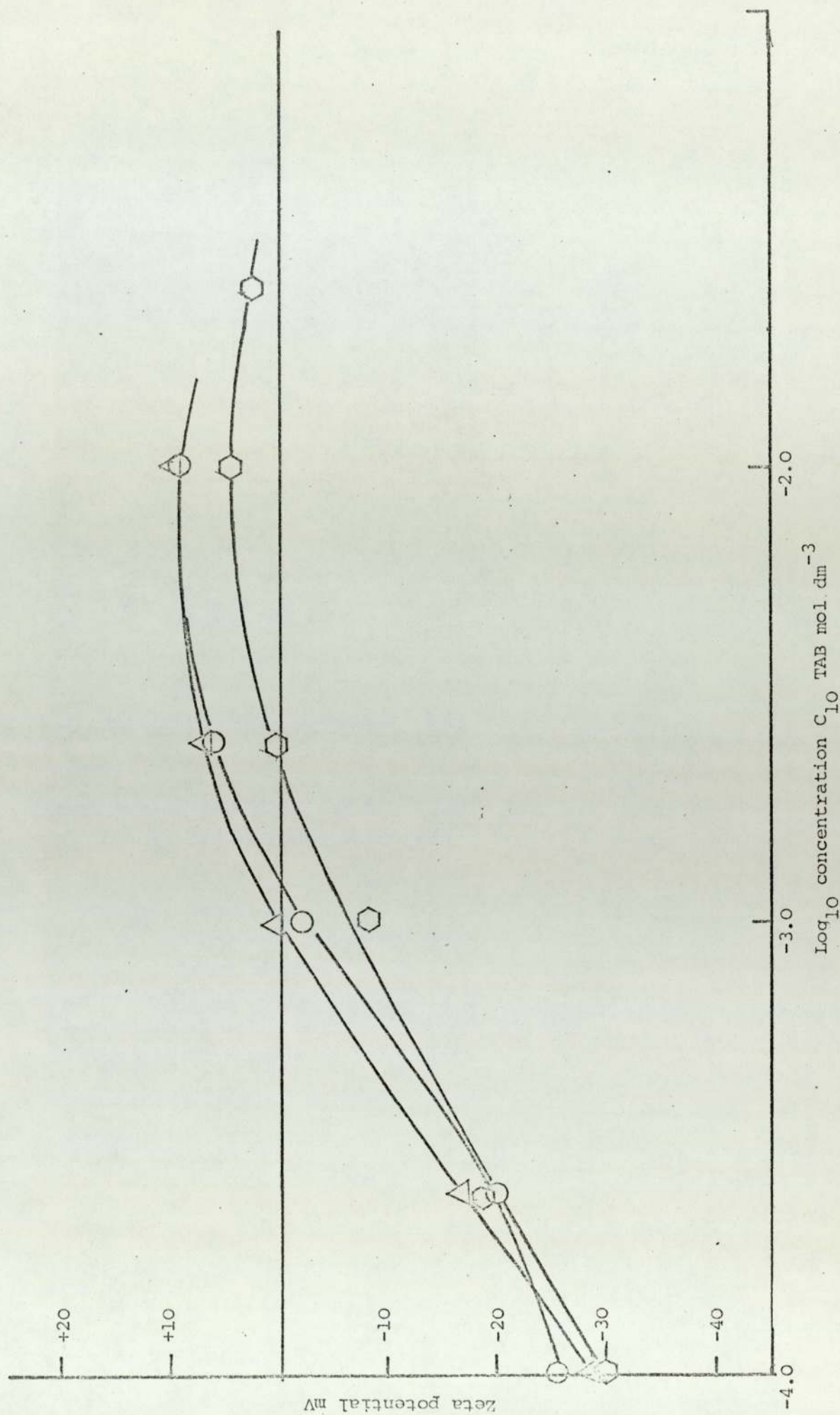


Fig XXV Zeta potential concentration C_{10} TAB with $C_{16}E_{6O}$; 10^{-2} mol dm^{-3} \circ ; 10^{-3} mol dm^{-3} \triangle ; 10^{-4} mol dm^{-3} Δ .

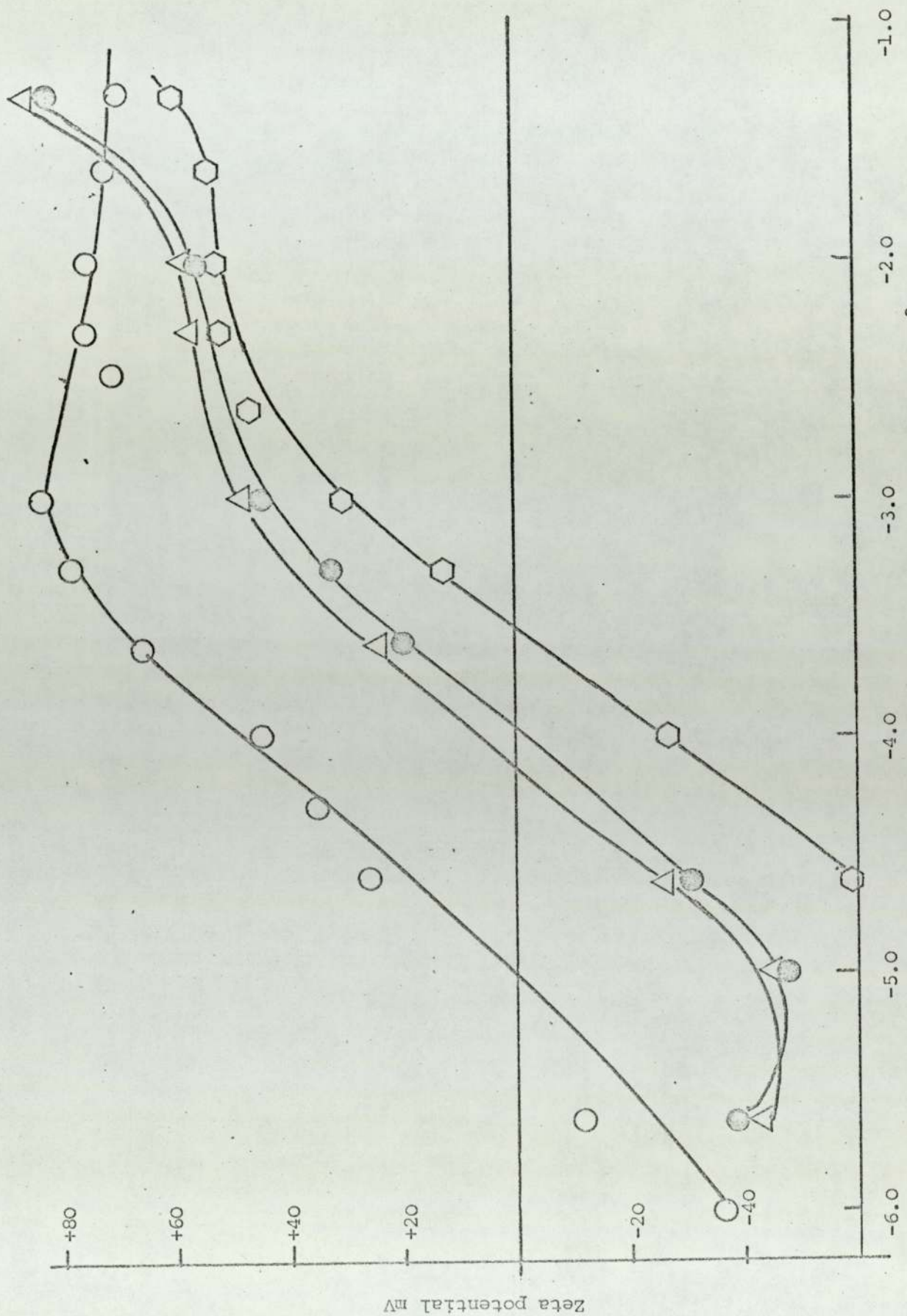


Fig XXVI Zeta potential - concentration C_{12}TAB mol dm^{-3} ; with 10^{-2} mol dm^{-3} $\text{C}_{16}\text{E}_{10}$; 10^{-3} mol dm^{-3} $\text{C}_{16}\text{E}_{10}$; 10^{-4} mol dm^{-3} $\text{C}_{16}\text{E}_{10}$

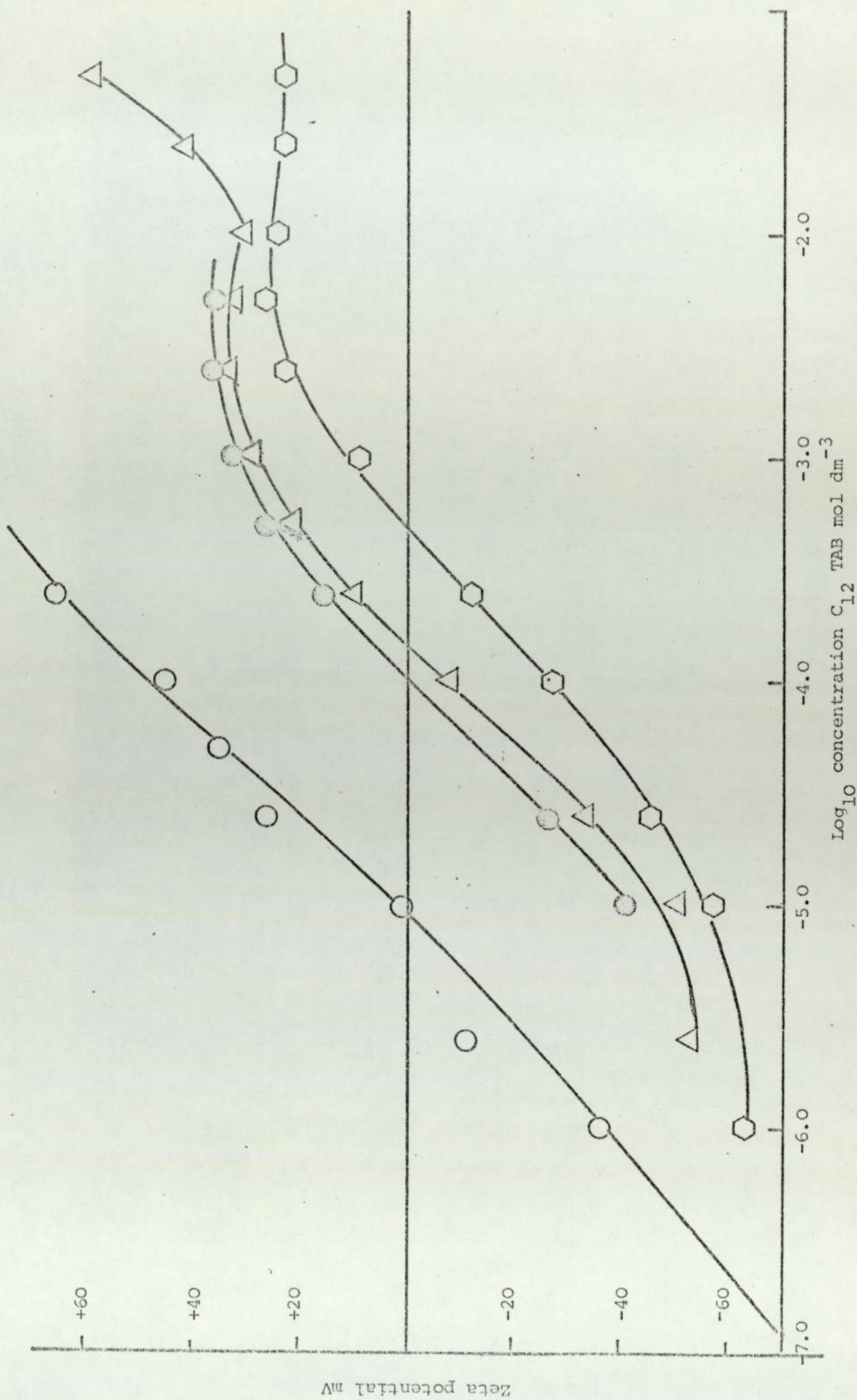


Figure XXVII Zeta potential - concentration C_{12} TAB 0; with C_{16} E₃₀, 10^{-2} mol dm^{-3} ○; 10^{-3} mol dm^{-3} △; 10^{-4} mol dm^{-3} ●.

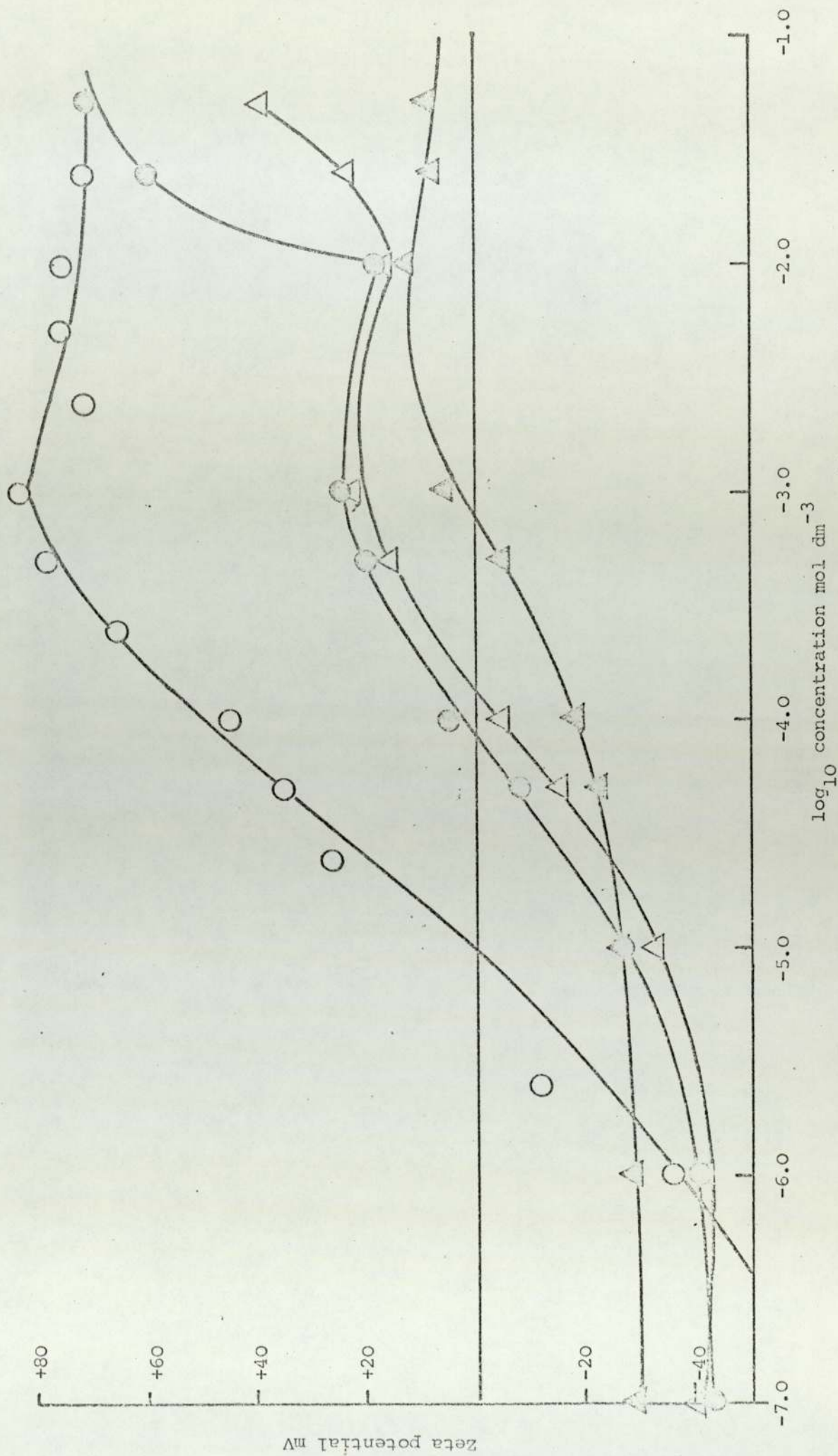


Fig XXVII Zeta potential - concentration C_{12} TAB \circ ; with $C_{16}E_{60}$, Δ 10^{-2} mol dm^{-3} , \triangle 10^{-3} mol dm^{-3} ; \bullet 10^{-4} mol dm^{-3}
 \log_{10} concentration mol dm^{-3}

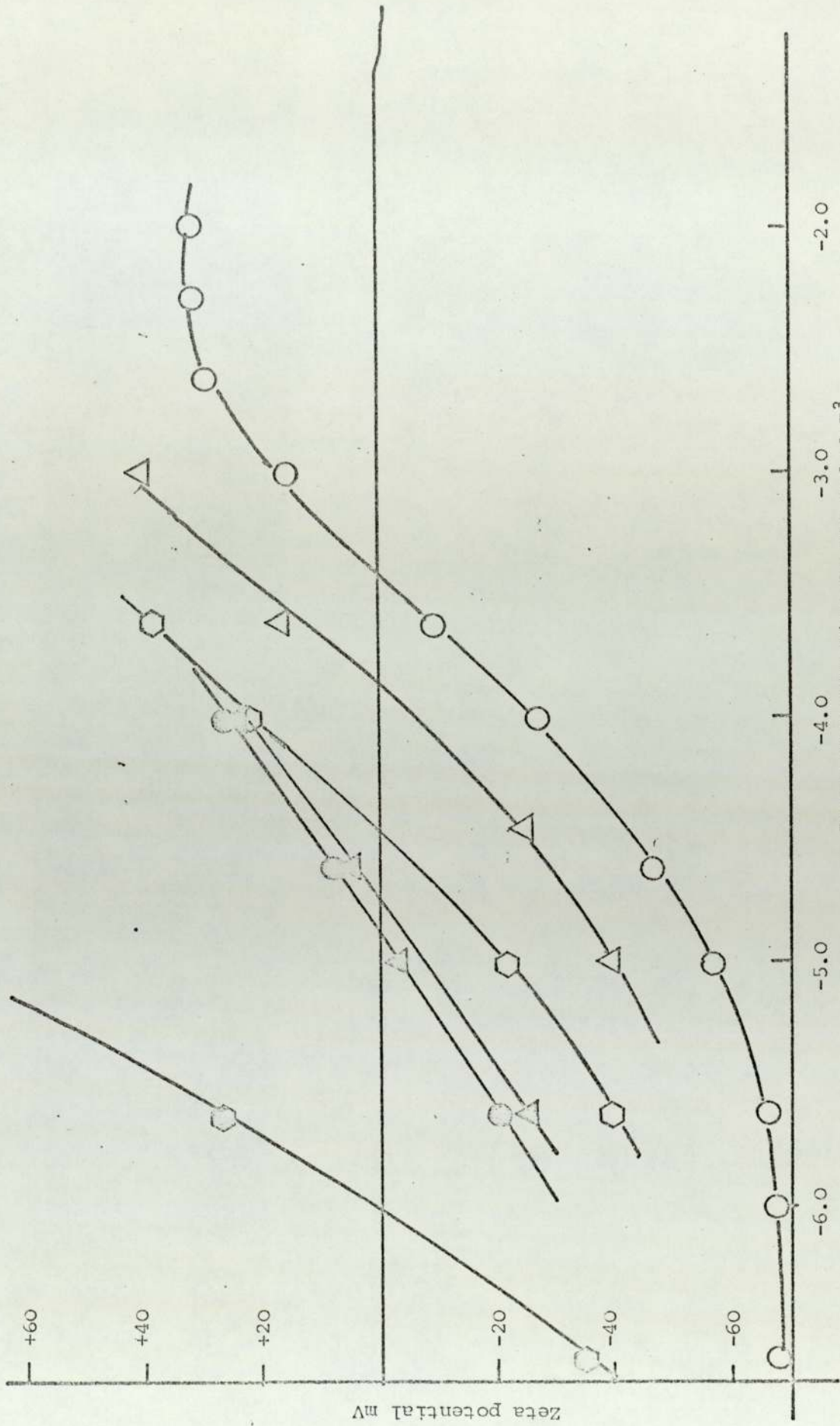


Figure XXIX
 Zeta potential - concentration $C_{14}\text{TAB}$ mol dm^{-3}
 10^{-2} mol dm^{-3} ○; 2×10^{-3} mol dm^{-3} △; 10^{-3} mol dm^{-3} □; 2×10^{-4} mol dm^{-3} ◇;
 10^{-4} mol dm^{-3} ●.

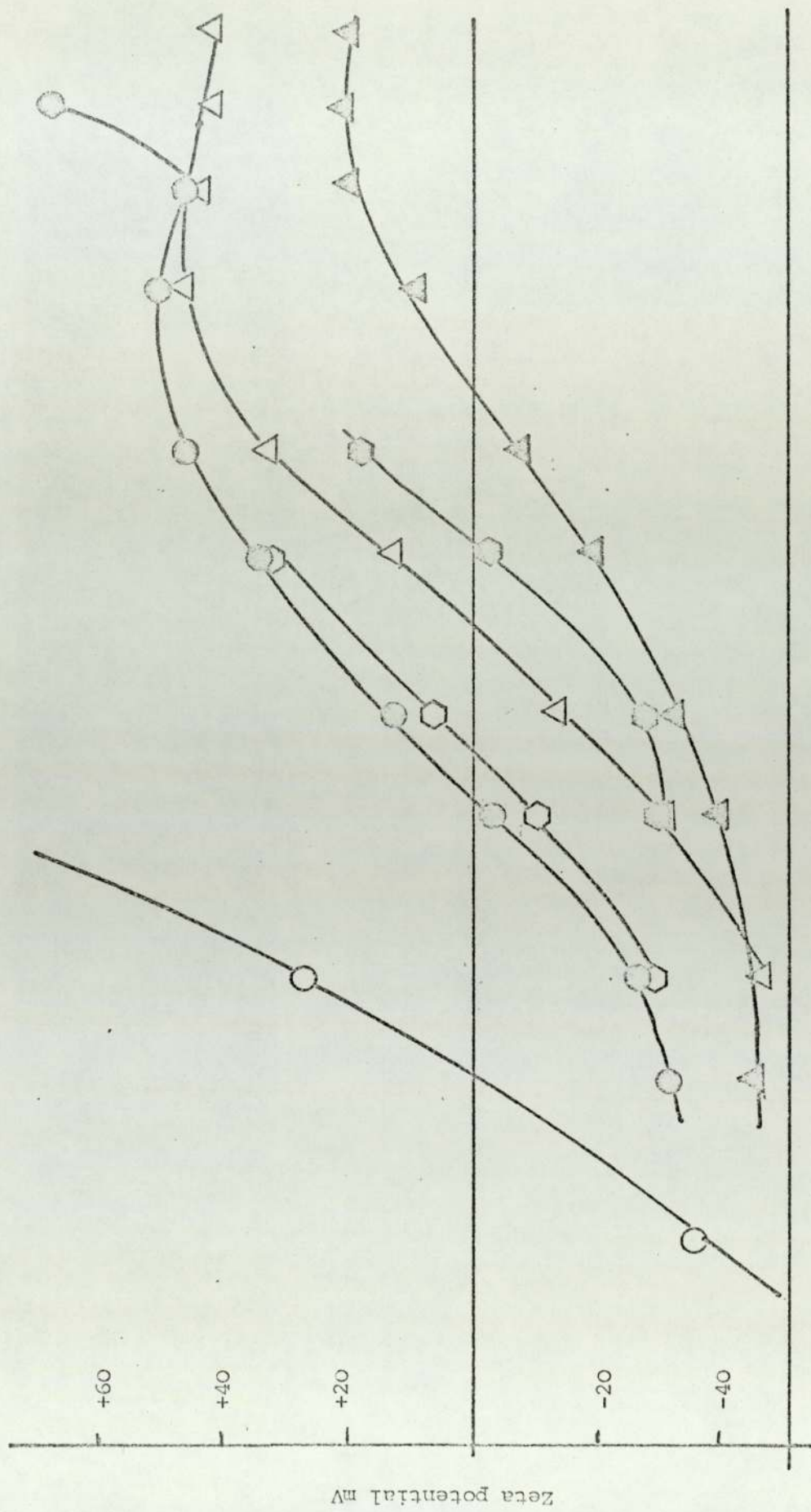


Figure XXX

Zeta potential - concentration C_{14} TAB mol dm^{-3} with C_{16} E₆₀, 10^{-2} mol dm^{-3} \blacktriangle ;
 2×10^{-3} mol dm^{-3} \square , 10^{-3} mol dm^{-3} \triangle ; 2×10^{-4} mol dm^{-3} \square ; 10^{-4} mol dm^{-3} \circ .
 Log_{10} concentration C_{14} TAB mol dm^{-3}

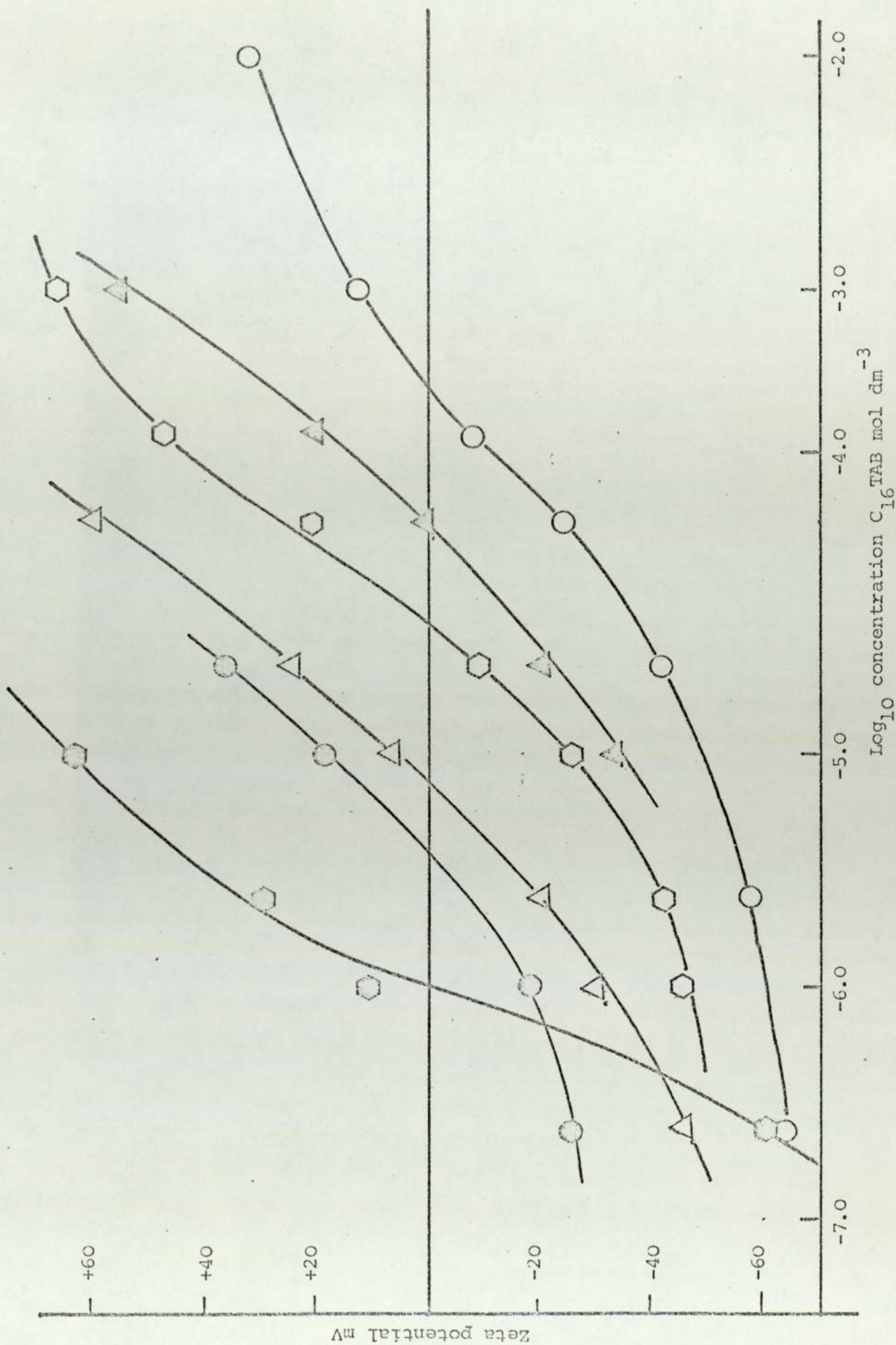


Fig XXXI Zeta potential - concentration $C_{16}TAB$; with $C_{16}E_{30}$, $10^{-2} \text{ mol dm}^{-3}$ ○, $2 \times 10^{-3} \text{ mol dm}^{-3}$ ◡, $10^{-3} \text{ mol dm}^{-3}$ ◢, $2 \times 10^{-4} \text{ mol dm}^{-3}$ ◣, $10^{-4} \text{ mol dm}^{-3}$ ◤.

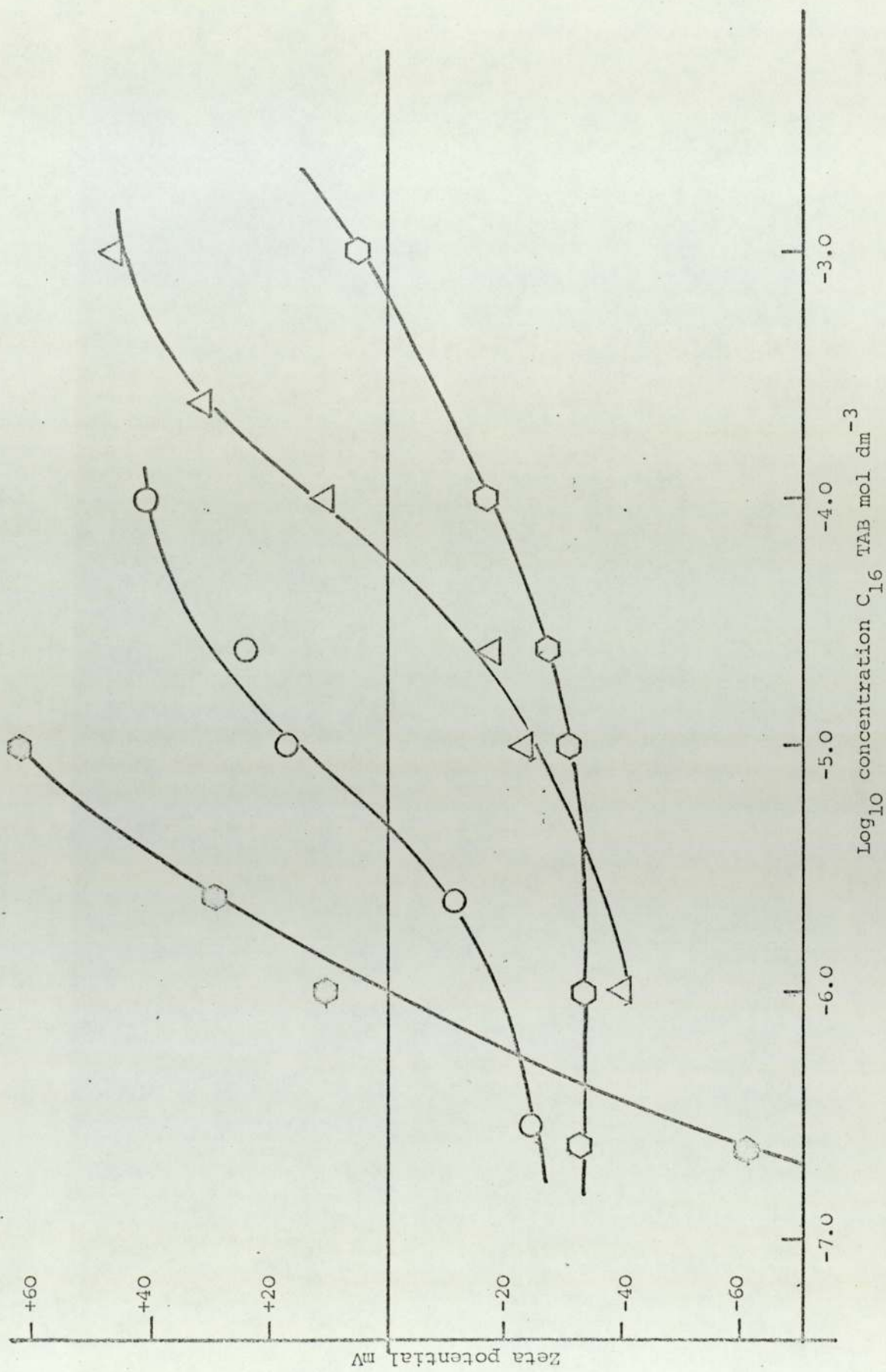


Fig XXXII Zeta potential - concentration $C_{16} \text{ TAB}$ with $C_{16} \text{ E}_{60}$,
 $10^{-2} \text{ mol dm}^{-3}$, $10^{-3} \text{ mol dm}^{-3}$, $10^{-4} \text{ mol dm}^{-3}$.

neutralization of the charge by the cationic species the particle would remain uncharged and this is not the case. If, however, this mechanism of adsorption was correct an explanation of the positive charge could be due to reverse orientation by hydrophobic association of two cationic alkyl chains; one cation associated with the carboxyl group and the other with its charge group orientated towards the aqueous medium. If this was the case it does not seem likely that there would be a dependence of displacement of RCC on the concentration of nonionic, as after a certain concentration of nonionic was reached no further displacement of RCC with concentration would occur.

The controlling factors seem to be therefore a dependence on relative alkyl chain length of cationic, and concentration of nonionic, surfactant, which supports the view of displacement of nonionic by cationic species. The fact that the RCC depends on the relative concentrations of cationic and nonionic, so that as the concentration of nonionic is increased there is further displacement of the RCC is shown by C_{12}^{TAB} :

with 10^{-4} mol dm $^{-3}$ $C_{16}^{E_{30}}$	RCC is 1.1×10^{-4} mol dm $^{-3}$,
with 10^{-3} mol dm $^{-3}$ $C_{16}^{E_{30}}$	RCC is 1.55×10^{-4} mol dm $^{-3}$, and
with 10^{-2} mol dm $^{-3}$ $C_{16}^{E_{30}}$	RCC is 7×10^{-4} mol dm $^{-3}$.

At high concentrations of cationic, as shown with $C_{16}^{E_{30}}$ 10^{-3} mol dm $^{-3}$ and concentrations of $C_{12}^{TAB} > 10^{-2}$ mol dm $^{-3}$, the curve approaches that for C_{12}^{TAB} alone on latex, suggesting either complete displacement of the nonionic or bimolecular layer formation by the cationic adsorbed in reverse orientation as indicated above.

Whilst it would seem possible, in the case where the nonionic surfactant has a longer alkyl chain than the cationic, that the former should be more strongly adsorbed onto the hydrophobic surface of the latex due to the hydrophobic effect, it may be that the adsorption energy of the nonionic is a balance between the hydrophobic effect with

the alkyl chain for, and the heavily hydrated ethylene oxide chains against, and that the resultant total energy is less than that of the cationic surfactant, i.e. it can be displaced by the latter species.

4.4.2. Calculations from zeta potential- \log_{10} concentration surfactant plots.

4.4.2.1. Effect of concentration of nonionic surfactant on the reversal of charge concentration.

The effect the concentration of nonionic surfactant has on the RCC has been indicated in the previous subsection and is shown in a general way in Figs. XXIV to XXXII.

Examination of these figures suggests that the displacement of the RCC is proportional to the concentration of nonionic species and depends on the alkyl chain length of the cationic surfactant used.

Table XVII records the variation of RCC's of the cationics used with varying concentrations of $C_{16}E_y$. Figs. XXXIII and XXXIV give a typical set of results for the $C_{16}E_{30}/C_{12}TAB$ system and Fig. XXXV shows how CxTAB RCC's alter with varying concentration of $C_{16}E_{30}$, these results confirm the suggested proportionality.

It is noticed, in Fig. XXXV, that the slope of the \log_{10} concentration $C_{16}E_{30}$ versus \log_{10} RCC CxTAB plots decreases as the alkyl chain length of the cationic ~~is~~ⁱⁿcreases, indicating that the longer the alkyl chain the more strongly is the cationic adsorbed, as was found in Section 4.3.3, and presumably the more easily is the nonionic displaced.

Regression analysis of the concentration values for each combination of cationic and nonionic surfactant was made and the results for the slopes of the lines for the plots \log_{10} concentration $C_{16}E_y - \log_{10}$ RCC CxTAB are shown in Table XVII. A plot of the values of slope of line versus number of C_{atoms} in the alkyl chain of CxTAB is shown in

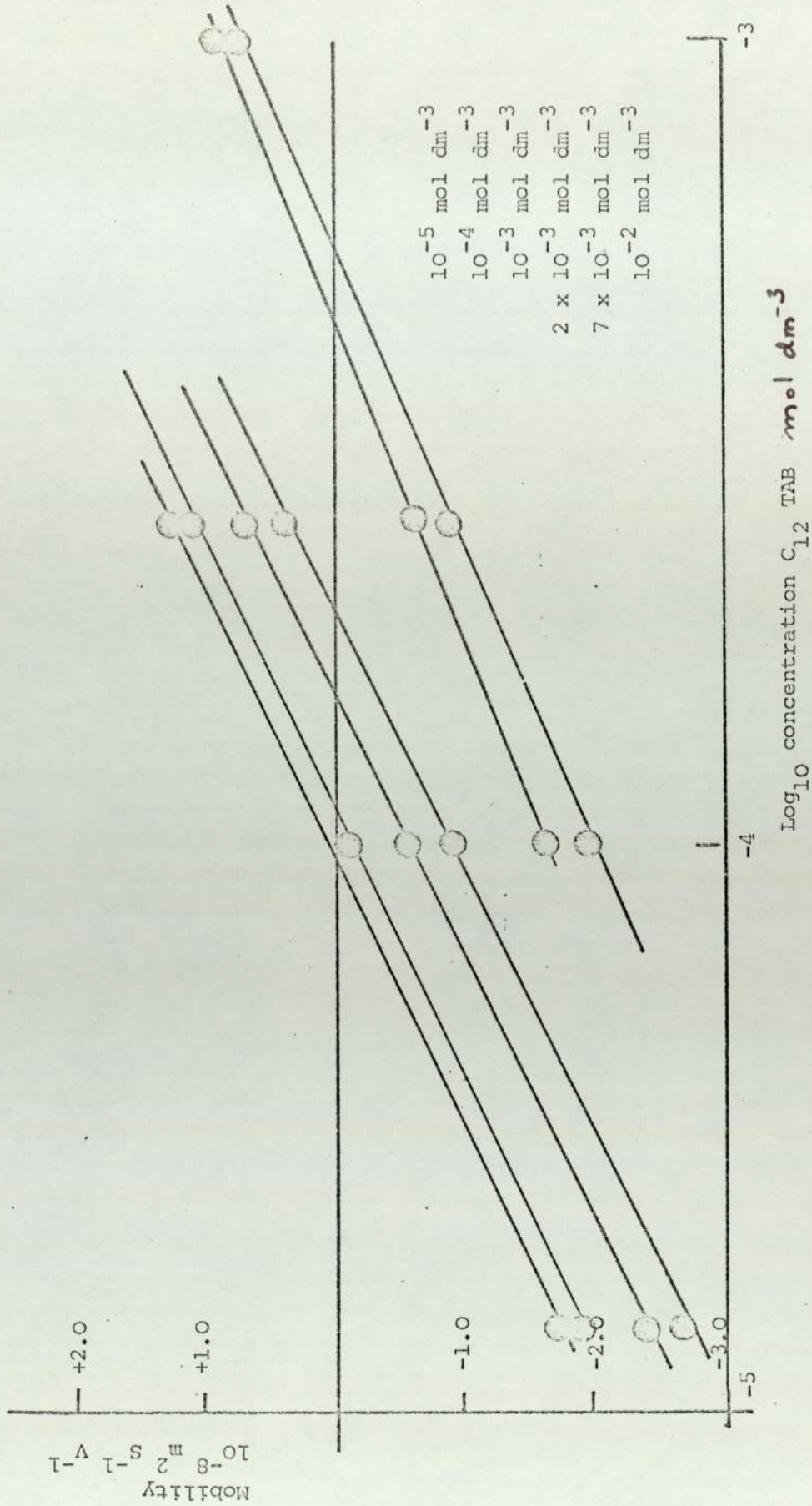


Figure XXXIII Variation of RCC with concentration $C_{16} E_{30}$

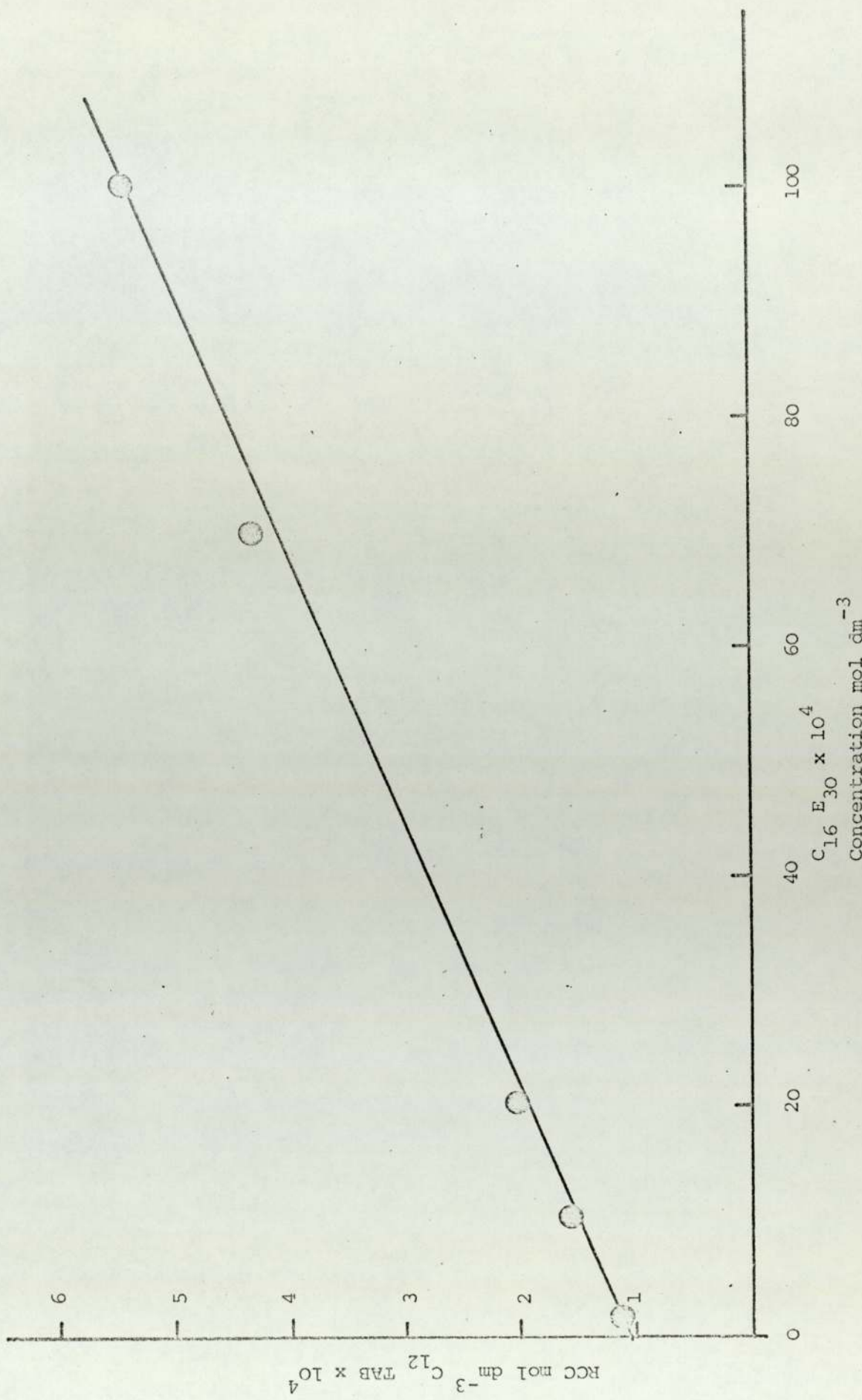


Figure XXXIV Effect of concentration of $C_{16} E_{30}$ on RCC of $C_{12} TAB$.

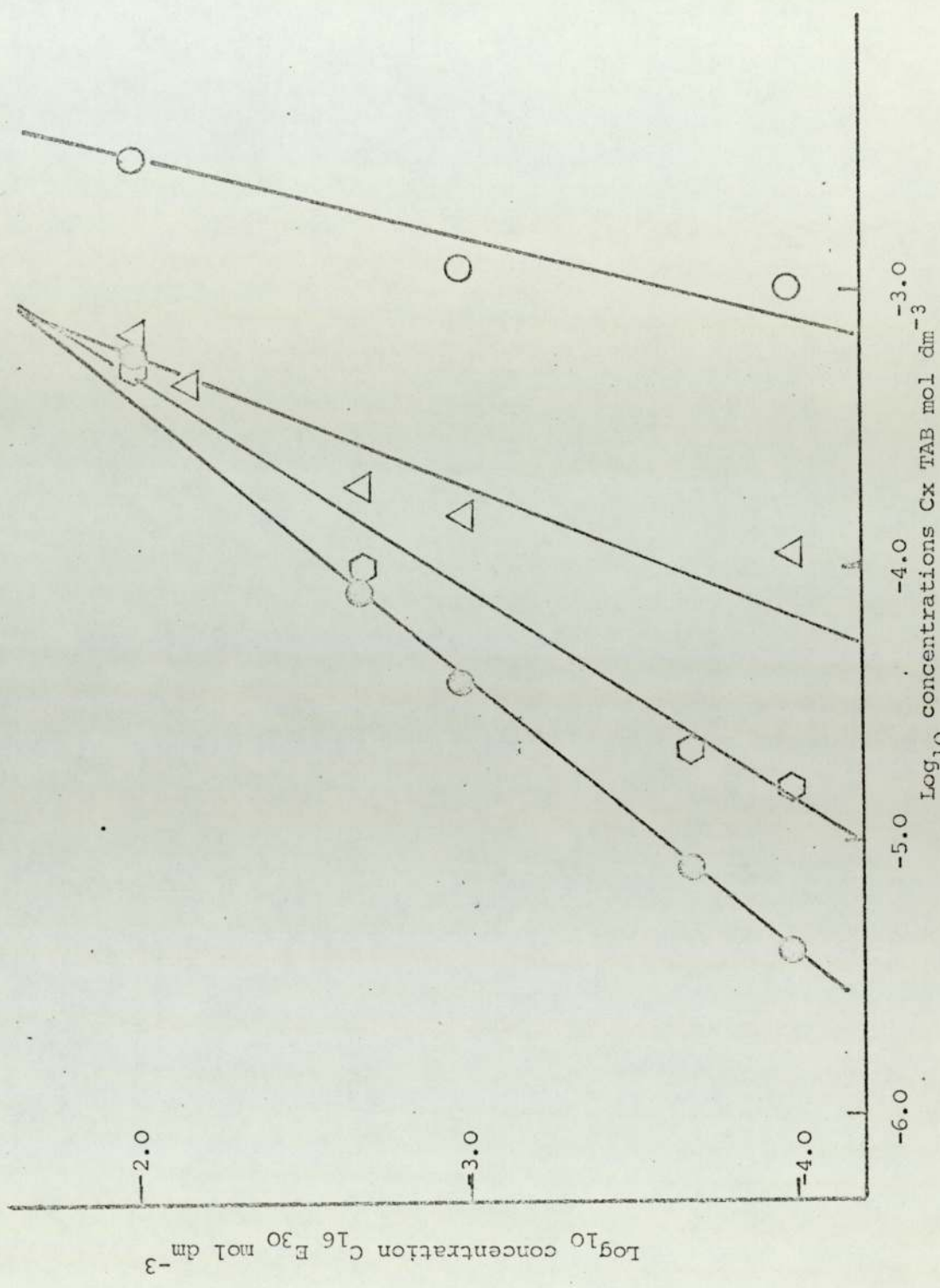


Fig XXXV Cx TAB concentrations for RCC in presence of varying concentrations of C₁₆ E₃₀. C₁₀ TAB ○; C₁₂ TAB ◻; C₁₄ TAB △; C₁₆ TAB ●

Fig. XXXVI. The plot is linear over the range C_{10} - C_{14} but there is deviation from linearity at greater C values; this plot is of similar form to that found in section 4.33 for the adsorption energies of cationics on polystyrene latex versus alkyl chain length. The slope of line -0.44 indicates that for each CH_2 group of the cationic alkyl chain the slope of the RCC versus C_{16}^{Ey} concentration plot will vary by a factor of 0.44, It is thus possible to predict the RCC for various concentrations of non-ionic of the series C_{16}^{Ey} when a single value is known.

4.4.2.2. Effect of ethylene oxide chain length on the reversal of charge concentration.

The effect of ethylene oxide chain length on RCC is shown by examining the results given in Fig. XXXVII and table XVIII, for the effect of 10^{-3} mol dm^{-3} $C_{16}^{E_{10}}$, $C_{16}^{E_{18}}$, $C_{16}^{E_{30}}$, $C_{16}^{E_{45}}$, $C_{16}^{E_{60}}$ on the zeta potential- \log_{10} concentration plot of C_{12}^{TAB} . The most significant feature of the curves is that the RCC for all species occurs, within the limits of experimental error, at about the same concentration - all results lie between 1.15×10^{-4} mol dm^{-3} and 1.8×10^{-4} mol dm^{-3} . This suggests that the ethylene oxide chain portion of the molecule plays no direct part in the adsorption pattern of mixed surfactants. Confirmation is given by reference to the results in the last section for different nonionics and the same cationic and to figure XXXV where the slope values for all the \log_{10} concentration C_{16}^{Ey} - \log_{10} concentration Cx^{TAB} plots are plotted against alkyl chain length of cationic surfactant. All points lie on the same line and as the only variant in the nonionic range is the number of ethylene oxide groups they can have no direct effect on the adsorption pattern.

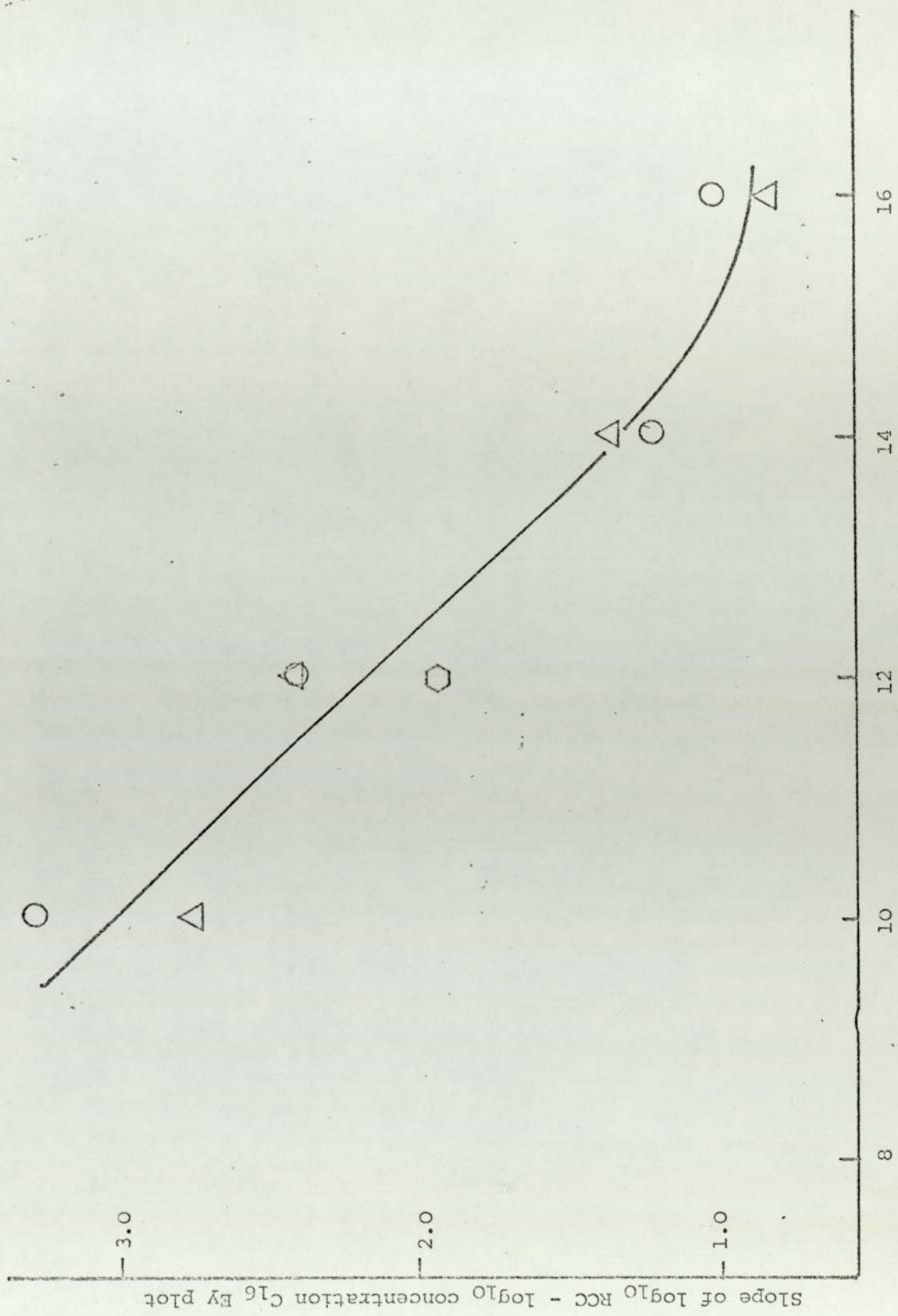


Fig XXXVI Effect of number of carbon atoms in alkyl chain of Cx TAB on slope of log₁₀ RCC - log₁₀ concentration C₁₆ Ey plot C₁₆ E₁₀ ○; C₁₆ E₃₀ △; C₁₆ E₆₀ ○.

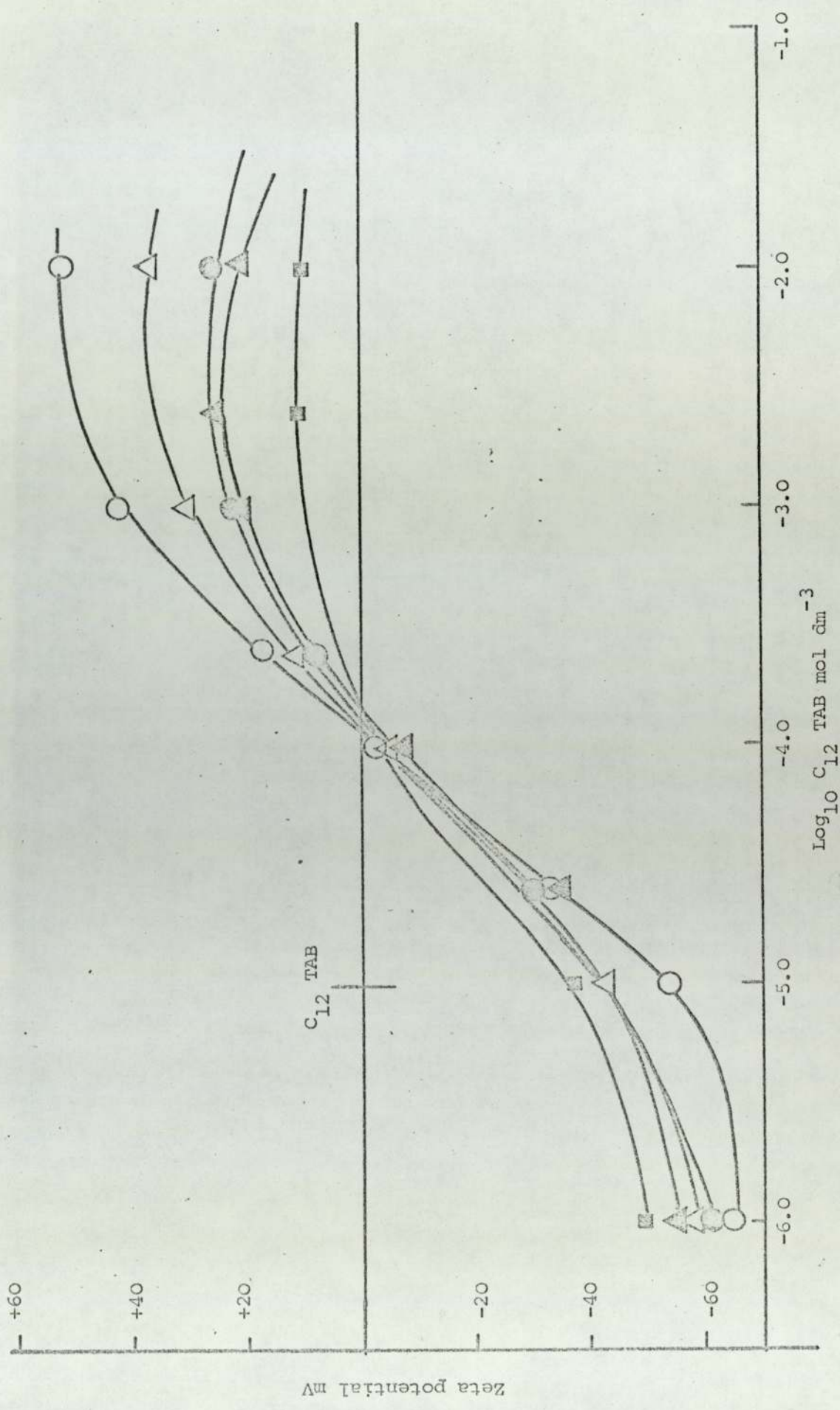


Fig XXXVII Zeta potential - concentration $C_{12} \text{ TAB}$ with $10^{-3} \text{ mol dm}^{-3}$ of $C_{16} E_{10}^{\circ}$; $C_{16} E_{18}^{\Delta}$; $C_{16} E_{30}^{\circ}$; $C_{16} E_{45}^{\circ}$; $C_{16} E_{60}^{\square}$.

4.5. Effect of anionic surface active agents on the electrophoretic mobility and zeta potential.

The adsorption of anionic surface active agents at the polystyrene solid-liquid interface differs from the system with cationic surface active agents in that the situation is one in which a negatively charged molecule is being adsorbed onto a negatively charged surface. After adsorption, the driving force for which will be the hydrophobic effect, the alkyl chain of the molecule associating with the hydrophobic surface of the latex 'between' the carboxylic acid groups, the adsorbed molecules will be orientated with the charge group directed towards the diffuse layer, so that there will be an increase of potential at the shear plane. The zeta potential should consequently increase with increasing concentration of surface active agent until the surface of the latex is 'full' and should then remain constant.

4.5.1. General characteristics of the zeta potential- \log_{10} concentration plots.

The anionic surface active agents used were sodium alkyl sulphates; sodium decyl sulphate, SDeS; sodium dodecyl sulphate, SDS; and sodium tetradecyl sulphate, STS. Variation in mobility with increasing concentration of surface active agent was measured and zeta potentials calculated, results are shown in Figures XXXVIII, XXXIX, XL and Table XIX.

Zeta potentials were calculated, as in Section 4.3.2, via Appendix 1 (99). In a number of cases the observed mobilities were too high to enable zeta potentials to be calculated from these computed tables. However mobilities with the three surfactants all followed the same pattern.

Complete zeta potential- \log_{10} concentration curves are presented for SDeS, Fig. XXXVIII and SDS, Fig. XXXIX, and the results for STS, Fig. XL, have been plotted as far as conversion of mobility values allows. The errors involved in measurement of mobility at these high zeta potentials

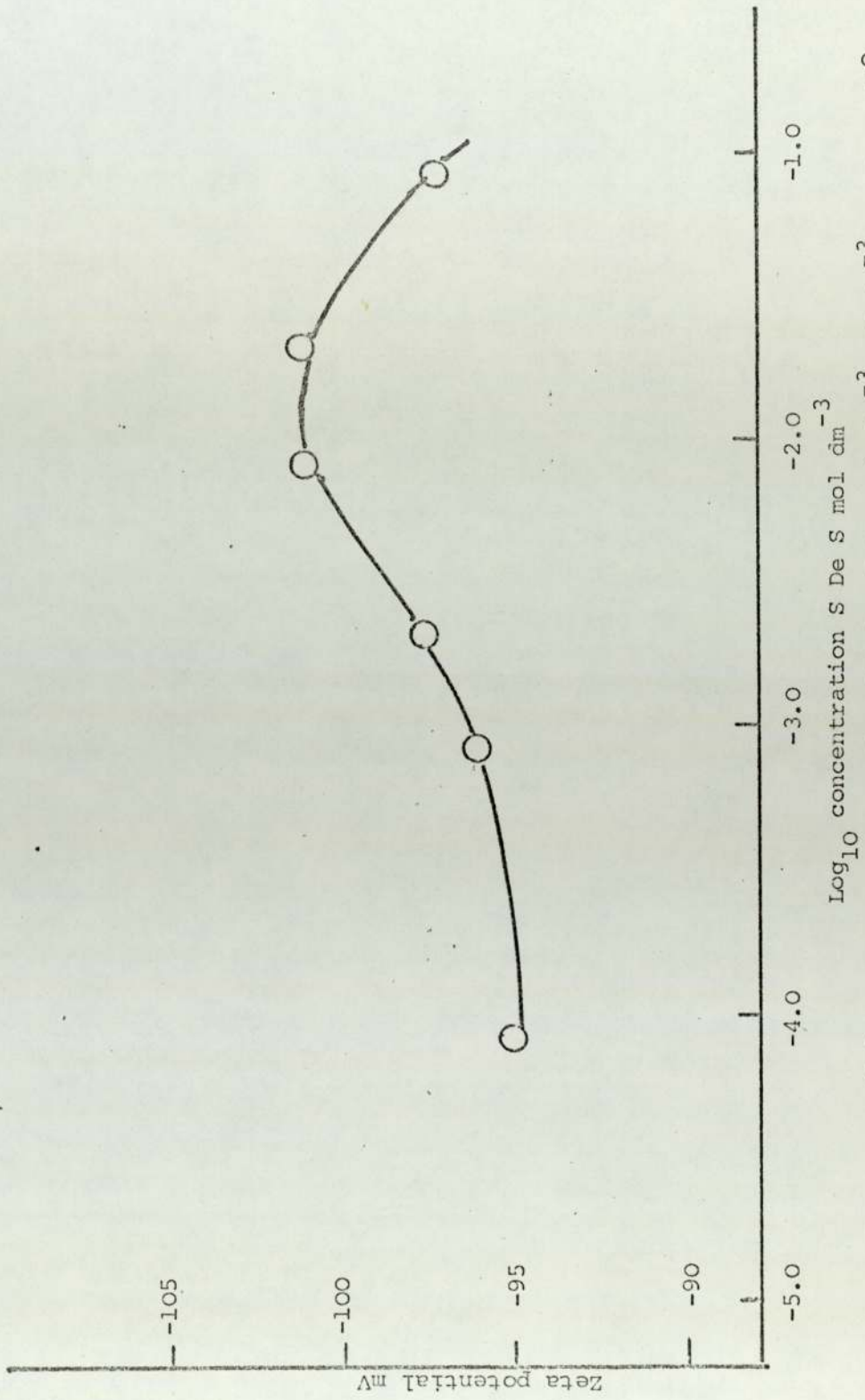


Figure XXXVIII Zeta potential - concentration sodium decyl sulphate in 10^{-3} mol dm^{-3} Na Cl at 25°C and pH 7.0

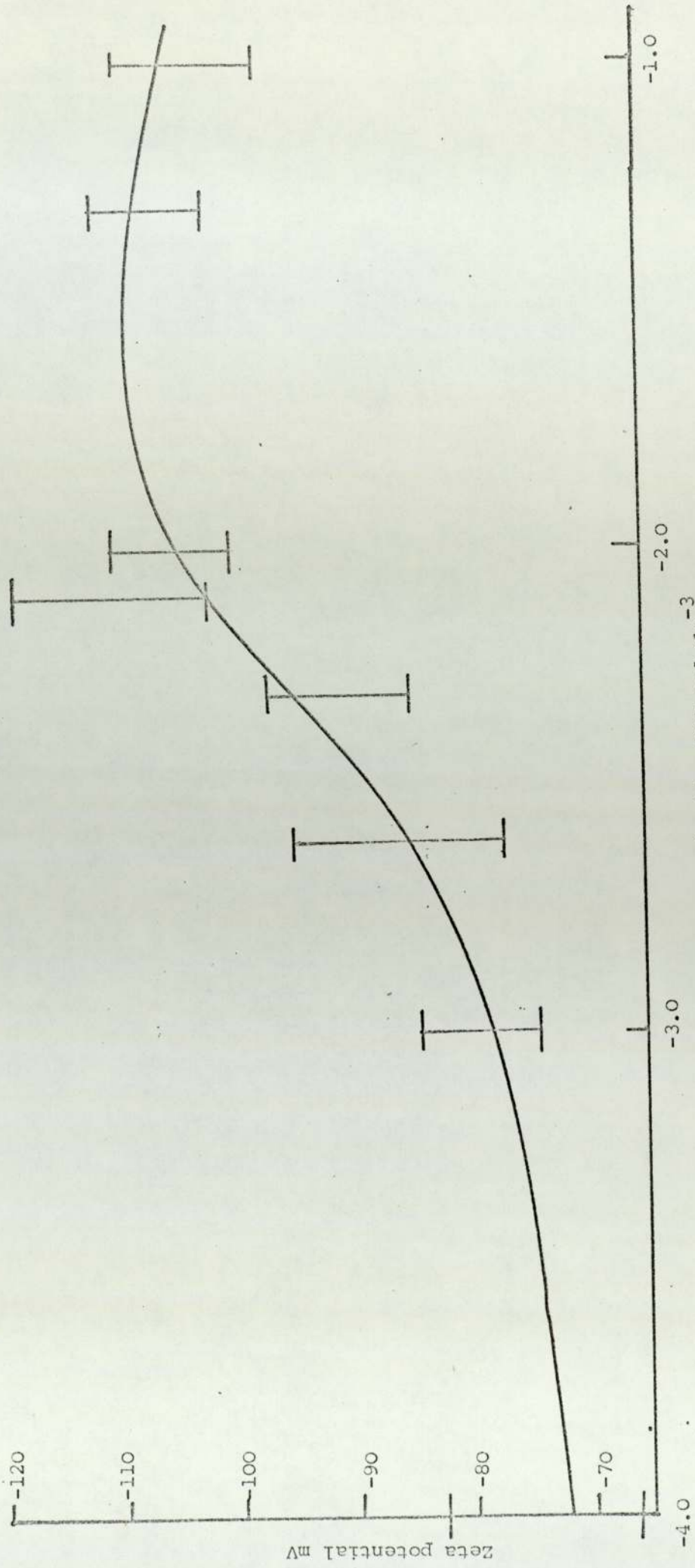


Figure XXXIX Zeta potential - concentration sodium dodecyl sulphate in 10⁻³ molar Na Cl at 25°C and pH 7.0

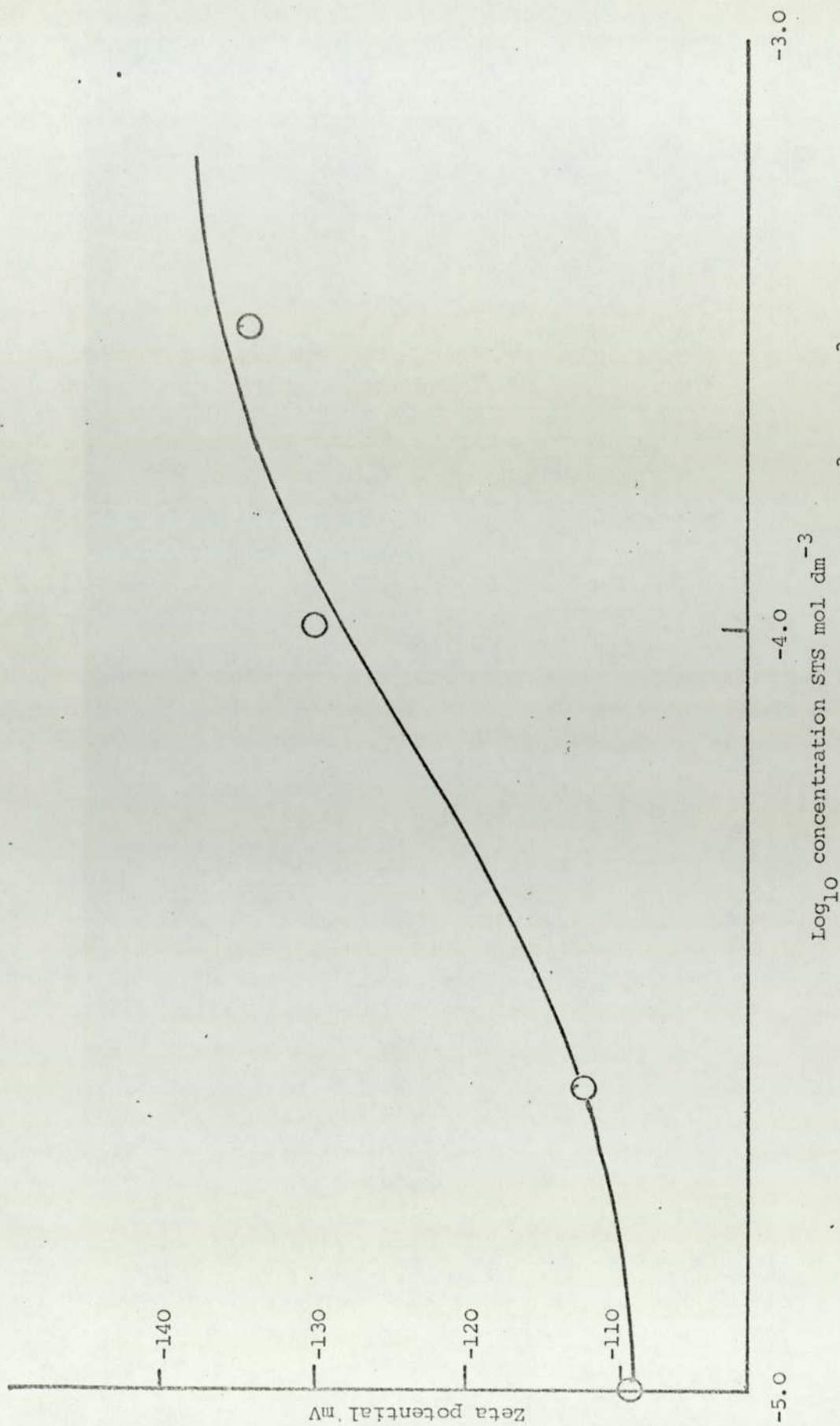


Fig XL Zeta potential - concentration sodium tetradecyl sulphate in 10^{-3} mol dm^{-3} Na Cl at 25°C and pH 7.0

are greatly magnified and Fig. XXXIX for SDS, has been plotted including error estimation to illustrate this point.

As indicated, curves are of the same form and will be discussed mainly by reference to that for SDS, Fig. XXXIX.

Between the concentrations of SDS 10^{-4} mol dm $^{-3}$ to 10^{-3} mol dm $^{-3}$ the zeta potential increases very slowly and here there is probably displacement by the surfactant molecules of ions already present in the Stern layer. Above 10^{-3} mol dm $^{-3}$ the potential rises rapidly, as adsorption of SDS by the hydrophobic effect occurs, and reaches a maximum at or before about 10^{-2} mol dm $^{-3}$. The cmc of SDS in water was found to 7.8×10^{-3} mol dm $^{-3}$ so that there appears to be a relationship between this maximum and the critical micelle concentration. The plot for SDeS, Fig. XXXVIII, shows that the maximum occurs before the cmc, 3.5×10^{-2} mol dm $^{-3}$ in water. This fact was noticed by Shaw (148) with polystyrene latex and sodium dodecanoate and is probably due to the fact that the surface concentration of surfactant molecules is higher than the bulk concentration, consequently the 'cmc' at the surface, with optimum conditions for the hydrophobic effect, occurs at a lower concentration than in the 'bulk' solution, as was discussed in Section 2.4.6. on hydrophobic bonding.

After the maximum the zeta potential falls off with increasing concentration of anionic due to ionic strength effects.

4.5.2. Calculations from zeta potential- \log_{10} concentration sodium alkyl sulphate curves.

In Section 4.5.3. equation 2.86, with zeta potentials replacing Stern potentials was used to calculate the number of adsorption sites N_1 available per unit area and from this, the adsorption constant k_2 and the chemical free energy of adsorption $\Delta \bar{G}$ were obtained.

The adsorption of the anionic surfactant molecules onto the negatively charged latex particle occurs by the hydrophobic effect. The adsorption energies involved should therefore depend on alkyl chain length and be similar to those found with cationic surfactants in Section 4.3.3. However opposing adsorption will be the electrostatic repulsion between the $-COO^-$ group of the latex and the $O-S(=O)_2O^-$ group of the anionic surfactant.

If the slope of the zeta potential- \log_{10} concentration sodium alkyl sulphate line is taken as it begins to rise rapidly, i.e. as adsorption due to the hydrophobic effect is taking place, then equation 2.85, with zeta potentials replacing Stern potentials, can be used to calculate the number of adsorption sites N_1

$$\left(\frac{d\zeta}{d \log_{10} C} \right) = \frac{4.606kT}{Ze} \left(\frac{\frac{\sinh Ze \zeta_1}{2kT} - \frac{\sinh Ze \zeta_2}{2kT}}{\cosh \frac{Ze \zeta_2}{2kT}} \right) \left[\frac{(8n_0\epsilon kT)^{1/2}}{Ze N_1} \frac{\frac{\sinh Ze \zeta_1}{2kT} - \frac{\sinh Ze \zeta_2}{2kT}}{-1} \right]$$

where ζ_1 and ζ_2 are zeta potentials on the line.

Further, k_2 the adsorption constant, can then be calculated from equation 2.81.

$$1/c = k_2 \left[\frac{Ze N_1}{(8n_0\epsilon kT)^{1/2} \left[\frac{\sinh \frac{Ze \zeta_1}{2kT} - \sinh \frac{Ze \zeta_2}{2kT}}{2kT} \right]} - 1 \right]$$

where C is chosen as the concentration at the zeta potential midpoint between ζ_1 and ζ_2 .

and the chemical free energy of adsorption $\Delta \bar{G}$ from equation 2.73a

$$k_2 = \frac{\exp \left[\frac{-\Delta \bar{G}}{kT} \right]}{55.6 \times 6 \times 10^3}$$

If one assumes that the $\Delta \bar{G}$ obtained above is the specific chemical free energy of adsorption $\Delta \phi$ of equation 2.87

$$\Delta \bar{G} = \Delta \phi + ze\psi_\delta$$

then a measure of the adsorption energy counteracting the electrostatic repulsion can be obtained from $ze\zeta$, where the value of ζ is the midpoint

value between \mathcal{S}_1 and \mathcal{S}_2 as mentioned above; thus a value for $\Delta\bar{G}$ can then be found. Results are shown in Table XX. The number of adsorption sites N_1 is constant which suggests that this method of calculation is applicable. The total chemical free energy of adsorption $\Delta\bar{G}$ (the last column of table XX) increases as alkyl chain length increases. The results found agree very well with those for adsorption of cationic surfactants of the same alkyl chain length (Table VI), showing that it is the length of the alkyl chain which is the important factor in considering adsorption of these compounds onto hydrophobic surfaces. Similar agreement was found by Ottewill & Watanabe (112) $-\Delta\bar{G} = 8,800 \text{ cal mole}^{-1}$ for SDS on silver iodide and Ottewill and Rastogi (147) $-\Delta\bar{G} = 9,200 \text{ cal mole}^{-1}$ for C_{12} TAB on silver iodide.

4.6. Effect of mixtures of anionic and nonionic surface active agents on the electrophoretic mobility and zeta potential.

The effect of adding nonionic surface active agents, $C_{16}E_y$ to the anionic surface active agents used in Section 4.5, and the combined effect on the mobility of the polystyrene latex was examined. Constant concentrations of the nonionic were used and the concentration of anionic varied as previously:

The surface active agent mixtures used were SDeS with $C_{16}E_{60}$; SDS with $C_{16}E_{10}$, $C_{16}E_{30}$ and $C_{16}E_{60}$; STS with $C_{16}E_{10}$ and $C_{16}E_{60}$.

4.6.1. General characteristics of the zeta potential- \log_{10} concentration sodium alkyl sulphate plots.

Results are shown in Figures XLI to XLVI and Tables XXI to XXV. Results for the various anionic nonionic mixtures follow a pattern which can be studied by examination of the results for SDS shown in Fig. XLII, SDS with $C_{16}E_{10}$; Fig. XLIII. SDS with $C_{16}E_{30}$; and Fig. XLIV SDS with $C_{16}E_{60}$.

TABLE XX

Free energies of adsorption anionic surface active agents

Compound	$d\zeta/d \log_{10} C$ mV	C mol m ⁻³	N_i m ⁻²	K_2 m ³ mol ⁻¹	$-\Delta\bar{G}(\Delta\phi)$ kJ mol ⁻¹	$Ze \zeta$ kJ mol ⁻¹	$-\Delta\bar{G}$ kJ mol ⁻¹
S De S	- 7.5	3×10^{-3}	3.53×10^{16}	0.138	22.17	9.53	31.70
SDS	-12.0	10^{-3}	2.24×10^{16}	0.633	25.95	7.65	33.60
STS	-25.0	1.4×10^{-4}	3.87×10^{16}	7.69	32.14	12.58	44.72

(a) Sodium dodecyl sulphate with $C_{16}E_{10}$.

The zeta potential - \log_{10} concentration plot is displaced to the right, with this short ethylene oxide chain compound only a high concentration is really effective in altering the pattern, however the magnitude of displacement would appear to be proportional to concentration of non-ionic. The suggestion is that both species are adsorbed onto the latex particle and that the nonionic species is hindering anionic adsorption. The effect of the adsorption of the nonionic surfactant will be to displace the shear plane and hence reduce the zeta potential. As the concentration of anionic increases it must displace the nonionic so that at 10^{-1} mol dm^{-3} SDS all concentrations show virtually the same potential as that of SDS on latex alone indicating that the nonionic molecules have been removed.

The explanation of the reason for displacement of the nonionic by the anionic surfactant, i.e. that the adsorption energy of the anionic is greater than that of the nonionic, must be substantially the same as that given for cationic/nonionic systems in Section 4.4.1.

(b) Sodium dodecyl sulphate with $C_{16}E_{30}$, and

(c) Sodium dodecyl sulphate with $C_{16}E_{60}$.

Both Fig. XLIII, SDS with $C_{16}E_{30}$, and Fig. XLIV, SDS with $C_{16}E_{60}$, show the same characteristics and so can be considered together. As with (a) there is displacement of the zeta potential- \log_{10} concentration curve by the various concentrations of nonionics used. The magnitude of lowering of zeta potential at 10^{-4} mol dm^{-3} SDS follows the effect found by nonionic surfactant on latex alone, i.e. the longer the ethylene oxide chain length the lower the zeta potential, as was discussed in Section 4.2; so that with $C_{16}E_{30}$ the zeta potential is lowered from -74mV to -53mV and with $C_{16}E_{60}$ from -74mV to -29mV both at 10^{-2} mol dm^{-3} concentration of nonionic surfactant.

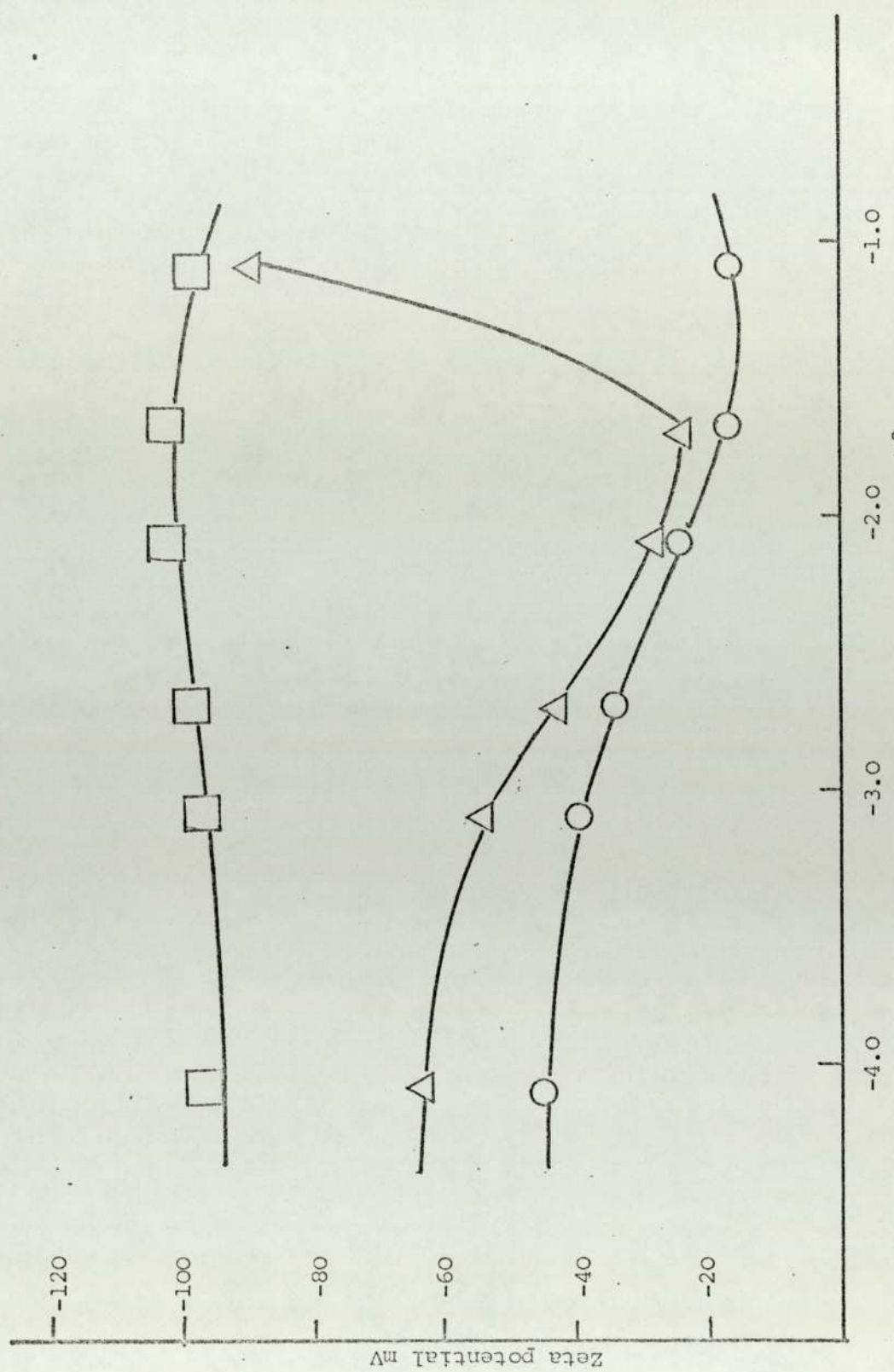


Fig XLI Zeta potential - concentration S De S \square ; with $\text{C}_{16}\text{E}_{60}$, $10^{-2} \text{ mol dm}^{-3}$ \triangle ; $10^{-3} \text{ mol dm}^{-3}$ \circ

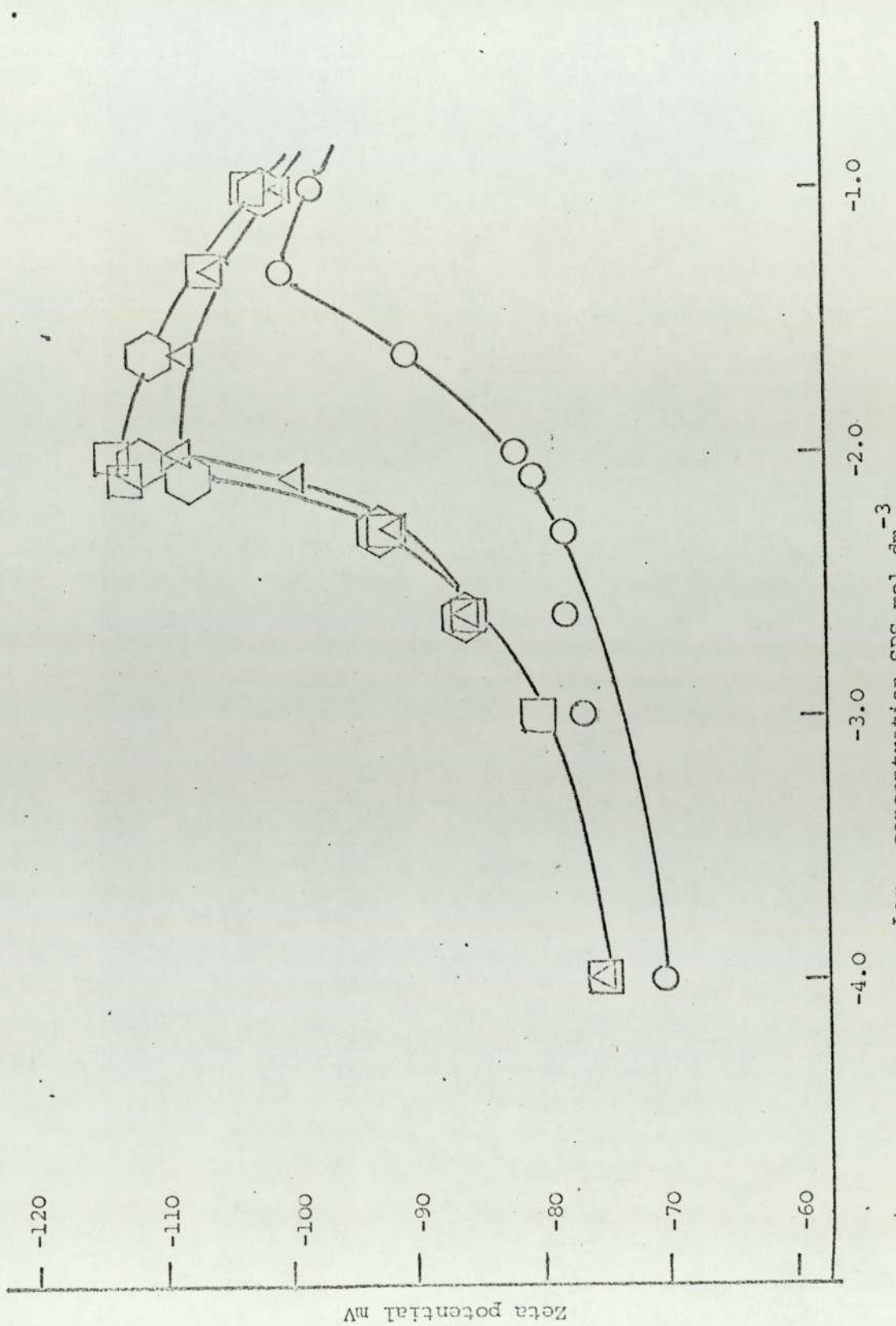


Fig XLII Zeta potential - concentration SDS \square with $C_{16}E_{10}$; 10^{-2} mol dm^{-3} \circ ; 10^{-3} mol dm^{-3} \triangle ;
 10^{-4} mol dm^{-3} \hexagon .

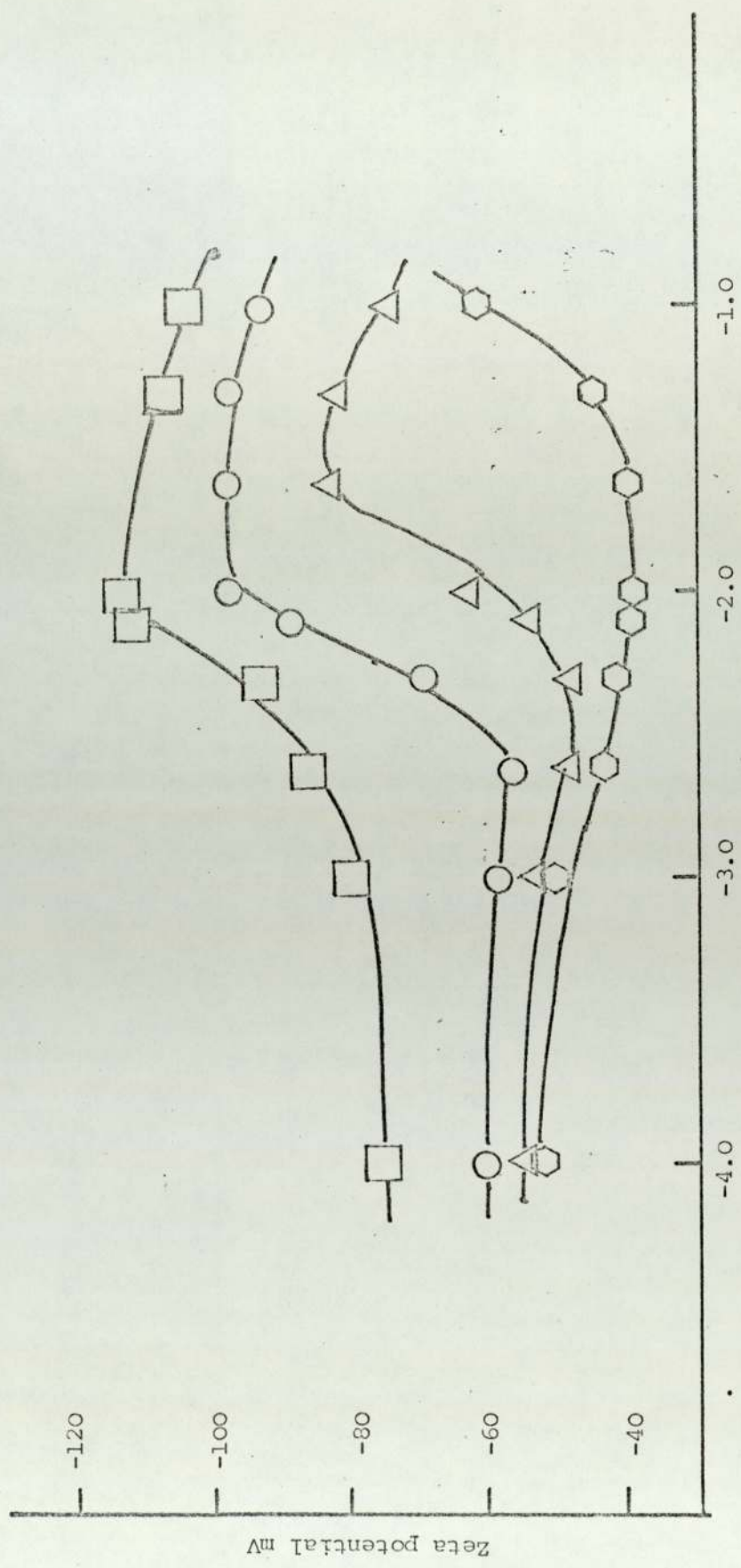


Fig XIII Zeta potential - concentration SDS \square ; with $\text{C}_{16}\text{E}_{30}$, 10^{-2} mol dm^{-3} \circ ; 10^{-3} mol dm^{-3} \triangle ; 10^{-4} mol dm^{-3} \diamond

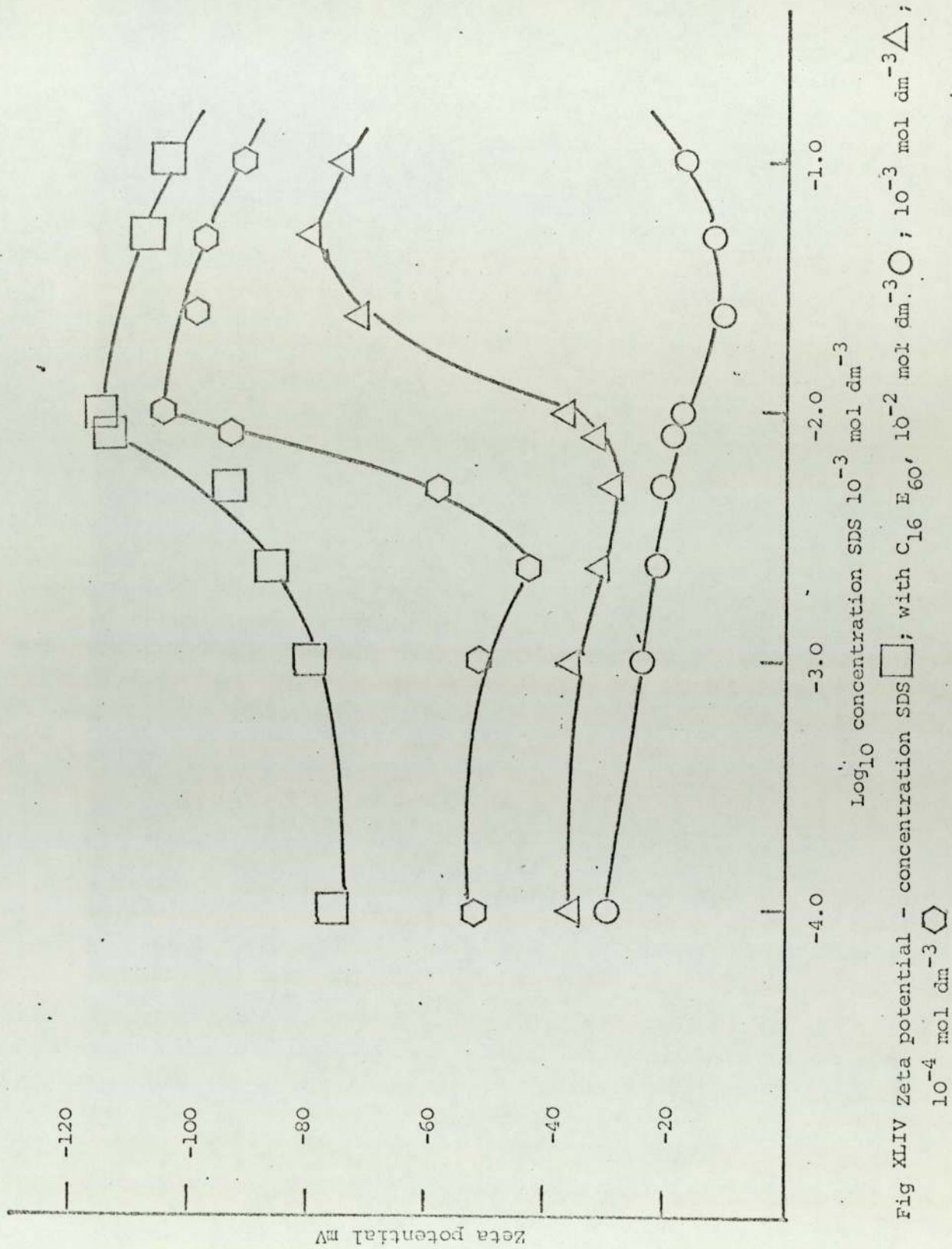


Fig XLIV Zeta potential - concentration SDS \square ; with $C_{16}E_{60}$, 10^{-2} mol dm^{-3} \circ ; 10^{-3} mol dm^{-3} \triangle ; 10^{-4} mol dm^{-3} \hexagon

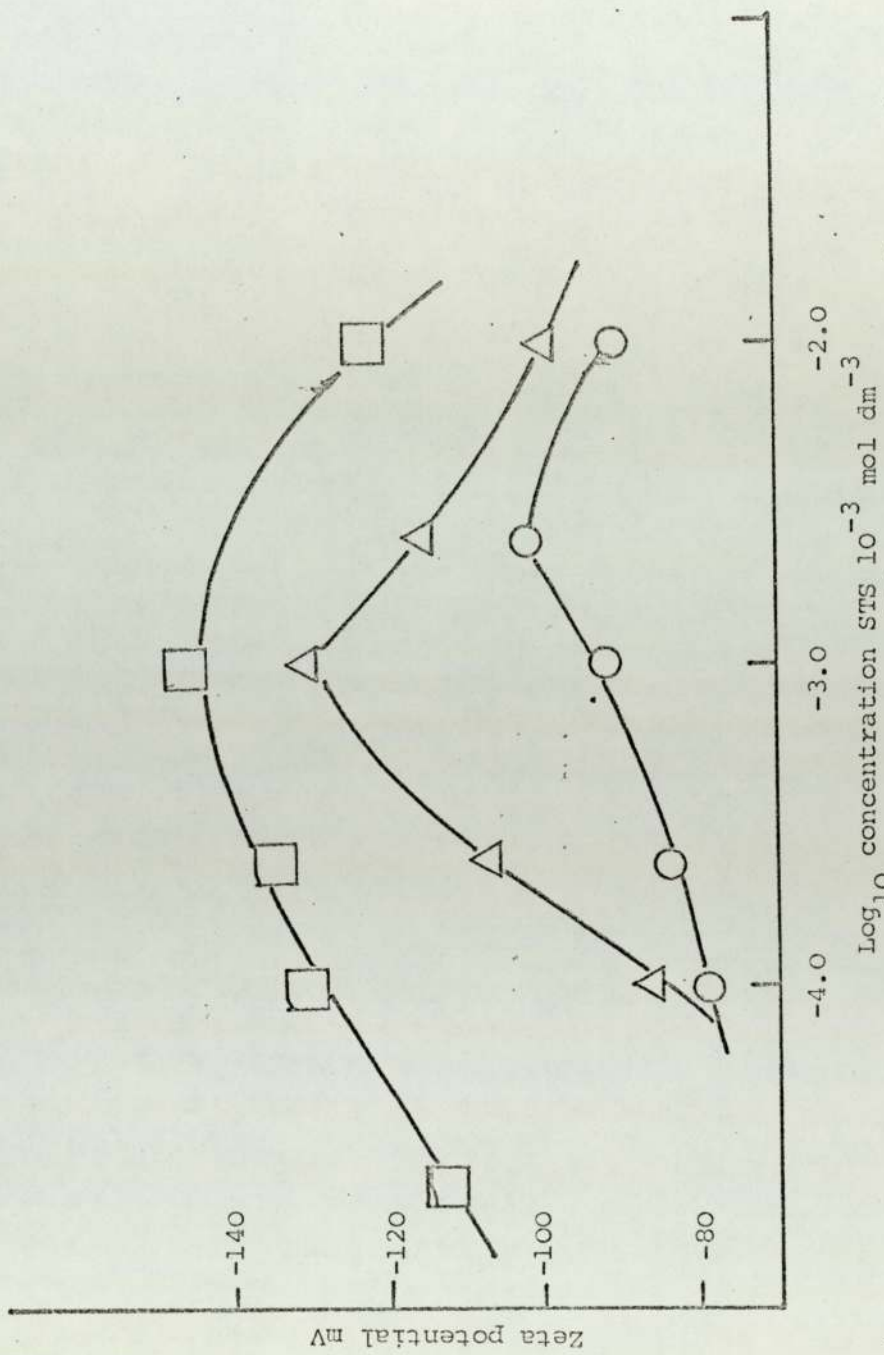


Fig XLV Zeta potential - concentration STS \square 10^{-3} mol dm^{-3} ; with $C_{16}E_{10}$, 10^{-2} mol dm^{-3} \circ ; 10^{-3} mol dm^{-3} \triangle .

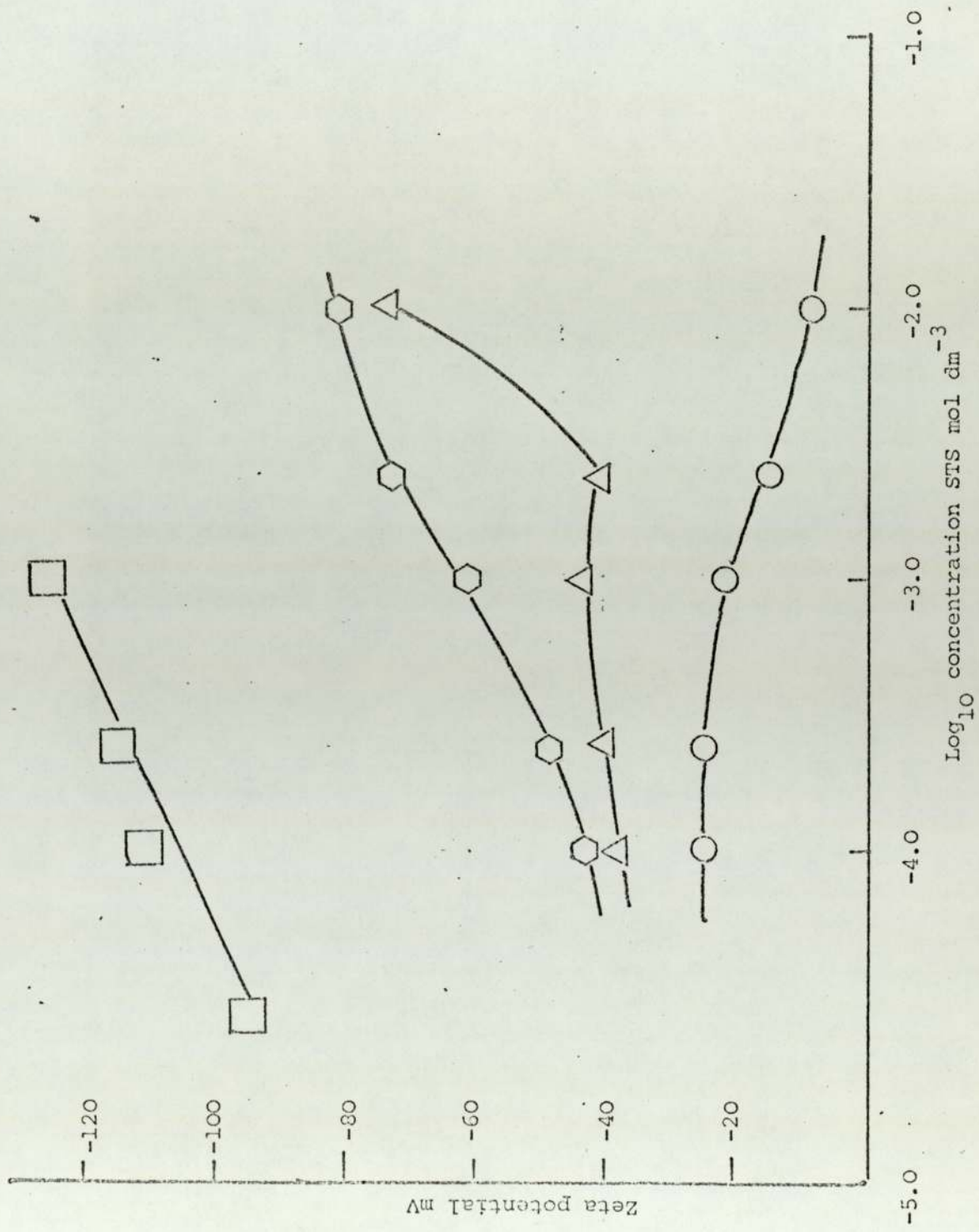


Fig XLVI Zeta potential - concentration STS ◻; with $C_{16} E_{60}$, 10^{-2} mol dm⁻³ ◻; 10^{-3} mol dm⁻³ △; 10^{-4} mol dm⁻³ ◻.

However as the concentration of SDS is increased the zeta potential falls still further to a minimum of, with 10^{-2} mol dm⁻³ C₁₆E₃₀, -39mV at a concentration of 1.5×10^{-2} mol dm⁻³ SDS, and with the same concentration of C₁₆E₆₀ to -10mV at a concentration of 3×10^{-2} mol dm⁻³ SDS. The potential then rises as SDS concentration is increased to 10^{-1} mol dm⁻³, apparently towards the line for SDS on latex alone, but concentration difficulties would not allow investigation beyond this concentration. At lower concentrations of nonionic the minima occur at lower concentrations of SDS and there is approximate proportionality between the concentrations of SDS at the minima and concentrations of nonionic surfactants, which varies with ethylene oxide chain length. The fall off in zeta potential which occurs with increasing concentration of SDS as shown in Fig. XLIII, SDS with C₁₆E₃₀, and Fig. XLIV, SDS with C₁₆E₆₀ is not shown in Fig. XLII, SDS with C₁₆E₁₀.

The explanation for the lowering must be that some form of complexation occurs between the nonionic and anionic surfactants. As the effect is reversible, i.e. the zeta potential rises again as SDS concentration is increased, the suggestion is that first of all a predominately nonionic layer is adsorbed onto the particle, taking, for example Fig. XLIV, SDS with C₁₆E₆₀, this is the effect between the concentrations 10^{-4} and 10^{-3} mol dm⁻³ SDS. As further SDS is added these molecules must complex with the nonionic in such a way that their nonpolar groups are directed towards the aqueous phase, the effect would be of bilayer formation with the plane of shear displaced still further out from the particle surface and a consequent fall in zeta potential. When the concentration of SDS is further increased presumably the effect of concentration and the differing adsorption energies of the complex and the SDS allows gradual displacement of the former from the particle surface and therefore a rise in the zeta potentials. With C₁₆E₁₀ presumably no such complex is formed.

Complex formation between nonionic polymers and ionic surfactants has been well established. Thus Moto et al (149) report complexation between SDS and an ethylene oxide block copolymer. Tadros (150) found interaction between both $C_{16}TAB$ and sodium dodecylbenzene sulphonate with polyvinyl alcohol, he considers that a complex can form by orientated adsorption of the surfactant ions through hydrophobic bonding between the hydrophobic end of the surfactant ion and the hydrophobic part of the polymer chain. Schwuger (151) points out that polymers such as polyvinyl pyrrolidone, polyglycol ethers and polyvinyl alcohol form complexes with ionic surfactants in aqueous solution and that especially strong interactions are observed with anionic surfactants. In contrast, cationic surfactants show only very weak effects, which sometimes cannot be detected using a number of general colloid chemistry techniques; this would explain the apparent lack of complexation effects found in this work with cationic and nonionic surfactant mixtures.

Whilst hydrophobic bonding is one of the contributory factors in complex formation Schwuger points to evidence that with polyethylene glycols complex formation is strongly dependent upon the length of the glycol chain. A polyethylene glycol of fifteen units shows only a low tendency towards complex formation, ^{but} as the number of units in the chain increases complex formation strongly increases. Obviously a factor other than hydrophobic bonding is involved. Schwuger's work indicates that there is association between the polar parts of the two molecules. He suggests that the oxygen atom of the ether linkage of the ethylene oxide chain could possibly become slightly positively charged, which would favour an adsorption of the negatively charged surfactant anion. The basis for this suggestion seems a little obscure; a possible alternative is that of hydrogen bonding between the ether oxygens and solvent molecules and similar bonding between the solvent molecules and the $-O-S(=O)-$ group

of the anionic surface active agent. Schwuger suggests that his findings, with polyethylenglycol-ionic surfactant complexes, can be applied to complexes formed between nonionic surfactants with ethylene oxide chains and ionic species.

Irrespective of the mechanism it therefore seems well founded that complexation between nonionic and ionic surfactants can occur because of association between polar regions. This supports the suggestion in this work that the anionic surfactant's polar group is associated with the ethylene oxide groups of the adsorbed nonionic thus bringing about a reduction in zeta potential due to shear plane displacement.

The fact that the lowering of zeta potential is reversed as concentration of SDS is increased, supports the hydrogen bonding theory as such association is relatively weak, and would be broken by the stronger adsorption energy of the anionic surfactant when a sufficient concentration of the latter was achieved.

The fact that Schwuger found no complex formation with a polyethylene glycol of 15 units gives a possible reason why no lowering of zeta potential occurs with the $C_{16}E_{10}$ anionic systems i.e. no complex is formed.

4.6.2. Effect of anionic surface active agent type, and nonionic surface active agent ethylene oxide chain length, on the zeta potential- \log_{10} concentration plots.

The general effect the increase of concentration of nonionic surface active agent has on the zeta potential- \log_{10} concentration curves has been indicated in the previous subsection. There is a general indication of proportional displacement of plot with increasing concentration of nonionic, but it is difficult to decide how to select a particular property for comparison to confirm this and to decide the effect of other factors such as anionic type and ethylene oxide chain length.

However in subsection 4.5.2., when calculating energies of adsorption of the three anionics a mid point potential of the slope of the line was used, for SDeS 98.5mV; SDS 79mV and STS 130mV. These values enable a comparative lowering of the zeta potential by, for example, $C_{16}^{E}60$ to be made. The results are shown below (the figures in brackets are calculated values to standardise the SDeS and STS values for comparison with the figures for SDS).

Lowering of zeta potential produced by $C_{16}^{E}60$

Concentration $C_{16}^{E}60$ mol dm ⁻³	SDeS mV	SDS mV	STS mV
10^{-4}	-	50	65 (40)
10^{-3}	38 (31)	35	58 (35)
10^{-2}	30 (24)	23	45 (27)

There is good agreement between the standardised figures and the values for SDS and the results show that the lowering of zeta potential produced by a concentration of $C_{16}^{E}60$ is the same irrespective of the anionic used. Similar results would be expected with other nonionics.

With SDS and the various nonionics at a 10^{-2} mol dm⁻³ concentration a comparison of the effect of the length of the ethylene oxide chain can be made by measuring the lowering of the zeta potential at the 79mV point as indicated above. The values are 5.5mV for $C_{16}^{E}10$; 31mV for $C_{16}^{E}30$ and 56mV for $C_{16}^{E}60$. These values plotted against ethylene oxide chain length show a direct proportionality between chain length and lowering produced, Fig. XLVII. This shows, that at this point, it is the displacement of the plane of shear by the nonionic which is important. The slope of the line is very near to 1 indicating a lowering

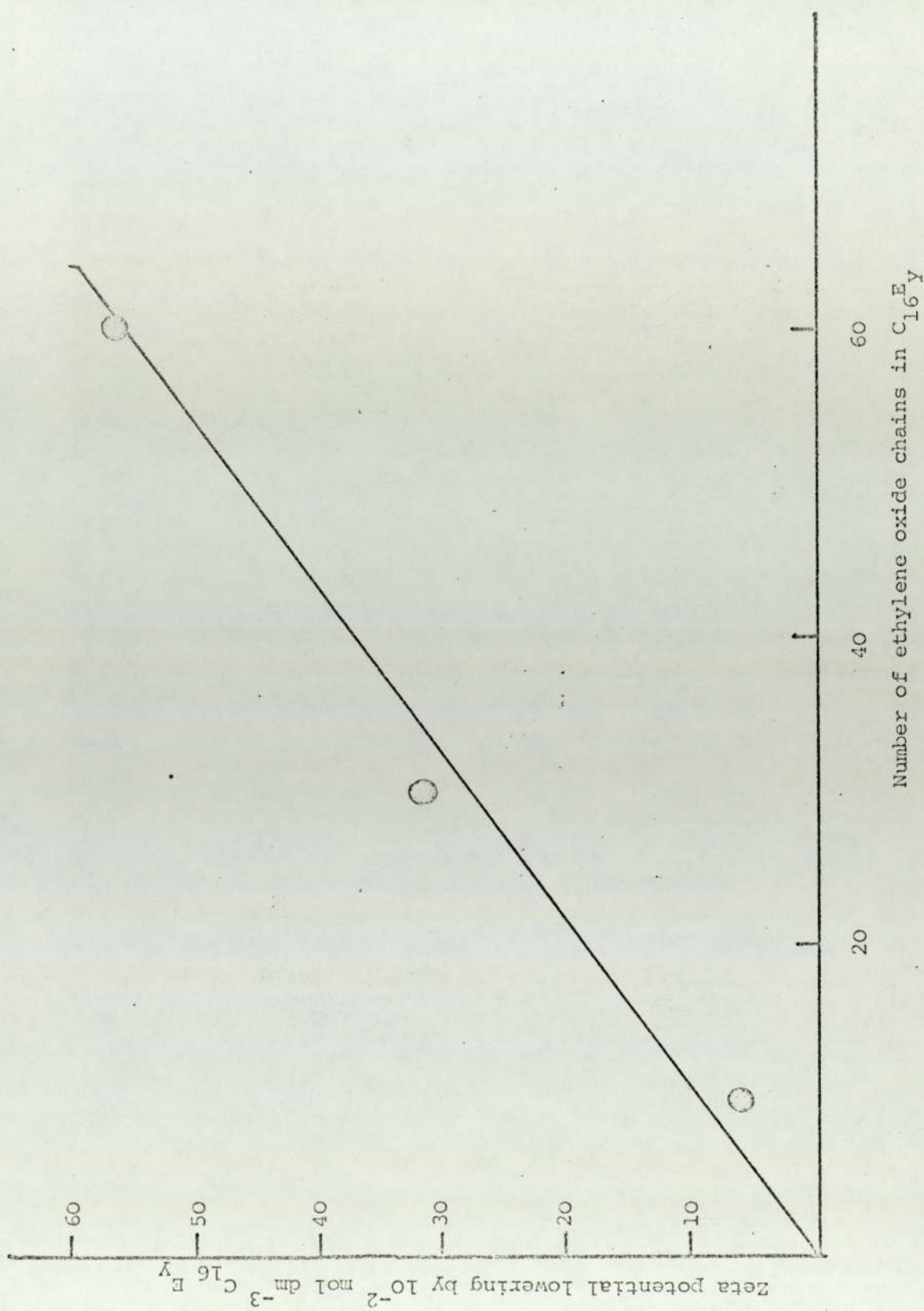


Fig XLVII

of $1mV$ for each additional ethylene oxide unit in the chain. It should thus be possible to predict the effect similar mixtures of anionic/non-ionic surfactants will have on other disperse systems.

SECTION 5.

MICROELECTROPHORETIC STUDIES ON GRISEOFULVIN, BETAMETHASONE,
NALIDIXIC ACID AND THIABENDAZOLE SUSPENSIONS,
RESULTS AND DISCUSSION.

The drugs chosen for this study are all of low water solubility. Betamethasone, Nalidixic Acid and Thiabendazole are available commercially as formulated suspensions. They all differ in chemical composition and hence a comparison can be made with this and their electrophoretic behaviour.

Suspensions of the drugs were made in solutions of the surface active agents used in the previous section with the polystyrene latex model system. The suspensions were shaken for 24 hours in a constant temperature water bath to allow time for complete adsorption of the surface active agent - Elworthy & Guthrie (119) had found that 16 hours was necessary for complete adsorption of nonionic surfactants, CxBy, on Griseofulvin. After storage of the suspensions at constant temperature for three days the sedimentation volume was measured in terms of the ultimate settled volume V_u to the original volume V_o :

$$\text{Sedimentation Volume} = \frac{V_u}{V_o}$$

The results are expressed as percentages. The appearance of the suspensions was examined and the ease of redispersion by shaking noted. The electrophoretic mobility of the particles was then measured.

5.1. Effect of pH on the electrophoretic mobility and zeta potential.

A suitable fraction of the suspension was placed in the flat cell assembly of the microelectrophoresis apparatus and the mobility of the drug particles measured as detailed in Section 3. Adjustment of pH was made by the addition of hydrochloric acid or sodium hydroxide and the suspension was shaken overnight in a constant temperature water

bath to equilibrate, the pH being checked before measurement, as above, was made.

Results are given in Table XXVI and the mobility/zeta potential - pH plots, which are discussed below in 5.1.2., in Figs. XLVIII to LI.

5.1.1. Conversion of mobility to zeta potential.

All measurements were carried out in 10^{-3} mol dm $^{-3}$ (1 mol m $^{-3}$) NaCl which gives a K value of $1.039 \times 10^8 \sqrt{c}$ m $^{-1}$, or 1.039×10^8 m $^{-1}$, so that

$$1/K \approx 1 \times 10^{-6} \text{ m or } 10\text{nm,}$$

for 10^{-2} mol dm $^{-3}$ solutions $1/K \approx 3\text{nm}$

and 10^{-1} mol dm $^{-3}$ $1/K \approx 1\text{nm}$

If the particle diameter is $2\mu\text{m}$ then Ka values in above concentrations are:

$$10^{-3} \text{ mol dm}^{-3}, \quad Ka \approx 100$$

$$10^{-2} \text{ mol dm}^{-3}, \quad Ka \approx 333$$

$$10^{-1} \text{ mol dm}^{-3}, \quad Ka \approx 1000$$

With the results found for these drug systems when mobilities are high; i.e. $> 4.0 \times 10^{-8} \text{ m}^2 \text{ s}^{-1} \text{ V}^{-1}$, then Ka is ≥ 333 . The majority of mobilities are $\ll 4.0$ where, when Ka is large ≥ 100 , variation in mobility with Ka has little effect on conversion of mobilities to zeta potentials (see tables of Ottewill and Shaw (99) Appendix I). It would seem therefore that the error involved in using the Smoluchowski equation, 2.58,

$$u = \frac{\epsilon \zeta}{\eta}$$

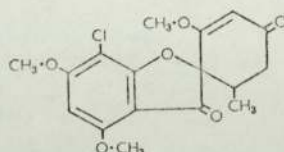
for conversion of mobilities to zeta potentials would be small and it was decided to use this conversion for all the drug systems. The equation reduces for aqueous solutions to:

$$\zeta = 12.85 \times u \text{ mV at } 25^\circ\text{C.}$$

5.1.2. Mobility/zeta potential - pH plots.

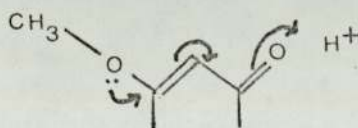
(a) Griseofulvin.

The plot Fig. XLVIII shows a positive charge of $\zeta = +25\text{mV}$ at pH 1.5 which rapidly decreases to zero at pH 2.4, there is then reversal of charge followed by an increase over the pH range 2.4 to 7.0 the zeta potential at the latter pH is -45mV . The potential then stays constant over the pH range 7 to 10. The chemical structure of Griseofulvin is (154)



Griseofulvin is (+)-7-chloro-4,6-dimethoxycoumaran-3-one-2-spiro-1'-(2'-methoxy-6'-methylcyclohex-2'-en-4'-one), an anti-fungal substance produced by the growth of certain strains of *Penicillium griseofulvum*.

and the positive charge at low pH can be attributed to the protonation of the $\alpha\beta$ unsaturated ketone aided by the positive donating mesomeric effect, (the +M effect) of the methoxyl group.



as pH increases this effect will diminish.

Above pH 2.4 where there is a gradual increase in negative potential to pH 7.0, which then stays constant, this must be due to adsorption of hydroxyl ions as discussed in Section 2.1(b). As the zeta potential stays steady at pH 7.0 and above further studies were carried out at this pH.

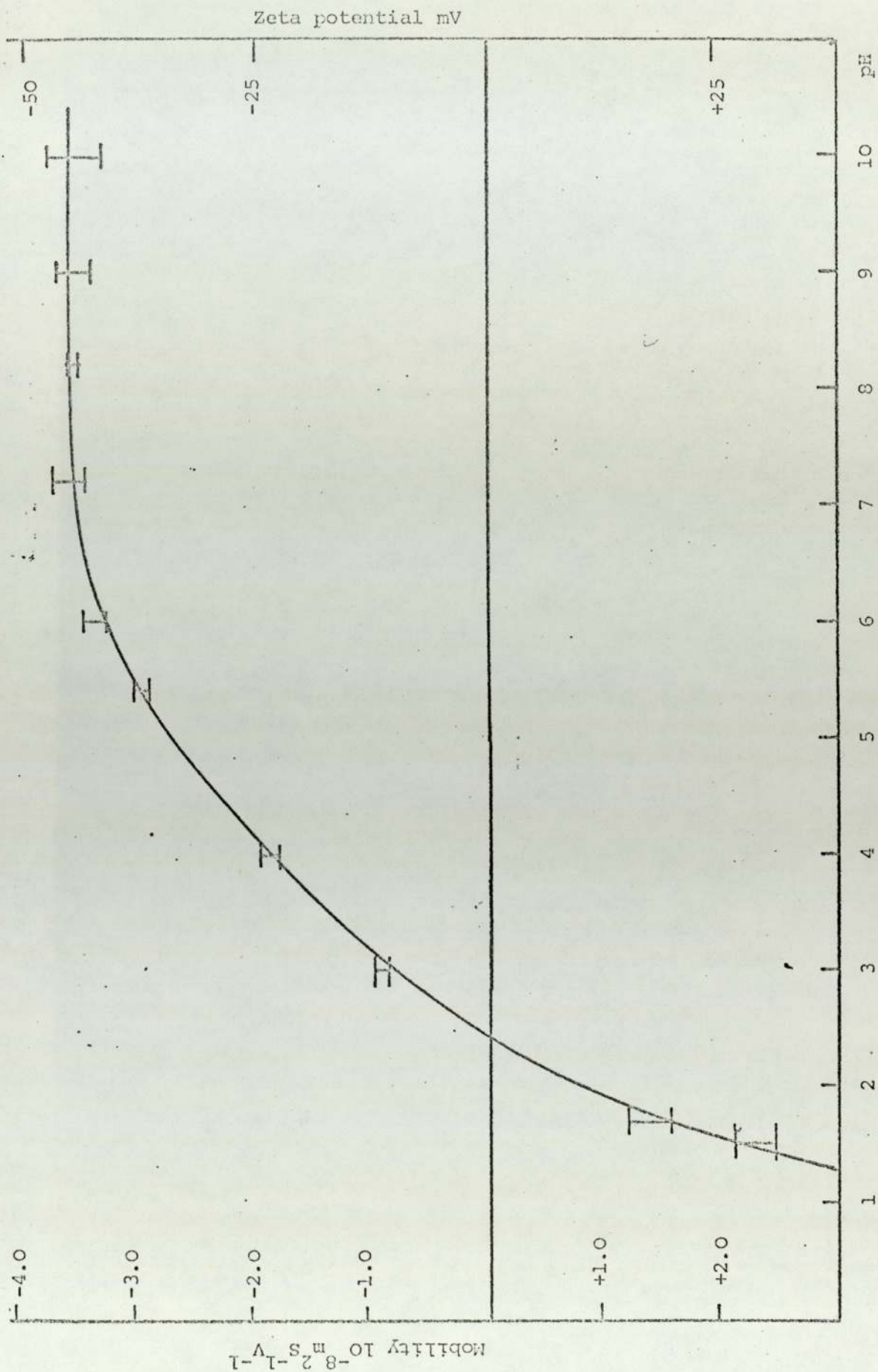
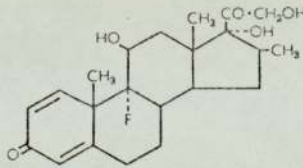


Figure XIVIII pH - mobility/zeta potential Griscofulvin

(b) Betamethasone.

Betamethasone Fig. XLIX shows little variation in mobility with pH. There is evidence that the particles are positively charged below pH 3.0, but movement was so slow even at high voltages that it was difficult to make measurement of the mobility. Reversal of charge occurs at ca. pH 3.0 and then from pH 3.0 to 5.0 there is a gradual increase in negative potential to a zeta potential of -6.5mV which then stays steady as pH is increased to 10.0. Such a pattern of mobility can only be due to ion adsorption as is expected from its structure (154):



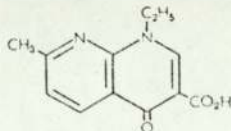
Betamethasone is 9 α -fluoro-11 β ,17 α ,21-trihydroxy-16 β -methylpregna-1,4-diene-3,20-dione.

As a steady state mobility occurs above pH 5.0, further studies were carried out at ca. pH 7.0.

(c) Nalidixic Acid

For Nalidixic Acid, Fig. L, the plot shows a positive zeta potential, virtually constant over the pH range 2-3.5, of +12mV. This decreases with increasing pH to charge reversal at pH 4.9. The zeta potential then rapidly increases with pH to pH 7.0 to a steady state value of -22mV. Above pH 8.0 the drug goes slowly into solution and it was not possible to achieve a steady pH above this value.

The structure of Nalidixic Acid is (155):



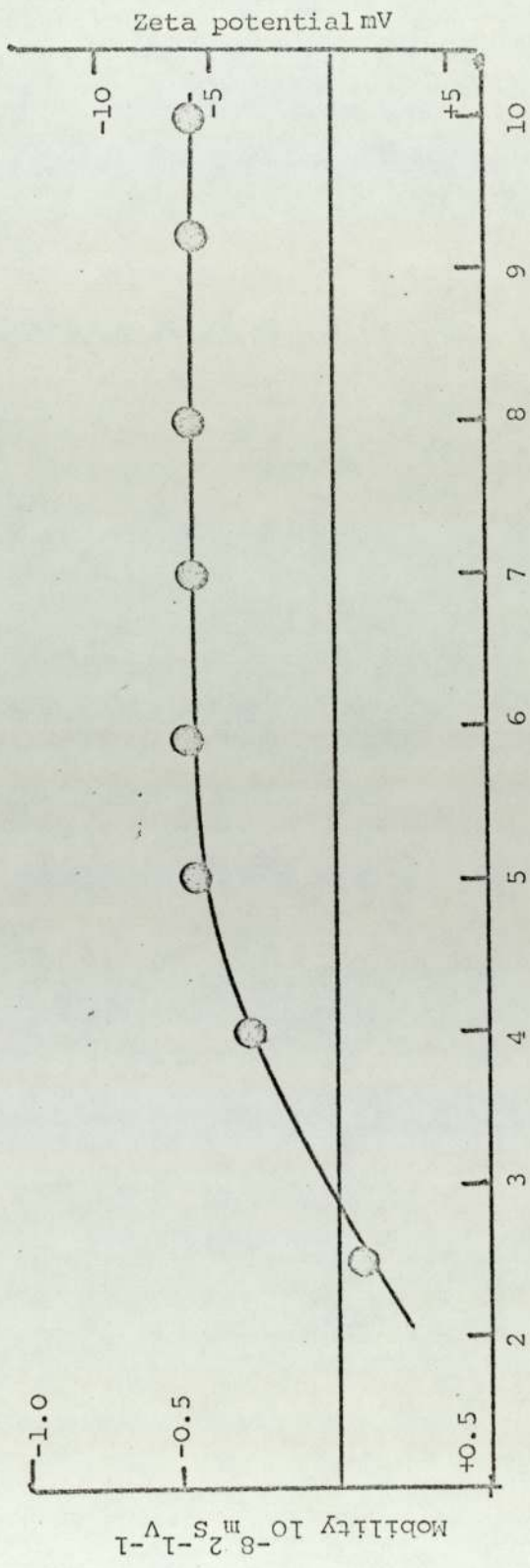


Fig XLIX pH - Mobility/zeta potential Betamethasone

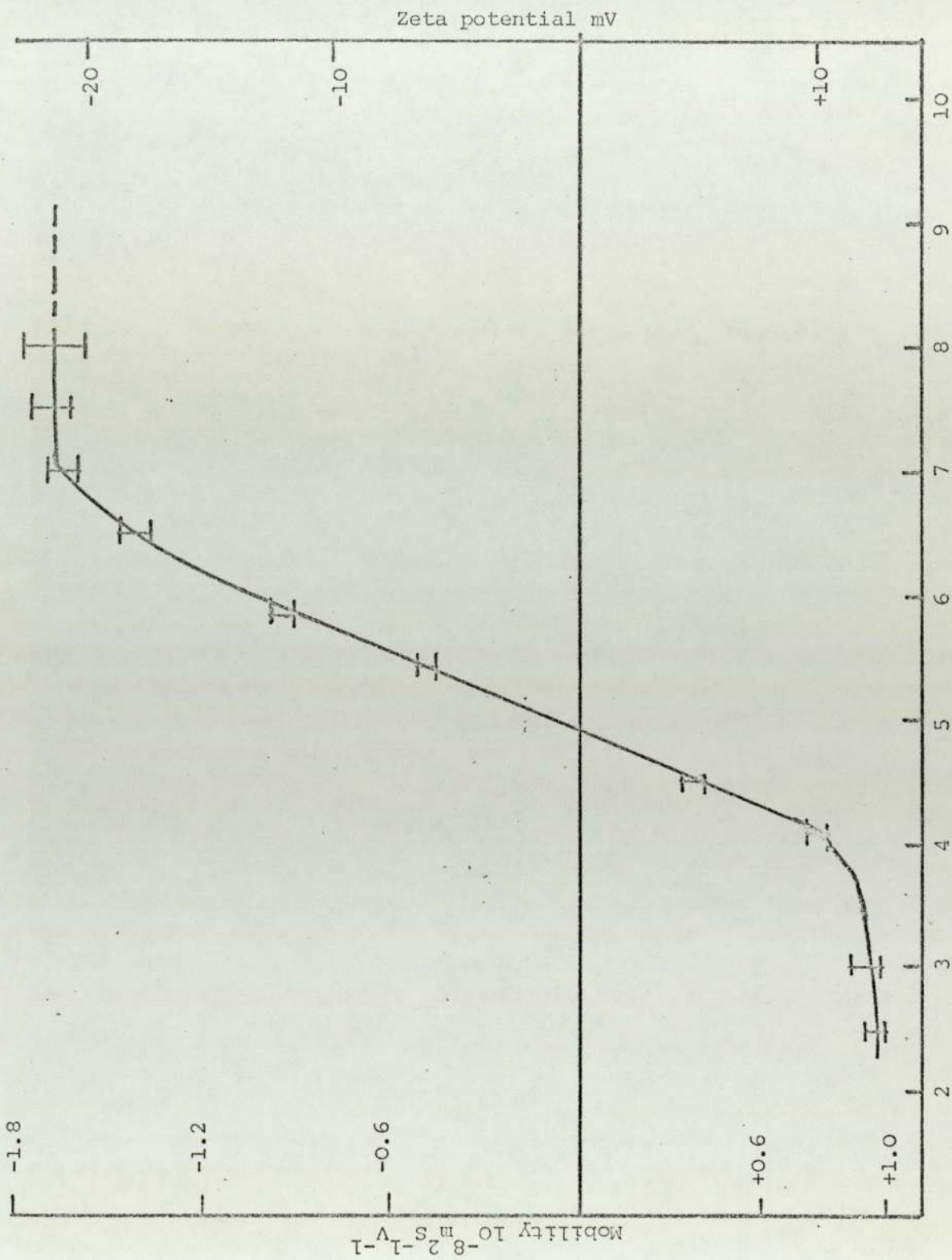


Fig 1 pH - Mobility/zeta potential Nalidixic Acid

Nalidixic Acid is 1-ethyl-7-methyl-4-oxo-1,8-naphthyridine-3-carboxylic acid.

The positive charge at low pH is attributed to protonation of the immino group, =N-, this effect would decrease as pH is increased. The gradual increase of negative potential over the pH range 4.9 to 7 is consistent with the ionization of the carboxyl group, -COOH. In section 4.1.1. it was shown that the bulk dissociation constant k_b of the carboxyl groups of the polystyrene latex could be obtained using equation 4.9.

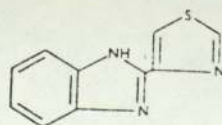
$$pk_b = pH_b \left(\zeta = \frac{1}{2} \zeta_0 \right)$$

use of this equation here gives a pk_b for Nalidixic Acid of 5.75 which agrees well with the value of 6.0 reported by Winningham et al (156). For further study, due to the rapid change of mobility over the pH range 4.0 to 7.0, a choice of either ^{of} the steady states i.e. 2.5 to 3.5 or 7.0 to 8.0 was necessary, it was decided to choose pH 7.0 as being the most suitable for the other additives to be used.

(d). Thiabendazole

The mobility/zeta potential - pH plot for Thiabendazole, Fig LI, shows a positive potential at low pH of +35mV which gradually decreases to the pH for charge reversal at 5.65. The potential then increases to a value of -27mV at pH 7.5, is steady over the range 7.5 to 8.5 and again increases to -37.5mV at pH 9.0, the zeta potential stays steady at this value over the pH range 9 to 11.

Thiabendazole has two immino groups =N= in its structure (155):



Thiabendazole is 2-(4-thiazolyl)benzimidazole.

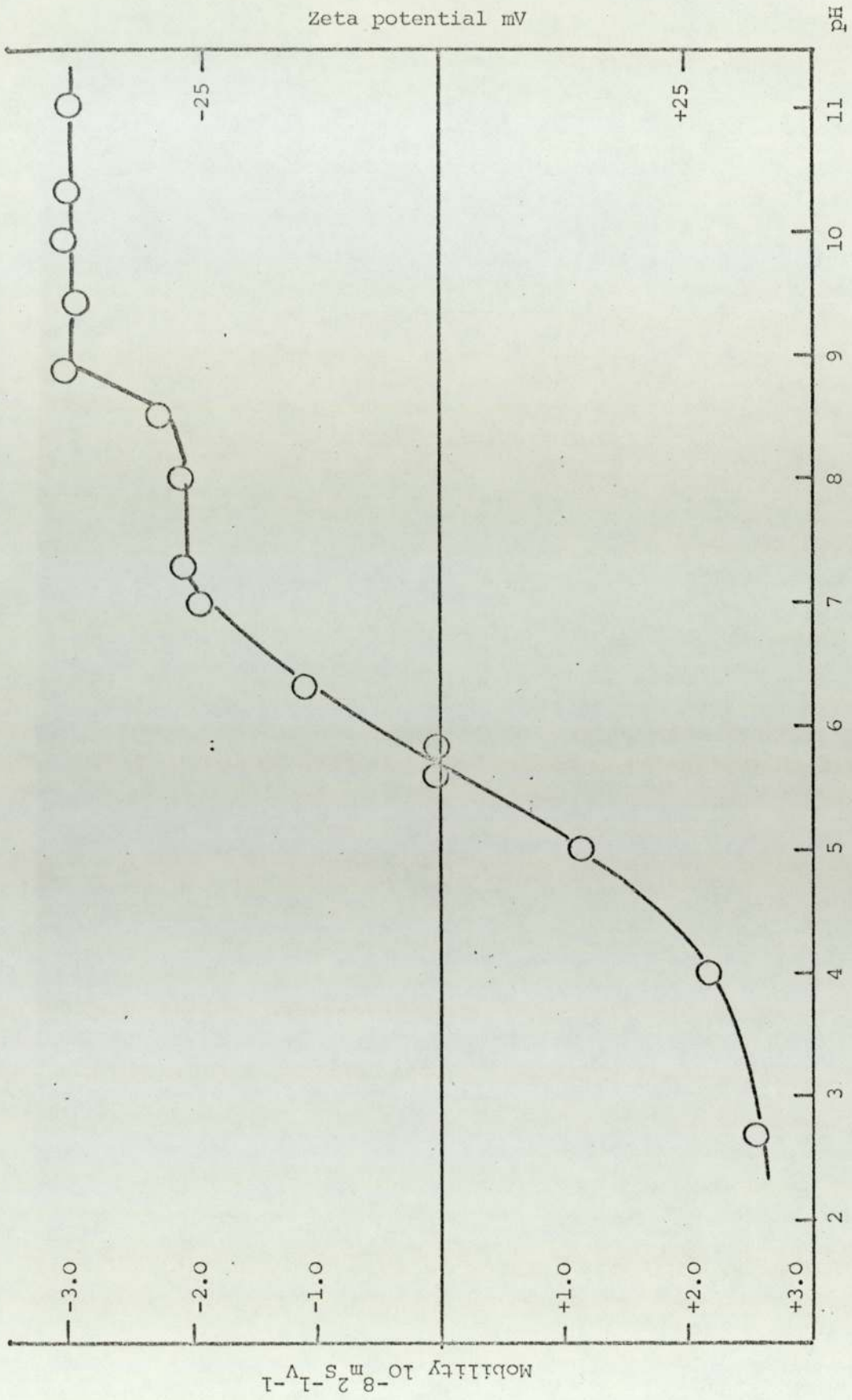


Fig LI pH - Mobility/zeta potential Thiabendazole

and these would account for the positive charge at low pH. The fact that the zeta potential here at pH 2.5 is ca. +33mV, with two imino groups in the structure, whilst with Nalidixic Acid at pH 2.5 it is +12mV with one imino group, supports this suggestion. The increase in negative potential which occurs over the pH range 5.65 to 7.5 is attributed to hydroxyl ion adsorption as discussed with Griseofulvin, and the step-wise increase between pH 8.5 and 9.0 to ionization of the =NH, secondary amino group. Again the pH for further studies was chosen to be in the steady state region close to pH 7.0, here pH 7.5.

5.2. Effect of nonionic surface active agents on the mobility and zeta potential.

To find if the effect of nonionic surfactant on the mobility of the drug particles was similar to that found with the polystyrene model system discussed in Section 4.2, one of the nonionics, C₁₆E₃₀, was used with all four drug systems. Results are shown in tables XXVII to XXX and Figs. LIII to LV. In all cases the plots show the characteristic fall off in mobility with increasing concentration of nonionic to a steady state value. This suggests that the adsorption pattern of the nonionic surfactant is similar to that of the nonionic onto polystyrene latex i.e. that there is adsorption of the alkyl chain onto a hydrophobic portion of the surface, by the hydrophobic effect, and also association of the ethylene oxide groups with some polar group at the surface probably by hydrogen bonding. As pointed out in Section 4.2. Elworthy and Guthrie (119) have shown that such adsorption does occur with these nonionics on Griseofulvin.

The fact that, although the surfaces of the particles are to some extent hydrophobic but also possess polar groups, are still different from each other, is typified by the fact that the percentage displacement of mobility at the steady state is not equal:- Griseofulvin steady

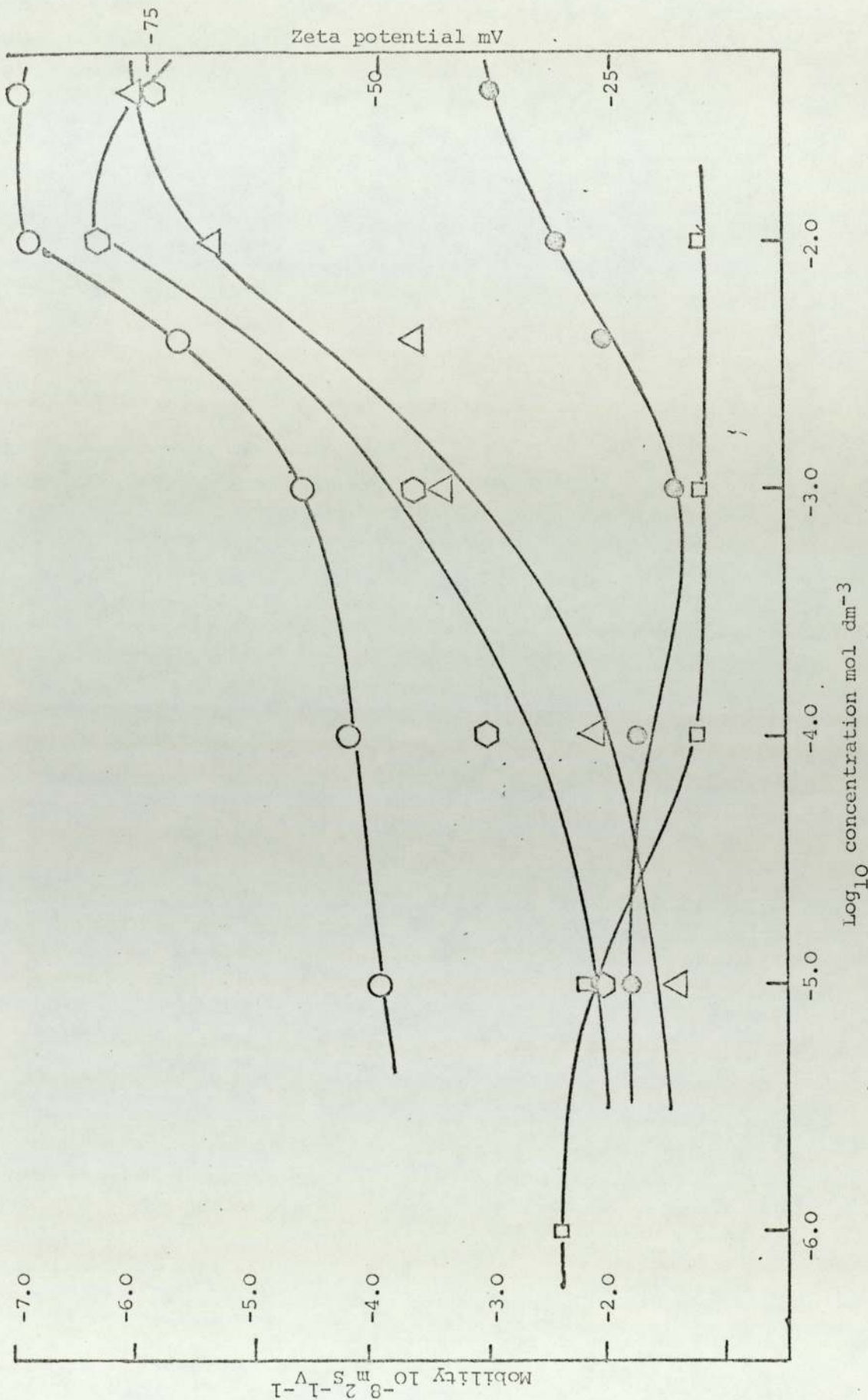


Fig LII Mobility/zeta potential Griseofulvin - concentration SDS ○ ; C₁₆E₃₀ △ ; SDS and C₁₆E₃₀ □ ; 10⁻² mol dm⁻³ ● , 10⁻³ mol dm⁻³ △ ; 10⁻⁴ mol dm⁻³ ○.

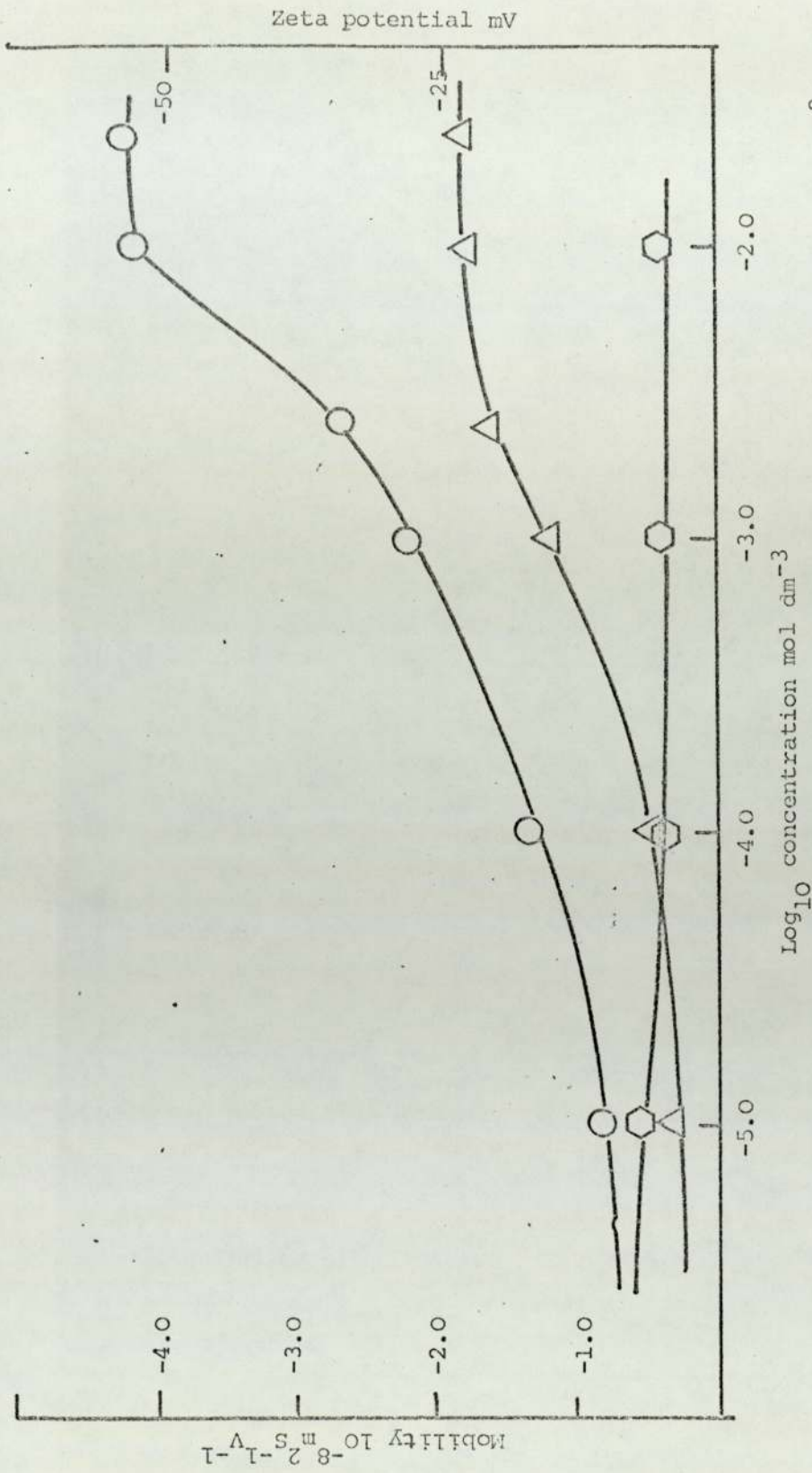


Fig LIII Mobility/zeta potential Betamethasone - concentration of SDS \circ ; SDS with 10^{-2} mol dm^{-3} $\text{C}_{16}\text{E}_{30}$ \triangle ; $\text{C}_{16}\text{E}_{30}$ \hexagon .

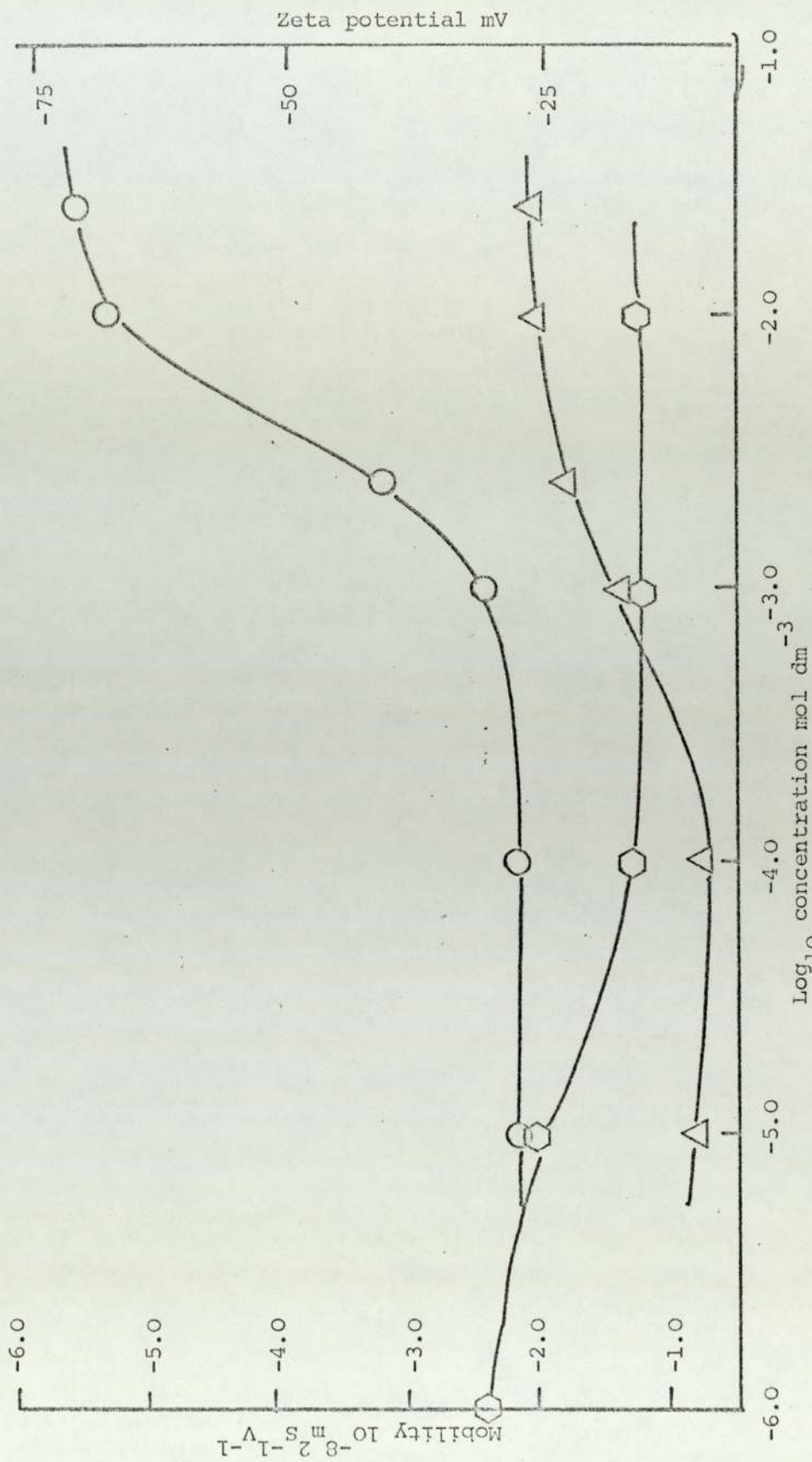


Fig LIV Mobility/zeta potential Nalidixic Acid - concentration of SDS ○ ; SDS with $10^{-2} \text{ mol dm}^{-3}$ C_{16} E₃₀ △ ; C_{16} E₃₀ ◻.

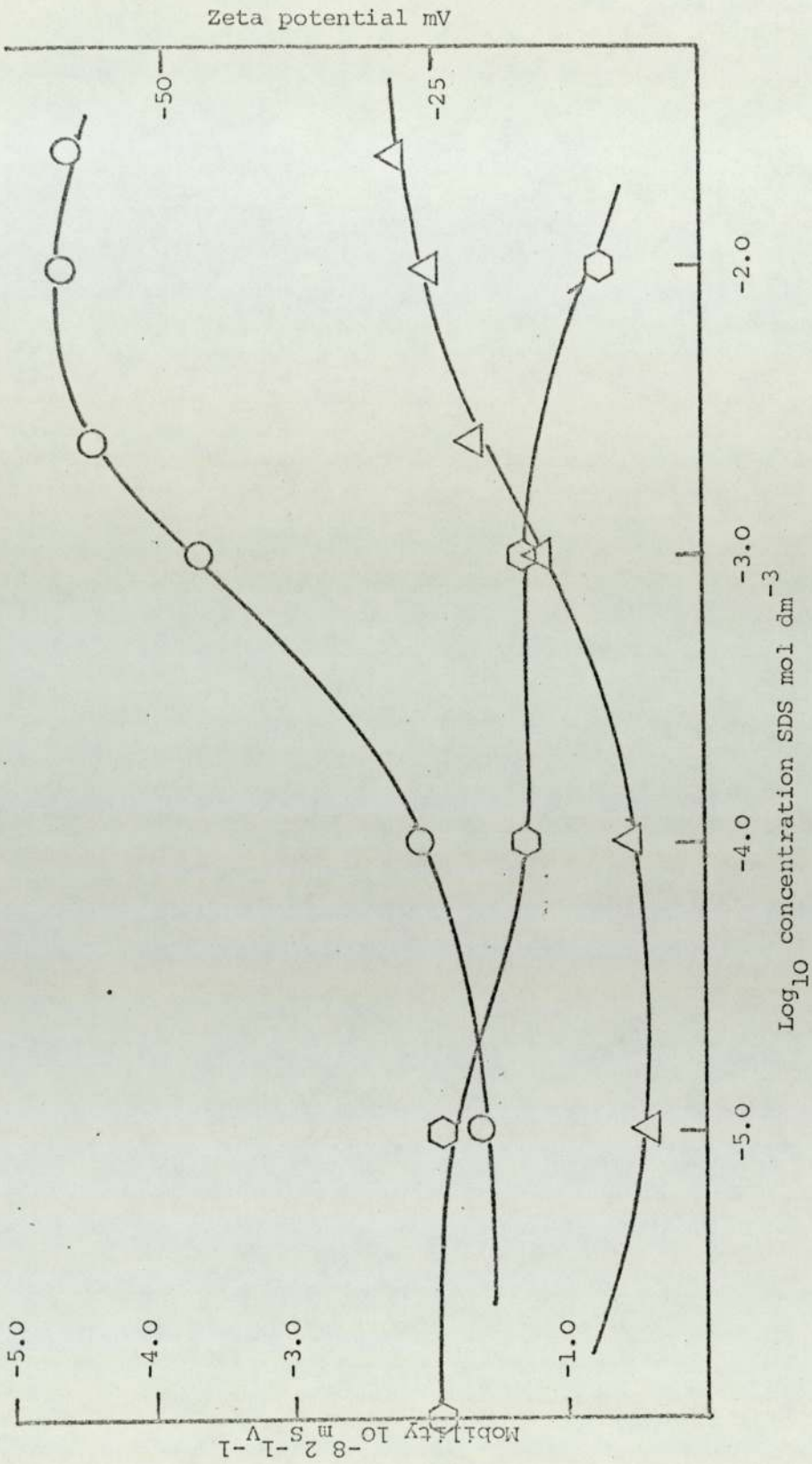


Fig LV Mobility/zeta potential Thiabendazole - concentration SDS \circ ; $\text{C}_{16} \text{ E}_{30}$ \square ; SDS with $10^{-2} \text{ mol dm}^{-3} \text{ C}_{16} \text{ E}_{30}$ \triangle .

state mobility $-3.5 \times 10^{-8} \text{ m}^2 \text{ s}^{-1} \text{ V}^{-1}$ displaced to $-1.29 \times 10^{-8} \text{ m}^2 \text{ s}^{-1} \text{ V}^{-1}$, a 67% displacement.

Betamethasone -0.45 to $-0.35 \times 10^{-8} \text{ m}^2 \text{ s}^{-1} \text{ V}^{-1}$ -22%

Nalidixic Acid -1.68 to $-1.25 \times 10^{-8} \text{ m}^2 \text{ s}^{-1} \text{ V}^{-1}$ -26%

Thiabendazole -2.10 to $-1.25 \times 10^{-8} \text{ m}^2 \text{ s}^{-1} \text{ V}^{-1}$ -40%

Differences would in fact be expected from the differences in chemical composition, but the results point to the nonionics being more strongly adsorbed onto Griseofulvin and Thiabendazole; this point is in fact suggested by the mobility -pH plots for Griseofulvin and Thiabendazole which show a rise to a fairly high negative value apparently solely by hydroxyl ion adsorption. Some difference in adsorption energies is also shown with anionic and cationic surfactants and is discussed later.

5.3. Effect of dodecyl trimethyl ammonium bromide on the electrophoretic mobility and zeta potential.

The adsorption of C_{12}TAB at the particle-liquid interface is dependent on the chemical structure of the particle and its charging mechanism. At the pH's used the charging mechanism of Griseofulvin, Betamethasone and Thiabendazole is ion adsorption. Nalidixic Acid acquires its charge by ionization of carboxylic acid groups.

The case of Nalidixic Acid is analagous to that of the polystyrene latex used in Section 4, i.e. adsorption is a two stage process. Firstly there is gradual neutralization of the negative charge as the charge group of the C_{12}TAB molecule associates with the $-\text{COO}'$ of the Nalidixic Acid. Secondly the cationic is adsorbed in reverse orientation by the alkyl chain associating with the hydrophobic areas of the particle surface by the hydrophobic effect, this gives rise to a positive zeta potential which will increase to a maximum as concentration of cationic increases.

With the other three drugs the $C_{12}TAB$ ions will adsorb onto the particle surface in reverse orientation by the hydrophobic effect, charging ions will thus be displaced from the Stern plane. In the early stages (at low concentration of $C_{12}TAB$) as a small number only of surface active molecules will be adsorbed, the net effect will be reduction of the Stern potential; this will be progressive as concentration of cationic is increased until charge reversal occurs. As the concentration of $C_{12}TAB$ is increased still further the ions must displace all other ions from the Stern plane and thus the zeta potential should reach a maximum positive value.

As with cationic surface active agents and polystyrene latex, Section 4.3.3, the slope of the zeta potential- \log_{10} concentration $C_{12}TAB$ plot at zero potential can be used to calculate the energy of adsorption of the surface active agent on the particle surface.

5.3.1. General characteristics of the zeta potential- \log_{10} concentration $C_{12}TAB$ plots.

The results for the systems Griseofulvin, $C_{12}TAB$; Betamethasone, $C_{12}TAB$; Nalidixic Acid, $C_{12}TAB$; and Thiabendazole, $C_{12}TAB$; are shown in tables XXXI to XXXIV and Figs. LVI to LIX respectively. They all follow the pattern outlined above and detailed with polystyrene latex in section 4.3. A similar pattern of results has been obtained by Takamura et al who studied the adsorption of $C_{16}TAB$ on sulphadiazine, sulphaphenazole and sulfisomidine and correlated their results with zeta potential measurements (157). The reversal of charge concentrations for the four drugs are shown below together with their steady state zeta potentials in the absence of $C_{12}TAB$.

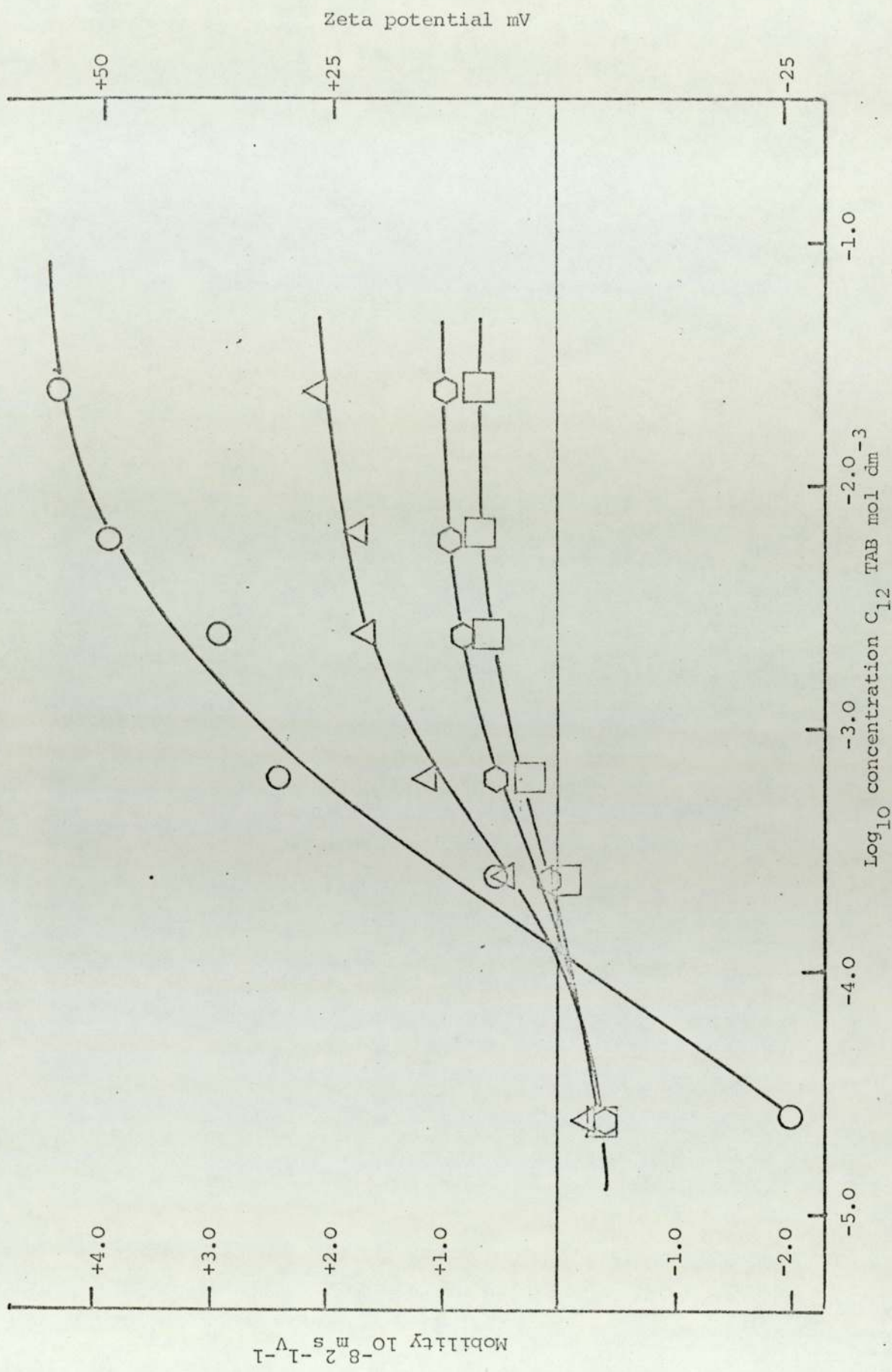


Fig LVI Mobility/zeta potential griseofulvin - concentration C_{12} TAB \circ ; with $10^{-2} \text{ mol dm}^{-3}$ C16 E60 \square ; $10^{-2} \text{ mol dm}^{-3}$ C16 E30 \diamond ; $10^{-2} \text{ mol dm}^{-3}$ C16 E10 \triangle .

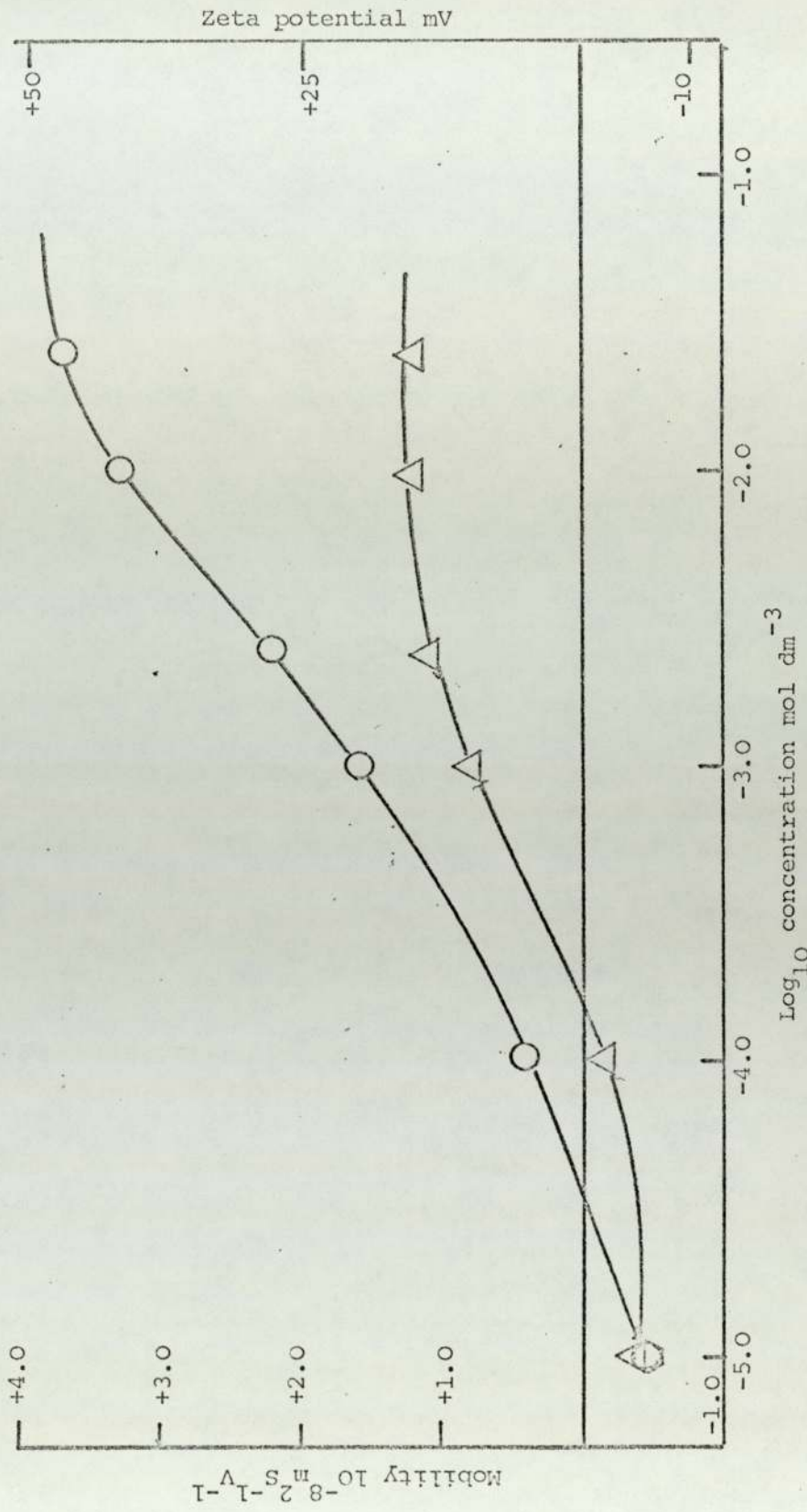


Fig LVII Mobility/zeta potential Betamethasone - concentration C₁₂ TAB ○ ; C₁₆ TAB with 10⁻² mol dm⁻³ C₁₆ E₃₀ △.

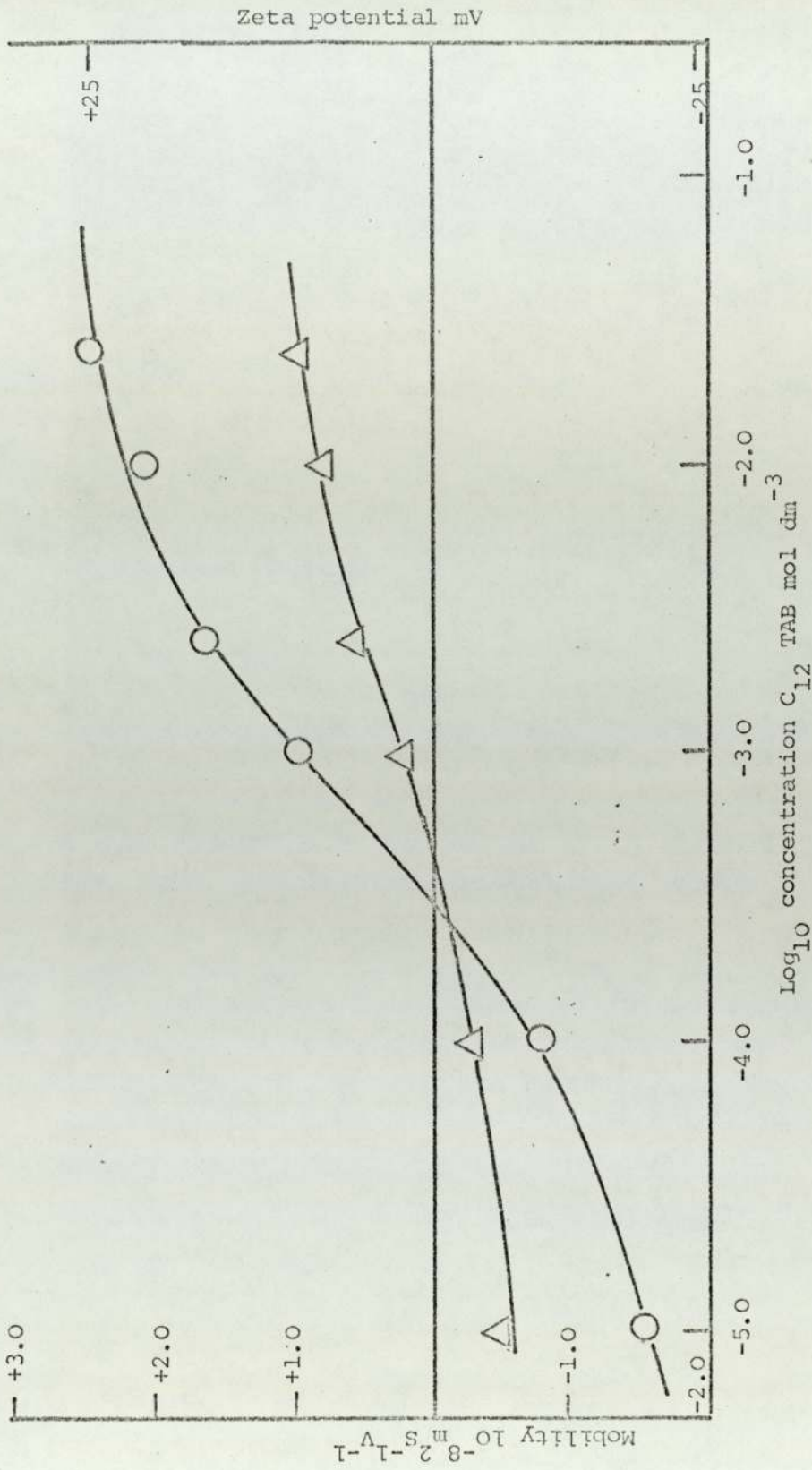


Fig LVIII Mobility/zeta potential Nalidixic Acid - concentration C_{12} TAB \circ ; C_{16} TAB with 10^{-2} mol dm^{-3} C_{16} E₃₀ \triangle .

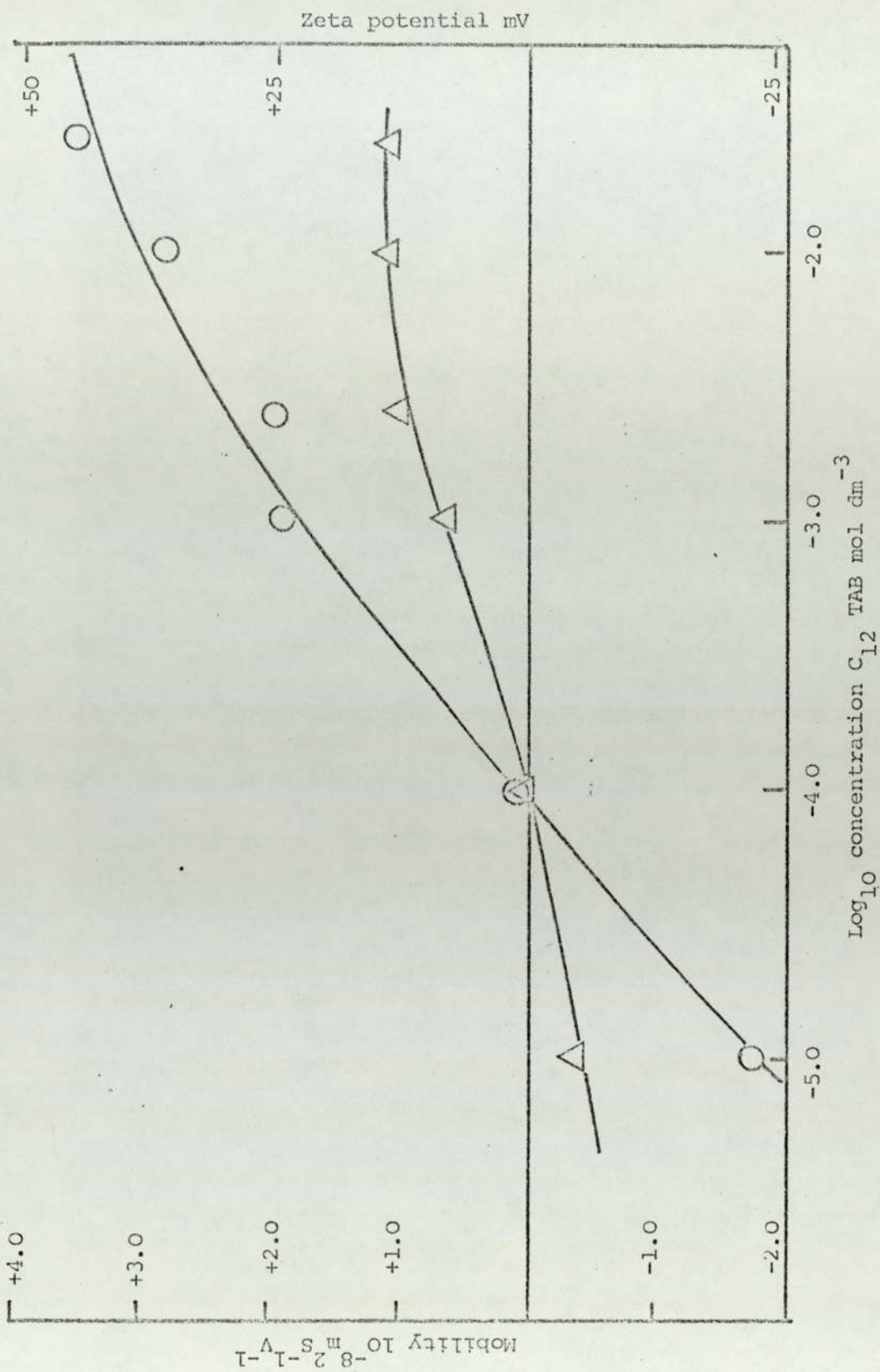


Fig LIX Mobility/zeta potential Thiazobenzazole - concentration C_{12} TAB \circ ; C_{12} TAB with 10^{-2} mol dm^{-3} C_{16} E 30 \triangle .

DRUG	R.C.C. of $C_{12}TAB$ $mol\ dm^{-3}$	Zeta potential mV (without $C_{12}TAB$)
Griseofulvin	1.3×10^{-4}	-45
Betamethasone	4.0×10^{-5}	-6.5
Nalidixic Acid	3.2×10^{-4}	-22
Thiabendazole	9.0×10^{-5}	-27

R.C.C.'s follow the original zeta potential for Griseofulvin, Betamethasone and Thiabendazole as might be expected from the ion adsorption charge mechanism. Nalidixic Acid is presumably different, i.e. the concentration for R.C.C. is greater than the others, due to the charge neutralization required - the corresponding concentration for $C_{12}TAB$ polystyrene latex is $10^{-5} mol\ dm^{-3}$. The maximum values for zeta potentials found at $2.5 \times 10^{-2} mol\ dm^{-3} C_{12}TAB$ are:-

Griseofulvin -54.6mV

Betamethasone -46.6mV

Nalidixic Acid -25mV

Thiabendazole -44.3mV.

These results suggest that approximately the same amount of $C_{12}TAB$ adsorbs onto Griseofulvin, Betamethasone and Thiabendazole but that Nalidixic Acid because of its chemical structure, i.e. presence of $-COOH$ groups, is not able to take up the same quantity of $C_{12}TAB$ molecules adsorbed in reverse orientation i.e. with their charge groups towards the aqueous phase. As those molecules adsorbed with their charge groups towards $-COO'$ will have their alkyl chains towards the aqueous phase consequently the 'saturation' potential will be lower than if they were all orientated

with their charge groups towards the aqueous phase.

5.3.2. Calculation of free energies of adsorption from zeta potential- \log_{10} concentration C_{12}^{TAB} plots.

As shown in Section 4.3.3. the slope of the zeta potential- \log_{10} concentration plot can be used to calculate the free energies of adsorption of cationic surface active agents using equation 2.86. The results are shown in table XXXV. The values of ΔG are all of the same order, however it is interesting that the values for Griseofulvin and Thiabendazole are higher than the other two and that this pattern the results found with nonionic surfactants in Section 5.2.

5.4. Effect of mixtures of cationic and nonionic surface active agents on the electrophoretic mobility and zeta potential.

The effect of adding nonionic surface active agents to the C_{12}^{TAB} drug suspension systems used in Section 5.3 was examined. As previously, constant concentrations of the nonionic were used and the concentration of C_{12}^{TAB} varied. The mixtures used were Griseofulvin with C_{12}^{TAB} and $C_{16}^{\text{E}10}$, $C_{16}^{\text{E}30}$ and $C_{16}^{\text{E}60}$; and Betamethasone, Nalidixic Acid, Thiabendazole with C_{12}^{TAB} and $C_{16}^{\text{E}30}$.

5.4.1. General characteristics of the zeta potential- \log_{10} concentration C_{12}^{TAB} with C_{16}^{E} plots.

Results are shown in Figures LVI to LIX and Tables XXXI to XXXIV.

The zeta potential- \log_{10} concentration plots follow a pattern similar to that for the polystyrene latex/ $C_x\text{TAB}$ /nonionic systems studied in Section 4.4. However there is one main difference in that the PCC is not displaced to the same extent as with the polystyrene systems; the actual magnitudes of displacement are shown below:

TABLE XXXV

Free energies of adsorption C_{12} TAB on various drugs						
Compound	$(d\zeta/d \log_{10} C)$ $\zeta = 0$ mV	RCC mol m^{-3}	Ni m^{-2}	K_2 $\text{m}^3 \text{mol}^{-1}$	C mol m^{-3} where $\zeta = +\text{mV}$	$-\Delta G$ kJ mol^{-1}
Betamethasone	10.3	4×10^{-2}	3.4×10^{14}	0.753	4.5 at 10^{-1}	26.36
Griseofulvin	37.5	1.4×10^{-1}	6.56×10^{15}	2.83	25.7 at 6×10^{-1}	29.66
Nalidixic Acid	25.0	3.4×10^{-1}	3.92×10^{15}	2.105	12.0 at 1	28.93
Thiabendazole	23.0	9.5×10^{-2}	2.86×10^{15}	2.5	17.8 at 4×10^{-1}	29.36

DRUG	RCC with C_{12}^{TAB} mol dm^{-3}	RCC with C_{12}^{TAB} and C_{16}^{E30} mol dm^{-3}	RCC Displacement
Griseofulvin	1.3×10^{-4}	2×10^{-4}	0.7
Betamethasone	4×10^{-5}	2×10^{-4}	1.6
Nalidixic Acid	3.2×10^{-4}	4.5×10^{-4}	1.3
Thiabendazole	9×10^{-5}	1.2×10^{-4}	0.3
(polystyrene latex	10^{-5}	6.0×10^{-4}	5.9)

It is significant that the displacement values follow the adsorption energies of C_{12}^{TAB} on the various drugs as reported in 5.3.2, showing that the form of the plot produced depends on the relative adsorption energies of the two surfactants on any particular drug system.

Fig. LVI Griseofulvin with C_{16}^{E10} , C_{16}^{E30} and C_{16}^{E60} and C_{12}^{TAB} shows that there is little significant difference produced by altering the ethylene oxide chain length. A similar result was found with polystyrene systems.

5.5. Effect of sodium dodecyl sulphate on the electrophoretic mobility and zeta potential.

At the pH's at which investigations were made all particles carry a negative charge - Griseofulvin, Betamethasone and Thiabendazole by ion adsorption and Nalidixic Acid by ionization of carboxylic acid groups. The charging mechanism of the latter is analagous to that of the polystyrene latex previously used and the adsorption pattern of the SDS is therefore likely to be affected in the same way. As with the polystyrene system the driving force for adsorption is the hydrophobic effect,

the molecules of SDS being adsorbed 'between' the $-COOH$ groups in the case of Nalidixic Acid, and onto the surface of the other three drugs replacing charging ions already present within the Stern layer. The zeta potential should consequently increase with increasing concentration of surface active agent until the surface is 'full' and should then remain constant.

As with anionic surface active agents and polystyrene latex, section 4.5.2, the slope of the zeta potential- \log_{10} concentration SDS plot, as adsorption begins to occur rapidly, can be used to calculate energy of adsorption of the surface active agent on the particle surface.

5.5.1. General characteristics of the zeta potential- \log_{10} concentration SDS plots.

The results for the systems Griseofulvin/SDS; Betamethasone/SDS; Nalidixic Acid/SDS; and Thiabendazole/SDS; are shown in tables XXXVI, XXVIII to XXX and Figs. LII to LV respectively.

All plots show the same pattern as found with anionic surface active agents and polystyrene latex, i.e. a small increase in negative zeta potential as concentration of SDS is increased, probably due to replacement of ions in the Stern layer by the SDS, followed by a fairly rapid rise to a maximum. The zeta potential then stays constant with increasing concentration of SDS or falls off slightly due to ionic strength effects. In all cases the maximum in potential occurs at about 10^{-2} mol dm $^{-3}$ SDS which is in the region of the cmc of this surfactant, in water at 25°C. A similar concentration for maximum zeta potential was found with the polystyrene latex/SDS system (Section 4.5.1).

The maximum values for zeta potentials found with the four drugs, when it can be assumed that the surface of the particles is covered with vertically orientated molecules of SDS, taken at 10^{-2} mol dm $^{-3}$ SDS are:

Griseofulvin - 89mV

Betamethasone - 54mV

Nalidixic Acid - 67mV

Thiabendazole - 59mV

it would be expected that all results would be of the same order at maximum adsorption - the $-COO'$ groups of Nalidixic Acid contributing an effect of the same magnitude as the $-SO_3'$ group of SDS.

5.5.2. Calculation of free energies of adsorption from zeta potential- \log_{10} concentration SDS plots.

The calculation of the free energies of adsorption of anionic surface active agents onto the surface of negatively charged polystyrene latex particles is discussed in Section 4.5.2. The situation here would seem to be analagous in the case of Nalidixic Acid. However for Griseofulvin, Betamethasone and Thiabendazole, where the negative charging mechanism is due solely to ion adsorption, there will not be any contribution due to electrostatic repulsion and the adsorption energies will be due solely to the hydrophobic effect. The slope of the zeta potential- \log_{10} concentration SDS plot was taken at the point where rapid rise in potential occurred i.e. 10^{-3} mol dm $^{-3}$ SDS in all cases. The results are shown in Table XXXVII, there is good agreement between the ΔG values for the four drugs with those found for C $_{12}$ TAB (see Table VI). The results confirm those found for C $_{12}$ TAB and SDS on polystyrene latex, i.e. that it is the alkyl chain which is the factor which controls the adsorption of these surfactants onto a hydrophobic surface.

5.6. Effect of mixtures of sodium dodecyl sulphate and nonionic surface active agents on the electrophoretic mobility and zeta potential.

The effect of adding nonionic surface active agents to the SDS - drug systems used in the previous sub-section was examined. Constant concentration of nonionic surfactant was used and the concentration of

TABLE XXXVII

Free energies of adsorption of sodium dodecyl sulphate with varying drugs							
Compound	$d\zeta/d \log_{10} C$ mV	C mol m ⁻³	Ni m ⁻²	K ₂ m ³ mol ⁻¹	$-\Delta G(\Delta\phi)$ kJ mol ⁻¹	Ze ζ kJ mol ⁻¹	$-\Delta G$ kJ mol ⁻¹
Betamethasone	-13	1	1.67×10^{16}	4.105	30.58		30.58
Griseofulvin	-13	1	3.00×10^{16}	6.67	31.78		31.78
Nalidixic Acid	-12	1	1.60×10^{16}	4.17	30.62	1.12	31.74
Thiabendazole	-26.5	1	4.24×10^{16}	5.42	31.27		31.27

SDS varied and the change in mobility was measured. The systems used were Griseofulvin with SDS and $C_{16}E_{10}$, $C_{16}E_{30}$ and $C_{16}E_{60}$; and Betamethasone, Nalidixic Acid and Thiabendazole with SDS and $C_{16}E_{30}$. Results are shown in tables XXXVIII, XXXIX, XXVIII, XXIX, XXX and Figs. LX, LIII, LIV, LV respectively.

5.6.1. General characteristics of the zeta potential- \log_{10} concentration SDS with $C_{16}E_y$ plots.

The results for the SDS nonionic mixtures follow the pattern found with the polystyrene/SDS/ $C_{16}E_y$ systems examined in Section 4.6.1. Study of Fig. LX which gives results for Griseofulvin, SDS with $C_{16}E_{10}$, $C_{16}E_{30}$, and $C_{16}E_{60}$ shows that displacement of the zeta potential- \log_{10} concentration plot occurs, the magnitude of displacement depending on ethylene oxide chain length. For example the displacement with 10^{-2} mol dm $^{-3}$ $C_{16}E_{30}$ was of 29mV and with the same concentration of $C_{16}E_{60}$ 40mV, both at SDS 10^{-4} mol dm $^{-3}$ concentration. The increased lowering of potential found with slightly higher concentrations of SDS with $C_{16}E_{30}$ and $C_{16}E_{60}$, is similar to that found with polystyrene latex/SDS/ $C_{16}E_{30}$ and $C_{16}E_{60}$, and is due to complex formation between the surfactants, as discussed in Section 4.6.1. As expected no such complexation effect was found with SDS/ $C_{16}E_{10}$.

The effect of SDS/ 10^{-2} mol dm $^{-3}$ $C_{16}E_{30}$ mixtures on the zeta potentials of Betamethasone, Nalidixic Acid and Thiabendazole is shown in Figs. LIII, LIV, and LV. The lowering of zeta potential produced by 10^{-2} mol dm $^{-3}$ $C_{16}E_{30}$ at 10^{-4} mol dm $^{-3}$ SDS is shown below, for polystyrene latex and all the four drugs:

Polystyrene latex	21mV
Griseofulvin	29mV
Betamethasone	11mV
Nalidixic Acid	21mV
Thiabendazole	21mV

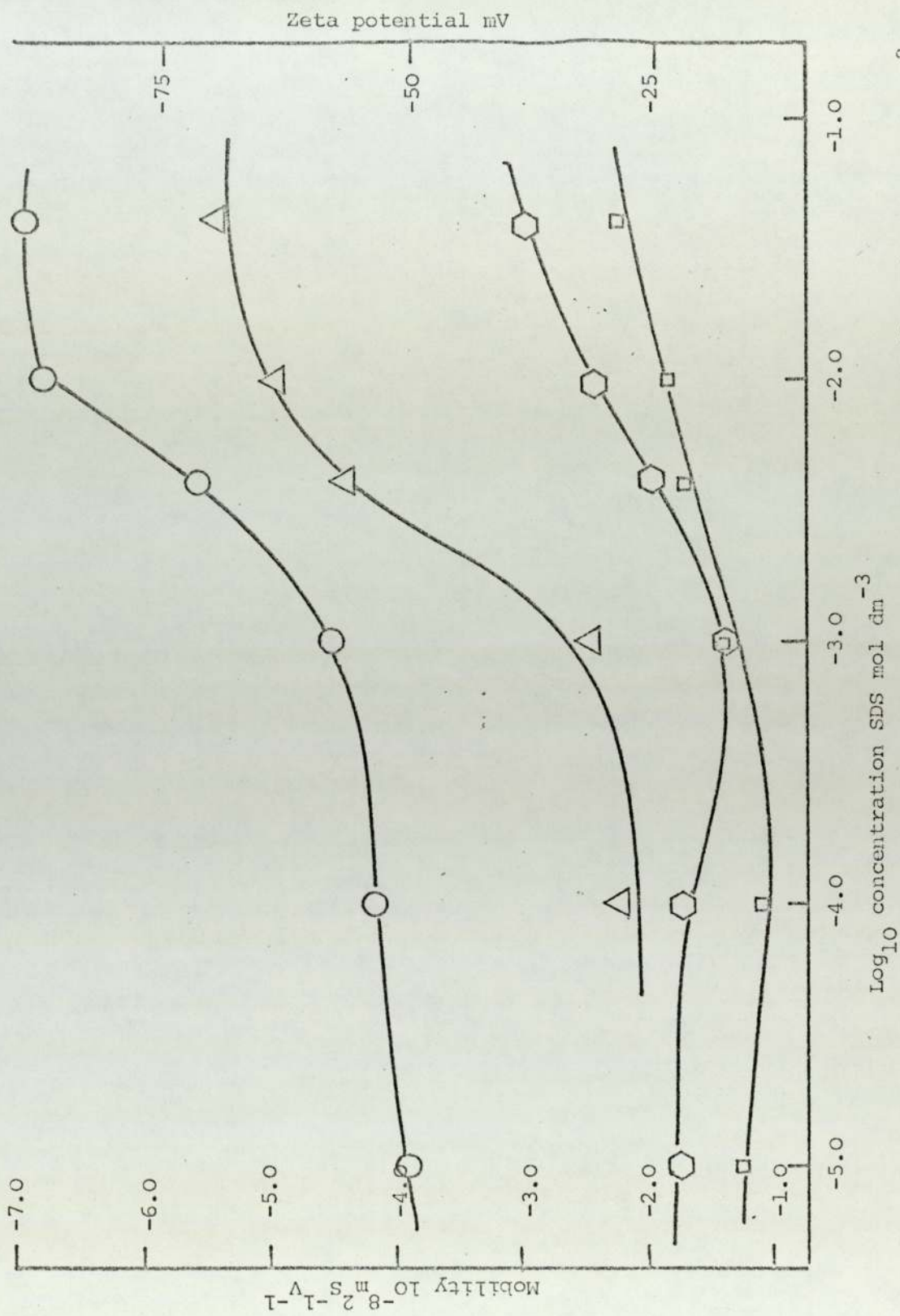


Fig LX Mobility/zeta potential Griseofulvin - concentration SDS \bigcirc ; with $\text{C}_{16}\text{E}_{60}$ 10^{-2} mol dm^{-3} \bigcirc ; $\text{C}_{16}\text{E}_{30}$ 10^{-2} mol dm^{-3} \square ; $\text{C}_{16}\text{E}_{10}$ 10^{-2} mol dm^{-3} \triangle .

These results are in good agreement (the zeta potential values for Beta-methasone are so low that it is difficult to make an accurate estimate of the effect). It is possible therefore to predict the lowering of zeta potential of a drug particle on addition of a nonionic surface active agent, $C_{16}E_y$, providing the same dispersion medium is used, this would be expected from the adsorption pattern discussed in Section 4.2.

5.6.2. Effect of sodium dodecyl sulphate with nonionic surface active agents of varying ethylene oxide chain length.

In Section 4.6.2. the effect of ethylene oxide chain length on the zeta potential of polystyrene latex in the system polystyrene latex/SDS/ $C_{16}E_y$ was investigated and a direct proportionality between chain length and lowering of zeta potential produced was found.

At 10^{-4} mol dm $^{-3}$ SDS, Fig. LXI shows a plot of zeta potential lowering produced by 10^{-2} mol dm $^{-3}$ $C_{16}E_y$, against ethylene oxide chain length in $C_{16}E_y$ for polystyrene/SDS/ $C_{16}E_y$ systems (results taken from Section 4.6.2). With the Griseofulvin/SDS/ $C_{16}E_y$ system shown in Fig. LX the lowering of zeta potentials produced by 10^{-2} mol dm $^{-3}$ $C_{16}E_y$ at SDS concentration of 10^{-4} mol dm $^{-3}$ are, $C_{16}E_{10}$ 25mV; $C_{16}E_{30}$ 31mV; and $C_{16}E_{60}$ 40mV; these results are included in Fig. LXI. There is reasonable agreement with the predicted line for $C_{16}E_{30}$ and $C_{16}E_{60}$ but the result for $C_{16}E_{10}$ shows wide variation; this is an anomalous result probably due to experimental error, as apart from the agreement just noted above, excellent agreement was found in the previous subsection for $C_{16}E_{30}$, at 10^{-2} mol dm $^{-3}$, with polystyrene latex and all four drugs.

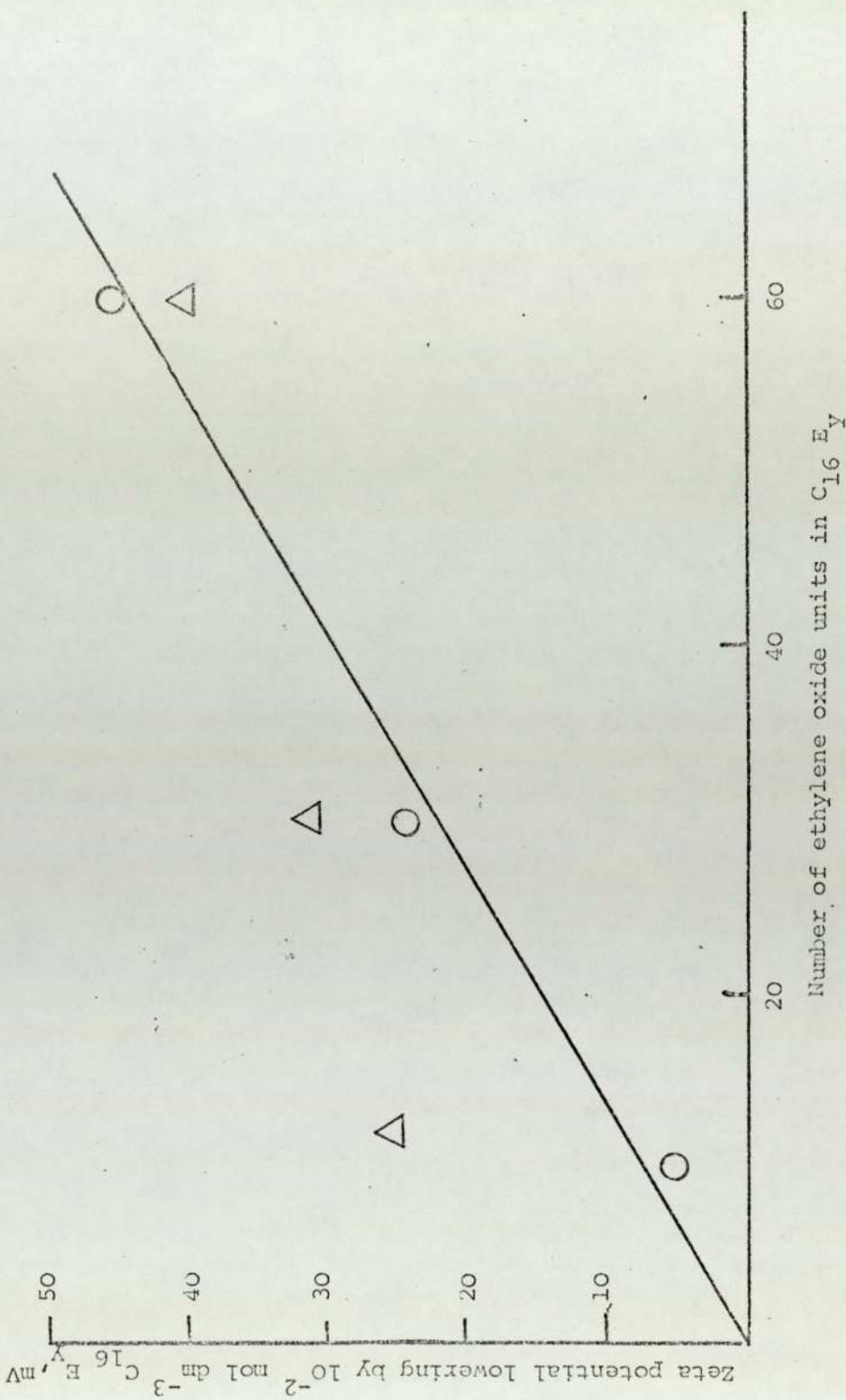


Fig LXI Variation in zeta potential with increase in ethylene oxide chain length of C₁₆E_Y.
 Polystyrene latex/SDS/C₁₆E_Y ○ ; Griseofulvin/SDS/C₁₆E_Y △.

SECTION 6.

RELATIONSHIP BETWEEN ZETA POTENTIAL, SEDIMENTATION
VOLUME AND REDISPERSIBILITY OF BETAMETHASONE,
GRISEOFULVIN, NALIDIXIC ACID AND THIABENDAZOLE SUSPENSIONS.

6.1 General Considerations

6.1.1 Sedimentation Volume

When sedimentation is studied in aggregated systems, it is observed that the aggregates tend to fall together, producing a distinct boundary between the sediment and the supernatant liquid. The liquid above the sediment is clear because even the small particles present in the system are associated with the aggregates. Such is not the case in deflocculated suspensions having a range of particle sizes, where, in accordance with Stoke's law, the larger particles sediment more rapidly than the smaller particles. No clear boundary is formed, sometimes not even on standing for some days, and the supernatant remains turbid for a considerable time - as found with the suspensions studied in this work, (see, for example tables XXVIII and XXX). The appearance of the supernatant liquid can give therefore a good indication of an aggregated or deflocculated system.

A useful parameter which may be derived from sedimentation studies is that of sedimentation volume. By itself the sedimentation volume is meaningless for lack of a reference value. To avoid this difficulty Robinson (158) and Ward and Kammermayer (159) used the ratio of the ultimate volume of the settled height to the original height:

$$F = H_u / H_o \quad 6.1.$$

H_u is the apparent height of the solids after sedimentation and H_o is the total height of the original suspension before settling.

Distenfass (160) used ^a ~~the same~~ ratio in terms of volumes to describe sedimentation volume:

$$F = V_u/V_o \quad 6.2.$$

and this expression with F expressed as a percentage is used in this work.

The ratio F thus gives a measure of the aggregated-deflocculated state of the system.

6.1.2. Redispersibility

An attempt was made to evaluate the suspension, by visual examination of the sediment, and by redispersion, inverting the container by hand, in as standard a way as possible, until the sediment was dispersed. Where necessary the time needed for redispersion was recorded. The term 'caked' was used here to indicate a deflocculated system which needs shaking for some time to disperse the sediment.

Results for sedimentation volumes and redispersibility of the suspensions described in Section 5 are shown in tables XXVII to XXXIV, XXXVI, XXXVIII & XXXIX.

6.1.3. Zeta potential, sedimentation volume and suspension stability.

The significance of the zeta potential to, and its relationship with, the sedimentation volume can be seen by plotting these parameters versus concentration of surfactant. In simple systems, as, for example, Fig. IXII for Thiabendazole and SDS, it is seen that as the sedimentation volume falls with increasing concentration of SDS, i.e. the system becomes deflocculated, so the zeta potential rises. The effect of nonionic/ionic surfactant mixtures is shown in the same way, see for example Fig. LXIII, Thiabendazole/SDS/C₁₆E₃₀.

Consideration of the total potential energy of interaction between the particles:

$$V = V_A + V_R \quad 1.1.$$

or in the case of nonionic and nonionic/ionic surfactant mixtures:

$$V = V_A + V_R + V_S \quad 1.2.$$

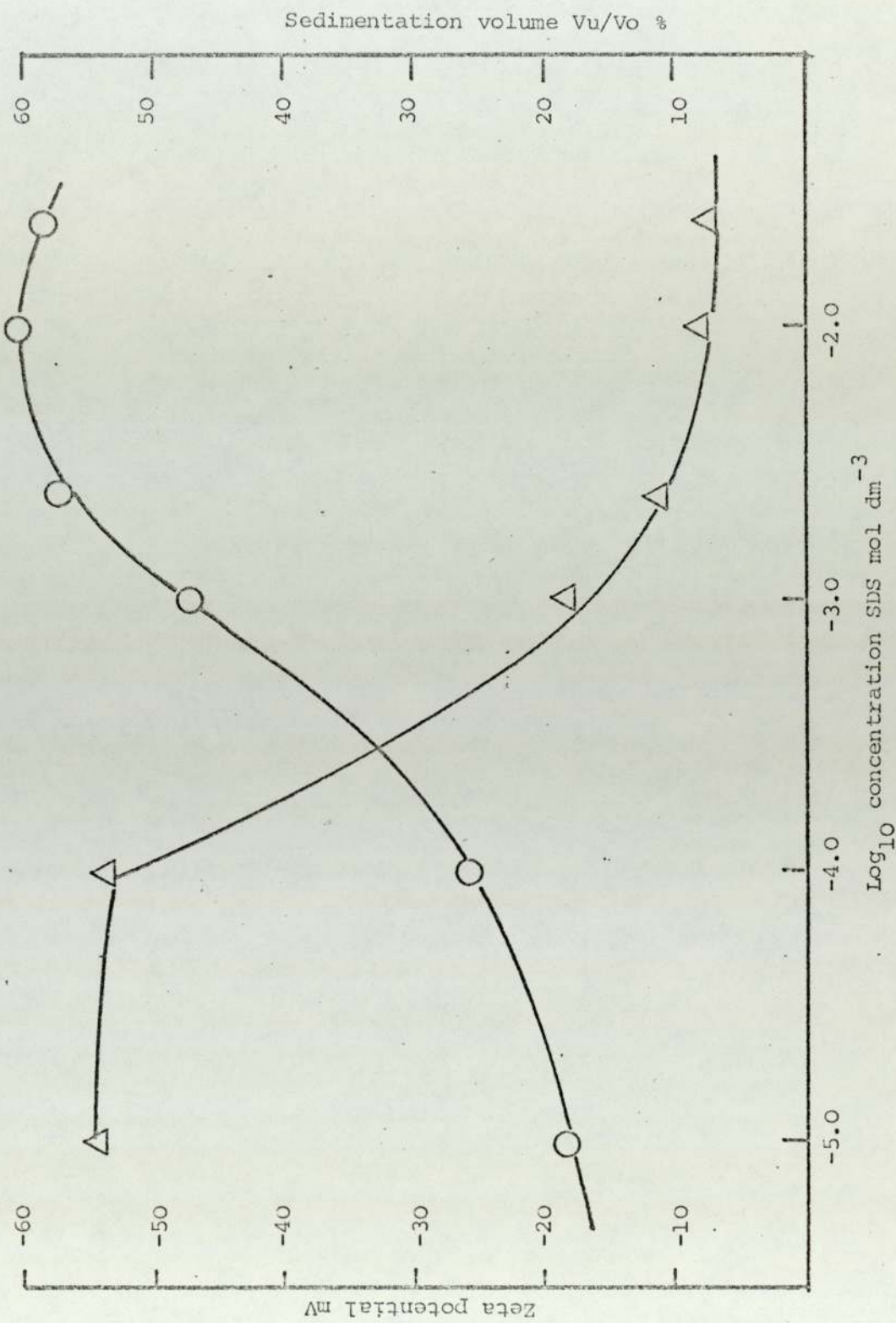


Fig LXII Zeta potential \circ , sedimentation volume \triangle , Thiabendazole - concentration SDS

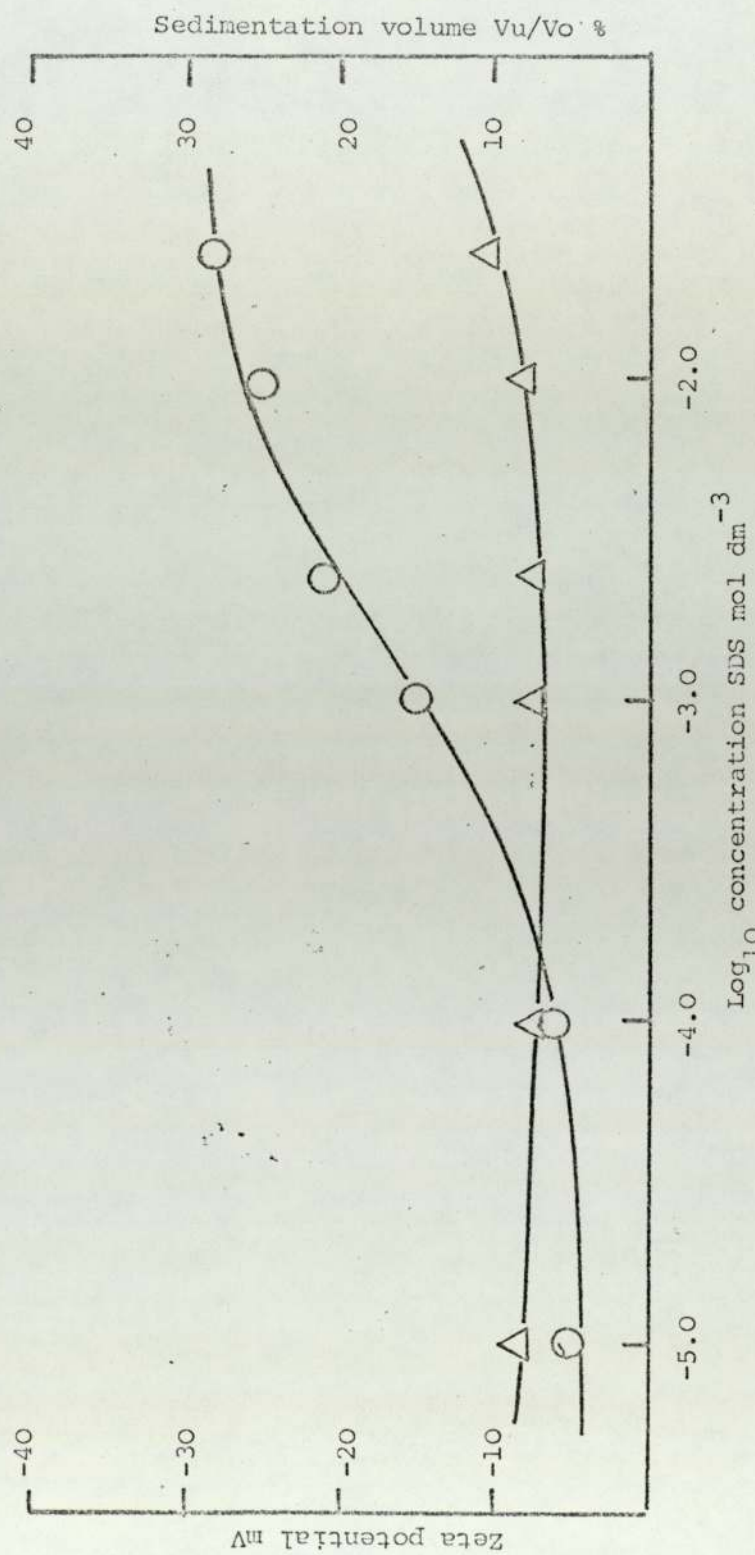


Fig LXIII Zeta potential \circ , sedimentation volume \triangle , Thiabendazole with $10^{-2} \text{ mol dm}^{-3}$
 $C_{16}E_{30}$ - concentration SDS

gives a measure of the coagulated or deflocculated state of the system. If the height of the potential energy barrier V_M (Fig. 1) i.e. the distance, H_0 , between particles where V is at a maximum, is $\geq 20kT$ (161) where the zeta potential is approximately 50mV; then the particles will not be able to get close enough to enter the primary minimum, P , where coagulation occurs.

The results quoted in this section enable an estimate of V to be made, thus V_A can be calculated from equation 2.4.1, (provided $H_0 \leq 15nm$, at greater distances the retardation effect is important and equation 2.45 must be used):

$$V_A = - \frac{\Lambda a}{12H_0} \quad 2.41.$$

for the simple particle/ionic surfactant systems (where Λ is the Hamaker constant of the solid in water). For particle/nonionic and particle/nonionic/ionic surfactant mixtures, equation 2.55 must be used:

$$V_A = - \frac{1}{12} \left\{ (\Lambda_M^{\frac{1}{2}} - \Lambda_S^{\frac{1}{2}})^2 H_S + (\Lambda_S^{\frac{1}{2}} - \Lambda_P^{\frac{1}{2}})^2 H_P + 2(\Lambda_M^{\frac{1}{2}} - \Lambda_S^{\frac{1}{2}})(\Lambda_S^{\frac{1}{2}} - \Lambda_P^{\frac{1}{2}}) H_{PS} \right\} \quad 2.55.$$

Ottewill and Walker (79) have indicated that this equation can be simplified, without causing great error, by putting $\Lambda_M = \Lambda_S = 3.7 \times 10^{-20}$ J i.e. the Hamaker constant of the adsorbed layer Λ_S may be taken to be equal to the value for water Λ_M - the error involved here is not likely to be great as for example the Hamaker constant of the nonionic Triton x35 (an alkyl aryl polyether alcohol) has a value of 3.32×10^{-20} J, ^{as} Visser (62). Equation 2.55 then becomes

$$V_A = - \frac{1}{12} (\Lambda_S^{\frac{1}{2}} - \Lambda_P^{\frac{1}{2}})^2 H_P \quad 6.1.$$

As shown in Section 2.3.3. the function H can be approximated to

$$\lim_{x \rightarrow 0} \frac{H(xy)}{x(1+y)} = \frac{y}{x(1+y)} \quad 2.57$$

where, for H_P ,

$$x = \frac{\Delta + 2\delta}{2a} \quad \text{and } y = 1.$$

In the case of two approaching particles both covered with an adsorbed layer as they touch $\Delta \rightarrow 0$ and x is given by δ (the thickness of the adsorbed layer) divided by the particle radius a . An estimate of the thickness of the layer of $C_{16}E_{30}$ on the Thiabendazole particles can be made using equation 2.10:

$$Kx = \ln \left[\frac{\exp Ze \zeta / 2kT + 1}{\exp Ze \zeta / 2kT - 1} \right] \left[\frac{\exp Ze \psi_0 / 2kT - 1}{\exp Ze \psi_0 / 2kT + 1} \right] \quad 2.10$$

For the 'steady state' zeta potential of $C_{16}E_{30}$ on Thiabendazole

$$\zeta = -16.5mV; \quad \psi_0 = -27mV; \quad \text{so that in } 10^{-3} \text{ mol dm}^{-3} \text{ NaCl}$$

$$x = 4.7nm = \delta$$

The mean radius of the Thiabendazole particle is $5.5\mu m$, so that the value of H_p is 5.9×10^2 , taking the value of the Hamaker constant for Thiabendazole as $8.55 \times 10^{-20} J$. (Schenkel and Kitchener (18) and Ho and Higuchi (163) have indicated that $1 \times 10^{-20} J$ is a reasonable value for the Hamaker constant of an organic substance in water; Visser (62) quotes values for hydrocarbons of $6-7 \times 10^{-20} J$ so the above would appear reasonable). V_A is then evaluated as $-120kT$.

An estimate of V_R can be obtained from equation 2.31:

$$V_R = \frac{\epsilon a \zeta^2}{2} \ln (1 + \exp^{-KH_0})$$

where ψ_0 is replaced by the zeta potential. The stabilizing effect of steric and solvation layers V_s can be calculated using equation 2.54 in the form:

$$\frac{V_s}{kT} = \frac{4\pi Nc^2}{3V_1\rho_2^2} [0.5 - \chi] \left[\delta - \frac{H_0}{2} \right]^2 \left[3a + 2\delta + \frac{H_0}{2} \right] \quad 6.2.$$

where N is Avogadro's number.

The thickness of the adsorbed layer of $C_{16}E_{30}$ is $4.7nm = \delta$, if interpenetration of layers is assumed to a small extent then H_0 the distance between the particles will be, say $2 \times 4.7 - 1.0 = 8.4nm$. The particle radius a is $5.5\mu m$, 2δ and $H_0/2$ are small compared with this value so

that the right hand bracket of equation 6.2 can be modified to be 3a. Florence and Rogers (162) report values for the interaction parameter K , for aqueous solutions of polyoxyethylene compounds and give, for $C_{16}E_{21}$ a value of 0.497, using these figures a value of +118 kT is obtained for V_s . A number of calculations of V have been made and the results are given in the detailed discussion below.

6.2. Characteristics of the zeta potential/sedimentation volume versus concentration of surface active agent plots, and calculation, in selected cases, of the total potential energy of interaction between particles.

6.2.1. Drug particle, nonionic surfactant systems.

Results for Thiabendazole/ $C_{16}E_{30}$ and Griseofulvin/ $C_{16}E_{30}$ are shown in Figs. LXIV and LXV and tables XXX and XXVII respectively.

The results are similar, that for Thiabendazole shows a fall off of P and zeta potential as concentration of nonionic is increased, so that for example at a concentration of 10^{-4} mol dm⁻³ $C_{16}E_{30}$, the system is deflocculated even though the zeta potential is only -16.5mV. It is likely therefore that the particles are sterically stabilized.

Calculation of V at the above concentration, assuming that a full layer of $C_{16}E_{30}$ is present on the particles:

$$\begin{aligned} V &= V_A + V_R + V_S \\ &= -102 + 43 + 104 \\ &= +45 \text{ kT.} \end{aligned}$$

signifying as found a deflocculated system.

However at 10^{-6} mol dm⁻³ assuming no contribution from V_S (i.e. V_A is unmodified) then at $H_o = 10\text{nm}$

$$\begin{aligned} V &= V_A + V_R \\ &= -112.5 + 88 = -24.5\text{kT.} \end{aligned}$$

i.e. the system should be coagulated.

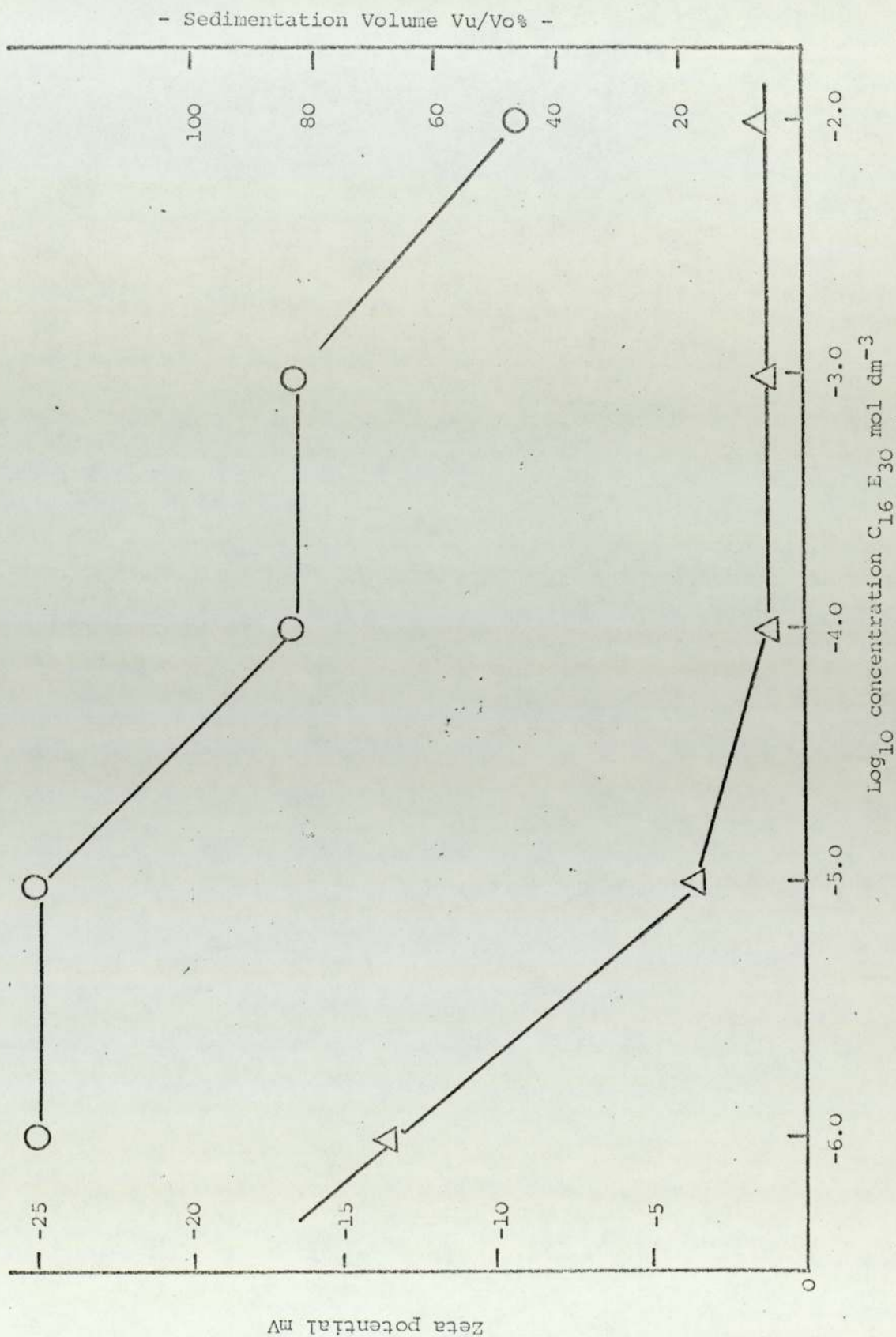


Fig LXIV Zeta potential O, sedimentation volume Δ , Thiabendazole - concentration $C_{16} E_{30}$

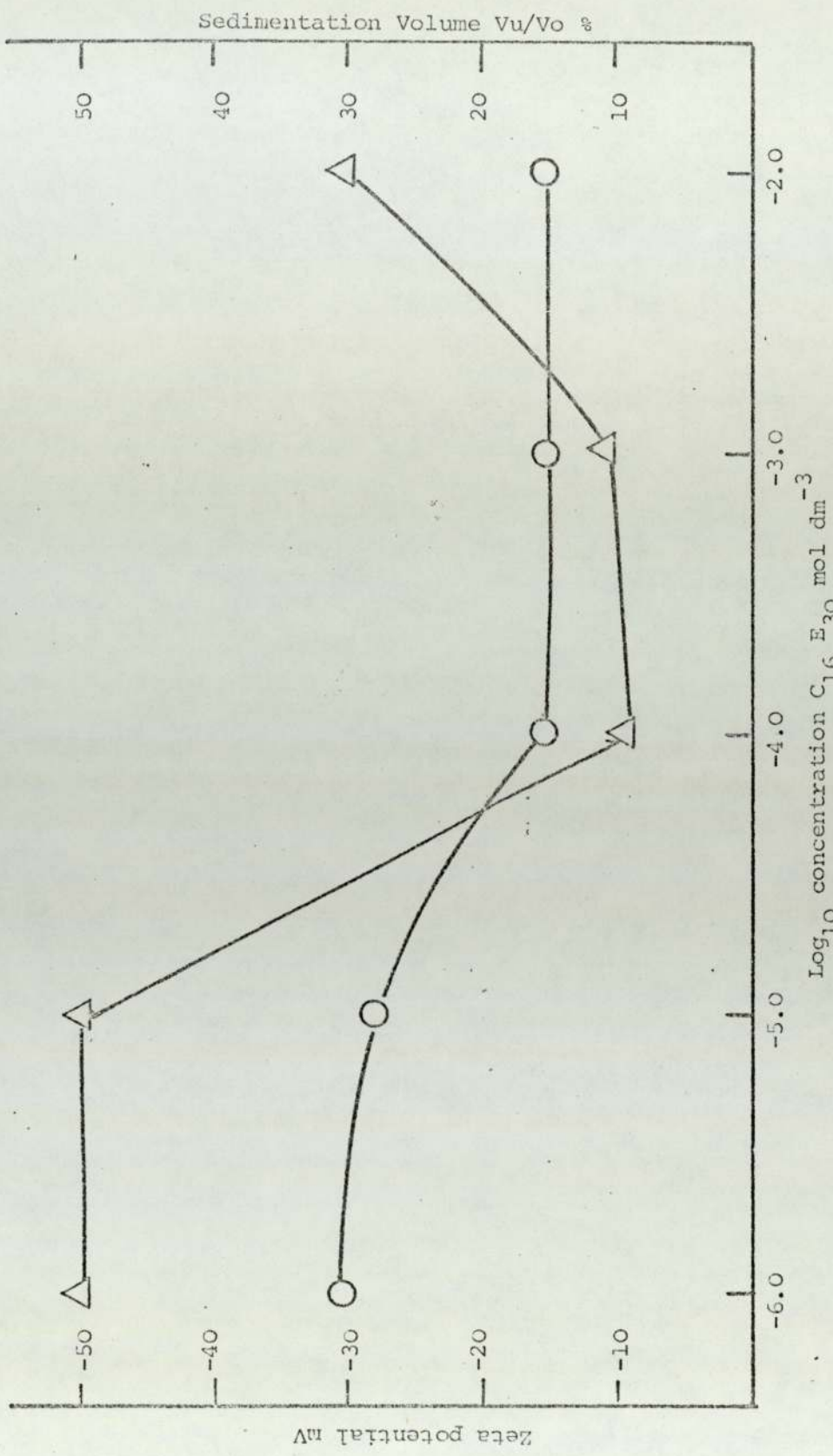


Fig LXV Zeta potential ○, sedimentation volume △, Griseofulvin - concentration C₁₆E₃₀

Experimentally the particles formed light fluffy aggregates and it is possible that flocculation due to polymer bridging had occurred because of the low concentration of nonionic surfactant, rather than coagulation.

The plot for Griseofulvin differs at concentrations of $C_{16}E_{30}$ above $10^{-3} \text{ mol dm}^{-3}$ when the sedimentation volume increases. This suspension was easily resuspended and the particles were not aggregated into groups, it is probable therefore that this suspension is showing controlled coagulation as suggested in Section 1. Whilst the layer of adsorbed nonionic surfactant will prevent coagulation of the particles deep in the primary minimum there will be a large enough attractive force to cause aggregation as soon as the distance between particles is greater than twice the thickness of the adsorbed layer. For example with Griseofulvin at $H_0 = 15\text{nm}$, $V_R = +3.6kT$, $V_A = -36kT$, V_S will not be effective at this distance - it contributes a "cut off" effect at 9.4nm (i.e. twice the thickness of the adsorbed layer). V is therefore $-31.4kT$ which is a large enough attraction for aggregation to occur.

6.2.2. Drug particle, cationic surfactant systems

Results are given for Thiabendazole/ $C_{12}\text{TAB}$, Fig. LXVI, table XXXIV; Griseofulvin/ $C_{12}\text{TAB}$, Fig. LXVII, table XXXI; Nalidixic Acid/ $C_{12}\text{TAB}$, Fig. LXVIII, table XXXIII.

The results all follow the same pattern and can be discussed by examining the plot for Thiabendazole/ $C_{12}\text{TAB}$, Fig. LXVI. This shows a rise in F as the zeta potential passes from the negative value to zero, at zero F is at a maximum, F then falls to a minimum as the positive zeta potential increases. Reference to table XXXIV shows that at 10^{-5} and $10^{-4} \text{ mol dm}^{-3}$ $C_{12}\text{TAB}$ light fluffy aggregates are present, the system gradually becomes deflocculated as the zeta potential increases. The suspension at $10^{-2} \text{ mol dm}^{-3}$ $C_{12}\text{TAB}$ was deflocculated but easily

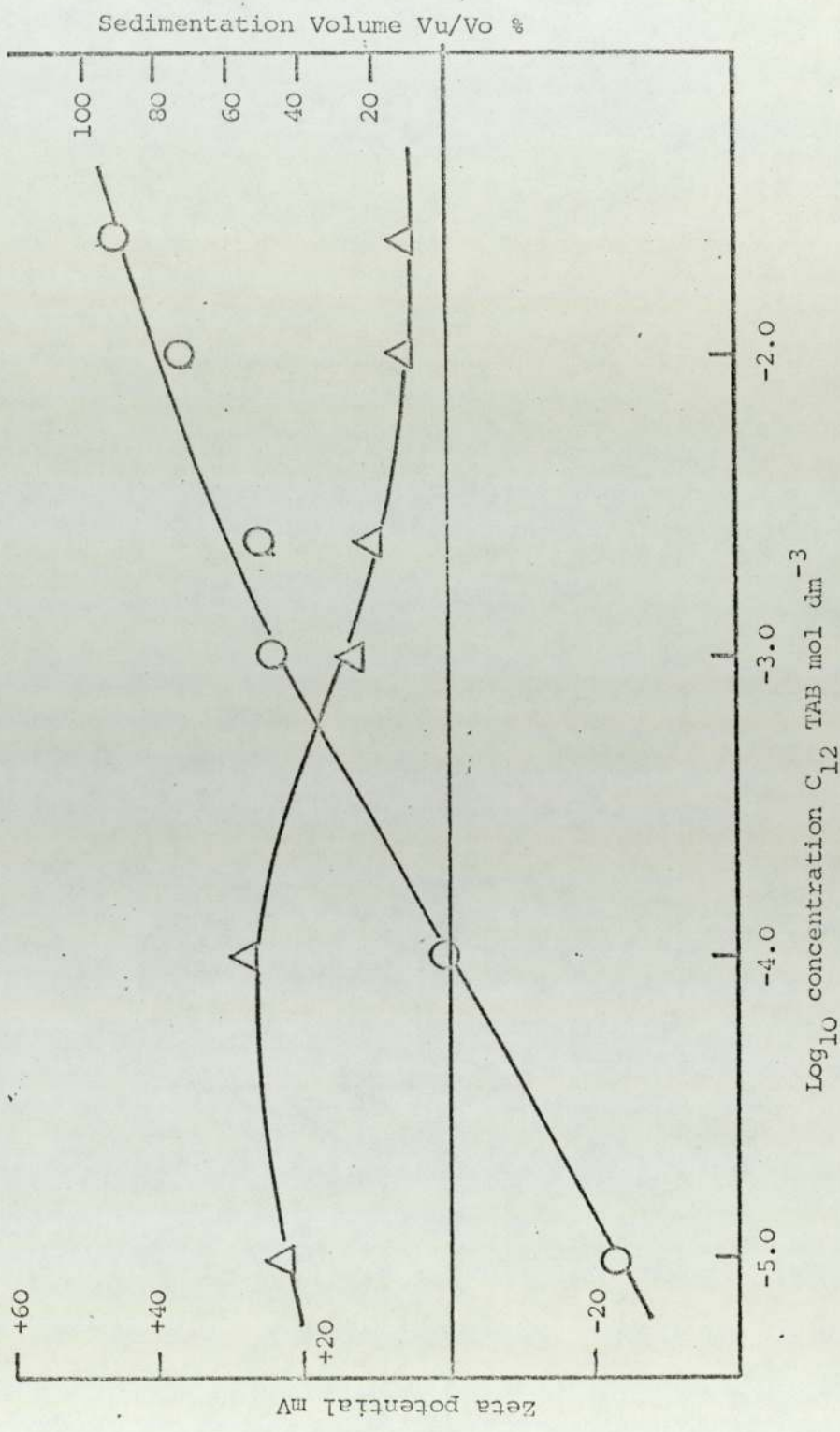


Fig LXVI Zeta potential \bigcirc , and Sedimentation volume \triangle , Thiabendazole - concentration C_{12} TAB

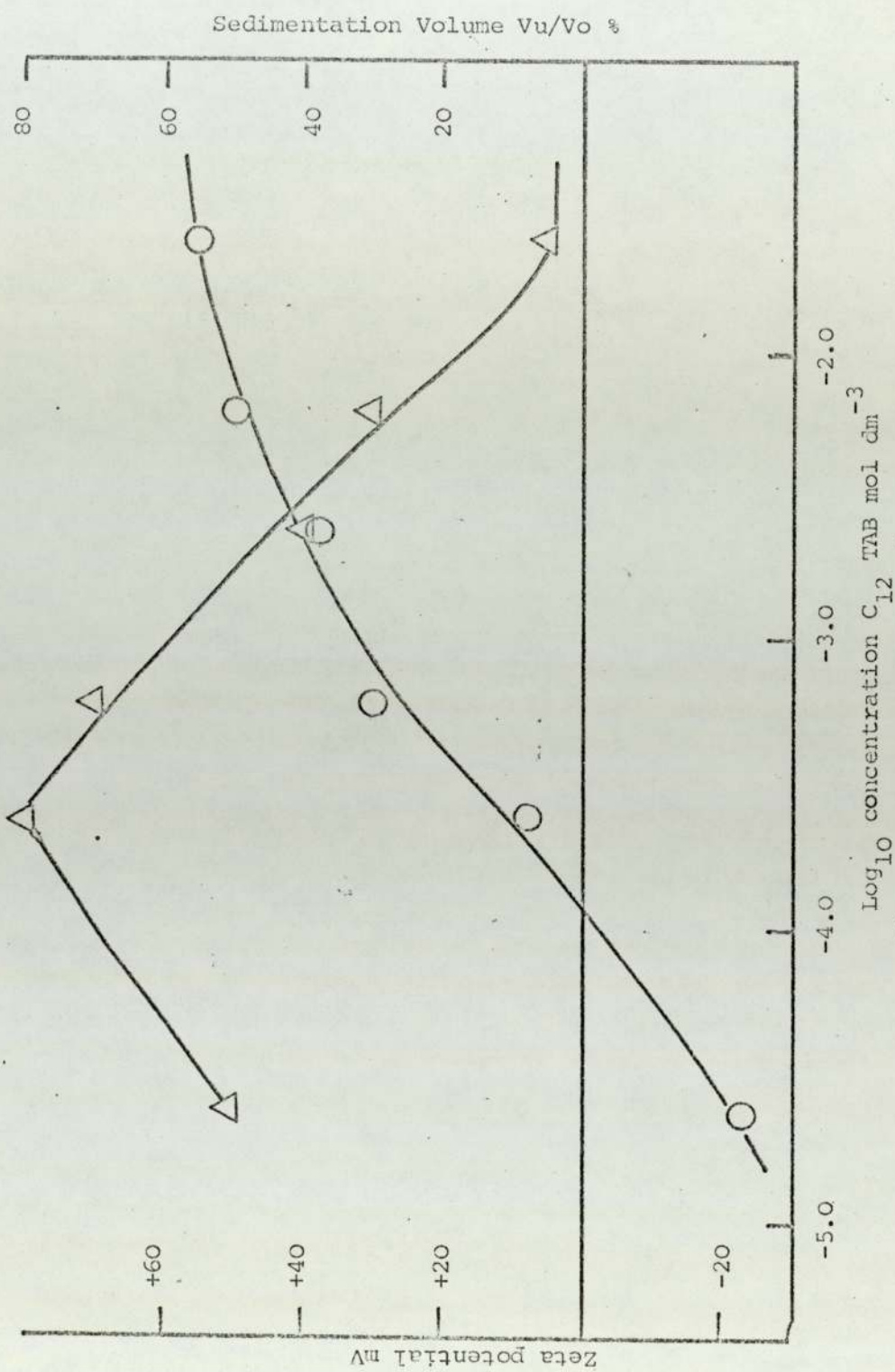


Fig LXVII Zeta potential \circ , sedimentation volume Δ , Griseofulvin - concentration C_{12} TAB

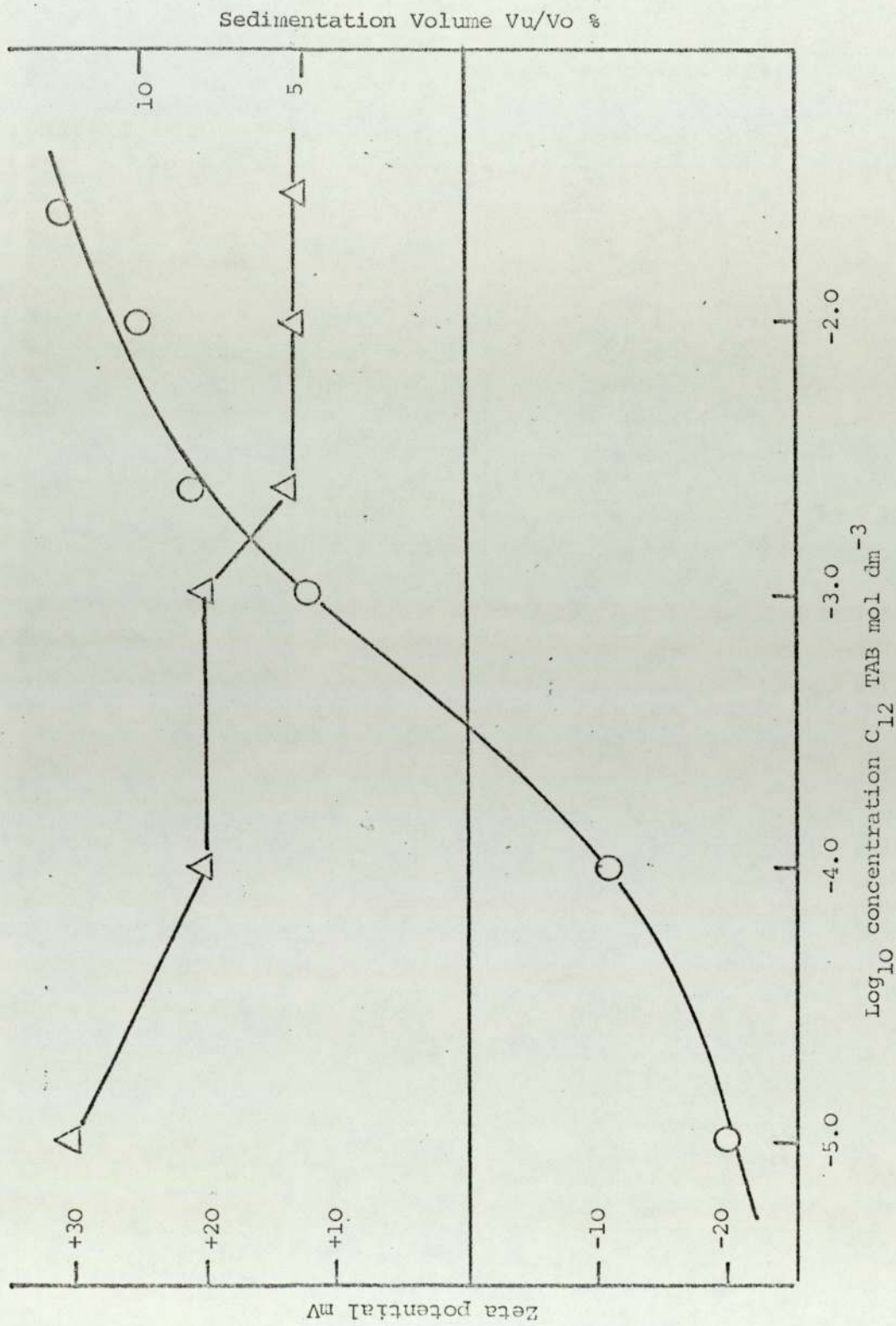


Fig LXVIII Zeta potential \circ , Sedimentation Volume Δ Nalidixic Acid - concentration C_{12} TAB

dispersed.

At zero zeta potential V_R is zero hence

$$V = V_A \rightarrow -450kT \text{ as } H_0 \rightarrow 2.5\text{nm and the system is coagulated.}$$

At $10^{-2} \text{ mol dm}^{-3}$, $\zeta = +35.5\text{mV}$; here

$$V = V_A + V_R, \text{ the magnitude of } V \text{ depends on distance such}$$

that at:-

$$H_0 = 2.5\text{nm} \quad V = -105 \text{ kT.}$$

$$H_0 = 5 \text{ nm} \quad V = +55 \text{ kT.}$$

$$H_0 = 10\text{nm} \quad V = +66.5\text{kT.}$$

$$H_0 = 15\text{nm} \quad V = +34.13\text{kT}$$

This system must be deflocculated with a value for V_m of ca. +66.5kT at H_0 about 10nm.

6.2.3. Drug particle, cationic/nonionic surfactant systems

Suspensions examined were Thiabendazole, Nalidixic Acid and Griseofulvin with C_{12} TAB and $10^{-2} \text{ mol dm}^{-3} C_{16}E_{30}$, and Griseofulvin with C_{12} TAB and $10^{-2} \text{ mol dm}^{-3} C_{16}E_{10}$ and $C_{16}E_{60}$, results are given in Figs. LXIX to LXXIII and tables XXXIV, XXXIII and XXXI.

The results for Thiabendazole, Fig. LXIX, are representative of them all. The sedimentation volume stays constant with increase in concentration of C_{12} TAB as the zeta potential moves from the value of -5mV at $10^{-5} \text{ mol dm}^{-3} C_{12}$ TAB to +14mV at $10^{-2} \text{ mol dm}^{-3} C_{12}$ TAB, thus showing that the presence of $10^{-2} \text{ mol dm}^{-3} C_{16}E_{30}$ confers stability upon the particles. Calculation of V at $10^{-4} \text{ mol dm}^{-3} C_{12}$ TAB, i.e. at zero zeta potential, where V_R is zero, can be made from:-

$$\begin{aligned} V &= V_A + V_S \\ &= -102 + 104 \\ &= +2\text{kT} \end{aligned}$$

This value of positive potential energy would not alone be sufficient to prevent coagulation, however the presence of the absorbed layer

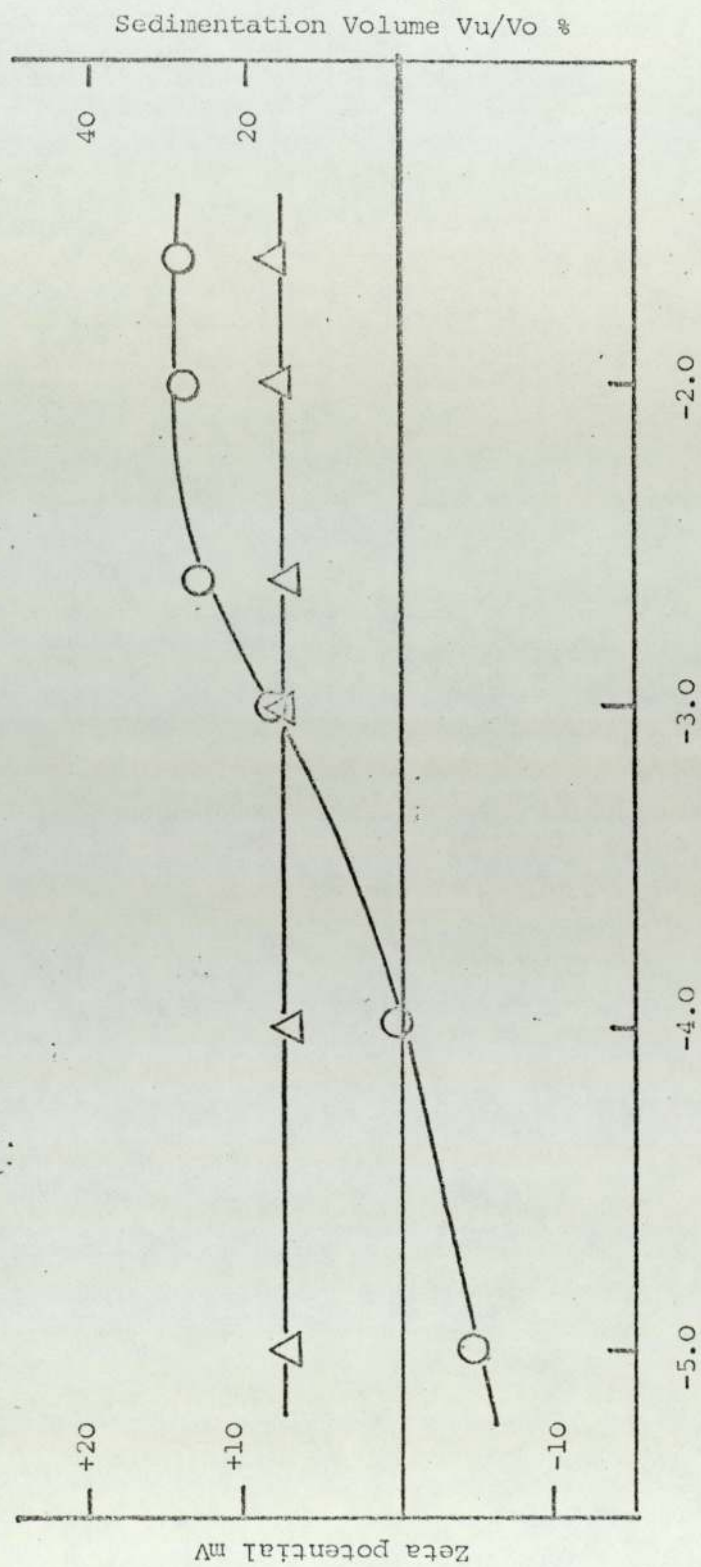


Fig LXIX Zeta potential O , sedimentation volume Δ , Thiabendazole with $10^{-2} \text{ mol dm}^{-3}$
 $C_{16} E_{30}$ - concentration $C_{12} \text{ TAB}$

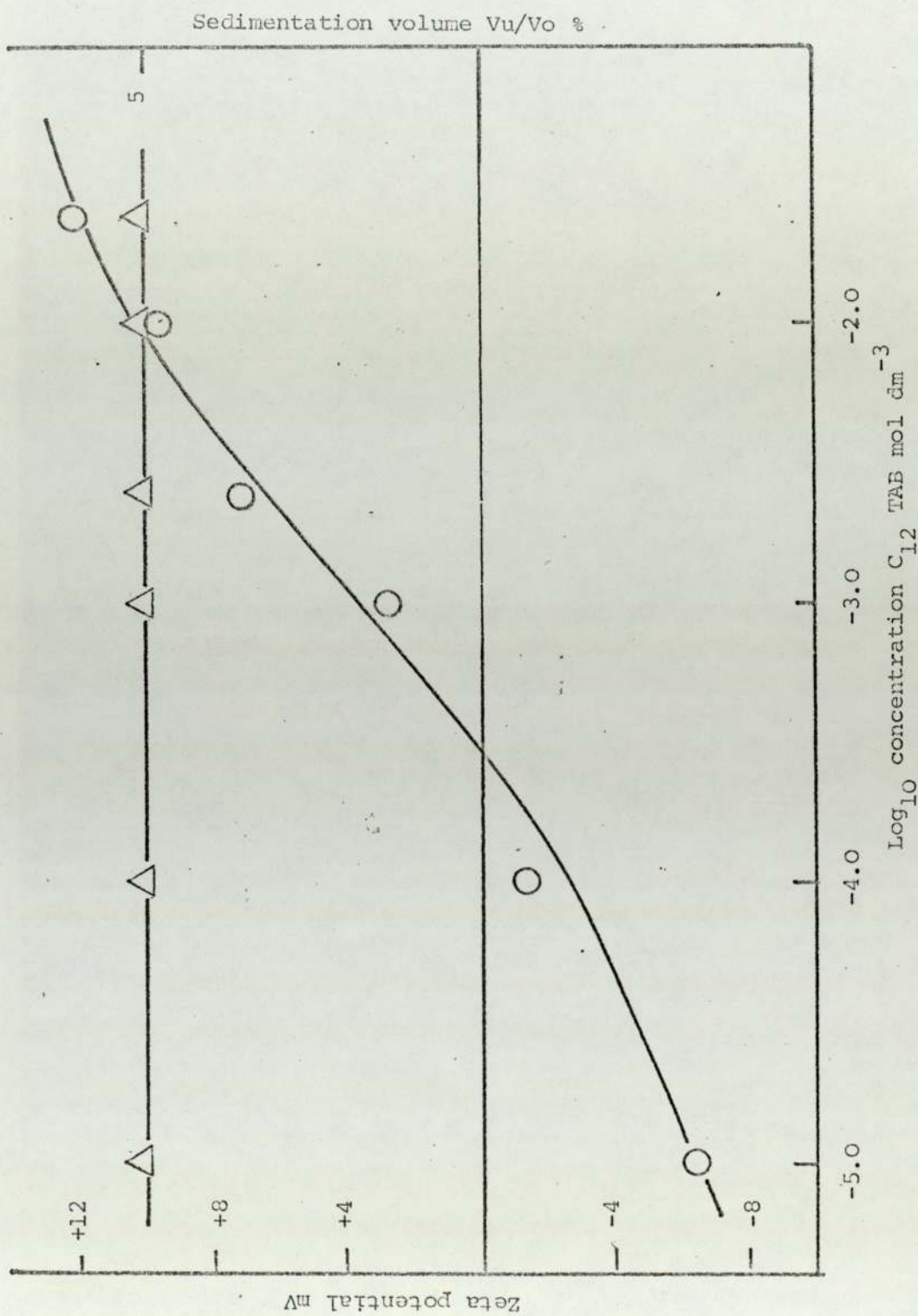


Fig LXX Zeta potential \circ , sedimentation volume Δ , Nalidixic Acid with 10^{-2} mol dm^{-3} $C_{16} E_{30}$ - concentration C_{12} TAB

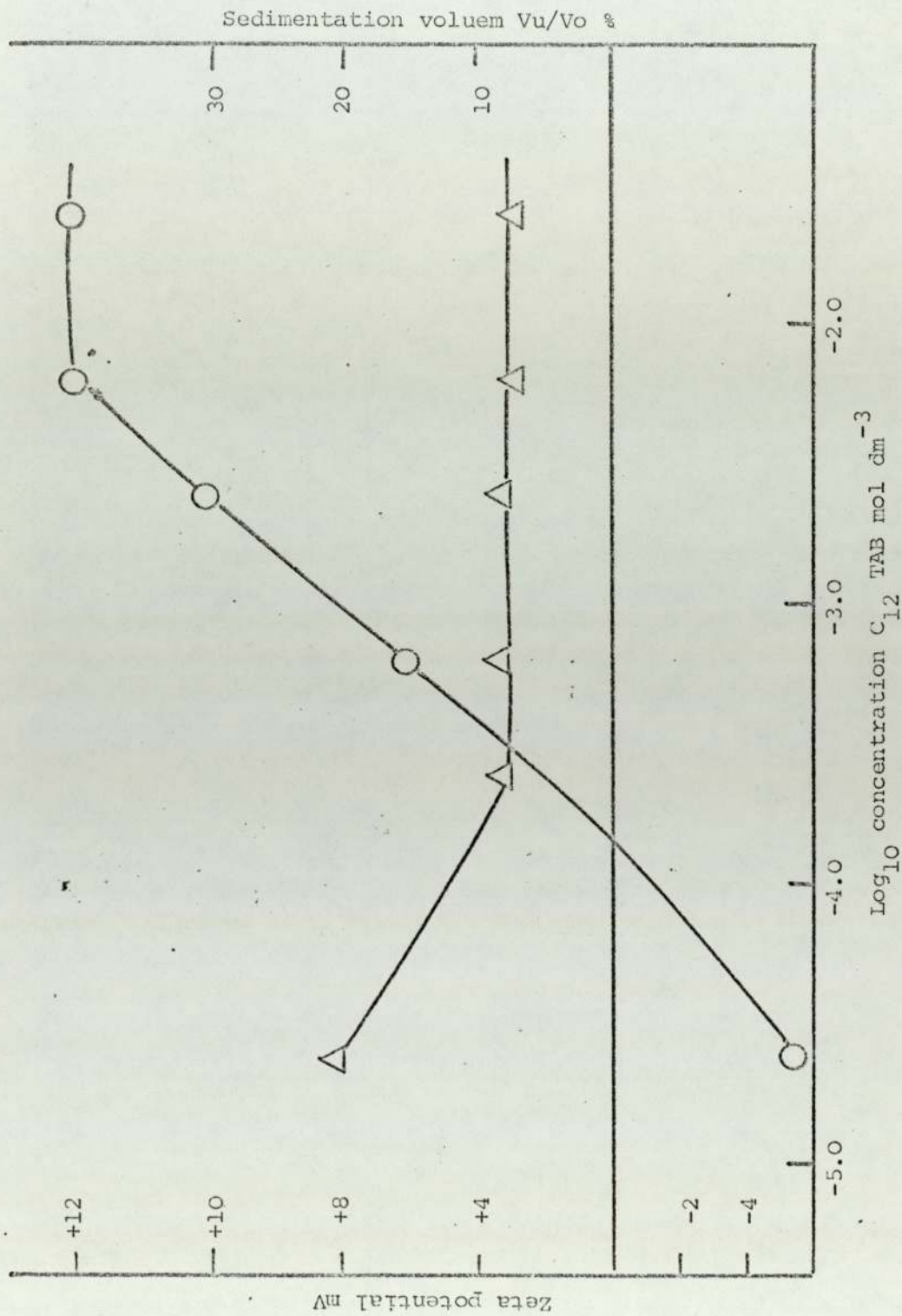


Fig LXXI Zeta potential \bigcirc , sedimentation volume \triangle , Griseofulvin with $C_{16} E_{30} 10^{-2}$ mol dm^{-3} - concentration C_{12} TAB

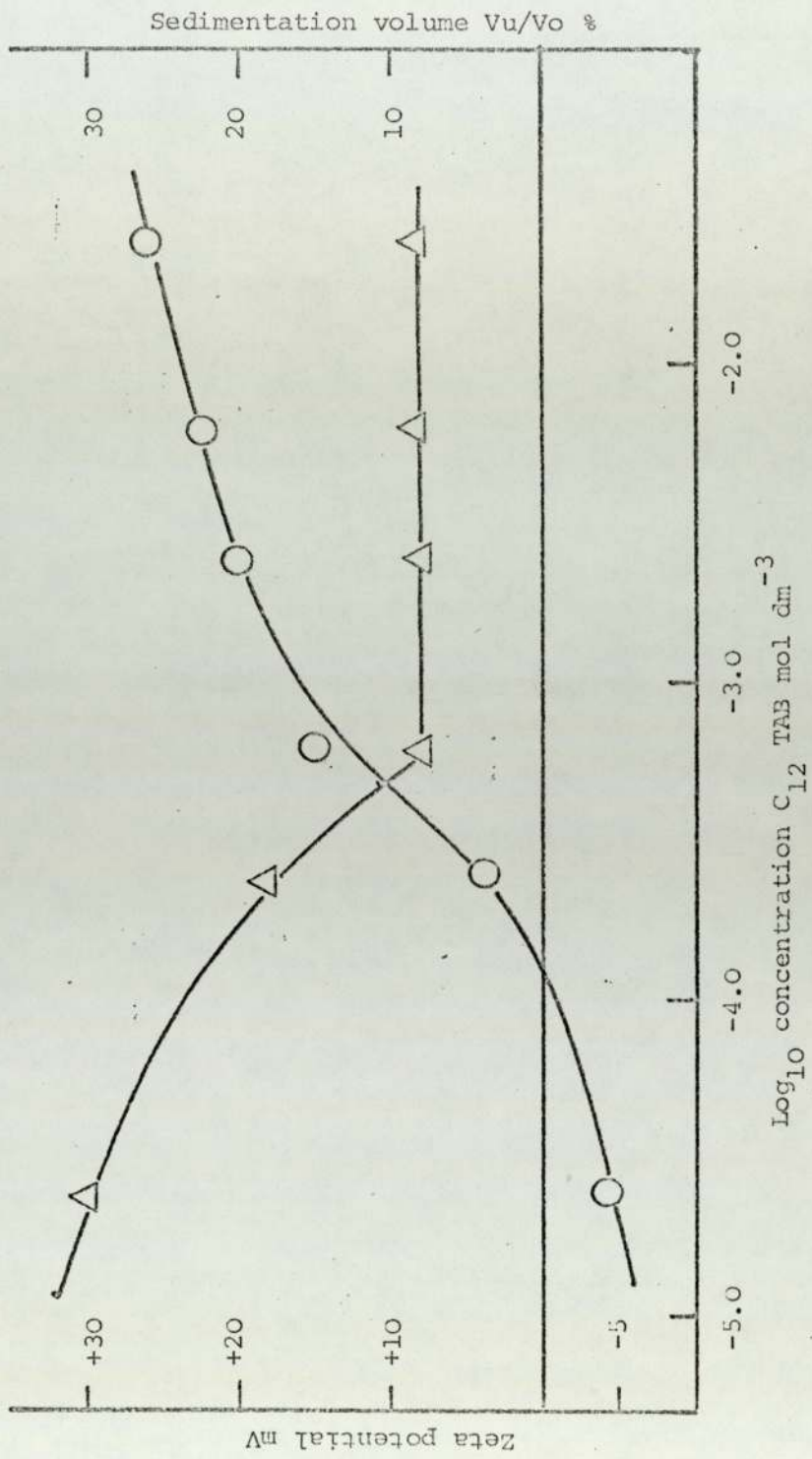


Fig LXXII Zeta potential O , sedimentation volume Δ , Griseofulvin with $C_{16} E_{10}$.
 $10^{-2} \text{ mol dm}^{-3}$ - concentration C_{12} TAB

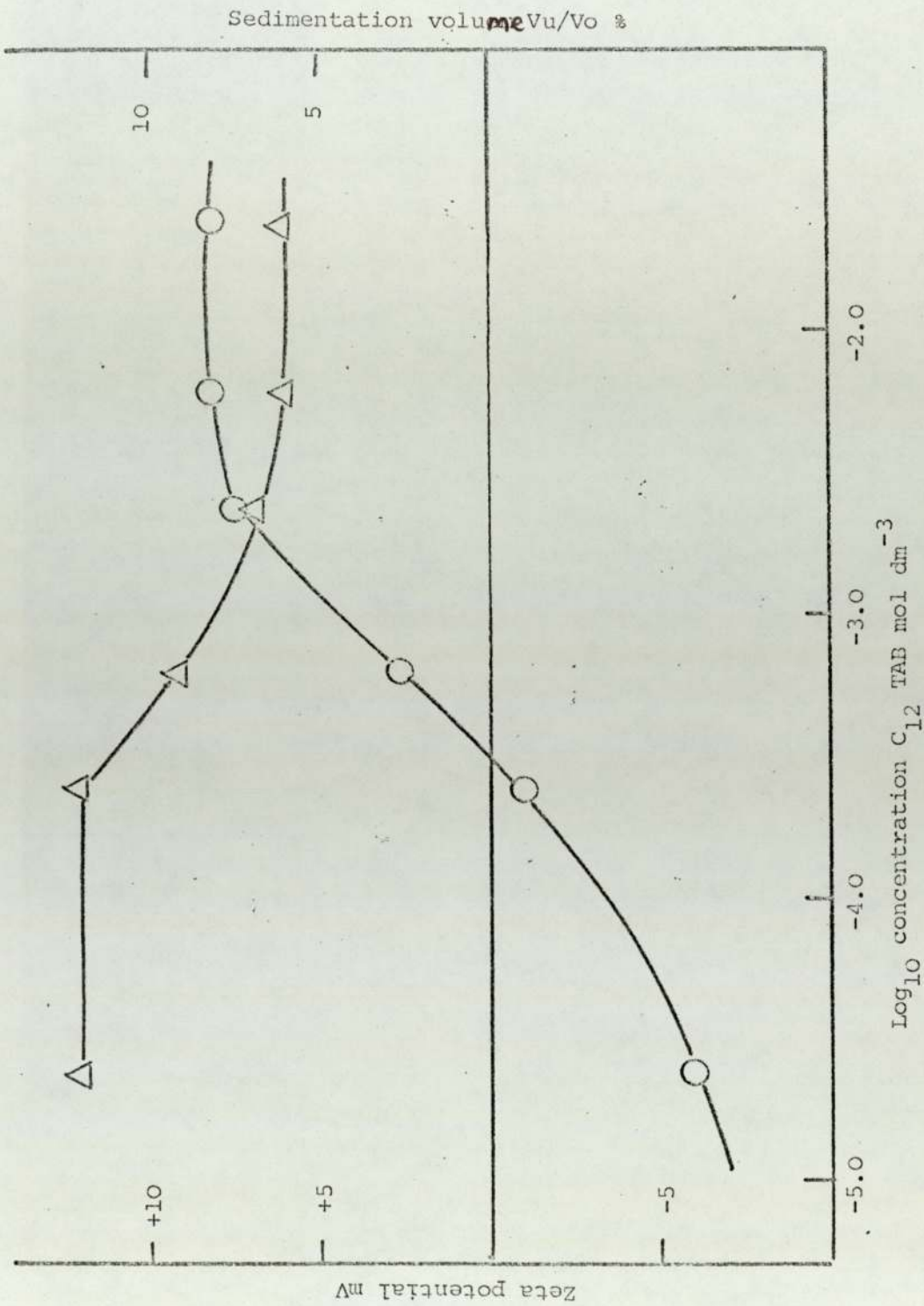


Fig LXXIII Zeta potential O, sedimentation volume Δ , Griseofulvin with $C_{16} E_{60}$
 10^{-2} mol dm^{-3} - concentration C_{12} TAB

prevents closer association of the particles, this is therefore an example of controlled coagulation i.e. primary minimum coagulation restricted by the steric layer.

Changing the ethylene oxide chain length as with Griseofulvin/ $C_{16}E_{10}$, $C_{16}E_{30}$ and $C_{16}E_{60}$, Figs. LXXI, LXXII and LXXIII respectively shows that as the ethylene oxide chain length is increased, so is the steric stabilizing effect, i.e. $C_{16}E_{10}$ at zero zeta potential gives a coagulated system whilst $C_{16}E_{30}$ and $C_{16}E_{60}$ sterically stabilize. Increasing stability with increasing ethylene oxide chain length has been found by other workers and is reported in Section 4.2.1. This effect with $C_{16}E_{10}$ is due to a thinner adsorbed layer, δ which will lead to a lower value for V_s such that V_A , at the resulting distance of approach (H_0 will also be smaller), will have a bigger effect leading to a primary minimum deep enough to cause coagulation even though some protection is given by the adsorbed layer.

6.2.4. Drug particle, anionic surfactant systems.

Results for Thiabendazole/SDS; Betamethasone/SDS; Nalidixic Acid/SDS and Griseofulvin/SDS are shown in Figs. LXII, LXXIV to LXXVI and tables XXX, XXVIII, XXIX and XXXVI. Examination of the zeta potential/sedimentation volume versus concentration SDS plot for Thiabendazole Fig. IXII shows a lowering of F as the zeta potential increases; this plot is typical of the group.

Fig. LXXVII shows how V , calculated from

$$V = V_R + V_A$$

varies with distance H_0 between particles, equations 2.41 and 2.45 being used to calculate V_A at distances of $< 15\text{nm}$ and $> 15\text{nm}$ respectively.

At $\zeta = -18\text{mV}$ the system shows an attractive potential energy at all distances, the suspensions should therefore be coagulated and this was found experimentally.

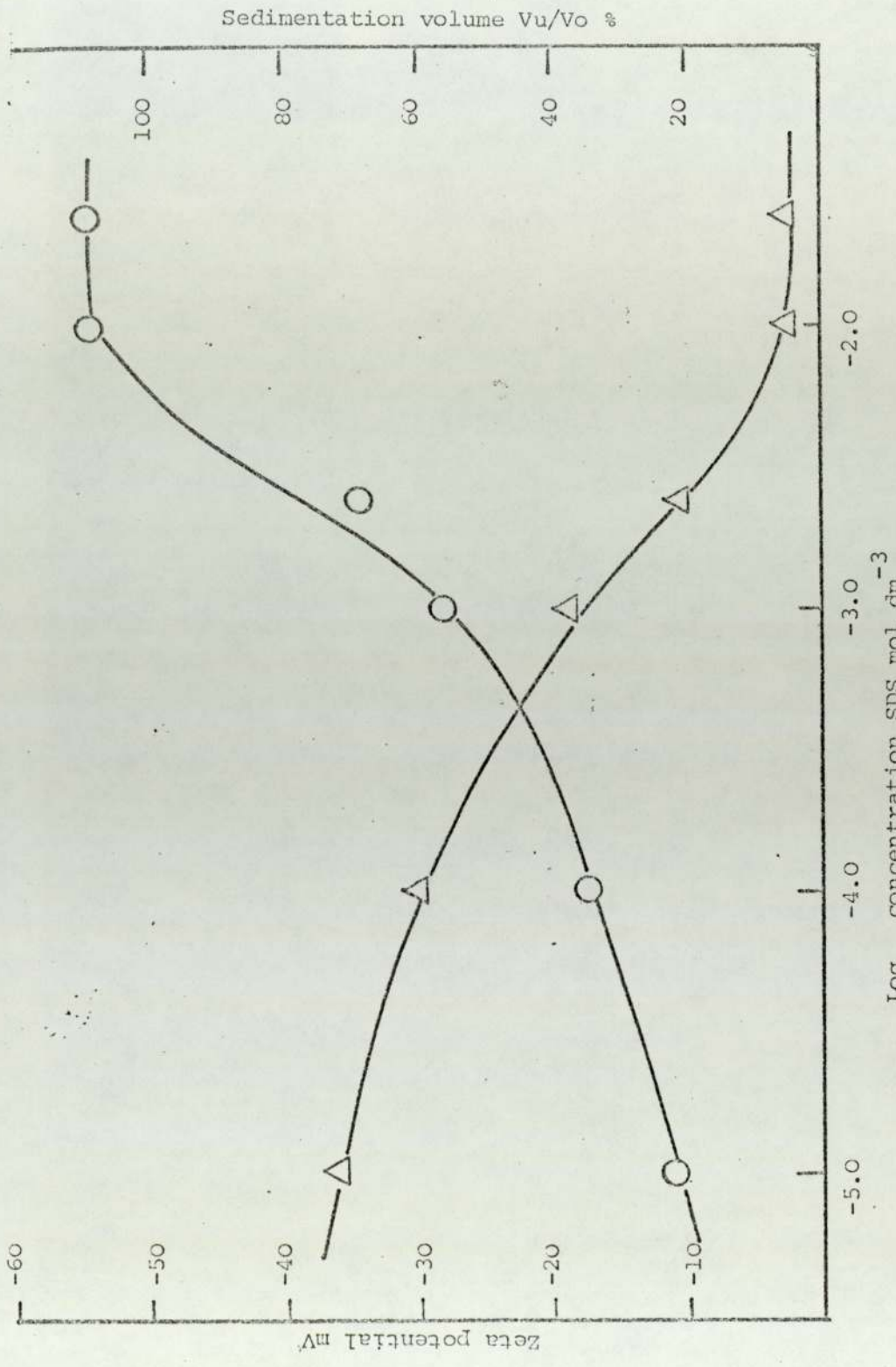


Fig LXXIV Zeta potential \circ , sedimentation volume \triangle , Betamethasone - concentration SDS

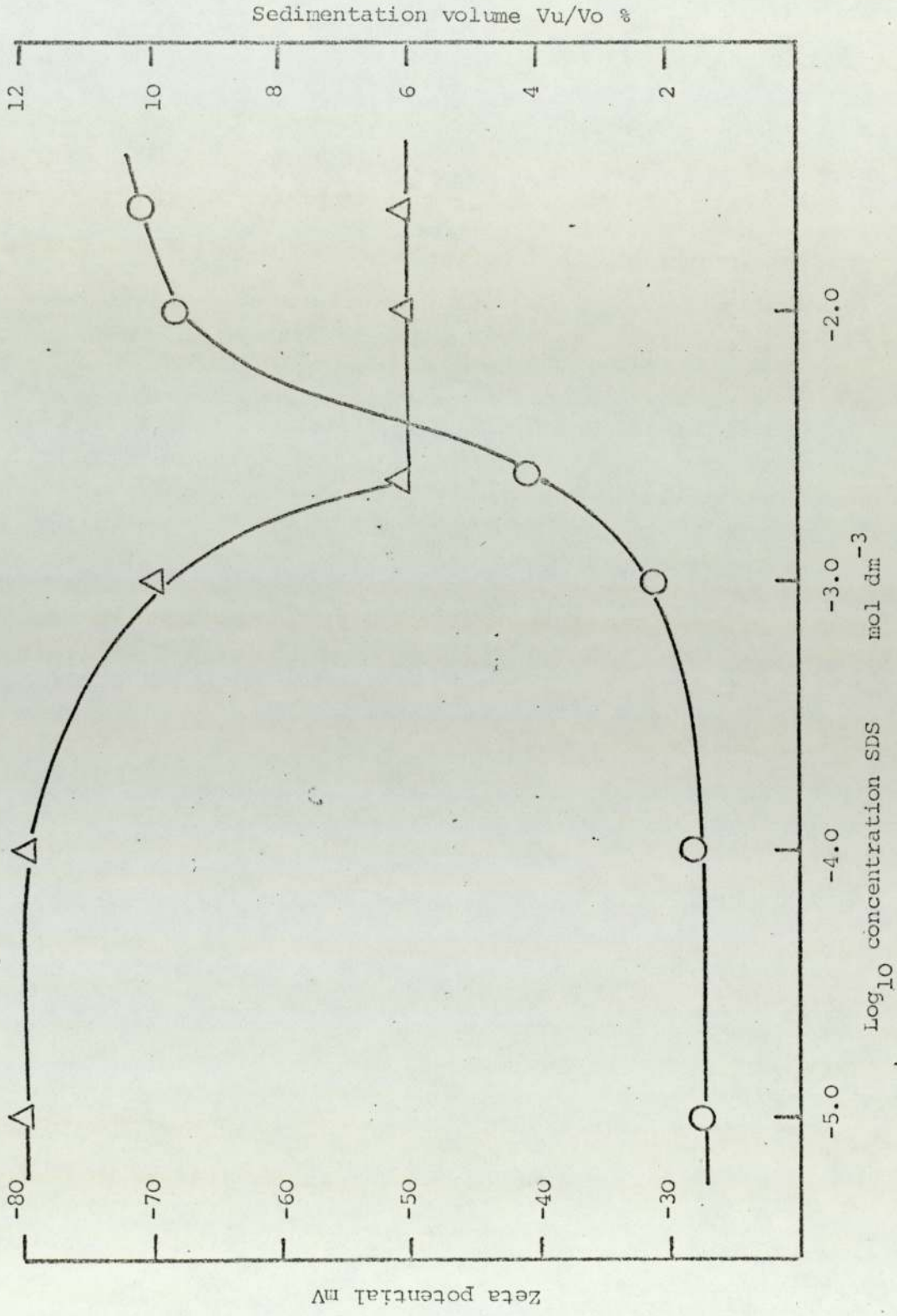


Fig LXXV Zeta potential ○, sedimentation volume Δ, Nalidixic Acid - concentration SDS

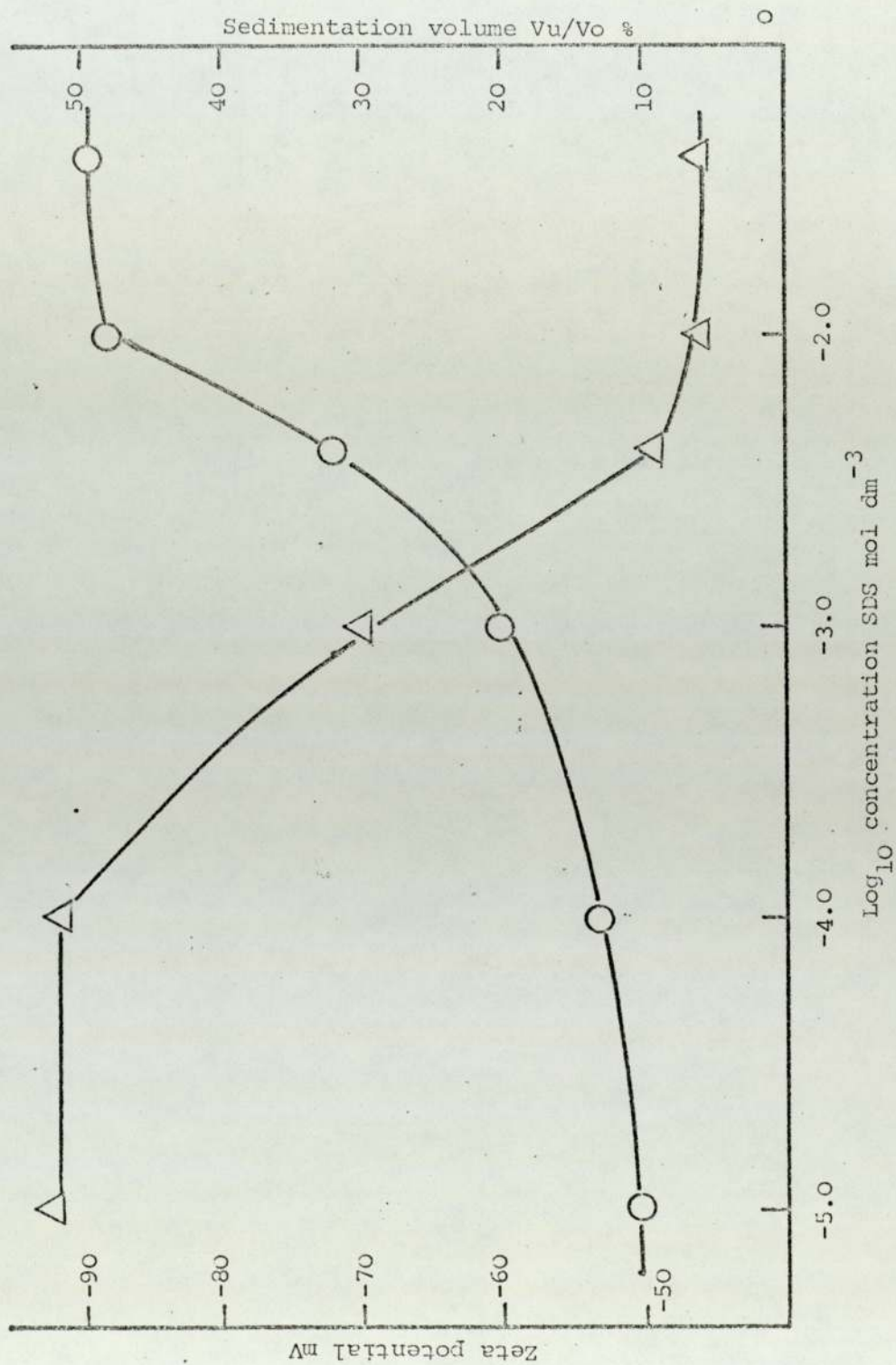
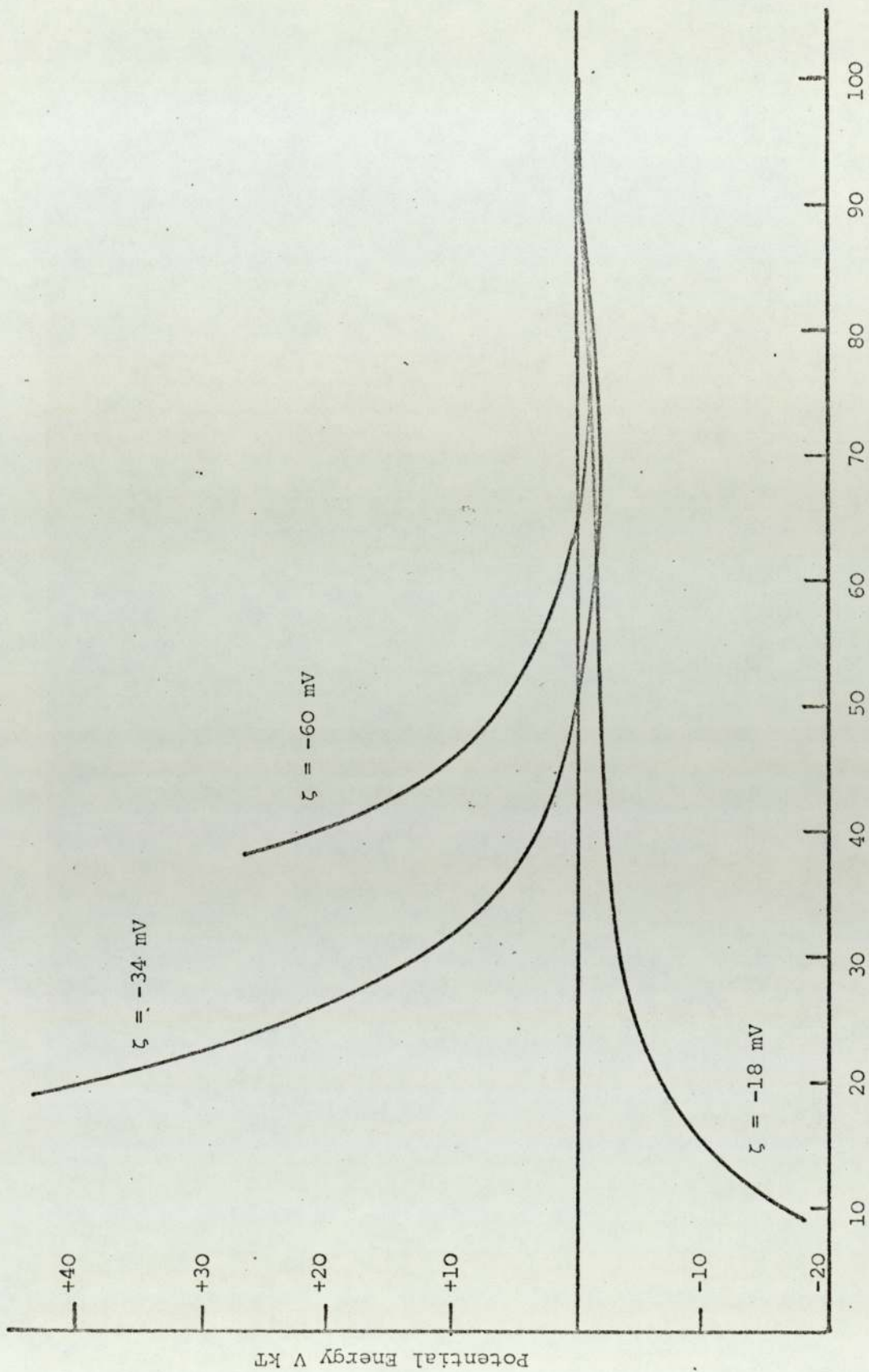


Fig LXXVI Zeta potential \circ , sedimentation volume \triangle , Griseofulvin - concentration SDS



Distance H_0 between particles in nm

Fig LXXVII Potential energy $V = V_R + V_A$ for Thibendazole with varying concentration of SDS; zeta potential = -60 mV 10^{-2} mol dm^{-3} SDS; -34 mV at 2.5×10^{-4} mol dm^{-3} SDS and -18 mV at 10^{-5} mol dm^{-3} SDS.

With $\zeta = -34\text{mV}$, V is positive at distances less than 50nm, a maximum V_m of potential energy is reached of ca. $+64kT$ which should be sufficient to prevent primary minimum coagulation. A shallow secondary minimum is seen at ca. 70nm of about $-2kT$, this suspension showed a sedimentation volume of 33%, aggregation of particles had occurred but these aggregates were easily dispersed, it is possible that this is secondary minimum flocculation, although a value of 5-10kT would be expected before such flocculation occurred. However Verwey and Overbeek (3) give an example of a suspension of $1\mu\text{m}$ particles in a solution of a $10^{-3}\text{ mol dm}^{-3}$ 1:1 electrolyte where there was a secondary minimum of 6kT and where loose aggregation occurred. In view of the approximations made in calculating V it may well be that the true secondary minimum is larger than that calculated. At $\zeta = -60\text{mV}$, V is always positive to ca. 60nm. A maximum of $+558kT$ is reached at 5nm. The depth of the secondary minimum barely reaches $-1kT$ and as expected the suspension was completely deflocculated and caked.

6.2.5. Drug particle, anionic/nonionic surfactant systems.

Here results are very similar in pattern to those found for cationic/nonionic surfactant mixtures. Fig. LXIII and table XXX shows results for Thiabendazole/SDS/ $C_{16}E_{30}$ and Figs. LXXVIII to LXXXII and tables XXVIII, XXIX and XXXVIII for Betamethasone/SDS/ $C_{16}E_{30}$, Nalidixic Acid/SDS/ $C_{16}E_{30}$ and Griseofulvin/SDS/ $C_{16}E_{10}$, $C_{16}E_{30}$ and $C_{16}E_{60}$, respectively.

The plot for Thiabendazole shows that the sedimentation volume F stays virtually constant as the concentration of SDS is increased. This indicates that this concentration of $C_{16}E_{30}$ is adsorbed sufficiently to sterically stabilise the suspension with little or no help from electrostatic repulsion. All samples show a cloudy supernatant.

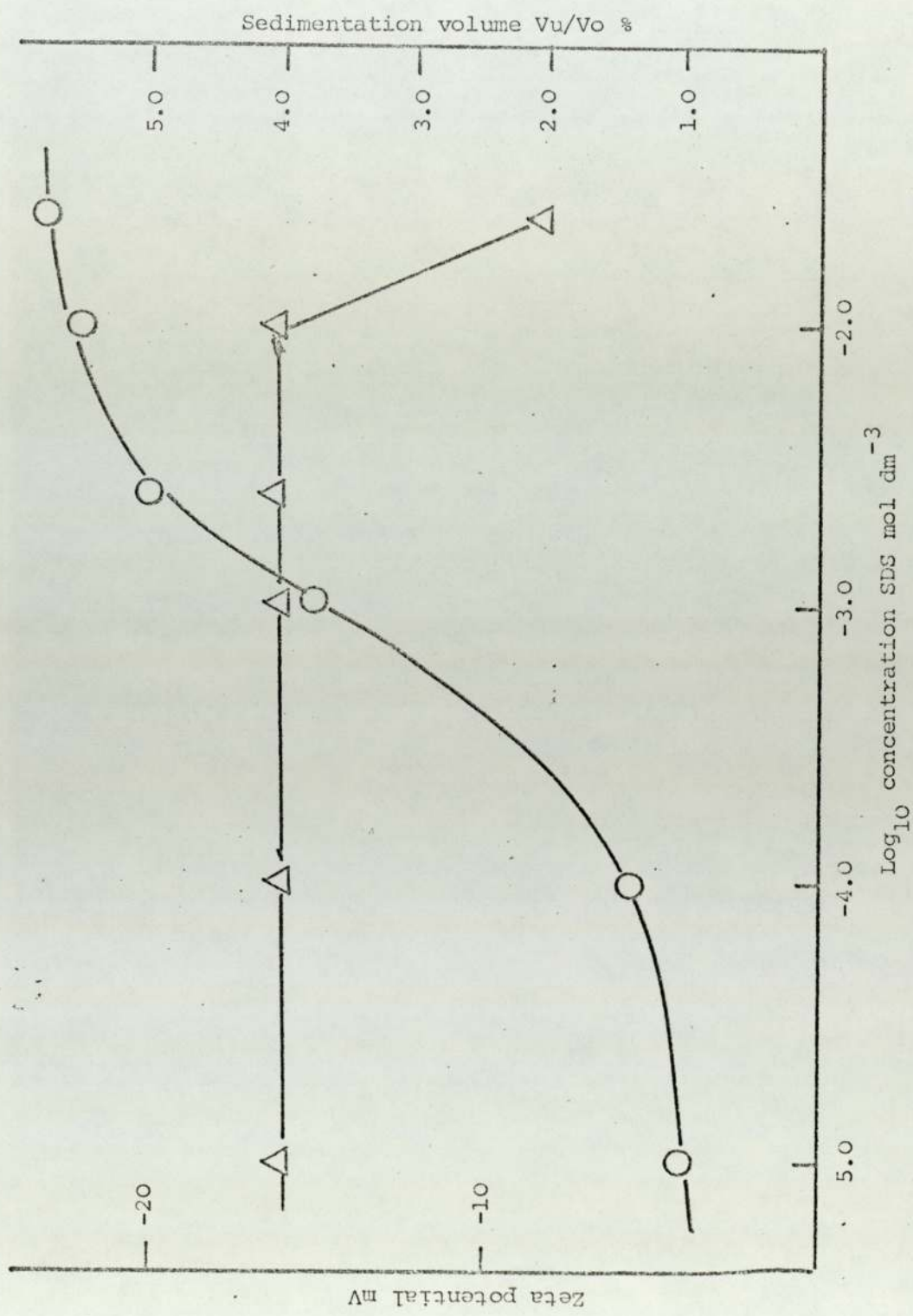


Fig LXXVIII Zeta potential \circ , sedimentation volume Δ , Betamethasone with 10^{-2} mol dm⁻³ C₁₆E₃₀ - concentration SDS

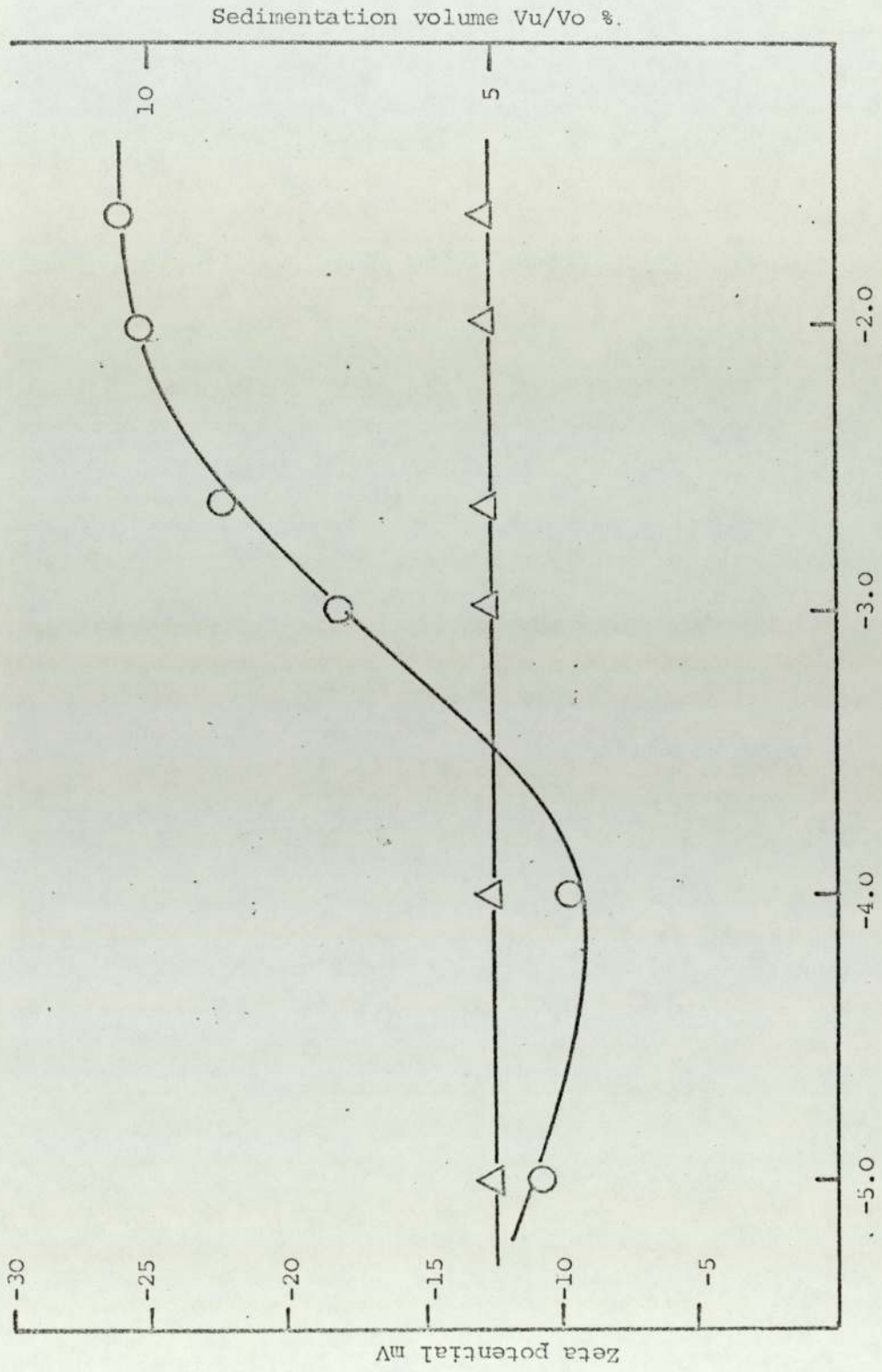


Fig LXXIX Zeta potential \bigcirc , sedimentation volume \triangle , Nalidixic Acid with $C_{16}E_{30}$
 $10^{-2} \text{ mol dm}^{-3}$ - concentration SDS

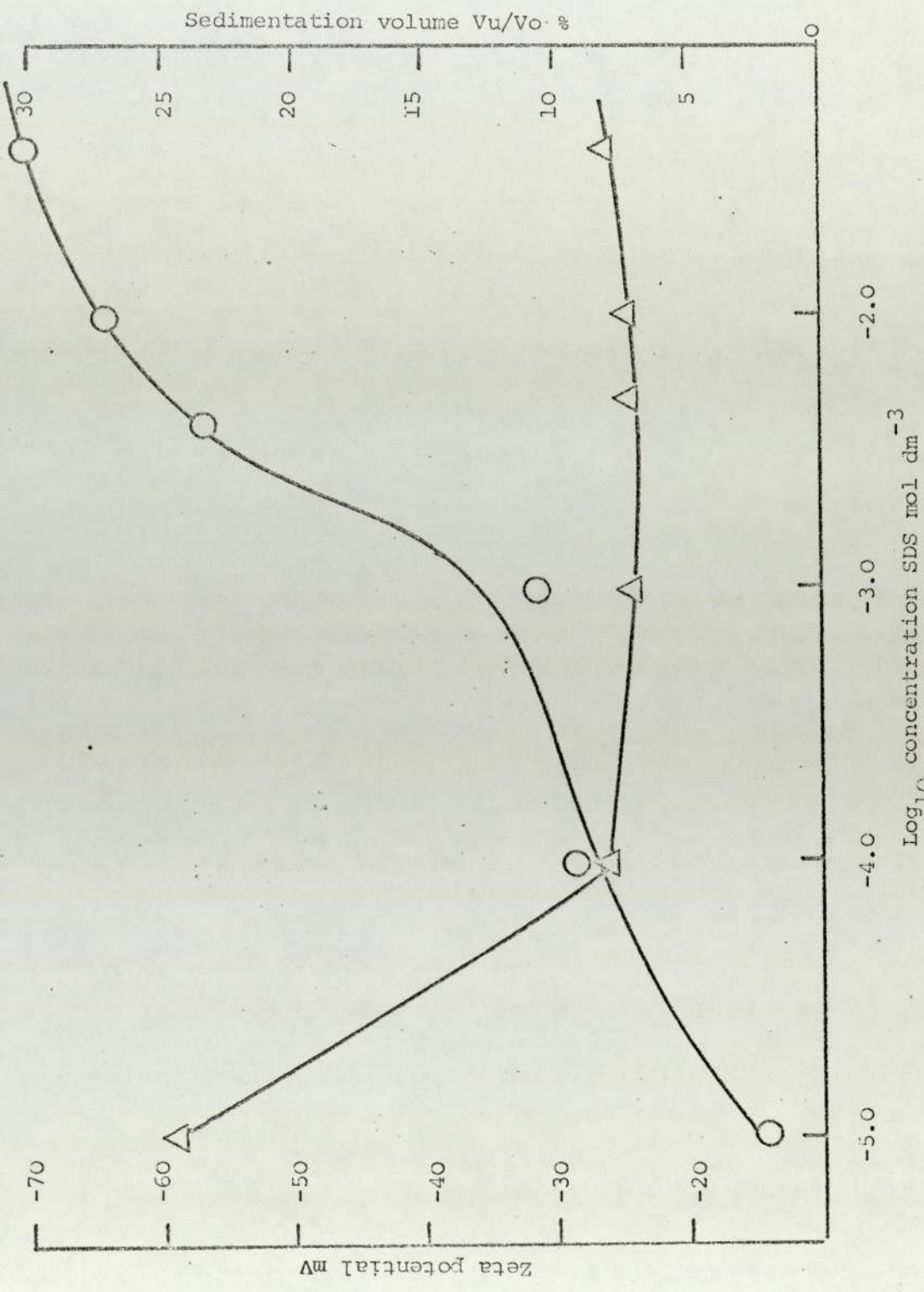


Fig LXXX Zeta potential \bigcirc , sedimentation volume \triangle , Griseofulvin with $10^{-2} \text{ mol dm}^{-3}$ $C_{16}E_{10}$ - concentration SDS

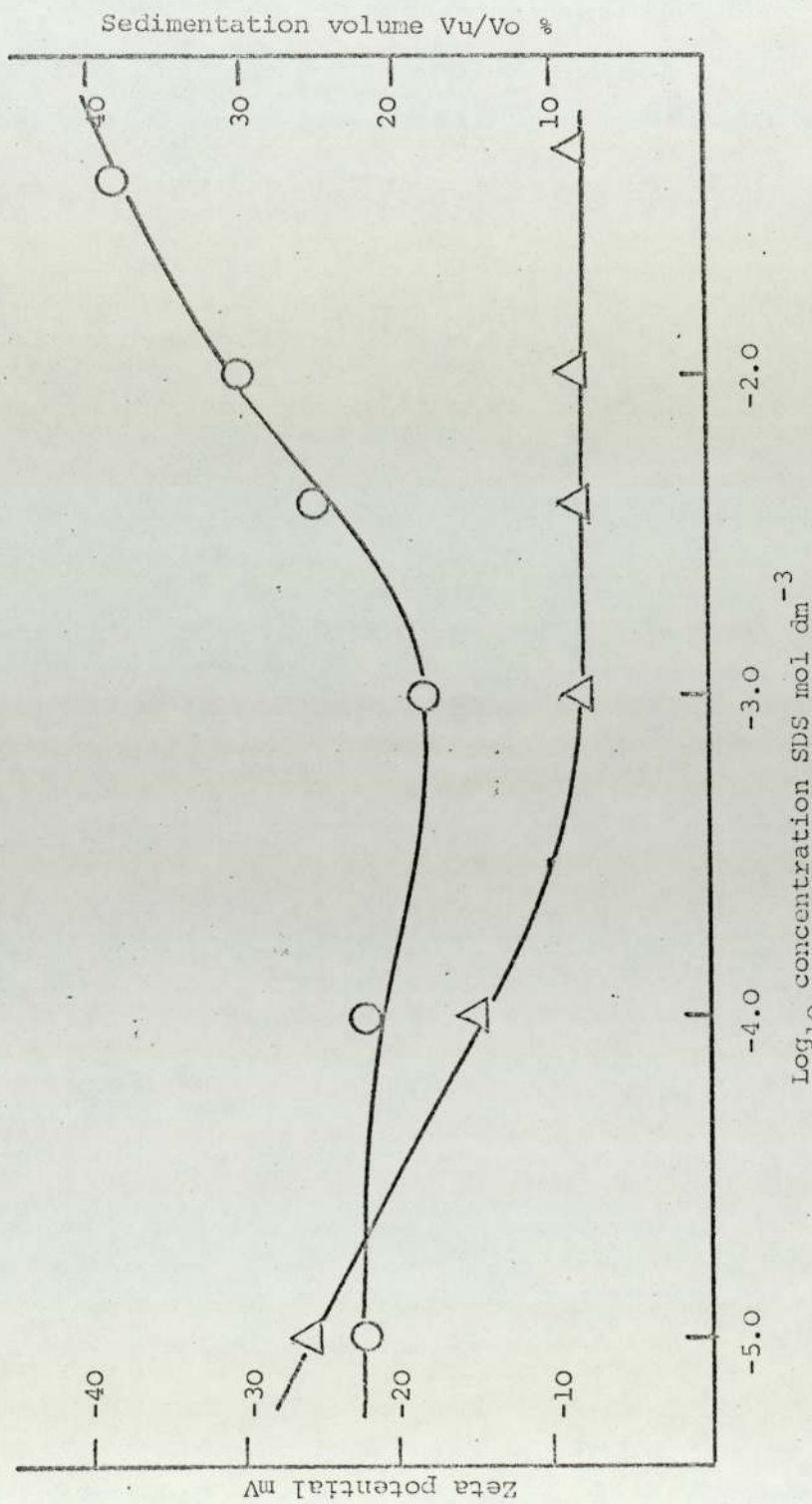


Fig LXXXI Zeta potential \bigcirc , sedimentation volume \triangle , Griseofulvin with $10^{-2} \text{ mol dm}^{-3}$
 $C_{16}E_{30}$ - concentration SDS

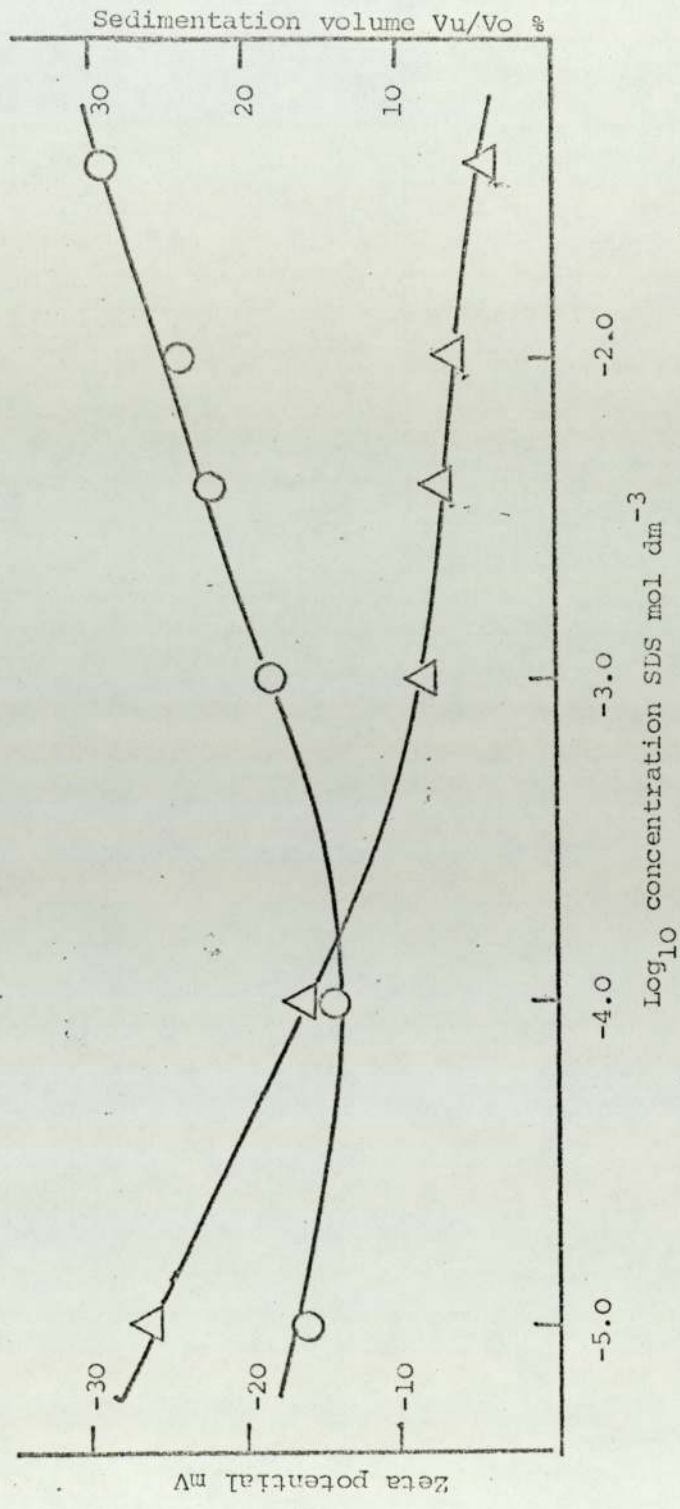


Fig LXXXII Zeta potential \circ , sedimentation volume \triangle , Griseofulvin with $C_{16}E_{60}$ 10^{-2} mol dm⁻³ - concentration SDS

Calculation of V at 10^{-3} mol dm $^{-3}$ SDS gives $+38kT$ a value sufficiently high to stabilize the suspension.

The results for Griseofulvin/SDS/ $C_{16}E_{10}$, $C_{16}E_{30}$ and $C_{16}E_{60}$ confirm the findings of the Griseofulvin/ C_{12} TAB/nonionic systems that increasing the ethylene oxide chain length increases the steric stabilizing effect of the nonionic surface active agent.

SECTION 7.

GENERAL DISCUSSION AND CONCLUSIONS

The effect surface active agents of various ionic types have on the electrophoretic mobility and zeta potential of polystyrene latex has been studied. Similar experiments were carried out with the four drugs Betamethasone, Griseofulvin, Nalidixic Acid and Thiabendazole. Suspensions of these drugs in solutions of the same surface active agents, as used with the polystyrene latex, being prepared so that sedimentation volumes could also be studied.

The results found with microelectrophoresis of the drug systems were similar to those found with the polystyrene latex dispersion, indicating that the latter is a suitable model system.

The effect nonionic surface active agents had on the various systems was to lower the electrophoretic mobility and zeta potential, the plane of shear around the particle being displaced by the adsorbed nonionic surfactant molecules. It was found that the nonionic surfactant molecule looped itself around the particle so that adsorption occurred until the particle was covered and then there was no further adsorption as there was a plateau in the electrophoretic mobility - \log_{10} concentration surface active agent plot. The mobility of the particle was correspondingly less as ethylene oxide chain length was increased showing that the increase in 'bulk' of the molecule further displaced the shear plane, i.e. the thickness of the adsorbed layer increased. Adsorption of the nonionic surfactant occurred by the hydrophobic effect with the alkyl chain on the hydrophobic areas of particle surface and by association of the ethylene oxide groups of that chain with suitable sites on the particle surface by hydrogen bonding. On studying sedimentation volumes e.g. Fig. LXIV for Thiabendazole, it is seen that such a layer is sufficient to sterically stabilize the suspended particles, the protection

improving as ethylene oxide chain length is increased.

With cationic surface active agents adsorption is a two stage process, first sufficient cationic molecules are adsorbed, either within the Stern layer or, in the case of polystyrene latex and Nalidixic Acid electrostatically associated with the charge group, to effectively neutralize the particle charge. Further adsorption then occurs by the hydrophobic effect, with the alkyl chain on the particle surface, and the particle acquires a positive charge which rises to a maximum as the surface eventually becomes packed with vertically orientated molecules. Consideration of the slope of the zeta potential- \log_{10} concentration CxTAB plot enables the free energy of adsorption of the surface active agent to be obtained, this increases as alkyl chain length increases. The driving force for the adsorption of cationics onto the particle surface is the hydrophobic effect. Suspensions of this group were coagulated at low concentrations of CxTAB (low positive or negative potential) but became deflocculated as cationic adsorption increased and the zeta potential increased - such suspensions were deflocculated and caked.

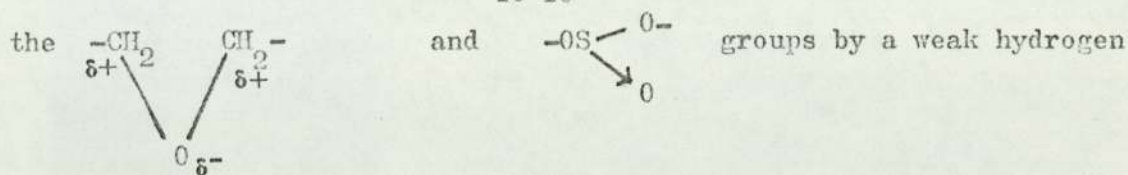
The addition of nonionic surface active agents to the cationic systems caused a displacement of the zeta potential- \log_{10} concentration plot to the right, the R.C.C. increasing depending on the relative concentrations. In the first place the concentration of nonionic is higher and more is adsorbed but this is gradually displaced as the concentration of cationic is increased. The magnitude of displacement of the R.C.C. is proportional both to concentration of nonionic and to the alkyl chain length of cationic used. The length of the ethylene oxide chain has no effect on the R.C.C. Prediction of displacement of the R.C.C. with specified systems is possible. Sedimentation volume results for the cationic nonionic systems shows that all suspensions are sterically stabilized by the adsorbed nonionic, the effect being proportional to

ethylene oxide chain length, $C_{16}E_{10}$ only partially stabilizes the system to coagulation, the presence of a charge on the particle also being necessary, whilst $C_{16}E_{30}$ and $C_{16}E_{60}$ stabilize at zero zeta potential.

The adsorption of a negatively charged surface active molecule, i.e. SDeS, SDS and STS, onto the negatively charged particles causes an increase in zeta potential. The alkyl chains are adsorbed onto the hydrophobic surface of the particles, the driving force being the hydrophobic effect. In the case of polystyrene latex and Nalidixic Acid the electrostatic repulsive force between the carboxyl group and the $-OSO_3^-$ of the surfactant molecule has to be overcome before the ~~particle~~ ^{molecule} can be adsorbed. As adsorption of molecules increases the zeta potential increases to a maximum; this maximum occurs just before the cmc of the bulk surfactant i.e. the surface is 'full' before the bulk cmc. This is due to the concentration of molecules at the particle surface being greater than in the bulk of the solution. The slope of the zeta potential- \log_{10} concentration anionic plot just as it begins to rise steeply, i.e. as adsorption was occurring strongly, was used to calculate the adsorption energies, allowance being made, where applicable, for the electrostatic repulsion effect. These energies increased as alkyl chain length increased but were reasonably constant for one surfactant species on various surfaces. DLVO potential energy curves were calculated for the system SDS/Thiabendazole, Fig. LXXVII and show that the coagulation/deflocculation state depended on the zeta potential of the particle. For mixtures of anionic/nonionic surface active agents certain interesting characteristics were found.

With nonionic/SDS systems the zeta potential- \log_{10} concentration SDS plot was displaced to the right, the $C_{16}E_{10}$ being displaced by the anionic at higher concentrations of the latter. However, with $C_{16}E_{30}$ and $C_{16}E_{60}$ there was evidence of complex formation occurring at median

concentration of anionic between the anionic and nonionic molecules. This complexation depended on the ethylene oxide chain length of the nonionic species and was not shown by $C_{16}E_{10}$; association appeared to be between



bond probably through water molecules. The weak bond was broken and the complex destroyed by the effect of the more strongly adsorbed anionic as the concentration of this latter increased.

The magnitude of displacement of the zeta potential- \log_{10} concentration anionic plot at low concentration of anionic is proportional to the ethylene oxide chain length. Here it is the displacement of the plane of shear which is the important effect and, at such low concentrations, it would seem possible to predict the effect such mixtures would have on other systems.

The mobility - pH plots for Betamethasone, Griseofulvin, Nalidixic Acid and Thiabendazole show that it is only over certain well defined pH regions - characteristic to a particular drug - that the charge of the particle is constant, e.g. Nalidixic Acid between pH 2.5 and 3.5 and pH 7.0-8.0, Griseofulvin pH 7.0 to 10.0. This suggests that when considering pharmaceutical suspension formulations a mobility-pH plot for the drug should be made and where necessary the pH of the formulation should be strictly controlled. It is interesting that the pH of the commercially available form of Nalidixic Acid is 6.5, just at the commencement of the plateau region.

Study of the zeta potential/sedimentation volume - concentration surfactant plots shows that apparently only coagulated, deflocculated or sterically stabilized systems were found. As in most cases the sterically stabilized systems were produced from mixtures of ionic/nonionic surfactants.

These are examples of controlled coagulation as discussed in the introduction of Section 1. From the size of the particles, and magnitude of charge, secondary minimum flocculation would have been expected in certain cases, as shown by the calculations for the SDS/Thiabendazole system. The method used for investigation of the sedimentation volume of the suspensions was to allow them to stand for 3 days after shaking in a water bath for 24 hours; the suspensions were not observed over this period. It is therefore possible that secondary minimum flocculation did occur, but, due to the weight, size and size distribution of the particles (the assumptions made in calculations are that they are monodisperse and spherical) on settling the particles are able to exclude water from between the flocs and to overcome the forces separating them such that they become deflocculated and caking occurs. This is particularly likely with large particles (164). Further factors involved could be the tunnel (12) and desorption effects (13) discussed in Section 1.

The results of this work show that the investigation of the charge characteristics of a drug particle, with or without additives, is an important factor to be considered in suspension formulation.

The use of polystyrene latex dispersions as model systems has been justified, the results found can be applied to drug systems qualitatively but the surface characteristics and size distributions of drug particles vary, so that the results cannot be applied quantitatively in all respects.

Nonionic surfactants would seem able to completely stabilize coarse suspensions against caking, but further long term studies with these and different types of nonionic stabiliser are needed.

The work confirms that of Mathews & Rhodes (23) that the DLVO theory of colloid stability and its modification to include a steric term, can be applied to coarse suspension systems. However the existence and importance of secondary minimum flocculation in coarse polydisperse

suspensions needs further investigation.

The terminology used in discussing coarse suspensions needs revision. It would seem that most suspensions described as flocculated are really coagulated, that the so called "controlled flocculation" approach is perhaps more correctly termed controlled coagulation, with added polymeric substance preventing access to the true primary minimum. It would seem desirable to use the words coagulated and decoagulated (instead of deflocculated) to describe the relevant states and to reserve flocculation for polymer bridging aggregation and secondary minimum flocculation.

References

1. Martin, A.N., Swarbrick, J. and Cammarata, A. "Physical Pharmacy" p.516 2nd Ed. Lea and Febiger Philadelphia 1969.
2. Derjaguin, B.V. and Landau, L. Acta Physicochim U.R.S.S. 1941, 14, 633.
3. Verwey, E.J.W. and Overbeek, J.Th.G. "Theory of the Stability of Lyophobic Colloids". Elsevier, Amsterdam. 1948.
4. Ottewill, R.H. "Particulate Dispersions" p.175 in "Colloid Science". Vol. 1. Chemical Society, London, 1973.
5. Koelmans, H. and Overbeek, J.Th.G. Discussions Faraday Soc. 1954, 18, 52.
6. Haines, B.A. and Martin, A.N. J. Pharm. Sci. 1961, 50, 228.
7. Weissberger, A. "Technique of Organic Chemistry" Vol. 3. Interscience, New York. 1950, p.388.
8. Kolthoff, I.M. and Naponen, G.E. J. Am. Chem. Soc. 1938, 60, 499.
9. Husa, W.J. "Pharmaceutical Dispensing" 4th Ed. Husa Bros. Iowa City. 1951, p.343.
10. Hiestand, E.N. J. Pharm. Sci. 1964, 53, 1.
11. Bondi, J.V., Schnaare, P.L., Niebergall, P.J. and Sugita, E.T. J. Pharm. Sci. 1973, 62, 1731.
12. Ottewill, R.H. University of Bristol. Personal communication April 1975.
13. Ash, S.G., Everett, D.H. and Radke, C. J.C.S. Faraday II, 1973, 69, 1256.
14. Haines, B.A. and Martin, A.N. J. Pharm. Sci. 1961, 50, 753.
15. Haines, B.A. and Martin, A.N. ibid. 1961, 50, 756.
16. Wilson, R.G. and Ecanow, B. ibid. 1963, 52, 757.
17. Ecanow, B., Grundman, R. and Wilson, R. Amer. J. Hosp. Pharm. 1966, 27, 404.
18. Schenkel, J.H. and Kitchener, J.A. Trans. Faraday Soc. 1960, 56, 161.
19. Srivastava, S.N. and Haydon, D.A. Trans. Faraday Soc. 1964, 60, 971.
20. Sherman, P. J. Colloid Interface Sci. 1968, 27, 282.

21. Wiese, G.R. and Healy, T.W. *Trans. Faraday Soc.* 1970, 66, 490.
22. Tabor, D. and Winterton, R.H.S. *Nature.* 1968, 219, 1120.
23. Tabor, D. and Winterton, R.H.S. *Proc. Roy. Soc.* 1969, A312, 435.
24. Tabor, D. *J. Colloid. Interface Sci.* 1969, 31, 364.
25. Mathews, B.A. and Rhodes, C.T. *J. Pharm. Pharmacol.* 1968, 20, 204S.
26. Mathews, B.A. and Rhodes, C.T. *J. Pharm. Sci.* 1968, 57, 569.
27. Jones, R.D.C., Mathews, B.A. and Rhodes, C.T. *ibid.* 1970, 59, 519.
28. Mathews, B.A. and Rhodes, C.T. *ibid.* 1970, 59, 521.
29. Ottewill, R.H. and Walker, T. *Kolloid. Z.u.Z. Polymere.* 1968, 227, 108.
30. Short, M.P. and Rhodes, C.T. *Canad. J. Pharm. Sci.* 1973, 8, 46.
31. Bondi, J.V., Schnaare, R.L., Niebergall, P.J. and Sugita, E.T. *J. Pharm. Sci.* 1973, 62, 1731.
32. Stanko, G.L. and DeKay, H.G. *J. Amer. Pharm. Sci. Ed.* 1958, 47, 104.
33. Nash, B.A. and Haeger, B.E. *J. Pharm. Sci.* 1966, 55, 829.
34. James, A.M. and Goddard, G.H. *Pharm. Acta. Helv.* 1971, 46, 708.
35. James, A.M. and Goddard, G.H. *ibid.* 1972, 47, 244.
36. Uno, H. and Tanaka, S. *Kolloid. Z.u.Z. Polymere.* 1972, 250, 238.
37. Green, R.N. and Hem, S.L. *J. Pharm. Sci.* 1974, 63, 635.
38. Nakamura, Y., Otsuka, A. and Nakagaki, M. *J. Pharm. Soc. Japan.* 1974, 94, 833.
39. Haydon, D.A. "Recent Progress in Surface Science". Academic Press. 1964, 1, 94.
40. Gouy, G. *J. Phys.* 1910, 2, 457.
41. Chapman, D.L. *Phil. Mag.* 1913, 25, 475.
42. Loeb, A.L., Overbeck, J.Th.G. and Wiersma, P.H. in "The Electrical Double Layer Around a Spherical Particle". 1961, M.I.T. Press.
43. Stern, O. *Z. Electrochem.* 1924, 30, 508.
44. Grahame, D.C. *Chem. Revs.* 1947, 41, 441.
45. Levine, S. and Bell, G.M. *J. Colloid. Sci.* 1962, 17, 838.
Levine, S., Mingins, J. and Bell, G.M. *J. Electroanal. Chem.* 1967, 13, 280.

46. Wiese, G.R., James, R.O. and Healy, T.W. Discuss. Faraday Soc. 1971, 52, 242.
47. Levine, S. and Bell, G.M. *ibid.* 1966, 42, 69.
48. Macdonald, J.K. and Barlow, C.A. First Australian Conference on Electrochemistry (1963). London. Pergamon.
49. Napper, D.H. and Hunter, R.J. in M.T.P. International Review of Science, Physical Chemistry Series One Vol. No. 7. Surface Chemistry & Colloids 1972. "Hydrosols" p.269.
50. Langmuir, I. J. Chem. Phys. 1938, 6, 893.
51. Watillon, A. and Joseph-Petit, A.M. Discuss. Faraday Soc. 1966, 42, 145.
52. Hogg, R., Healy, T.W., Fuerstenau, D.W. Trans. Farad. Soc. 1966, 62, 1638.
53. Honig, E.P. and Mul, P.M. J. Colloid. Interface Sci. 1971, 36, 258.
54. Glasstone, S. "A Textbook of Physical Chemistry". Macmillan 1947.
55. Keesom, H. Proc. Akad. Sci. Amsterdam. 1920, 18, 939.
56. Debye, P. Phys. Z. 1920. 178. 1921. 301.
57. London, F. Z.F. Physik. 1930, 60, 245.
58. Kallmann, H. and Willstatter, M. Naturwiss. 1932, 20, 952.
59. deBoer, J.H. Trans. Farad. Soc. 1936, 32, 10.
60. Hamaker, H.C. Physica. 1937, 4, 1058.
61. Gregory, J. Adv. Colloid. Interface Sci. 1969, 2, 396.
62. Visser, J. *ibid.* 1972, 3, 331.
63. Ottewill, R.H. "Particulate Dispersions" p.177 in "Colloid Science". Vol. 1. Chemical Society, London 1973.
64. Lifshitz, E.M. Zhur. eksp. teor. Fiz. 1955, 29, 94.
65. Parsegian, V.A. and Ninham, B.W. Nature. 1969, 224, 1197.
66. Ninham, B.W. and Parsegian, V.A. J. Chem. Phys. 1970, 52, 4578.
67. Parsegian, V.A. and Ninham, B.W. J. Colloid. Interface Sci. 1971, 37, 332.
68. Parsegian, V.A. and Ninham, B.W. Biophys. J. 1970, 10, 664.
69. Langbein, D. Phys. Rev. (B). 1970, 3371.

70. Langbein, D. J. Chem. and Phys. Solids. 1971, 32, 1657.
71. ~~Niestand, E.N. J. Pharm. Sci. 1964, 53, p.270. Ref.49 p270~~
72. Heller, W. and Pugh, T.L. J. Chem. Phys. 1954, 22, 1778.
73. Freundlich, H. "Colloid and Capillary Chemistry". Methuen, London. 1926, p.589.
74. Barclay, L. and Ottewill, R.H. Special Discuss. Faraday Soc. 1970, No. 1. 169.
75. Krieger, I.M. Advan. Colloid. Interface Sci. 1972, 3, 111.
76. Bagchi, P. J. Colloid. Interface Sci. 1974, 47, 86.
77. Osmond, D.W.J., Vincent, B. and Waite, F.A. J. Colloid. Interface Sci. 1973, 42, 262. and Vincent, B. ibid. 1973, 42, 270.
78. Ottewill, R.H. and Walker, T. Kolloid Z. 1968, 227 108.
79. Ottewill, R.H. and Walker, T. J.C.S. Faraday I. 1974, 70, 917.
80. Glass, J.E., Lundberg, R.D. and Bailey, F.E. J. Colloid. Interface Sci. 1970, 33, 491.
81. Niestand, E.N. J. Pharm. Sci. 1964, 53, p.279.
82. Mackor, E.L. J. Colloid Sci. 1951, 6, 492.
83. Evans, R. and Napper, D.H. Kolloid Zu.Z. Polymere. 1973, 251, 409.
84. Fischer, E.W. Kolloid Z. 1958, 160, 120.
85. Flory, P.J. "Principles of Polymer Chemistry". Ithaca, Cornell University Press. 1953.
86. Ottewill, R.H. "Particulate Dispersions" p. 210 in "Colloid Science". Vol. 1. Chemical Society, London. 1973.
87. Evans, R. and Napper, D.H. Kolloid Z.u.Z. Polymer. 1973, 251, 329.
88. Vold, M.J. J. Colloid Sci. 1961, 16, 1.
89. Napper, D.H. and Netschey, A. J. Colloid Interface Sci. 1971, 37, 528.
90. Mathai, K.G. and Ottewill, R.H. Kolloid ZuZ Polymere. 1970, 236, 147.
91. Lyklema, J. and Overbeek, J.Th.G. J. Colloid Sci. 1961, 16, 501.
92. von Helmholtz, H. Ann. Physik. 1879, 7, 337.
93. von Smoluchowski, M. Bull. Acad. Sci. Cracovie. 1903, p.182.
94. Hückel, E. Phys. Z. 1924, 25, 204.

95. Henry, D.C. Proc. Roy. Soc. 1931, 133A, 106.
96. Overbeek, J.Th.G. Kolloidchem. Beih. 1943, 54, 287.
97. Booth, F. Nature, Lond. 1948, 161, 83; Proc. Roy. Soc. 1950, A203, 514.
98. Wiersema, P.H., Loeb, A.L. and Overbeek, J.Th.G. J. Colloid Interface Sci. 1966, 22, 78.
99. Ottewill, R.H. and Shaw, J.N. J. Electroanal. Chem. 1972, 37, 133.
100. Hunter, R.J. and Alexander, A.E. J. Colloid Sci. 1963, 18, 820.
101. Stigter, D. J. Phys. Chem. 1964, 68, 3600.
102. Hunter, R.J. J. Colloid. Sci. 1966, 22, 231.
103. Overbeek, J.Th.G. and Wiersema, P.H. in "Electrophoresis" (M Bier ed.) Vol. II, Chapter I. Academic Press. New York and London, 1967.
104. Overbeek, J.Th.G. Philips Res. Rept. 1946, 1, 315.
105. Ottewill, R.H. Rastogi, M.C. and Watanabe, A. Trans. Farad. Soc. 1960, 56, 854.
106. Chen, S.F. Ph.D. Thesis, Bristol. 1974.
107. Parsons, R. in "Modern Aspects of Electrochemistry" ed. J.O'M. Bockris and B.E. Conway, Butterworth. London 1954
108. Langmuir, I. J. Amer. Chem. Soc. 1918, 40, 1361.
109. Tanford, C. in "The Hydrophobic Effect" John Wiley and Sons, 1973.
110. Kauzmann, W. in "The Mechanism of Enzyme Action" John Hopkins Baltimore 1954.
111. Hartley, G.S. in "Aqueous Solutions of Paraffin Chain Salts" Hermann and Cie, Paris 1936.
112. Ottewill, R.H. and Watanabe, A. Kolloid. Z. 1960, 170, 152.
113. Fuerstenau, D.W. in "The Chemistry of Biosurfaces" ed. M.L. Hair, Marcel Dekker Inc. New York. 1971, p.152.
114. Guveli, D. University of Aston. Personal communication 1974.
115. Goodwin, J.W., Hearn, J., Ho, C.C. and Ottewill, R.H. Br. Polym. J. 1973, 5, 347.
116. Goodwin, J.W. University of Bristol. Personal communication 1972.
117. Mukerjee, P. and Mysels, K.J. in "Critical Micelle Concentrations of Aqueous Surfactant Systems" National Bureau of Standards. Washington D.C. 1971.

118. Guveli, D., Davis, S.S. and Kayes, J.B. *J. Pharm. Pharmac.* 1974, 26, Suppl. 127P.
119. Elworthy, P.H. and Guthrie, W.G. *J. Pharm. Pharmacol.* 1970, 22, 114S.
120. Ottewill, R.H. and Shaw, J.N. *Kolloid. ZuZ. Polymere.* 1967, 218, 314.
121. Hearn, J. Ottewill, R.H. and Shaw, J.N. *Br. Polym. J.* 1970, 2, 116.
122. Van der Koff, D.M.E. and van den Hul, H.J. *J. Polym. Sci.* 1960, 48, 175.
123. Allen, T. "Particle Size Measurement" Chapman and Hall Ltd. London. 1968, p.127.
124. Allen, T. "Particle Size Measurement" Chapman and Hall Ltd. London. 1968, p. 178.
125. Allen, T. "Particle Size Measurement" Chapman and Hall Ltd. London. 1968, p.82.
126. Shaw, D.J. in "Electrophoresis" Academic Press London and New York 1969.
127. Rank Bros. "Operating Instructions and Manual for the Particle Microelectrophoresis Apparatus Mark II" 1971.
128. Komagata, S. *J. electrochem. Soc. Japan.* 1933, 1, 97.
129. Abramson, H.A., Moyer, L.S. and Gorin, M.H. "Electrophoresis of Proteins and the Chemistry of Cell Surfaces" Reinhold, New York. 1942.
130. van Gils, G.E. and Kruyt, H.T. *Kolloid. Chem. Beith.* 1936, 45, 60.
131. Davies, J.T. and Rideal, E.K. "Interfacial Phenomena" 2nd Ed. Academic Press, London. 1963, p.143.
132. Ottewill, R.H. in "Non Ionic Surfactants" ed by Schick, M.J. 1967, Arnold, London. P.636.
133. Ottewill, R.H. in "Non Ionic Surfactants" ed by Schick, M.J. 1967, Arnold, London. P.629.
134. Mathai, K.G. and Ottewill, R.H. *Trans. Farad. Soc.* 1966, 62, 750-759.
135. Ottewill, R.H. University of Bristol. Personal communication 1975.
136. Watanabe, A., Tsuji, F. and Ueda, S. *Kolloid Z.* 1963, 195, 39.
137. Daluja, K.L. and Srivastava, S.N. *Indian J. Chem.* 1969, 7, 790.
138. Corkill, J.M., Goodman, J.F. and Harrold, S.P. *Trans. Farad. Soc.* 1964, 60, 202.

139. Corkill, J.M., Goodman, J.F. and Tate, J.R. *ibid.* 1964, 60, 996.
140. Glazman, Yu.M. *Disc. Faraday Soc.* 1966, 42, 255.
141. Elworthy, P.H. and Florence, A.T. *J. Pharm. Pharmac.* 1967, 19, 140S.
142. Glazman, Yu.M. and Kabysch, G.M. *Colloid. J. U.S.S.R.* 1969, 31, 27.
143. Schick, M.J. *J. Colloid. Sci.* 1963, 18, 378.
144. Elworthy, P.H. and Florence, A.T. *J. Pharm. Pharmac.* 1969, 21, 705.
145. Connor, P. *Proc. Vth Int. Congr. Surface Active Substances, Barcelona.* 1969, II, 469.
146. Connor, P. and Ottewill, R.H. *J. Colloid. Interface Sci.* 1971, 37, 642.
147. Ottewill, R.H. and Bastogi, M.C. *Trans. Faraday Soc.* 1960, 56, 880.
148. Shaw, J.N. *Ph.D. Thesis, Cambridge University.* Cambridge 1965.
149. Moto, S., Ino, T. and Meguro, K. *J. Amer. Oil. Chem. Soc.* 1972, 49, 437.
150. Tadros, Th.F. *J. Colloid. Inter. Sci.* 1974, 46, 528.
151. Schwuger, M.J. *J. Colloid. Inter. Sci.* 1973, 43, 491.
152. Guveli, D. *University of Aston; Personal communication* 1975.
153. Staudinger, H. and others in "Non-Ionic Surfactants" Ed. by M.J. Schick. *Arnold London* 1967. Chapter 22 "Configuration of the polyoxyethylene chain in bulk".
154. *British Pharmacopoeia.* Her Majesty's Stationery Office, London 1973.
155. *British Pharmaceutical Codex.* Pharmaceutical Press, London 1973.
156. Winningham, D.G., Nemoy, N.J. and Stoney, T.A. *Nature*, 1968, 213, 139.
157. Takamura, K., Kaveniwa, N. and Imagawa, K. *J. Pharm. Soc. Japan.* 1974, 94, 1580.
158. Robinson, C.S. *Ind. Eng. Chem.* 1926, 18, 869.
159. Ward, H.T. and Kammermeyer, K. *ibid.* 1940, 32, 622.
160. Distenfass, L. *Kolloid Z.* 1959, 163, 48.
161. Napier, D.H. *Sci. Progr.* 1967, 55, 91.
162. Florence, A.T. and Rogers, J.A. *J. Pharm. Pharmacol.* 1971, 23, 153.
163. Ho, N.F.H., and Higuchi, W.I. *J. Pharm. Sci.* 1968, 57, 436.
164. Ottewill, R.H. *University of Bristol. Personal communication* 1975.

Table 3 of Reference 99

THEORETICAL VALUES OF MOBILITY ($\mu\text{m cm s}^{-1} \text{V}^{-1}$) AS A FUNCTION OF ζ -POTENTIAL (mV) AND κa FOR A POSITIVELY OR NEGATIVELY CHARGED SPHERE IN THE PRESENCE OF A 1:1 ELECTROLYTE WITH $m_2 = 0.184$ AT 25°C

ζ	$\kappa a = 0.01$	0.02	0.05	0.1	0.2	0.5	1	2	5	10	20	50	100	200	500	1000
10	0.52	0.52	0.52	0.52	0.52	0.52	0.53	0.55	0.60	0.64	0.70	0.74	0.76	0.77	0.78	0.78
20	1.04	1.04	1.04	1.04	1.04	1.04	1.05	1.09	1.17	1.27	1.38	1.48	1.52	1.53	1.55	1.56
30	1.55	1.55	1.55	1.54	1.54	1.52	1.56	1.60	1.73	1.88	2.02	2.21	2.26	2.28	2.32	2.33
40	2.06	2.06	2.06	2.05	2.04	2.01	2.03	2.09	2.24	2.45	2.66	2.91	3.00	3.04	3.09	3.10
50	2.58	2.57	2.57	2.57	2.53	2.48	2.50	2.54	2.71	2.96	3.27	3.59	3.72	3.80	3.86	3.87
60	3.10	3.08	3.06	3.04	3.00	2.93	2.91	2.92	3.13	3.41	3.80	4.23	4.42	4.54	4.61	4.64
70	3.61	3.60	3.56	3.52	3.47	3.34	3.27	3.25	3.44	3.82	4.27	4.83	5.14	5.26	5.36	5.40
80	4.13	4.08	4.06	3.99	3.91	3.72	3.60	3.54	3.70	4.16	4.67	5.36	5.78	5.98	6.12	6.19
90	4.64	4.60	4.55	4.46	4.33	4.06	3.88	3.76	3.90	4.42	5.00	5.84	6.40	6.67	6.87	6.95
100	5.15	5.10	5.05	4.91	4.73	4.39	4.10	3.94	4.06	4.56	5.22	6.27	7.00	7.37	7.62	7.72
110	5.66	5.60	5.54	5.34	5.10	4.66	4.30	4.08	4.16	4.61	5.37	6.61	7.56	8.01	8.37	8.50
120	6.17	6.10	6.00	5.76	5.45	4.90	4.46	4.18	4.20	4.63	5.45	6.86	8.00	8.64	9.12	9.27
130	6.69	6.60	6.46	6.18	5.78	5.09	4.61	4.28	4.21	4.62	5.46	7.00	8.33	9.25	9.36	10.0
140	7.20	7.10	6.90	6.58	6.10	5.26	4.72	4.32	4.18	4.58	5.41	7.08	8.60	9.81	10.6	10.8
150	7.72	7.60	7.35	6.96	6.36	5.41	4.81	4.35	4.13	4.50	5.31	7.09	8.78	10.2	11.3	11.6

Table 4 of Reference 99

THEORETICAL VALUES OF MOBILITY ($\mu\text{m cm s}^{-1} \text{V}^{-1}$) AS A FUNCTION OF ζ -POTENTIAL (mV) AND κa FOR A NEGATIVELY CHARGED SPHERICAL PARTICLE IN SODIUM CHLORIDE SOLUTIONS AT 25°C

ζ	$\kappa a = 0.01$	0.02	0.05	0.1	0.2	0.5	1	2	5	10	20	50	100	200	500	1000
10	0.52	0.52	0.52	0.52	0.52	0.52	0.53	0.55	0.60	0.64	0.70	0.74	0.76	0.77	0.78	0.78
20	1.04	1.04	1.04	1.04	1.04	1.04	1.05	1.09	1.17	1.27	1.38	1.48	1.51	1.53	1.55	1.56
30	1.55	1.55	1.55	1.54	1.54	1.52	1.55	1.60	1.72	1.88	2.02	2.21	2.26	2.28	2.32	2.33
40	2.06	2.06	2.06	2.05	2.04	2.01	2.03	2.09	2.24	2.45	2.66	2.91	3.00	3.04	3.09	3.10
50	2.58	2.58	2.57	2.55	2.53	2.47	2.49	2.51	2.70	2.93	3.26	3.58	3.72	3.80	3.86	3.87
60	3.10	3.08	3.06	3.02	3.00	2.90	2.87	2.88	3.06	3.36	3.77	4.20	4.40	4.54	4.61	4.64
70	3.61	3.60	3.56	3.50	3.45	3.30	3.22	3.20	3.37	3.76	4.22	4.79	5.08	5.26	5.36	5.40
80	4.13	4.08	4.06	3.98	3.88	3.68	3.54	3.49	3.64	4.10	4.62	5.32	5.72	5.98	6.12	6.19
90	4.64	4.60	4.54	4.42	4.28	4.02	3.80	3.68	3.84	4.28	4.90	5.76	6.34	6.66	6.87	6.95
100	5.15	5.10	5.04	4.87	4.67	4.31	4.00	3.84	3.96	4.41	5.10	6.15	6.92	7.35	7.62	7.72
110	5.66	5.60	5.52	5.29	5.04	4.56	4.19	3.96	4.01	4.47	5.22	6.46	7.42	7.98	8.37	8.50
120	6.17	6.10	5.96	5.69	5.38	4.87	4.33	4.05	4.04	4.45	5.24	6.68	7.81	8.60	9.12	9.27
130	6.69	6.60	6.40	6.08	5.69	4.96	4.46	4.11	4.06	4.40	5.22	6.78	8.16	9.20	9.86	10.0
140	7.20	7.10	6.84	6.46	6.00	5.11	4.56	4.15	4.04	4.30	5.16	6.82	8.43	9.75	10.6	10.8
150	7.72	7.60	7.24	6.80	6.24	5.26	4.64	4.18	4.02	4.23	5.08	6.82	8.68	10.2	11.3	11.6

Appendix II.

(Tables I, III to V, VII to XIX, XXI to XXXIV,
XXXVI, XXXVIII & XXXIX).

TABLE I

Mobility and zeta potential of polystyrene latex in 10^{-3} mol dm^{-3} Na Cl and varying pH at 25°C		
pH	Mobility $10^{-8} \text{ m}^2 \text{ S}^{-1} \text{ V}^{-1}$	Zeta potential mV
1.5	0	0
2.0	-0.69 ± 0.03	-9.5
2.6	-4.01 ± 0.14	-61.0
3.4	-4.63 ± 0.23	-73.5
3.8	-5.15 ± 0.25	-86.5
4.5	-5.47 ± 0.30	-98.0
5.0	-5.96 ± 0.21	-130.0
5.6	-5.85 ± 0.21	-117.5
6.4	-5.86 ± 0.31	-117.5
7.1	-5.56 ± 0.25	-101.0
7.5	-5.82 ± 0.19	-115.0
9.1	-5.86 ± 0.20	-117.5
10.1	-6.21 ± 0.19	-
10.9	-6.27 ± 0.12	-

TABLE III

Mobility and zeta potential of polystyrene latex with increasing concentration $C_{16} E_y$ in 10^{-3} mol dm^{-3} Na Cl at 25°C and pH 7.0

Concentration of $C_{16} E_y$ mol dm^{-3}	$C_{16} E_{10}$		$C_{16} E_{18}$		$C_{16} E_{23}$	
	Mobility $10^{-8} m s^{-1} V^{-1}$	Zeta potential mV	Mobility $10^{-8} m s^{-1} V^{-1}$	Zeta potential mV	Mobility $10^{-8} m s^{-1} V^{-1}$	Zeta potential mV
10^{-7}	-5.89 ± 0.26		-5.54 ± 0.28		-6.05 ± 0.34	
10^{-6}	-5.81 ± 0.17		-5.32 ± 0.26		-5.36 ± 0.25	
10^{-5}	-5.71 ± 0.18		-5.32 ± 0.30		-5.16 ± 0.16	
10^{-4}	-5.73 ± 0.13		-5.38 ± 0.31		-5.25 ± 0.24	
10^{-3}	-5.67 ± 0.19		-5.41 ± 0.26		-5.28 ± 0.17	
10^{-2}	-5.62 ± 0.19		-5.27 ± 0.23		-4.97 ± 0.16	

TABLE IV

Mobility and zeta potential of polystyrene latex with increasing concentration $C_x E_y$ in 10^{-3} mol dm^{-3} Na Cl at 25°C and pH 7.0

Concentration of $C_x E_y$ mol dm^{-3}	Mobility $10^{-8} \text{ m s}^{-1} \text{ V}^{-1}$	Zeta potential mV	Mobility $10^{-8} \text{ m s}^{-1} \text{ V}^{-1}$	Zeta potential mV	Mobility $10^{-8} \text{ m s}^{-1} \text{ V}^{-1}$	Zeta potential mV
	C_{16}	E_{30}	C_{16}	E_{45}	C_{16}	E_{60}
10^{-7}	-5.14 ± 0.26		-4.76 ± 0.19		-4.15 ± 0.24	
10^{-6}	-4.94 ± 0.25		-4.61 ± 0.25		-4.12 ± 0.27	
10^{-5}	-5.0 ± 0.28		-4.49 ± 0.29		-4.10 ± 0.15	
10^{-4}	-4.90 ± 0.34		-4.49 ± 0.24		-3.98 ± 0.23	
10^{-3}	-4.88 ± 0.26		-4.40 ± 0.06		-3.89 ± 0.22	
10^{-2}	-4.41 ± 0.31		-3.48 ± 0.17		-3.02 ± 0.19	
	C_{12}	E_{23}				
10^{-7}	-6.07 ± 0.16					
10^{-6}	-5.56 ± 0.18					
10^{-5}	-5.20 ± 0.16					
10^{-4}	-5.29 ± 0.24					
10^{-3}	-5.28 ± 0.20					
10^{-2}	-5.00 ± 0.17					

TABLE Va

Mobility and zeta potential of polystyrene latex with increasing concentration C_x TAB in 10^{-3} mol dm $^{-3}$ Na Cl at 25°C and pH 7.0

Concentration of C_x TAB mol dm $^{-3}$	C_{10} TAB			C_{12} TAB		
	Mobility $10^{-8} \text{ m s}^{-1} \text{ V}^{-1}$	Zeta potential mV	Mobility $10^{-8} \text{ m s}^{-1} \text{ V}^{-1}$	Zeta potential mV	Mobility $10^{-8} \text{ m s}^{-1} \text{ V}^{-1}$	Zeta potential mV
10^{-7}						
10^{-6}						
2.5×10^{-6}	-2.09	-29	-4.51	-71		
10^{-5}	-1.95	-27	-1.22	-12		
2.5×10^{-5}			No movement			
5×10^{-5}			+1.85	+26		
10^{-4}	+0.58	+8	+2.45	+34.5		
2.5×10^{-4}	+1.14	+15.5	+3.17	+44		
5×10^{-4}			+4.21	+65		
10^{-3}	+2.47	+35	+4.8	+77.5		
2.5×10^{-3}	+2.77	+38	+4.99	+82.5		
5×10^{-3}			+4.91	+70		
10^{-2}	+2.66	+35	+5.31	+74.5		
2.5×10^{-2}	+2.32	+30	+5.33	+74.5		
5×10^{-2}	+2.84	+36	+5.31	+71		
10^{-1}	+3.86	+50	+5.19	+68		

TABLE Vb

Mobility and zeta potential of polystyrene latex with increasing concentration C_x TAB in 10⁻³ mol dm⁻³ Na Cl at 25°C and pH 7.0

Concentration of C _x TAB mol dm ⁻³	C ₁₄ TAB			C ₁₆ TAB		
	Mobility 10 ⁻⁸ m s ⁻¹ V ⁻¹	Zeta potential mV	Mobility 10 ⁻⁸ m s ⁻¹ V ⁻¹	Zeta potential mV	Mobility 10 ⁻⁸ m s ⁻¹ V ⁻¹	Zeta potential mV
10 ⁻⁷	-3.91	-59	-4.86	-79		
2.5 x 10 ⁻⁷	-2.54	-36	-4.07	-61		
5.0 x 10 ⁻⁷	Small negative charge?					
10 ⁻⁶	Small positive charge?		+0.76	+10		
2.5 x 10 ⁻⁶	+1.85	+26	+2.01	+28		
10 ⁻⁵	+4.86	+79	+4.09	+62		
2.5 x 10 ⁻⁵	+5.38	+94	+4.55	+72		
10 ⁻⁴	+6.33	-	+5.05	+83.5		
2.5 x 10 ⁻⁴	+5.96	+110	+5.06	+83.5		
10 ⁻³	-	-				
2.5 x 10 ⁻³	+6.42	+99				
5.0 x 10 ⁻³	+7.52	+115				
10 ⁻²	+7.69	+110				

TABLE VII

Mobility and zeta potential of polystyrene latex with increasing concentration C_{10} TAB in 10^{-3} mol dm^{-3} Na Cl and with constant concentration of C_{16} E₃₀ at 25°C and pH 7.0

Concentration of C_{10} TAB mol dm^{-3}	Mobility $10^{-8} \text{ m s}^{-1} \text{ V}^{-1}$	Zeta potential mV	Mobility $10^{-8} \text{ m s}^{-1} \text{ V}^{-1}$	Zeta potential mV	Mobility $10^{-8} \text{ m s}^{-1} \text{ V}^{-1}$	Zeta potential mV
	C_{16} E ₃₀ 10^{-2} mol dm^{-3}		C_{16} E ₃₀ 10^{-3} mol dm^{-3}		C_{16} E ₃₀ 10^{-4} mol dm^{-3}	
10^{-4}	-2.55 ± 0.05	-37	-2.57 ± 0.06	-37	-2.52 ± 0.07	-37
2.5×10^{-4}	-1.86 ± 0.05	-26.5	-1.57 ± 0.04	-22	-1.52 ± 0.04	-21
10^{-3}	-0.48 ± 0.03	-7	Small negative charge?		-0.28 ± 0.01	-4
2.5×10^{-3}	Ca -0.33	-4	Ca +0.42	+6	+0.38 ± 0.02	+5
10^{-2}	Ca +0.33	+4	+0.70 ± 0.02	+9	+0.91 ± 0.03	+12
2.5×10^{-2}	+0.50 ± 0.02	+6.5				
5×10^{-2}	Ca +0.45	+6				
10^{-1}	Ca +0.45	+5.5				
	C_{16} E ₃₀	2×10^{-4}				
10^{-4}	-2.56 ± 0.04	-37				
2.5×10^{-4}	-1.52 ± 0.06	-21				
10^{-3}	Ca +0.25	-3				
2.5×10^{-3}	+0.61 ± 0.01	+8				
10^{-2}	+0.91 ± 0.02	+12				
			Difficulties with heating effects at high ionic strengths			

TABLE VIII

Mobility and zeta potential of polystyrene latex with increasing concentration $C_{10\text{TAB}}$ in 10^{-3} mol dm^{-3} Na Cl and with constant concentration of $C_{16\text{E60}}$ at 25°C and pH 7.0

Concentration of $C_{10\text{TAB}}$ mol dm^{-3}	Mobility $10^{-8} \text{ m s}^{-1} \text{ V}^{-1}$	Zeta potential mV	Mobility $10^{-8} \text{ m s}^{-1} \text{ V}^{-1}$	Zeta potential mV	Mobility $10^{-8} \text{ m s}^{-1} \text{ V}^{-1}$	Zeta potential mV
	$C_{16\text{E60}} 10^{-2}$	mol dm^{-3}	$C_{16\text{E60}} 10^{-3}$	mol dm^{-3}	$C_{16\text{E60}} 10^{-4}$	mol dm^{-3}
10^{-4}	-2.05 ± 0.03	-30	-1.84 ± 0.05	-26	-2.02 ± 0.04	-29
2.5×10^{-4}	-1.30 ± 0.03	-18	-1.45 ± 0.05	-20.5	-1.21 ± 0.03	-17
10^{-3}	-0.62 ± 0.02	-8.5	Ca -0.20	-2.5	No charge	+6.5
2.5×10^{-3}	No charge	+4	$+0.41 \pm 0.01$	+5.5	$+0.49 \pm 0.02$	+8
10^{-2}	Ca +0.33	+2	$+0.58 \pm 0.02$	+8.5	$+0.57 \pm 0.01$	-
2.5×10^{-2}	Ca +0.17		-	-	-	-

TABLE IX

Mobility and zeta potential of polystyrene latex with increasing concentration C_{16}^{TAB} in 10^{-3} mol dm $^{-3}$ NaCl and with constant concentration of C_{16}^E at 25°C and pH 7.0

Concentration of C_{12}^{TAB} mol dm $^{-3}$	Mobility $10^{-8} \frac{cm^2}{Vs}$	Zeta potential mV	Mobility $10^{-8} \frac{cm^2}{Vs}$	Zeta potential mV	Mobility $10^{-8} \frac{cm^2}{Vs}$	Zeta potential mV
	C_{16}^E 10^{-2}	mol dm $^{-3}$	C_{16}^E 10^{-3}	mol dm $^{-3}$	C_{16}^E 10^{-4}	mol dm $^{-3}$
10^{-6}	-4.50 ± 0.13	-71	-	-	-	-
2.5×10^{-6}	-5.25 ± 0.11	-90	-2.76 ± 0.08	-39	-3.04 ± 0.16	-43.5
10^{-5}	-4.70 ± 0.15	-75	-3.34 ± 0.09	-48	-3.22 ± 0.10	-46
2.5×10^{-5}	-3.92 ± 0.09	-59.5	-2.27 ± 0.05	-31.5	-1.94 ± 0.06	-27
10^{-4}	-1.95 ± 0.06	-27.5	Small negative charge?		Small positive charge?	
2.5×10^{-4}	No movement		+1.41 ± 0.08	+19.5	+1.72 ± 0.05	+23.5
5.0×10^{-4}	+0.94 ± 0.03	+13	+2.27 ± 0.06	+31.5	-	-
10^{-3}	+2.13 ± 0.06	+30	+3.11 ± 0.09	+44.5	+3.31 ± 0.12	+47.5
2.5×10^{-3}	+3.24 ± 0.09	+45.5	-	-	-	-
5.0×10^{-3}	+3.58 ± 0.09	+48.5	+3.78 ± 0.11	+51	+4.12 ± 0.08	+56.5
10^{-2}	+3.90 ± 0.10	+52	+4.07 ± 0.10	+54	+4.33 ± 0.13	+58
2.5×10^{-2}	+4.06 ± 0.14	+53	-	-	-	-
5.0×10^{-2}	+4.57 ± 0.24	+59	+6.04 ± 0.20	+81	+6.41 ± 0.13	+86

TABLE X

Mobility and zeta potential of polystyrene latex with increasing concentration $C_{12}TAB$ in 10^{-3} mol dm^{-3} Na Cl and with constant concentration of $C_{16}E_{30}$ at 25°C and pH 7.0

Concentration of $C_{12}TAB$ mol dm^{-3}	Mobility $10^{-8} \frac{cm^2}{Vs}$	Zeta potential mV	Mobility $10^{-8} \frac{cm^2}{Vs}$	Zeta potential mV	Mobility $10^{-8} \frac{cm^2}{Vs}$	Zeta potential mV
	$C_{16}E_{30} 10^{-5}$	mol dm^{-3}	$C_{16}E_{30} 5 \times 10^{-5}$	mol dm^{-3}	2×10^{-3}	mol dm^{-3}
10^{-5}	-2.47 ± 0.07	-34.5	-25.4 ± 0.08	-36	-	-
2.5×10^{-5}	-1.77 ± 0.04	-24.5	-1.73 ± 0.04	-24	-2.69 ± 0.08	-48
10^{-4}	No movement		Small negative charge?		-1.06 ± 0.07	-14.5
2.5×10^{-4}	$+1.21 \pm 0.04$	+17	$+1.08 \pm 0.04$	+15	Ca $+0.38$	Ca +5.0
5.0×10^{-4}	$+1.97 \pm 0.04$	+28	$+1.85 \pm 0.04$	+26	$+0.92 \pm 0.03$	+13
10^{-3}	$+2.50 \pm 0.07$	+35	$+2.35 \pm 0.07$	+33.5	-	-
	$C_{16}E_{30} 7 \times 10^{-3}$	mol dm^{-3}				
10^{-4}	-1.65	-23				
2.5×10^{-4}	-0.67	-9				
5.0×10^{-4}	No movement					
10^{-3}	+0.83	+11.5				

TABLE XI

Mobility and zeta potential of polystyrene latex with increasing concentration C_{12} TAB in 10^{-3} mol dm $^{-3}$ Na Cl and with constant concentration of C_{16} E₆₀ at 25°C and pH 7.0

Concentration of C_{12} TAB mol dm $^{-3}$	Mobility $10^{-8} \text{ m s}^{-1} \text{ V}^{-1}$	Zeta potential mV	Mobility $10^{-8} \text{ m s}^{-1} \text{ V}^{-1}$	Zeta potential mV	Mobility $10^{-8} \text{ m s}^{-1} \text{ V}^{-1}$	Zeta potential mV
	$C_{16} \text{ E}_{30} 10^{-2}$	mol dm $^{-3}$	$C_{16} \text{ E}_{30} 10^{-3}$	mol dm $^{-3}$	$C_{16} \text{ E}_{30} 10^{-4}$	mol dm $^{-3}$
10^{-6}	-4.11 ± 0.11	-63	-2.94 ± 0.08	-41.5	-2.89 ± 0.09	-41
2.5×10^{-6}	-	-	-3.57 ± 0.10	-53	-3.76 ± 0.13	-56.5
10^{-5}	-3.77 ± 0.08	-57.5	-3.39 ± 0.09	-50.5	-2.89 ± 0.11	-41
2.5×10^{-5}	-3.25 ± 0.07	-46	-2.43 ± 0.07	-34	-1.93 ± 0.04	-27
10^{-4}	-2.00 ± 0.04	-28	-0.59 ± 0.04	-8.5	Small negative charge?	
2.5×10^{-4}	-0.95 ± 0.04	-13	+0.66 ± 0.03	+9	+1.07 ± 0.03	+15
5.0×10^{-4}	No movement		+1.47 ± 0.04	+20.5	+1.84 ± 0.04	+26
10^{-3}	+0.68 ± 0.01	+8.5	+2.05 ± 0.05	+28.5	+2.32 ± 0.08	+32.5
2.5×10^{-3}	+1.58 ± 0.04	+22	+2.37 ± 0.08	+33.5	+2.58 ± 0.08	+36
5.0×10^{-3}	+1.77 ± 0.03	+26	+2.31 ± 0.06	+32.5	+2.52 ± 0.08	+35.5
10^{-2}	+1.67 ± 0.05	+23.5	+2.12 ± 0.06	+30	+2.25 ± 0.06	+30
2.5×10^{-2}	+1.60 ± 0.05	+22.5	+3.13 ± 0.14	+41	+5.45 ± 0.16	+72
5.0×10^{-2}	+1.62 ± 0.04	+22.5	+4.44 ± 0.11	+58	+5.73 ± 0.15	+77

TABLE XII

Mobility and zeta potential of polystyrene latex with increasing concentration C_{12TAB} in 10^{-3} mol dm $^{-3}$ Na Cl and with constant concentration of C_{16E60} at 25°C and pH 7.0

Concentration of C_{12TAB} mol dm $^{-3}$	Mobility $10^{-8} \text{ m s}^{-1} \text{ V}^{-1}$	Zeta potential mV	Mobility $10^{-8} \text{ m s}^{-1} \text{ V}^{-1}$	Zeta potential mV	Mobility $10^{-8} \text{ m s}^{-1} \text{ V}^{-1}$	Zeta potential mV
	$C_{16E60} 10^{-2}$	mol dm $^{-3}$	$C_{16E60} 10^{-3}$	mol dm $^{-3}$	$C_{16E60} 10^{-4}$	mol dm $^{-3}$
10^{-7}	-2.16 ± 0.06	-30	-2.84 ± 0.07	-40	-2.95 ± 0.06	-41.5
10^{-6}	-2.11 ± 0.07	-29.5	-2.86 ± 0.10	-40	-2.93 ± 0.08	-41
10^{-5}	-2.07 ± 0.08	-27.5	-2.42 ± 0.08	-34	-2.05 ± 0.06	-27.5
5×10^{-5}	-1.67 ± 0.05	-23.5	-1.10 ± 0.03	-15.5	Ca -0.61	-8.5
10^{-4}	-1.35 ± 0.06	-19	Ca -0.37	Ca -5.0	Small positive charge	
10^{-4}	Small negative potential?	Small negative potential?	+1.03 ± 0.01	+14.5	+1.29 ± 0.06	+18
10^{-3}	Small negative potential?	Small negative potential?	+1.53 ± 0.03	+21.5	+1.69 ± 0.04	+23.5
10^{-2}	+0.88 ± 0.02	+12	+1.09 ± 0.04	+15	+1.20 ± 0.06	+17
2.5×10^{-2}	+0.70 ± 0.02	+10	+1.59 ± 0.04	+22.5	+4.5 ± 0.18	+59
5×10^{-2}	+0.63 ± 0.02	+8	+2.80 ± 0.05	+39	+5.21 ± 0.13	+69

TABLE XIII

Mobility and zeta potential of polystyrene latex with increasing concentration C_{14}^{TAB} in 10^{-3} mol dm^{-3} Na Cl and with constant concentration of $C_{16} E_{30}$ at 25°C and pH 7.0

Concentration of C_{14}^{TAB} mol dm^{-3}	Mobility $10^{-8} \text{ m}^2 \text{ s}^{-1} \text{ V}^{-1}$	Zeta potential mV	Mobility $10^{-8} \text{ m}^2 \text{ s}^{-1} \text{ V}^{-1}$	Zeta potential mV	Mobility $10^{-8} \text{ m}^2 \text{ s}^{-1} \text{ V}^{-1}$	Zeta potential mV
	$C_{16} E_{30} 10^{-2}$	mol dm^{-3}	$C_{16} E_{30} 10^{-3}$	mol dm^{-3}	$C_{16} E_{30} 10^{-4}$	mol dm^{-3}
2.5×10^{-7}	-4.41 ± 0.11	-69				
10^{-6}	-4.34 ± 0.14	-67.5				
2.5×10^{-6}	-4.29 ± 0.14	-66.5	-2.80 ± 0.08	-40	-1.55 ± 0.05	-21.5
10^{-5}	-3.68 ± 0.10	-55.5	-1.59 ± 0.06	-22	Small negative charge?	
2.5×10^{-5}	-3.17 ± 0.12	-46.5	Small negative charge?		$+0.44 \pm 0.05$	+6
10^{-4}	-1.94 ± 0.06	-27.0	$+1.54 \pm 0.06$	+21	$+1.70 \pm 0.66$	+23.5
2.5×10^{-4}	-0.74 ± 0.02	-10	$+2.70 \pm 0.10$	+38		
10^{-3}	$+1.09 \pm 0.04$	+15				
2.5×10^{-3}	$+2.09 \pm 0.08$	+29				
5.0×10^{-3}	$+2.23 \pm 0.09$	+31				
10^{-2}	$+2.31 \pm 0.07$	+32				
	$C_{16} E_{30} 2 \times 10^{-4}$	mol dm^{-3}	$C_{16} E_{30} 2 \times 10^{-3}$	mol dm^{-3}		
2.5×10^{-6}	-1.80 ± 0.06	-25.6				
10^{-5}	Ca - 0.25	- 3.5	-2.71 ± 0.10	-39.6		
2.5×10^{-5}	Small positive charge		-1.76 ± 0.66	-25		
10^{-4}	$+1.50 \pm 0.06$	+21	No charge			
2.5×10^{-4}	-	-	$+1.16 \pm 0.11$	+16		
10^{-3}	-	-	$+2.73 \pm 0.09$	+40		

TABLE XIV

Mobility and zeta potential of polystyrene latex with increasing concentration C_{14}^{TAB} in 10^{-3} mol dm $^{-3}$ NaCl and with constant concentration of C_{16}^{E60} at 25°C and pH 7.0

Concentration of C_{14}^{TAB} mol dm $^{-3}$	Mobility $10^{-8} \frac{m^2}{m s} V^{-1}$	Zeta potential mV	Mobility $10^{-8} \frac{m^2}{m s} V^{-1}$	Zeta potential mV	Mobility $10^{-8} \frac{m^2}{m s} V^{-1}$	Zeta potential mV
	$C_{16}^{E60} 10^{-2}$	mol dm $^{-3}$	$C_{16}^{E60} 10^{-3}$	mol dm $^{-3}$	$C_{16}^{E60} 10^{-4}$	mol dm $^{-3}$
10^{-6}	-3.21 ± 0.06	-46	-3.62 ± 0.08	-52.5	-2.25 ± 0.09	-31.5
2.5×10^{-6}	-3.13 ± 0.07	-45	-3.27 ± 0.08	-46.5	-2.03 ± 0.06	-28
10^{-5}	-2.80 ± 0.08	-40	-2.19 ± 0.05	-30.5	Ca -0.30	Ca -04
2.5×10^{-5}	-2.37 ± 0.05	-33	-1.04 ± 0.04	-14	$+0.89 \pm 0.04$	+12
10^{-4}	-1.47 ± 0.04	-20	$+0.91 \pm 0.04$	+12.5	$+2.34 \pm 0.07$	+32.5
2.5×10^{-4}	-0.65 ± 0.02	-9	$+2.28 \pm 0.09$	+32	$+3.13 \pm 0.06$	+45
10^{-3}	$+0.66 \pm 0.02$	+9	$+3.16 \pm 0.05$	+45	$+3.39 \pm 0.06$	+49
2.5×10^{-3}	$+1.43 \pm 0.05$	+19	$+3.07 \pm 0.08$	+42	$+3.19 \pm 0.08$	+44.5
5.0×10^{-3}	$+1.51 \pm 0.06$	+20	$+3.02 \pm 0.06$	+41	$+4.77 \pm 0.13$	+66
10^{-2}	$+1.49 \pm 0.05$	+19	$+3.17 \pm 0.07$	+41	$+6.52 \pm 0.14$	+88
	$C_{16}^{E60} 2 \times 10^{-3}$ mol dm $^{-3}$		$C_{16}^{E60} 2 \times 10^{-4}$ mol dm $^{-3}$			
2.5×10^{-6}	-	-	-2.10 ± 0.07	-29		
10^{-5}	-2.54 ± 0.06	-36	-0.78 ± 0.02	-11		
2.5×10^{-5}	-1.97 ± 0.05	-27.5	Ca -0.44	+6		
10^{-4}	Ca -0.30	Ca - 4	$+2.30 \pm 0.05$	+32		
2.5×10^{-4}	$+1.27 \pm 0.03$	+17.5	-	-		

TABLE XV

Mobility and zeta potential of polystyrene latex with increasing concentration C_{16}^{TAB} in 10^{-3} mol dm^{-3} Na Cl and with constant concentration of $C_{16} E_{30}$ at $25^{\circ}C$ and pH 7.0

Concentration of C_{16}^{TAB} mol dm^{-3}	Mobility $10^{-8} m^2 s^{-1} V^{-1}$	Zeta potential mV	Mobility $10^{-8} m^2 s^{-1} V^{-1}$	Zeta potential mV	Mobility $10^{-8} m^2 s^{-1} V^{-1}$	Zeta potential mV
	$C_{16} E_{30} 10^{-2}$	mol dm^{-3}	$C_{16} E_{30} 10^{-3}$	mol dm^{-3}	$C_{16} E_{30} 2 \times 10^{-3}$	mol dm^{-3}
2.5×10^{-7}	-4.07 ± 0.14	-64	-	-	-	-
10^{-6}	-	-	-3.11 ± 0.09	-46	-	-
2.5×10^{-6}	-3.87 ± 0.10	-58.5	-2.94 ± 0.07	-43	-	-
10^{-5}	-	-	-1.86 ± 0.05	-26.5	-2.35 ± 0.06	-34
2.5×10^{-5}	-2.85 ± 0.08	-42	-0.72 ± 0.02	-10	-1.48 ± 0.04	-21
10^{-4}	-1.76 ± 0.05	-25	$+1.40 \pm 0.04$	+20	No charge	+19
2.5×10^{-4}	-0.58 ± 0.02	-8	$+3.10 \pm 0.09$	+46	$+1.37 \pm 0.04$	+54
10^{-3}	$+0.86 \pm 0.03$	+12	$+4.21 \pm 0.06$	+65		
10^{-2}	$+2.38 \pm 0.05$	+32	-			
	$C_{16} E_{30} 10^{-4}$	mol dm^{-3}	$C_{16} E_{30} 2 \times 10^{-4}$	mol dm^{-3}		
2.5×10^{-7}	-1.81 ± 0.07	-26	-3.12 ± 0.05	-46		
10^{-6}	-1.38 ± 0.04	-20	-2.28 ± 0.07	-30		
2.5×10^{-6}	No charge		-1.48 ± 0.05	-21		
10^{-5}	$+1.25 \pm 0.04$	+18	$+0.43 \pm 0.03$	+6		
2.5×10^{-5}	$+2.39 \pm 0.05$	+35	$+1.69 \pm 0.05$	+24		
10^{-4}	-	-	$+3.93 \pm 0.09$	+59		

TABLE XVI

Mobility and zeta potential of polystyrene latex with increasing concentration $C_{16} \text{TAB}$ in 10^{-3} mol dm^{-3} Na Cl and with constant concentration of $C_{16} \text{E}_{60}$ at 25°C and pH 7.0

Concentration of $C_{16} \text{TAB}$ mol dm^{-3}	Mobility $10^{-8} \text{ m s}^{-1} \text{ V}^{-1}$	Zeta potential mV	Mobility $10^{-8} \text{ m s}^{-1} \text{ V}^{-1}$	Zeta potential mV	Mobility $10^{-8} \text{ m s}^{-1} \text{ V}^{-1}$	Zeta potential mV
	$C_{16} \text{E}_{60} 10^{-2}$	mol dm^{-3}	$C_{16} \text{E}_{60} 10^{-3}$	mol dm^{-3}	$C_{16} \text{E}_{60} 10^{-4}$	mol dm^{-3}
2.5×10^{-7}	-2.40 ± 0.07	-33.5	-	-	-1.80 ± 0.05	-2.5
10^{-6}	-2.44 ± 0.08	-34.5	-2.82 ± 0.09	-40	-	-
2.5×10^{-6}	-	-	-	-	-0.83 ± 0.05	-11.5
10^{-5}	-2.27 ± 0.07	-31.5	-1.73 ± 0.06	-23.5	$+0.46 \pm 0.04$	+16.5
2.5×10^{-5}	-2.02 ± 0.03	-28	-1.35 ± 0.05	-18.5	$+1.69 \pm 0.07$	+23.5
10^{-4}	-1.29 ± 0.05	-18	$+0.74 \pm 0.03$	+10	$+2.85 \pm 0.11$	+40.5
2.5×10^{-4}	Small negative charge?		$+2.19 \pm 0.08$	+30.5	-	-
10^{-3}	+0.345	+4.5	$+3.18 \pm 0.11$	+45.5	-	-

Variation of RCC with concentration of non ionic surfactant C₁₆E₄ with C₁₆E₆

a) C ₁₀ TAB	R. C. C. mol dm ⁻³ with concentrations of non ionic:-						Slope of log ₁₀ RCC versus log ₁₀ conc. non ionic
	10 ⁻²	7 x 10 ⁻³	2 x 10 ⁻³	10 ⁻³	2 x 10 ⁻⁴	10 ⁻⁴	
Non ionic							
C ₁₆ E ₃₀	3 x 10 ⁻³			1.2 x 10 ⁻³		10 ⁻³	2.74
C ₁₆ E ₆₀	3 x 10 ⁻³			1.4 x 10 ⁻³		10 ⁻³	3.27
b) C ₁₂ TAB							
C ₁₆ E ₁₀	2.9 x 10 ⁻⁴			1.1 x 10 ⁻⁴		8 x 10 ⁻⁵	1.94
C ₁₆ E ₃₀	7 x 10 ⁻⁴	4.3 x 10 ⁻⁴	2 x 10 ⁻⁴	1.55 x 10 ⁻⁴		1.1 x 10 ⁻⁴	2.41
C ₁₆ E ₆₀	6.5 x 10 ⁻⁴			1.6 x 10 ⁻⁴		9.5 x 10 ⁻⁵	2.41
c) C ₁₄ TAB							
C ₁₆ E ₃₀	4.2 x 10 ⁻⁴		10 ⁻⁴	4 x 10 ⁻⁵	2.2 x 10 ⁻⁵	1.6 x 10 ⁻⁵	1.37
C ₁₆ E ₆₀	4.5 x 10 ⁻⁴		1.05 x 10 ⁻⁴	6 x 10 ⁻⁵	2 x 10 ⁻⁵	1.45 x 10 ⁻⁵	1.22
d) C ₁₆ TAB							
C ₁₆ E ₃₀	4.5 x 10 ⁻⁴		8.2 x 10 ⁻⁵	4 x 10 ⁻⁵	8 x 10 ⁻⁶	4.0 x 10 ⁻⁶	0.85
C ₁₆ E ₆₀	5 x 10 ⁻⁴			6 x 10 ⁻⁵		6 x 10 ⁻⁶	1.07

TABLE XVIII

Mobility and zeta potential of polystyrene latex with increasing concentration $C_{12}TAB$ in 10^{-3} mol dm^{-3} Na Cl and with constant concentration of $C_{16}E_y$ at $25^\circ C$ and pH 7.0

Concentration of C_{12} TAB mol dm^{-3}	Mobility $10^{-8} \frac{cm^2}{Vs}$		Zeta potential mV		Mobility $10^{-8} \frac{cm^2}{Vs}$		Zeta potential mV	
	E_{10}	E_{18}	E_{10}	E_{18}	E_{30}	E_{30}	E_{10}	E_{18}
	10^{-3}		$mol \ dm^{-3}$		10^{-3}		$mol \ dm^{-3}$	
10^{-6}	-4.24 ± 0.13	-3.83 ± 0.08	-65.5	-3.83 ± 0.08	-4.03 ± 0.09	-3.83 ± 0.08	-58	-4.03 ± 0.09
10^{-5}	-3.62 ± 0.09	-2.99 ± 0.09	-54	-2.99 ± 0.09	-2.93 ± 0.10	-2.99 ± 0.09	-44	-2.93 ± 0.10
2.5×10^{-5}	-2.30 ± 0.06	-2.12 ± 0.07	-33.5	-2.12 ± 0.07	-2.06 ± 0.06	-2.12 ± 0.07	-30.5	-2.06 ± 0.06
10^{-4}	Ca -0.25	-0.43 ± 0.01	-3	-0.43 ± 0.01	-0.52 ± 0.03	-0.43 ± 0.01	-6	-0.52 ± 0.03
2.5×10^{-4}	$+1.20 \pm 0.04$	$+0.73 \pm 0.03$	$+16.5$	$+0.73 \pm 0.03$	$+0.53 \pm 0.02$	$+0.73 \pm 0.03$	$+10.2$	$+0.53 \pm 0.02$
10^{-3}	$+2.85 \pm 0.09$	$+2.07 \pm 0.05$	$+41.5$	$+2.07 \pm 0.05$	$+1.57 \pm 0.05$	$+2.07 \pm 0.05$	$+30$	$+1.57 \pm 0.05$
2.5×10^{-3}	-	-	-	-	-	-	-	-
10^{-2}	$+3.84 \pm 0.08$	$+2.75 \pm 0.07$	$+51.5$	$+2.75 \pm 0.07$	$+1.92 \pm 0.04$	$+2.75 \pm 0.07$	$+36.5$	$+1.92 \pm 0.04$
$C_{16}E_{45}$	10^{-3}		$mol \ dm^{-3}$		10^{-3}		$mol \ dm^{-3}$	
	$mol \ dm^{-3}$		$C_{16}E_{60}$		$mol \ dm^{-3}$			
10^{-6}	-3.72 ± 0.08	-3.35 ± 0.12	-56	-3.35 ± 0.12		-3.35 ± 0.12	-50	
10^{-5}	-2.83 ± 0.09	-2.57 ± 0.07	-42	-2.57 ± 0.07		-2.57 ± 0.07	-38	
2.5×10^{-5}	-2.38 ± 0.08	-2.42 ± 0.06	-35	-2.42 ± 0.06		-2.42 ± 0.06	-35	
10^{-4}	-0.65 ± 0.01	-0.49 ± 0.02	-9	-0.49 ± 0.02		-0.49 ± 0.02	-7	
2.5×10^{-4}	No apparent movement	No apparent movement	No apparent movement	No apparent movement		No apparent movement	No apparent movement	
10^{-3}	$+1.38 \pm 0.05$	$+1.38 \pm 0.05$	$+19.5$	$+1.38 \pm 0.05$		$+1.38 \pm 0.05$	$+10$	
2.5×10^{-3}	$+1.88 \pm 0.06$	$+1.88 \pm 0.06$	$+25$	$+1.88 \pm 0.06$		$+1.88 \pm 0.06$	$+10$	
10^{-2}	$+1.53 \pm 0.04$	$+1.53 \pm 0.04$	$+20$	$+1.53 \pm 0.04$		$+1.53 \pm 0.04$	$+12$	

TABLE XIX

Mobility and zeta potential of polystyrene latex with increasing concentration anionic in 10^{-3} mol dm^{-3} Na Cl at 25°C and pH 7.0

Concentration of Anionic mol dm^{-3}	S De S			SDS			STS		
	Mobility $10^{-8} \text{ m}^2 \text{ s}^{-1} \text{ V}^{-1}$	Zeta potential mV	Mobility $10^{-8} \text{ m}^2 \text{ s}^{-1} \text{ V}^{-1}$	Zeta potential mV	Mobility $10^{-8} \text{ m}^2 \text{ s}^{-1} \text{ V}^{-1}$	Zeta potential mV	Mobility $10^{-8} \text{ m}^2 \text{ s}^{-1} \text{ V}^{-1}$	Zeta potential mV	
10^{-6}									
10^{-5}									
2.5×10^{-5}									
8.3×10^{-5}	-5.42 ± 0.17	-95							-108
10^{-4}									
2.5×10^{-4}									
8.3×10^{-4}	-6.10 ± 0.11	-96			-4.62 ± 0.37	-66	-5.93 ± 0.15	-82.5	-130
10^{-3}									
2.075×10^{-3}	-6.33 ± 0.13	-97.5			-4.84 ± 0.22	-74	-6.62 ± 0.15	-84	-134
2.5×10^{-3}									
5.0×10^{-3}					-5.11 ± 0.33	-77	-6.64 ± 0.11	-95	
8.0×10^{-3}					-6.36 ± 0.34	-85		-97	
10^{-2}					-1.71 ± 0.39	-102		-118.5	
2.075×10^{-2}	-6.52 ± 0.17	-101							
5×10^{-2}					-7.87 ± 0.39	-100		-110	
8.3×10^{-2}	-6.68 ± 0.10	-101							
10^{-1}					-8.01 ± 0.31	-102.5		-11.5	
	-7.29 ± 0.15	-97			-7.72 ± 0.37	-97.5		-109.5	

TABLE XXI

Mobility and zeta potential of polystyrene latex with increasing concentration of SDeS in 10^{-3} mol dm $^{-3}$ NaCl and with constant concentration of C_{16} E $_{60}$ at 25°C and pH 7.0

Concentration of S De S mol dm $^{-3}$	Mobility $10^{-8} \text{ m s}^{-1} \text{ V}^{-1}$	Zeta potential mV	Mobility $10^{-8} \text{ m s}^{-1} \text{ V}^{-1}$	Zeta potential mV	Mobility $10^{-8} \text{ m s}^{-1} \text{ V}^{-1}$	Zeta potential mV
	C_{16} E $_{60}$ 10^{-2}	mol dm $^{-3}$	C_{16} E $_{60}$ 10^{-3}	mol dm $^{-3}$	C_{16} E $_{60}$ 10^{-3}	mol dm $^{-3}$
8.3×10^{-5}	-3.03	-44.5	-4.05	-62	-4.05	-62
8.3×10^{-4}	-2.69	-39	-3.55	-53	-3.55	-53
2.075×10^{-3}	-2.45	-33	-3.12	-42.5	-3.12	-42.5
8.3×10^{-3}	-1.73	-22.5	-2.07	-27	-2.07	-27
2.075×10^{-2}	-1.26	-16.5	-1.74	-23	-1.74	-23
8.3×10^{-2}	-1.29	-16.5	-6.68	-89	-6.68	-89

TABLE XXII

Mobility and zeta potential of polystyrene latex with increasing concentration of SDS in 10^{-3} mol dm $^{-3}$ NaCl and with constant concentration of $C_{16}E_{10}$ at 25°C and pH 7.0

Concentration of SDS mol dm $^{-3}$	Mobility $10^{-8} \frac{cm^2}{Vs}$	Zeta potential mV	Mobility $10^{-8} \frac{cm^2}{Vs}$	Zeta potential mV	Mobility $10^{-8} \frac{cm^2}{Vs}$	Zeta potential mV	Mobility $10^{-8} \frac{cm^2}{Vs}$	Zeta potential mV
	$C_{16}E_{10} 10^{-2}$	mol dm $^{-3}$	$C_{16}E_{10} 10^{-3}$	mol dm $^{-3}$	$C_{16}E_{10} 10^{-4}$	mol dm $^{-3}$	$C_{16}E_{10} 10^{-4}$	mol dm $^{-3}$
10^{-4}	-4.42 ± 0.18	-69	-4.85 ± 0.10	-74	-	-	-	-
10^{-3}	-4.86 ± 0.12	-76	-	-	-	-	-	-
2.5×10^{-3}	-5.44 ± 0.12	-77.5	-5.82 ± 0.10	-85	-5.77 ± 0.12	-86	-5.77 ± 0.12	-86
5×10^{-3}	-5.31 ± 0.16	-77	-6.45 ± 0.16	-91	-6.50 ± 0.11	-92.5	-6.50 ± 0.11	-92.5
8×10^{-3}	-5.84 ± 0.18	-80	-7.28 ± 0.23	-99	-7.65 ± 0.16	-109	-7.65 ± 0.16	-109
10^{-2}	-5.93 ± 0.21	-81.5	-7.68 ± 0.11	-108	-7.74 ± 0.31	-111	-7.74 ± 0.31	-111
2.5×10^{-2}	-6.54 ± 0.18	-90	-8.02 ± 0.17	-107.5	-7.99 ± 0.22	-110	-7.99 ± 0.22	-110
5×10^{-2}	-7.45 ± 0.23	-100	-7.95 ± 0.21	-105	-	-	-	-
10^{-1}	-7.30 ± 0.26	-97.5	-7.70 ± 0.18	-100	-7.81 ± 0.23	-101	-7.81 ± 0.23	-101

TABLE XXIII

Mobility and zeta potential of polystyrene latex with increasing concentration of SDS in 10^{-3} mol dm $^{-3}$ Na Cl and with constant concentration of $C_{16}E_{30}$ at 25°C and pH 7.0

Concentration of SDS mol dm $^{-3}$	Mobility $10^{-8} \text{ m}^2 \text{ V}^{-1} \text{ s}^{-1}$	Zeta potential mV	Mobility $10^{-8} \text{ m}^2 \text{ V}^{-1} \text{ s}^{-1}$	Zeta potential mV	Mobility $10^{-8} \text{ m}^2 \text{ V}^{-1} \text{ s}^{-1}$	Zeta potential mV
	$C_{16}E_{30} 10^{-2}$	mol dm $^{-3}$	$C_{16}E_{30} 10^{-3}$	mol dm $^{-3}$	$C_{16}E_{30} 10^{-4}$	mol dm $^{-3}$
10^{-4}	-3.46 ± 0.07	-51.5	-3.56 ± 0.07	-53	-3.92 ± 0.12	-59.5
10^{-3}	-3.34 ± 0.10	-49	-3.53 ± 0.12	-52.5	-3.82 ± 0.12	-57.5
2.5×10^{-3}	-3.22 ± 0.05	-42	-3.47 ± 0.09	-47.2	-3.98 ± 0.10	-55.5
5.0×10^{-3}	-3.02 ± 0.06	-40	-3.53 ± 0.07	-47.6	-4.90 ± 0.11	-67.5
8.0×10^{-3}	-2.89 ± 0.06	-38.4	-4.02 ± 0.09	-53.5	-6.88 ± 0.12	-97
10^{-2}	-2.85 ± 0.07	-37.6	-4.62 ± 0.09	-62	-7.47 ± 0.11	-106.5
2.5×10^{-2}	-2.86 ± 0.06	-37.6	-6.11 ± 0.12	-82	-7.81 ± 0.15	-107
5.0×10^{-2}	-3.36 ± 0.08	-44	-5.92 ± 0.13	-81	-7.90 ± 0.38	-107
10^{-1}	-4.65 ± 0.01	-60	-5.62 ± 0.12	-73.5	-7.67 ± 0.19	-102

TABLE XXIV

Mobility and zeta potential of polystyrene latex with increasing concentration of SDS in 10^{-3} mol dm $^{-3}$ Na Cl and with constant concentration of $C_{16}E_{60}$ at 25°C and pH 7.0

Concentration of SDS mol dm $^{-3}$	Mobility $10^{-8} \text{ m}^2 \text{ s}^{-1} \text{ V}^{-1}$	Zeta potential mV	Mobility $10^{-8} \text{ m}^2 \text{ s}^{-1} \text{ V}^{-1}$	Zeta potential mV	Mobility $10^{-8} \text{ m}^2 \text{ s}^{-1} \text{ V}^{-1}$	Zeta potential mV
	$C_{16}E_{60} 10^{-2}$	mol dm $^{-3}$	$C_{16}E_{60} 10^{-3}$	mol. dm $^{-3}$	$C_{16}E_{60} 10^{-4}$	mol dm $^{-3}$
10^{-4}	-1.98 ± 0.09	-28.6	-2.41 ± 0.12	-35	-3.41 ± 0.10	-51
10^{-3}	-1.64 ± 0.05	-23	-2.46 ± 0.12	-36	-3.38 ± 0.08	-50
2.5×10^{-3}	-1.54 ± 0.06	-20.4	-2.24 ± 0.20	-30	-3.12 ± 0.10	-41.4
5.0×10^{-3}	-1.53 ± 0.05	-20	-2.04 ± 0.14	-27	-4.16 ± 0.09	-57
8.0×10^{-3}	-1.36 ± 0.05	-18	-2.34 ± 0.11	-31	-6.60 ± 0.12	-92
10^{-2}	-1.26 ± 0.07	-16.6	-2.70 ± 0.11	-35.8	-7.30 ± 0.18	-103.5
2.5×10^{-2}	-0.72 ± 0.04	-9.4	-5.40 ± 0.27	-71.5	-7.23 ± 0.21	-98
5.0×10^{-2}	-0.84 ± 0.04	-11	-5.93 ± 0.30	-79	-7.19 ± 0.15	-97
10^{-1}	-1.19 ± 0.03	-15.6	-5.59 ± 0.25	-73.5	-6.83 ± 0.15	-90

TABLE XXV

Mobility and zeta potential of polystyrene latex with increasing concentration of STS in 10^{-3} mol dm $^{-3}$ Na Cl and with constant concentration of $C_{16}E_9$ at 25°C and pH 7.0

Concentration of STS mol dm $^{-3}$	Mobility $10^{-8} \text{ m s}^{-1} \text{ V}^{-1}$	Zeta potential mV	Mobility $10^{-8} \text{ m s}^{-1} \text{ V}^{-1}$	Zeta potential mV	Mobility $10^{-8} \text{ m s}^{-1} \text{ V}^{-1}$	Zeta potential mV
	$C_{16}E_9 \cdot 10^{-2}$	mol dm $^{-3}$	$C_{16}E_9 \cdot 10^{-3}$	mol dm $^{-3}$	$C_{16}E_9 \cdot 10^{-4}$	mol dm $^{-3}$
10^{-4}	-2.97 ± 0.08	-44	-3.80 ± 0.08	-57.5	-4.06 ± 0.07	-62
2.5×10^{-4}	-2.97 ± 0.08	-44	-3.90 ± 0.09	-59	-4.38 ± 0.06	-68
10^{-3}	-2.80 ± 0.07	-41	-4.12 ± 0.10	-63	-4.90 ± 0.10	-80
2.5×10^{-3}	-2.50 ± 0.07	-34	-4.29 ± 0.07	-60	-6.10 ± 0.15	-92
10^{-2}	-2.06 ± 0.04	-27	-6.38 ± 0.17	-92.5	-7.10 ± 0.19	-100
	$C_{16}E_{10} \cdot 10^{-2}$	mol dm $^{-3}$	$C_{16}E_{10} \cdot 10^{-3}$	mol dm $^{-3}$		
10^{-4}	-4.82 ± 0.11	-78	-5.09 ± 0.14	-85		
2.5×10^{-4}	-5.00 ± 0.12	-82.5	-5.66 ± 0.15	-107.5		
10^{-3}	-5.31 ± 0.11	-91	-6.23 ± 0.13	-130		
2.5×10^{-3}	-5.82 ± 0.13	-103	-6.97 ± 0.14	-114		
10^{-2}	-6.52 ± 0.17	-90	-7.07 ± 0.16	-99		

TABLE XXVII

Griseofulvin in 10^{-3} mol dm $^{-3}$ Na Cl at 25°C and
pH 7, with C₁₆E₃₀

Concentration of C ₁₆ E ₃₀ mol dm $^{-3}$	Sedimentation Volume	Mobility 10 $^{-8}$ m 2 s $^{-1}$ V $^{-1}$	Suspension appearance, case of redispersibility etc.
10 $^{-6}$	50	-2.36 ± 0.10	} Highly aggregated
10 $^{-5}$	50	-2.14 ± 0.08	
10 $^{-4}$	9	-1.18 ± 0.05	} Cloudy supernatant, caked
10 $^{-3}$	11	-1.17 ± 0.04	
10 $^{-2}$	30	-1.14 ± 0.04	Clear supernatant easily redispersed

TABLE XXVIII

Betamethasone in 10^{-3} mol dm $^{-3}$ Na Cl at 25°C and
pH 7.0, with SDS and C₁₆ E₃₀

Concentration of SDS mol dm $^{-3}$	Sedimentation Volume %	Mobility 10 $^{-8}$ 2 $^{-1}$ V $^{-1}$	Suspension appearance, ease of redispersibility etc.
a) <u>SDS alone</u>			
10 $^{-5}$	72	-0.82 ± 0.04	Highly
10 $^{-4}$	60	-1.30 ± 0.05	aggregated
10 $^{-3}$	37	-2.16 ± 0.10	Supernatant
2.5 x 10 $^{-3}$	20	-2.65 ± 0.07	cloudy
10 $^{-2}$	4	-4.17 ± 0.17	Supernatant cloudy caked
2.5 x 10 $^{-2}$	4	-4.22 ± 0.19	Supernatant opalescent caked
b) <u>SDS with C₁₆ E₃₀ 10$^{-2}$ mol dm$^{-3}$</u>			
10 $^{-5}$	4	-0.31 ± 0.02	Supernatant contains suspension of small particles. Presumably sterically stabilized
10 $^{-4}$	4	-0.43 ± 0.03	
10 $^{-3}$	4	-1.18 ± 0.04	
2.5 x 10 $^{-3}$	4	-1.57 ± 0.04	Supernatant cloudy
10 $^{-2}$	4	-1.73 ± 0.04	Supernatant opalescent
2.5 x 10 $^{-2}$	2	-1.77 ± 0.05	Supernatant almost clear
c) <u>C₁₆ E₃₀ alone</u>			
10 $^{-6}$		-0.46 ± 0.04	
10 $^{-5}$		-0.51 ± 0.04	
10 $^{-4}$		-0.36 ± 0.02	
10 $^{-3}$		-0.35 ± 0.02	
10 $^{-2}$		-0.34 ± 0.01	

Nalidixic Acid in $10^{-3} \text{ mol dm}^{-3}$ Na Cl at 25°C and
 pH 7.0, with SDS and $\text{C}_{16}\text{E}_{30}$

Concentration of SDS mol dm^{-3}	Sedimentation Volume %	Mobility $10^{-8} \text{ m}^2 \text{ s}^{-1} \text{ V}^{-1}$	Suspension appearance, ease of redispersibility etc.
a) <u>SDS alone</u>			
10^{-5}	12	-2.13 ± 0.09	Highly aggregated
10^{-4}	12	-2.15 ± 0.09	
10^{-3}	10	-2.40 ± 0.12	Slightly aggregated
2.5×10^{-3}	6	-3.15 ± 0.15	Deflocculated easily resuspended
10^{-2}	6	-5.30 ± 0.19	Deflocculated caked
2.5×10^{-2}	6	-5.48 ± 0.23	
b) <u>SDS with $\text{C}_{16}\text{E}_{30} 10^{-2} \text{ mol dm}^{-3}$</u>			
10^{-5}	5	-0.81 ± 0.05	Deflocculated
10^{-4}	5	-0.68 ± 0.02	
10^{-3}	5	-1.37 ± 0.04	
2.5×10^{-3}	5	-1.72 ± 0.05	
10^{-2}	5	-1.98 ± 0.09	
2.5×10^{-2}	5	-2.02 ± 0.09	
c) <u>$\text{C}_{16}\text{E}_{30}$ alone</u>			
10^{-6}		-1.99 ± 0.11	
10^{-5}		-1.97 ± 0.06	
10^{-4}		-1.28 ± 0.03	
10^{-3}		-1.22 ± 0.07	
10^{-2}		-1.24 ± 0.08	

Thiabendazole in 10^{-3} mol dm $^{-3}$ Na Cl at 25°C and
pH 7.5, with SDS and C $_{16}$ E $_{30}$

Concentration of SDS mol dm $^{-3}$	Sedimentation Volume %	Mobility $10^{-8} \frac{2^{-1} - 1}{m^2 s^{-1} V}$	Suspension appearance, case of redispersibility etc.
a) <u>SDS alone</u>			
10^{-5}	32	-1.37 ± 0.07	} Highly aggregated Aggregated Caked but easily redispersed Caked Caked
10^{-4}	54	-2.05 ± 0.04	
10^{-3}	18	-3.65 ± 0.09	
2.5×10^{-3}	11	-4.41 ± 0.16	
10^{-2}	8	-4.64 ± 0.23	
2.5×10^{-2}	7	-4.54 ± 0.20	
b) <u>SDS with 10^{-2} mol dm$^{-3}$ C$_{16}$ E$_{30}$</u>			
10^{-5}	8	-0.39 ± 0.03	} Cloudy Caked Supernatant Caked Caked Caked Caked Easily resuspended
10^{-4}	7	-0.46 ± 0.04	
10^{-3}	7	-1.15 ± 0.05	
2.5×10^{-3}	7	-1.63 ± 0.05	
10^{-2}	8	-1.93 ± 0.04	
2.5×10^{-2}	10	-2.18 ± 0.07	
c) <u>C$_{16}$ E$_{30}$ alone</u>			
10^{-6}	68	-1.92 ± 0.09	} Aggregated Deflocculated and caked
10^{-5}	17	-1.93 ± 0.12	
10^{-4}	4	-1.28 ± 0.04	
10^{-3}	5	-1.27 ± 0.03	
10^{-2}	7	-0.96 ± 0.06	

Griseofulvin in 10^{-3} mol dm $^{-3}$ NaCl at 25°C and pH 7.0, with C₁₂ TAB and C₁₆ Ey 10^{-2} mol dm $^{-3}$

Concentration of C ₁₂ TAB mol dm $^{-3}$	Sedimentation Volume %	Mobility $10^{-8} \frac{m^2}{Vs} V^{-1}$	Suspension appearance, ease of redispersibility etc.
a)			
2.5 x 10 $^{-5}$	50	-1.76 ± 0.07	} Highly aggregated
2.5 x 10 $^{-4}$	80	+0.51 ± 0.04	
6.25 x 10 $^{-4}$	70	+2.37 ± 0.11	
2.5 x 10 $^{-3}$	40	+2.87 ± 0.10	Aggregated, not satisfactory
6.25 x 10 $^{-3}$	30	+3.85 ± 0.23	Aggregated satisfactory.
2.5 x 10 $^{-2}$	4	+4.26 ± 0.10	Deflocculated, caked, opalescent supernatant
b) <u>C₁₆ E₁₀</u>			
2.5 x 10 $^{-5}$	30	-0.34	Aggregated
2.5 x 10 $^{-4}$	18	+0.45	Sediment 'two layered'
6.25 x 10 $^{-4}$	8	+1.12 ± 0.03	Caked
2.5 x 10 $^{-3}$	8	+1.58 ± 0.04	Caked
6.25 x 10 $^{-3}$	8	+1.69 ± 0.06	Caked
2.5 x 10 $^{-2}$	8	+2.02 ± 0.04	Caked
c) <u>C₁₆ E₃₀</u>			
2.5 x 10 $^{-5}$	20.5	-0.43 ± 0.04	Immediately dispersed
2.5 x 10 $^{-4}$	8	? small negative charge	Immediately dispersed
6.25 x 10 $^{-4}$	8	+0.55 ± 0.01	Immediately dispersed
2.5 x 10 $^{-3}$	8	+0.80 ± 0.02	Caked
6.25 x 10 $^{-3}$	7	+0.90 ± 0.02	Caked
2.5 x 10 $^{-2}$	7	+0.90 ± 0.02	Caked
d) <u>C₁₆ E₆₀</u>			
2.5 x 10 $^{-5}$	12	-0.46 ± 0.04	} Cloudy supernatant easily resuspended
2.5 x 10 $^{-4}$	12	? small negative charge	
6.25 x 10 $^{-4}$	9	Ca +0.2	} Clear, caked
2.5 x 10 $^{-3}$	7	+0.58 ± 0.02	
6.25 x 10 $^{-3}$	6	+0.64 ± 0.01	
2.5 x 10 $^{-2}$	6	+0.65 ± 0.01	

TABLE XXXII

Betamethasone in 10^{-3} mol dm $^{-3}$ Na Cl at 25°C and
pH 7.0 , with C₁₂ TAB and C₁₆ E₃₀

Concentration of C ₁₂ TAB mol dm $^{-3}$	Sedimentation Volume	Mobility 10 $^{-8}$ m 2 s $^{-1}$ V $^{-1}$	Suspension appearance, ease of redispersibility etc.
a)			
10 $^{-5}$		-0.43 ± 0.04	Aggregated
10 $^{-4}$		+0.38 ± 0.02	
10 $^{-3}$		+1.53 ± 0.05	Partial aggregation
2.5 x 10 $^{-3}$		+2.17 ± 0.07	
10 $^{-2}$		+3.24 ± 0.08	Deflocculated
2.5 x 10 $^{-2}$		+3.67 ± 0.05	
b) C ₁₂ TAB with 10 $^{-2}$ mol dm $^{-3}$ C ₁₆ E ₃₀			
10 $^{-5}$		-0.35 ± 0.04	
10 $^{-4}$		-0.22 ± 0.01	
10 $^{-3}$		+0.77 ± 0.01	All deflocculated
2.5 x 10 $^{-3}$		+1.07 ± 0.03	
10 $^{-2}$		+1.14 ± 0.01	
2.5 x 10 $^{-2}$		+1.11 ± 0.03	

Nalidixic Acid in 10^{-3} mol dm^{-3} Na Cl at 25°C and
pH 7.0, with C_{12} TAB and C_{16} E₃₀

Concentration of C_{12} TAB mol dm^{-3}	Sedimentation Volume %	Mobility $10^{-8} \frac{\text{m}^2}{\text{s}} \frac{-1}{\text{V}}$	Suspension appearance, ease of redispersibility etc.
a) C_{12} TAB alone			
10^{-5}	12	-1.56 ± 0.06	} aggregated
10^{-4}	8	-0.85 ± 0.03	
10^{-3}	8	$+0.93 \pm 0.03$? slightly aggregated
2.5×10^{-3}	5.5	$+1.61 \pm 0.03$	
10^{-2}	5	$+0.98 \pm 0.03$	} Deflocculated
2.5×10^{-2}		$+2.44 \pm 0.06$	
b) C_{12} TAB with 10^{-2} mol dm^{-3} C_{16} E ₃₀			
10^{-5}	5	-0.5 ± 0.03	All deflocculated
10^{-4}	5	? small negative charge	
10^{-3}	5	? small positive charge	
2.5×10^{-3}	5	$+0.57 \pm 0.02$	
10^{-2}	5	$+0.73 \pm 0.04$	
2.5×10^{-2}	5	$+0.90 \pm 0.04$	

Thiabendazole in 10^{-3} mol dm $^{-3}$ Na Cl at 25°C and
pH 7.5, with C₁₂ TAB and C₁₆ E₃₀

Concentration of C ₁₂ TAB mol dm $^{-3}$	Sedimentation Volume	Mobility $10^{-8} \frac{m^2}{s} V^{-1}$	Suspension appearance, case of redispersibility etc.
a) <u>C₁₂ TAB alone</u>			
10^{-5}	45	-1.81 ± 0.07	Light 'fluffy' aggregates Aggregates not so 'loose' Deflocculated easily dispersed 'good' suspension
10^{-4}	54	No movement	
10^{-3}	24	$+1.83 \pm 0.07$	
2.5×10^{-3}	20	$+1.93 \pm 0.05$	
10^{-2}	10	$+2.78 \pm 0.11$	
2.5×10^{-2}	10	$+3.52 \pm 0.17$	
b) <u>C₁₂ TAB with 10^{-2} mol dm$^{-3}$ C₁₆ E₃₀</u>			
10^{-5}	7	-0.39 ± 0.03	All deflocculated and caked
10^{-4}	7	No movement	
10^{-3}	8	$+0.60 \pm 0.01$	Most easily dispersed
2.5×10^{-3}	7	$+1.00 \pm 0.02$	
10^{-2}	8	$+1.05 \pm 0.04$	
2.5×10^{-2}	8	$+1.05 \pm 0.04$	

Griseofulvin in 10^{-3} mol dm^{-3} Na Cl at 25°C and
pH 7.0 , with SDS

Concentration of SDS mol dm^{-3}	Sedimentation Volume %	Mobility $10^{-8} \text{ m}^2 \text{ s}^{-1} \text{ V}^{-1}$	Suspension appearance, ease of redispersibility etc.
10^{-5}	52	-3.90 ± 0.13	
10^{-4}	52	-4.15 ± 0.12	
10^{-3}	30	-4.51 ± 0.12	
4×10^{-3}	9	-5.57 ± 0.18	
10^{-2}	6	-6.82 ± 0.15	
4×10^{-2}	6	-6.91 ± 0.13	

TABLE XXXVIII

Griseofulvin in 10^{-3} mol dm^{-3} Na Cl at 25°C and pH 7, with SDS and C_{16}E_y 10^{-2} mol dm^{-3}			
Concentration of SDS mol dm^{-3}	Sedimentation Volume %	Mobility $10^{-8} \frac{\text{m}^2}{\text{s}} \frac{-1}{\text{V}}$	Suspension appearance, ease of redispersibility etc.
a) $\text{C}_{16}\text{E}_{10}$			
10^{-5}	24.5	-1.07 ± 0.11	Immediate resuspension } Cloudy } Caked } } Clear
10^{-4}	8	-2.22 ± 0.08	
10^{-3}	7	-2.42 ± 0.05	
4×10^{-3}	7	-4.40 ± 0.07	
10^{-2}	7	-4.95 ± 0.09	
4×10^{-2}	8	-5.42 ± 0.11	
b) $\text{C}_{16}\text{E}_{30}$			
10^{-5}	26	-1.73 ± 0.07	} Immediate resuspension } 10 seconds resuspension 10 seconds resuspension 15 seconds resuspension 15 seconds resuspension
10^{-4}	15	-1.71 ± 0.05	
10^{-3}	8	-1.37 ± 0.04	
4×10^{-3}	8	-1.98 ± 0.06	
10^{-2}	8	-2.33 ± 0.05	
4.5×10^{-2}	8	-2.93 ± 0.05	
c) $\text{C}_{16}\text{E}_{60}$			
10^{-5}	26	-1.22 ± 0.03	} Immediate } resuspension } Resuspended by shaking: } 5 seconds } Caked 20 seconds } Caked 20 seconds } Caked 30 seconds
10^{-4}	16	-1.11 ± 0.04	
10^{-3}	8	-1.40 ± 0.04	
4×10^{-3}	7	-1.70 ± 0.06	
10^{-2}	6	-1.86 ± 0.04	
4×10^{-2}	4	-2.26 ± 0.06	

TABLE XXXIX

Griseofulvin in 10^{-3} mol dm $^{-3}$ Na Cl at 25°C and
pH 7.0, with SDS and 10^{-2} mol dm $^{-3}$ C $_{16}$ E $_{30}$

Concentration of SDS mol dm $^{-3}$	Sedimentation Volume %	Mobility 10 $^{-8}$ 2 $^{-1}$ 1 $^{-1}$ m 2 s $^{-1}$ V $^{-1}$	Suspension appearance, case of redispersibility etc.
10^{-5}	25	-1.73 ± 0.07	Immediate dispersion
10^{-4}	15	-1.71 ± 0.05	Immediate dispersion
10^{-3}	8	-1.37 ± 0.04	10 seconds shaking
4 x 10^{-3}	8	-1.98 ± 0.06	10 seconds shaking
10^{-2}	8	-2.33 ± 0.05	15 seconds shaking
4 x 10^{-2}	8	-2.93 ± 0.05	15 seconds shaking
			10 $^{-3}$ "Cloudy" supernatant
	with 10^{-3} mol dm $^{-3}$ C $_{16}$ E $_{30}$		
10^{-5}	11	-1.40 ± 0.06	Immediate dispersion
10^{-4}	7	-2.07 ± 0.01	5 seconds shaking
10^{-3}	7	-3.32 ± 0.10	5 seconds shaking
4 x 10^{-3}	7	-3.53 ± 0.10	5 seconds shaking
10^{-2}	6	-5.31 ± 0.09	10+ seconds shaking
4 x 10^{-2}	7	-5.96 ± 0.18	10+ seconds shaking
			All 'Cloudy' supernatant
	with 10^{-4} mol dm $^{-3}$ C $_{16}$ E $_{30}$		
10^{-5}	8	-2.03 ± 0.04	All deflocculated
10^{-4}	7	-2.96 ± 0.07	and slightly
10^{-3}	9	-3.53 ± 0.07	caked
4 x 10^{-3}	8	-6.13 ± 0.14	
10^{-2}	8	-6.24 ± 0.11	
4 x 10^{-2}	8	-5.76 ± 0.18	All 'Cloudy' supernatant